Catalytic Oxidation of Volatile Organic Compounds

(Oxidação Catalítica de Compostos Orgânicos Voláteis)

Vera Patrícia da Costa Oliveira Santos

Dissertation presented for the Ph.D. Degree in Chemical and Biological Engineering at the Faculty of Engineering, University of Porto, Portugal

Supervisors: **Prof. José Luís Cabral da Conceição Figueiredo**
Prof. José Joaquim de Melo Órfão

Laboratório de Catálise e Materiais
Laboratório Associado LSRE/LCM
Departamento de Engenharia Química
Faculdade de Engenharia
Universidade do Porto

2010

À minha filha, Beatriz

Ao meu marido, José Pedro

Agradecimentos

Em primeiro lugar quero agradecer aos meus orientadores, Prof. José Luís Cabral C. Figueiredo e Prof. José Joaquim M. Órfão, por todo o apoio e acompanhamento neste trabalho. Agradeço todos os conhecimentos que me transmitiram, bem como todas as sugestões e críticas.

Agradeço ao Prof. Manuel Fernando R. Pereira por todo o seu apoio, motivação e enorme disponibilidade para a discussão de ideias no decurso deste trabalho.

Agradeço à Fundação para a Ciência e Tecnologia (bolsa de doutoramento SFRH/BD/23731/2005 e Projecto PTDC/AMB/69065/2006) e ao Laboratório de Catálise e Materiais (LCM) que disponibilizou os meios materiais para a execução deste trabalho.

Agradeço à Dr. Sónia Carabineiro a preparação dos metais nobres suportados obtidos pelo método LPRD.

Ao professor Dr. Carlos Sá, Director do Centro de Materiais da Universidade do Porto (CEMUP), agradeço o apoio prestado no tratamento dos resultados XPS.

Agradeço à Elodie a ajuda na elaboração do Résumé.

Agradeço a todos os meus colegas do LCM, em especial à Salomé, à Cláudia, à Patrícia, à Filomena, ao Bruno e ao Adrián, a amizade, o companheirismo e todos os bons momentos que passamos juntos. Agradeço também aos novos elementos do grupo, nomeadamente a Raquel, a Juliana, Carla, Alexandra, Rita, João e Victor.

Agradeço a toda a minha família, em particular aos meus pais e à minha irmã, pelo seu constante incentivo e motivação para fazer mais e melhor. Não poderia deixar de agradecer também à Sofia e ao José Armando o seu apoio incondicional.

Finalmente, ao José Pedro, agradeço o amor, a paciência e o apoio nos momentos mais difíceis.

Preface

This PhD thesis was carried out at Laboratório de Catálise e Materiais (LCM), Laboratório Associado LSRE/LCM, at the Department of Chemical Engineering, Faculty of Engineering of the University of Porto.

The thesis is divided in five parts. Parts I and V corresponds to the introduction and main conclusions, respectively. The main core of the text (Parts II, III and IV) is based on 6 scientific papers, 5 of which already published in refereed Journals, while the other is in the last phase of preparation to be submitted.

List of publications:

V.P. Santos, M.F.R. Pereira, J.J.M. Órfão, J.L. Figueiredo, *Synthesis and characterization of manganese oxide catalysts for the total oxidation of ethyl acetate.* Top. Catal. 52 (2009) 470.

V.P. Santos, M.F.R. Pereira, J.J.M. Órfão, J.L. Figueiredo, *The role of lattice oxygen on the activity of manganese oxides towards the oxidation of VOC,* Appl. Catal. B-Environ. (2010), doi:10.1016/j.apcatb.2010.07.007.

V.P. Santos, M.F.R. Pereira, J.J.M. Órfão, J.L. Figueiredo, *Catalytic oxidation of ethyl acetate over a cesium modified cryptomelane catalyst*, Appl. Catal. B-Environ., 88 (2009) 550.

V.P. Santos, S.S.T. Bastos M.F.R. Pereira, J.J.M. Órfão, J.L. Figueiredo, *Stability of a cryptomelane catalyst in the oxidation of toluene*, Catal. Today (2010), doi: 10.1016/j.cattod.2009.12.005.

V.P. Santos, S.A.C. Carabineiro, P.B. Tavares, M.F.R. Pereira, J.J.M. Órfão, J.L. Figueiredo, *Total oxidation of CO, ethanol and toluene over TiO_2 supported noble metal catalysts,* Appl. Catal. B-Environ. (2010), doi:10.1016/j.apcatb.2010.06.020.

V.P. Santos, M.F.R. Pereira, J.J.M. Órfão, J.L. Figueiredo, *Mixture effects during the oxidation of toluene, ethyl acetate and ethanol over cryptomelane catalyst*, submitted.

Abstract

Catalytic oxidation is a promising technology to control the emissions of volatile organic compounds (VOC). From a practical point, the integration of such a process with an adsorption system would be of great interest. The main goal of this thesis was the development of active catalytic systems for the elimination of VOC. Three organic compounds were chosen as a model of volatile organic compounds: ethyl acetate, ethanol and toluene. The catalytic oxidation of these compounds was studied individually and in mixtures.

In the first part of this work the oxidation of ethyl acetate, ethanol and toluene was investigated over several catalysts (supported noble metals, mixed oxides and base metal oxides) in order to select the most promising catalytic systems for further development. Cryptomelane type manganese oxide and noble metal supported on titania were the catalysts selected.

The second part of this work describes the preparation, characterization and application of manganese oxides in the oxidation of ethyl acetate, ethanol and toluene. Concerning catalyst preparation, it was observed that it is possible to tailor the shape, crystalline phase and chemical composition of manganese oxide materials by controlling the pH and the template cation.

Cryptomelane was found to be very active in the oxidation of VOC, and its performance was significantly affected by the presence of other phases, namely Mn_2O_3 and Mn_3O_4. The latter improves the catalytic performance by increasing the reactivity and mobility of lattice oxygen, while the former has the opposite effect. A correlation between the redox properties and the activity of the manganese oxides was proposed, and a Mars and van Krevelen mechanism was established. The reactivity of VOC (in terms of conversion into CO_2) was found to increase in the following order: Toluene<Ethanol<Ethyl Acetate.

A cesium modified cryptomelane catalyst, prepared by ion-exchange, was also tested in the oxidation of ethyl acetate. It was shown that the presence of cesium improves catalyst performance, since it enhances its basic properties.

Stability tests of cryptomelane in the oxidation of toluene show a gradual deactivation at low temperatures. Besides deactivation, the catalyst also shows an oscillatory behaviour in the conversion into CO_2 in a restrited temperature range, which results from the cyclic accumulation and oxidation of adsorbed reactant and reaction products.

Remarkable mixture effects were observed in the oxidation of two-component mixtures in the presence of cryptomelane. Toluene was found to inhibit both ethyl acetate and ethanol oxidation. Toluene oxidation was slightly inhibited by the presence of ethyl acetate, while the presence of ethanol had a promoting effect. In the mixtures of ethyl acetate and ethanol, it was observed that both molecules have a mutual inhibitory effect, which is more evident in the case of ethyl acetate.

Noble metals supported on titania were also tested in the oxidation of VOC. The catalysts were prepared by incipient wetness impregnation and liquid phase reduction deposition. It was concluded that the preparation method has a significant effect on the metal dispersion and consequently on the performance of the catalyst. Platinum was considered the most active catalyst for VOC oxidation. In addition, the oxidation of ethyl acetate, ethanol and toluene was found to be structure sensitive in the presence of this catalyst.

The effects of the crystalline phase of the support, the amount of platinum and the activation conditions were also assessed in the case of ethyl acetate oxidation. It was concluded that the crystalline phase does not significantly affect catalyst performance while the presence of pre-reduced platinum increases the activity.

The oxidation of ethanol/toluene mixtures was also studied over platinum supported on titania. Mutual inhibitory effects were observed, much more evident in the case of ethanol.

Sumário

A oxidação catalítica é considerada uma tecnologia promissora no controlo das emissões dos compostos orgânicos voláteis (COV). Do ponto de vista prático, esta técnica deve ser associada a um sistema de adsorção, de forma a minimizar os custos energéticos. O principal objectivo desta tese consiste no desenvolvimento de sistemas catalíticos activos para a eliminação de COV. Foram escolhidos três compostos representativos de três classes de COV: acetato de etilo, etanol e tolueno. A oxidação catalítica destes compostos foi estudada individualmente e em misturas.

Numa primeira fase avaliou-se a actividade catalítica de vários catalisadores (metais nobres suportados, óxidos metálicos e óxidos mistos) na oxidação do acetato de etilo, etanol e tolueno, no sentido de seleccionar os sistemas catalíticos mais promissores. Os catalisadores seleccionados foram o criptomelano e metais nobres supportados em dióxido de titanio.

A preparação, caracterização e avaliação da actividade catalítica dos óxidos de manganês encontra-se descrita na segunda parte deste trabalho. Relativamente à preparação dos catalisadores, verificou-se que é possível controlar a forma, fase cristalina e composição química dos óxidos de manganês através do pH e do *template* usado.

De entre os vários óxidos de manganês testados verificou-se que o criptomelano era muito activo, sendo a sua eficiência alterada significativamente em presença de outras fases, nomeadamente Mn_2O_3 e Mn_3O_4. Em particular o Mn_3O_4 melhorou o desempenho do catalisador devido ao aumento da reactividade e mobilidade das espécies de oxigénio, enquanto que a presença de Mn_2O_3 teve o efeito oposto. A actividade catalítica dos óxidos de manganês parece estar correlacionada com as propriedades redox do catalisador, o que implica a presença de um mecanismo de oxidação do tipo Mars e van Krevelen. A reactividade dos COV (em termos de conversão em CO_2) aumenta na seguinte ordem: tolueno < etanol < acetato de etilo.

A oxidação do acetato de etilo também foi testada na presença de criptomelano permutado com césio. Observou-se que a presença de césio na estrutura porosa do criptomelano melhorou o seu desempenho, devido à modificação das propriedades ácido-base.

Os testes de estabilidade do catalisador na oxidação do tolueno revelaram uma desactivação gradual a temperaturas baixas. Para além da desactivação, o catalisador também originou um comportamento oscilatório numa zona restrita de temperaturas, o qual foi atribuído a ciclos de acumulação/oxidação de coque.

Na oxidação de misturas binárias na presença de criptomelano verificou-se que o tolueno inibe a oxidação dos compostos oxigenados; por outro lado, a oxidação do referido hidrocarboneto é parcialmente inibida na presença de acetato de etilo e promovida na presença de etanol. Na oxidação de misturas de acetato de etilo e etanol verificou-se que existe um efeito mútuo de inibição, sendo esta mais pronunciada no caso do acetato de etilo.

A oxidação dos COV também foi estudada na presença de metais nobres suportados em dióxido de titânio. Estes catalisadores foram preparados por impregnação incipiente e pelo método de deposição redutiva em fase líquida. Verificou-se que o método de preparação tem um efeito significativo na dispersão metálica e consequentemente na eficiência do catalisador. Para todos os COV estudados verificou-se que a platina era o metal mais activo. Adicionalmente, provou-se que a oxidação do acetato de etilo, etanol e tolueno era uma reacção sensível à estrutura.

No caso da oxidação do acetato de etilo, estudou-se também a influência de outras variáveis, tais como a estrutura cristalina do suporte, a quantidade de metal nobre e o estado electrónico da platina. Verificou-se que a estrutura cristalina do suporte não é um parâmetro muito importante na optimização deste sistema catalítico, mas a presença de platina reduzida aumenta consideravelmente a actividade do catalisador.

A oxidação de misturas etanol/tolueno também foi estudada na presença de metais nobres suportados. Verificou-se que a oxidação de ambos os componentes na mistura eram afectados negativamente, sendo esse efeito mais pronunciado no caso do etanol.

Résumé

L'oxydation catalytique est une technologie prometteuse pour contrôler les émissions de composés organiques volatiles. D'un point de vue pratique, l'intégration de ce processus à un système d'adsorption serait d'un grand intérêt. Le principal objectif de cette thèse est le développement de systèmes catalytiques pour l'élimination de composés organiques volatils (COV). Trois composés organiques ont été choisis comme modèle de composés organiques volatils: l'acétate d'éthyle, l'éthanol et le toluène. L'oxydation catalytique de ces composés a été étudiée individuellement et en mélange.

Dans la première partie de ce travail, l'oxydation de l'acétate d'éthyle, de l'éthanol et du toluène a été évaluée par plusieurs catalyseurs (métaux nobles supportés, oxydes de métaux et oxydes mixtes) afin de choisir les systèmes catalytiques les plus prometteurs. L'oxyde de manganèse du type cryptomélane et les métaux nobles supportés sur l'oxyde de titane ont été les catalyseurs sélectionnés.

La préparation, la caractérisation et l'application des oxydes de manganèse sur l'oxydation de l'acétate d'éthyle, l'éthanol et le toluène sont présentées dans la deuxième partie de ce travail. En ce qui concerne la préparation des catalyseurs, il a été constaté qu'il est possible de contrôler la forme, la phase cristalline et la composition chimique des oxydes de manganèse à travers le pH et le template utilisé.

La cryptomélane a été considerée très active dans l'oxydation des COV et sa performance a été significativement affectée par la présence d'autres phases, à savoir, Mn_2O_3 and. En particulier, Mn_3O_4 améliore les performances du catalyseur, car il augmente la réactivité et la mobilité des espèces d'oxygène, tandis que le premier a l'effet inverse. Une corrélation entre les propriétés redox et l'activité des oxydes de manganèse a été proposé et un mécanisme du type Mars et van Krevelen a été établi. La réactivité des COV (en termes de conversion en CO_2) augmente dans l'ordre suivant: toluène < éthanol < acétate d'éthyle.

Le catalyseur cryptomélane césium, préparé par échange ionique, a également été testé dans l'oxydation d'acétate d'éthyle. Il a été observé que la présence de césium améliore les performances du catalyseur, car il modifie ses propriétés acide-base.

Des essais de stabilité du catalyseur dans l'oxydation du toluène ont montré une désactivation progressive à basse température. Outre la désactivation, le catalyseur a également révélé un comportement instable (oscillant) dans une zone de température restreinte, qui a été attribué à des cycles d'accumulation/ oxydation du coke.

Dans l'oxydation de mélanges binaires en présence de cryptomélane, il a été constaté que le toluène inhibe l'oxydation des composés oxygénés, cependant, son oxydation est partiellement inhibée en présence d'acétate d'éthyle et promue en présence d'éthanol. Dans l'oxydation de mélanges d'acétate d'éthyle et d'éthanol, il a été constaté un effet d'inhibition mutuelle, mais celui-ci est plus prononcé dans le cas de l'acétate d'éthyle.

Des métaux nobles supportés sur du dioxyde de titane ont également été testés dans l'oxydation des COV. Ces catalyseurs ont été préparés par imprégnation en phase liquide et par la méthode de dépôt en phase liquide. Il a été verifié que la méthode de préparation a un effet significatif sur la dispersion métallique et donc sur la performance du catalyseur. La platine a été considéré comme le catalyseur le plus actif dans l'oxydation des COV. En outre, l'oxydation de l'acétate d'éthyle, de l'éthanol et du toluène en présence de ce catalyseur a été considérée sensible à la structure.

Dans le cas de l'oxydation de l'acétate d'éthyle, l'influence de la phase cristalline du support, le quantité de platine et les conditions d'activation ont également été évaluées. Il a été conclu que la phase cristalline n' a pas un effet majeur sur les performances du titane, tandis que la présence de platine réduite améliore considérablement la performance du catalyseur.

L'oxydation d'éthanol/toluène a également été étudiée en presence de metaux nobles. Il a été constaté que l'oxydation des deux composants d´un mélange est affectée négativement, etant cet effet plus prononcé dans le cas de l'éthanol.

Contents

List of Figures

List of Tables

Part I

Introduction

A summary of the impact of the volatile organic compounds (VOC) in the environment is described in the first part of this chapter. Stratospheric ozone depletion, enhancement of the global greenhouse effect, photochemical smog, and human health effects are some of the aspects evaluated. Special emphasis is given to the participation of VOC on photochemical smog. The major sources of VOC emissions, including the biogenic and anthropogenic sources, are also included, together with an outline of the existing legislation in Europe that directly or indirectly acts to reduce VOC emissions. An overview of the emissions of pollutants in Europe, during the 1990-2006 period is provided. A short description of the available technologies for control of VOC emissions is presented, focusing on catalytic oxidation processes. The type of catalysts used, catalyst deactivation and reactivity of the reactants are some of the aspects evaluated. The main objectives and layout of this thesis are presented at the end of this chapter.

1 Introduction

1.1 Impact of Volatile organic compounds in the atmosphere

Air pollution is both a local and a trans-boundary problem caused by the emission of certain pollutants that, either alone or through chemical reaction, have negative environmental and health impacts [1].

Volatile organic compounds (VOC) are an important class of air pollutants and cover a wide ranging class of compounds that differ in their properties and chemistry, but display similar behaviour in the atmosphere. Several definitions can be found to describe VOC. For instance, the United States Environmental Protection Agency (US EPA) defines a VOC based on their relative photochemical reactivity in the atmosphere, whilst under European Union (EU) it is defined in terms of volatility and reactivity [2, 3]. The definition used here (EU) includes any organic compound having a vapour pressure of 0.01 kPa or more at 293.15 K [2]. VOC are also sometimes designated as non-methane volatile organic compound (NMVOC), as methane is inert and does not participate in the formation of photochemical smog.

The release of VOC into the atmosphere has widespread environmental implications and has been linked to the *stratospheric ozone depletion*, *the formation of ground level ozone (photochemical smog)* and the enhancement *of the global greenhouse effect* [1, 4, 5]. Even so, these compounds require special attention due their toxicity (human health effects), high stability and persistence in the environment.

1.1.1 VOC as precursor of ground level ozone

Ground level ozone is the major component of photochemical smog [1]. High concentrations of ozone can cause impacts ranging from minor effects on the respiratory system to premature mortality.

The production of ozone can be illustrated by the following scheme (Figure 1.1):

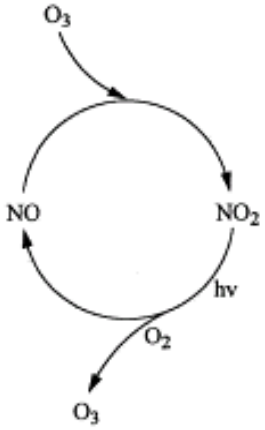

Figure 1.1 Cycle of NO_x in troposphere.

This cycle is initiated by the decomposition of NO_2 to NO and $O^{\bullet}$, which reacts to O_2 to form O_3. On the other hand, O_3 is used to oxidize NO into NO_2. This cycle generates a small contribution to the background ozone concentration. It is important to notice that the concentration of ozone is only a function of the intensity of the light and does not depend strongly on the concentration of NO_x.

In the presence of VOC a new cycle is reestablished (see Figure 1.2) and the role of VOC is to convert NO to NO_2 without using up ozone. In this case ozone will not be consumed by reacting with NO and it will accumulate in the atmosphere. In this way, although VOC do not take part in the main reaction of ozone formation, their presence will cause accumulation of ozone at ground level.

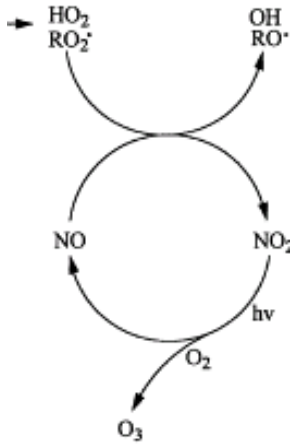

Figure 1.2 Cycle of NO_x in the presence of VOC.

1.2 Sources and control strategies for VOC

The environmental and human health issues have led to a variety of standards and legislation. Table 1.1 summarizes the most important European policies that directly or indirectly act to reduce VOC emissions in Portugal [5]. One of the most important is the 2001/81/EC directive (NECD). This directive establishes ceilings for the emission of certain atmospheric pollutants (SO_2, NO_x, VOC and NH_3) for the different members, which should be reached by 2010. The aim is to minimize the adverse effects from acidification, soil eutrophication and ground level ozone [3].

The sources of VOC emissions can be divided into biogenic and anthropogenic sources [1, 4]. The biogenic sources cannot be easily controlled, and includes the emissions from plants, trees, wild animals, natural forest fires, and anaerobic processes.

The emissions of VOC as a result of human activities arise from transport, evaporation, solvent usage, industrial processes (oil refining or chemical manufacture), petrol storage and distribution, landfilled wastes, food manufacture and agriculture. A recent study by the European Environment Agency (EEA) shows that during the period 1990-2006 the most significant sources of VOC emissions in the countries of European Union were the use of solvents (38%) and the road transport sector (18%) (see Figure 1.3) [6].

Table 1.1 European legislation for reduction of VOC.

European Directive	Objectives
96/61/EC	Ambient air quality assessment and management
1999/13/EC	Limitations to the use of organic solvents
2001/81/EC	National emission ceilings for SO_2, NH_3, NO_x and VOC, to be attained in 2010 for each member state
2002/3/EC	Limits and/or target values to tropospheric ozone
2004/42/EC	Limitation in the use of organic solvents in certain paints and varnishes

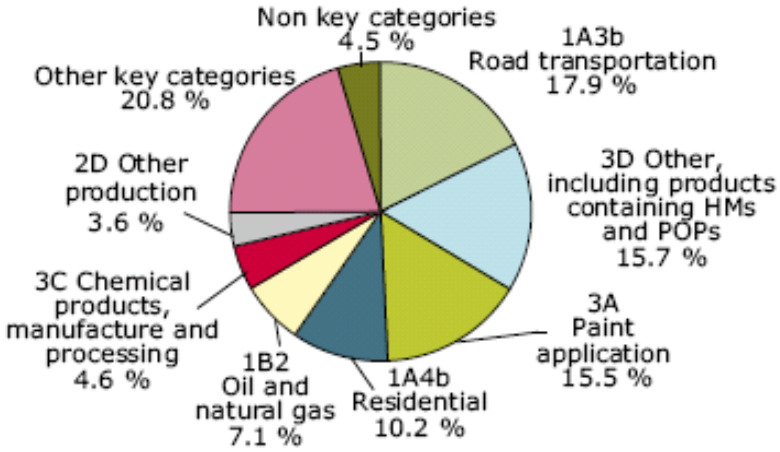

Figure 1.3 Contributions to VOC emissions by sectors in 2006 for EU-27.

1.3 Emissions of VOC in Europe, 1990-2006

Significant progress has already been made in reducing the main air pollutants, and the EU-27 emissions of VOC have decreased 41% since 1990. This reduction has primarily been due to the significant reduction achieved in the road transport (due to the introduction of vehicle catalytic converters and the switching from petrol to diesel cars) and in the use solvents (as a result of the introduction and implementation of the solvent emissions and paints directives (1999/13/EC) [2]). For instance, the Netherlands and Finland reported a decline in emissions of 69% and 64% from the solvent usage sector, as a result of compliance with the 1999/13/EC directive.

Figure 1.4 shows the changes in the emissions of VOC since 1990 compared with the 2010 NECD targets (%) [2]. In general, the EU-27 member's states have made good progress towards reducing emissions, and some of them have already reduced their national VOC emissions below the level of their respective emission ceiling.

However, six Member States (Belgium, Denmark, Greece, Hungary, Portugal and Spain) have emissions still significantly above their respective emission ceilings and thus must make significant reductions over the coming years if they are to comply with the NECD. In these countries other additional measures should be taken into account in order to reduce VOC emissions.

A recent study shows that even with the full implementation of existing laws, environmental and health problems will persist in 2020, if no further action is taken. Against this background, a policy choice has to be made on the level of health and environmental protection that can be achieved by 2020. The chosen strategy sets a review in the current legislation, mainly the NECD directive, in order to ensure a reduction of 82% in SO_2 emissions, 60% in NO_x, 51% in VOC, 27% in NH_3 relative to emissions in 2000.

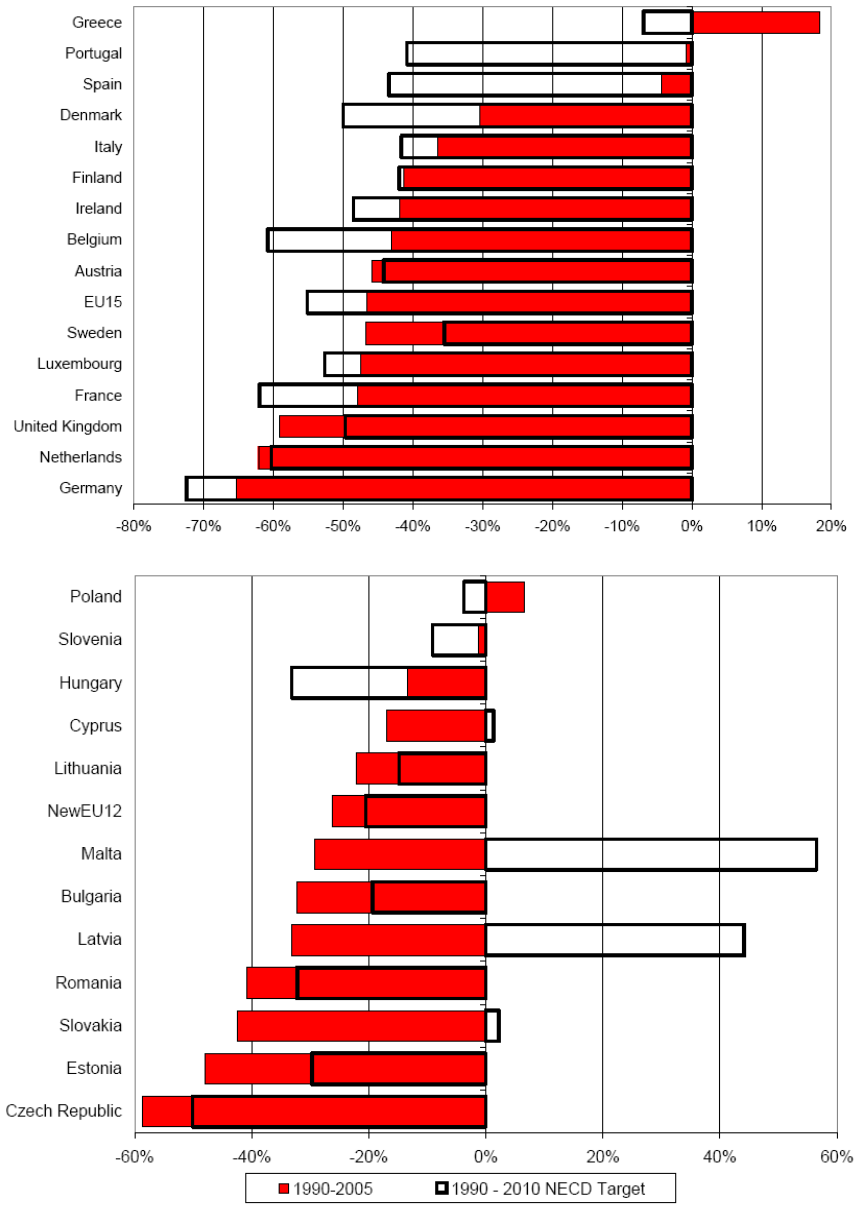

Figure 1.4 Changes in the emissions of VOC in EU-27 since 1990 compared with the 2010 NECD targets (%).

1.4 VOC control technologies

The reduction in VOC emissions from stationary sources can be achieved by two different approaches, either alone or in combination [7-9]:

- process and equipment modification

- add-on-control techniques

In the first group, the control is achieved by prevention, improving or modifying the equipment used, changing the operation conditions or choosing other raw materials. Add-on-control techniques are generally divided into recovery (adsorption, condensation, membrane separation, condensation, absorption) and destruction (biofiltration, thermal oxidation, catalytic oxidation, reverse flow reactor).

The main selection criteria for VOC abatement technologies are costs, VOC type and concentration, gas flow-rate and the required control level, although air flow rate and pollutant loading are the two most important design criteria for VOC control devices. Table 1.2 lists the most common control technologies, as well as the operation conditions in which each process operates most efficiently and cost-efficiently. The main secondary impacts of each method are also indicated [5, 7].

Adsorption, condensation, absorption and membrane separation are the most common recovery techniques.

Table 1.2 Evaluation of various techniques for the control of VOC emissions.

Process	VOC concentration (ppmv)	Flow-rate (m^3/s)	Performance (%)	Impact
Adsorption	20-10,000	0.05-3	90-99	Solid waste
Condensation	5,000-10,000	0.05-10	70-85	Solid waste, waste-water
Absortion	500-5,000	1-50	90-98	Solid waste, waste-water
Membranes	<20,000	0.1-1	90-99	Solid waste
Bio-filtration	10-5,000	< 7	60-95	CO_2, solid waste
Thermal oxidation	20-20,000	0.5-250	95-99	CO_2, SOx, Nox
Catalytic oxidation	100-2000	0.5-25	90-99	CO_2, SOx, NOx, solid waste

Adsorption is one of the most promising recovery technologies for treating low concentration VOC streams. The design of an adsorber system depends on the chemical characteristics of the VOC being recovered, the physical properties of the inlet stream (temperature, pressure and volumetric flow-rate) and the physical properties of the adsorbent. Common industrial adsorption systems often use activated carbon [10-12], zeolites [13, 14] and mesoporous silicas [15, 16]. Activated carbon is the most universal and widely applied adsorbent, due to its high adsorption capacity and great affinity for both polar and non-polar compound. However, this system shows some disadvantages, namely, it is a flammable material, it does not desorb efficiently high-boiling solvents, and it is a hygroscopic material requiring humidity control. In spite of their lower adsorption capacity, zeolites may be advantageous due to their incombustibility, great stability, and regenerability at low temperature. Bed regeneration is typically done by heating or applying vacuum to desorb the adsorbed gases; the bed is then cooled and dried, and the concentrated vapours are routed to a recovery system such as condenser, decanter or distillation tower.

Condensation is a suitable technology for low flow-rate concentrated VOC streams. The driving force for this process is over-saturation which is achieved by chilling or pressurization of the waste gas stream. The basic equipment is a refrigerated condenser system which includes a condenser, refrigeration unit(s) and auxiliary equipment (e.g., pre-cooler, recovery/storage tank, pump/blower and piping). From a practical point of view, this process should be avoided for the recovery of highly volatile compounds.

Absorption (scrubbing) is especially used to separate water-soluble compounds, by contacting the contaminated air with a liquid solvent. The choice of a suitable solvent, the availability of vapour/liquid equilibrium data for the design of the absorber and the required regeneration of the VOC containing solvent by stripping are some of the limitations of this method.

Gas permeation and reverse osmosis are the available membrane separation techniques. This recovery technology is only applied for low-flow waste gas streams. Cost and complexicity are the main factors limiting the application of this technology.

However, destruction rather than separation methods should be preferable in VOC control emission. A range of destruction technologies have been developed and these include bio-filtration, thermal and catalytic oxidation.

Bio-filtration is an effective and inexpensive method for the removal of VOC. In this technique, VOC are destroyed by microorganisms, under aerobic conditions, to carbon dioxide, water, inorganic products and bio-mass. The key component of this process is a bio-filter that contains the adequate type of microorganisms for the oxidation of a specific type of VOC. High performance is achieved in the oxidation of low molecular weight oxygenated compounds. On the other hand, in the presence of waste streams containing halogenated VOC and polyaromatic compounds, the efficiency of this process is very low.

Thermal oxidation is a process in which the VOC are oxidised to carbon dioxide and water, by increasing the temperature above the auto-ignition point, in the presence of oxygen. Time, temperature, turbulence and the amount of oxygen affect the rate and the efficiency of the combustion process [17]. The operation temperatures are in the range 600-1100 ºC depending on the nature of the VOC. At these temperatures, gas phase radicals are formed and the oxidation reactions proceed very rapidly. Furthermore the feed composition has to be chosen within certain limits, in order to operate outside the explosion boundaries. There are three types of thermal oxidation systems: *direct flame*, *recuperative* and *regenerative.* They are differentiated by the equipment and heat recovery system. A *direct flame thermal oxidiser*, also known as an afterburner, consists of a combustion chamber and does not include any heat recovery. The *recuperative* and *regenerative* oxidisers use the heat of combustion to heat the incoming gas stream prior to entering the combustion zone. In the recuperative oxidiser the waste gas is preheated with hot, clean gas leaving the combustion chamber. The regenerative oxidiser uses a high-density medium such as a ceramic packed bed still hot from a previous cycle to pre-heat the incoming feed containing VOC; such systems generally have lower fuel requirements because of higher recovery (up to 95%).

Catalytic oxidisers operate similarly to thermal oxidisers. The main difference is the presence of a catalyst that increases the oxidation reaction rate, allowing the reaction

to occur at lower temperatures (between 200 ºC to 500 ºC), which is the main advantage of this process [5, 8]. However, the presence of poisons, such as sulphur and particulates in the waste stream can decrease significantly the performance of this process. Furthermore, this process should not be feasible in the oxidation of large flow rate streams with very low VOC concentrations. In this case, a dual function adsorbent/catalyst system, which integrates the adsorption and catalytic combustion into a single control unit, should be preferable [5, 18, 19]. An overview of many scientific aspects relating to this process, namely the type of catalysts used and the nature of the different reactivities of VOC, will be provided in the following section.

Other emerging technologies include ultraviolet oxidation and plasma technology. The UV radiation excites the oxidants, which destroy the VOC through direct oxidation. This process is highly energy efficient for very dilute streams, and no pollutant by-products are created. However, the use of a water scrubber could require wastewater treatment. Plasma technology is a high-temperature ionized gas that is very reactive. The decomposition reaction is initiated by a free-radicals mechanism. It is important to establish optimum conditions to generate enough free radicals for the reactions to reach completion.

1.5 Catalytic Oxidation of VOC- General Overview

Catalytic oxidation of VOC is a promising technology that offers high destructive efficiency at lower operating temperatures, lower capital cost and smaller units [5, 7].

The key parameter of this technology is the type of catalyst used which depends on several variables, namely the type of effluent to be treated (composition, type of VOC and flow-rate), the presence of poisons or/and inhibitors in the gas stream, and any inlet temperature constraints.

The optimization of a catalyst formulation is not an easy task, due to the large variety of VOC compounds and the complex nature of VOC mixtures. The catalyst itself must respect a number of characteristics: it must be both very active (due to the low concentration of VOC and large volumes to be treated) and selective (in the sense that only CO_2 and H_2O should be produced), it must withstand the conditions of operation and, in particular, it must be thermal stable and allow ignition at low temperatures.

Intensive research has been ongoing in this field since the early of 1970s, in order to produce the best catalytic formulation [18, 20, 21]. A brief description of the type of catalysts used will be reviewed, in the following sections, as well as the basic understanding of the reactivities of the different classes of VOC.

1.5.1 Catalysts

Two type of catalysts can be applied in catalytic oxidation: single/mixed metal oxides (Cu, Mn, Cr, Fe, Ni) and supported noble metal catalysts [5, 20, 21]. The following sections will described the most important features related with these catalysts, as well as the most recent advances in this field.

1.5.1.1 Metal Oxides

It is generally accepted that noble metal catalysts are more active than metal oxides, but their high cost and limited availability have been encouraging their replacement. Furthermore, by choosing the proper composition, higher thermal stability and activity can be achieved with metal oxides.

During the oxidation reactions over metal oxides, oxygen can be activated by interacting with oxide surfaces. Coordination, electron transfer, dissociation, and incorporation into the oxide lattice may be steps in the activation process. Two possible states of activated oxygen can be recognized [22]:

1. Adsorbed oxygen (O^-);
2. Lattice-incorporated oxygen species (O^{2-}).

The participation of these species is a function of the type of catalyst used (*p-oxide or n-oxide*) and the oxidation temperature. For instance, p-type semiconductors easily adsorb oxygen as O^-, which are the active species in oxidation, while in n-type semiconductors lattice oxygen is usually involved (Mars Van Krevelen mechanism) [22]. Arai and co-workers [23] confirmed the participation of both types of oxygen species in the complete oxidation of methane. At low temperatures the oxidation reaction proceeds with the participation of adsorbed surface oxygen, while at higher temperatures lattice oxygen dominated the oxidation reaction.

Transition metal oxides have been extensively studied in the oxidation of VOC, the most used being Mn [24-26], Cr [27], and Fe [28] being most used. In some cases, these catalysts show performances as high or higher than supported noble metal catalysts [29].

Ceria-based catalysts are also very active in VOC oxidation, because of the unique features of their oxygen storage capacity (OSC). However, thermal instability and deactivation by Cl_2 and HCl are some of the disadvantages of these catalysts [30]. Modifying CeO_2 with other metals, namely, zirconium, enhances thermal stability and improve catalyst performance [31, 32].

Zeolites can also be used as supports or even as catalysts for the oxidation of VOC. Tsou et al. showed that basic zeolites can be very efficient in the oxidation of MIBK and o-xylene[33-35]. The main disadvantage associated with this type of catalysts is the coke formation inside the pores, which may cause deactivation or/and an oscillatory behaviour [36, 37].

Mixed metal oxides are also an important class of catalysts, due their unique properties of activity and selectivity in comparison to the individual oxides. The perovskites (general formula ABO_3, where A represents a lanthanide and/or alkaline earth metal ion and B a transition metal ion) are also used with high efficiency in the catalytic oxidation of VOC, especially for oxygenated compounds [38-40]. Pecchi et al. [41] reported on the catalytic activity of $LaFe_{1-y}NiO_3$ perovskite oxides for ethanol and ethyl acetate oxidation. The incorporation of iron by nickel strongly enhances catalyst performance, due to the cooperative effect of iron and nickel. Other mixed oxides like Co-Mn-Al [42], $CuO\text{-}CeO_2$ [43] , $MnO_x\text{-}CeO_2$ [44], $CuMn_2O_4$ [45], Ce_xZrO_2 [46], were also studied.

The oxidation of VOC over manganese based catalysts will be discussed in more detail in the following sections.

Manganese Oxides

Manganese oxides (α–MnO_2, β–MnO_2, γ–MnO_2, Mn_3O_4, Mn_2O_3) have been extensively studied as catalytic materials in the oxidation of many pollutants such as ethanol [47, 48], acetone [26], propane and propene [24] and ethyl acetate [29]. The

catalytic properties of MnO_x are attributed to the ability of manganese to form oxides with different oxidation states and their high oxygen storage capacity (OSC). Although the nature of the active sites for catalytic oxidation is not well established, several authors attribute their high activity to the mixed valence of framework manganese and to the higher mobility of lattice oxygen, suggesting the participation of lattice oxygen in the oxidation process [47, 49]. Moreover, the presence of structural (cationic vacancies) and chemical defects was also found to improve catalyst performance [48, 50, 51].

Octahedral molecular sieves (OMS) have received considerable attention for over 50 years, due to their exceptional catalytic properties and their shape-selective character [52-55]. The open frameworks of these materials are composed of edge and corner shared MnO_6 octahedra, the internal pores being occupied by cations and water molecules.

Cryptomelane-type manganese oxide (K-OMS-2) is one group of the octahedral molecular sieves family (OMS) called hollandite, and has tunnel structures that consist of 2 x 2 arrays of MnO_6 octahedra (see Figure 1.5) [55]. Inside the tunnels, potassium cations and small amounts of water stabilize the structure, and can be partially ion-exchanged with other cations with appropriate sizes. The tunnel dimensions are 0.46 nm x 0.46 nm and the average manganese oxidation state is around 3.8, which corresponds to a larger proportion of Mn (IV) with lower amounts of Mn (III) [52-56]. The open tunnel structure and mixed valences of OMS-2 make this material very attractive for oxidation catalysis and, therefore, the synthesis of cryptomelane material with high purities, small particle size, high surface areas, and high yield has been a challenge in recent years.

There are some studies concerning the oxidation of several VOC over cryptomelane, namely, benzene [57, 58], toluene [59], ethanol [60, 61] and ethyl acetate [60]. The high activity of this catalyst was attributed to the presence of the redox couple Mn(III)/Mn(IV), high mobility of lattice oxygen, open structure and high hydrophobicity [51, 61].

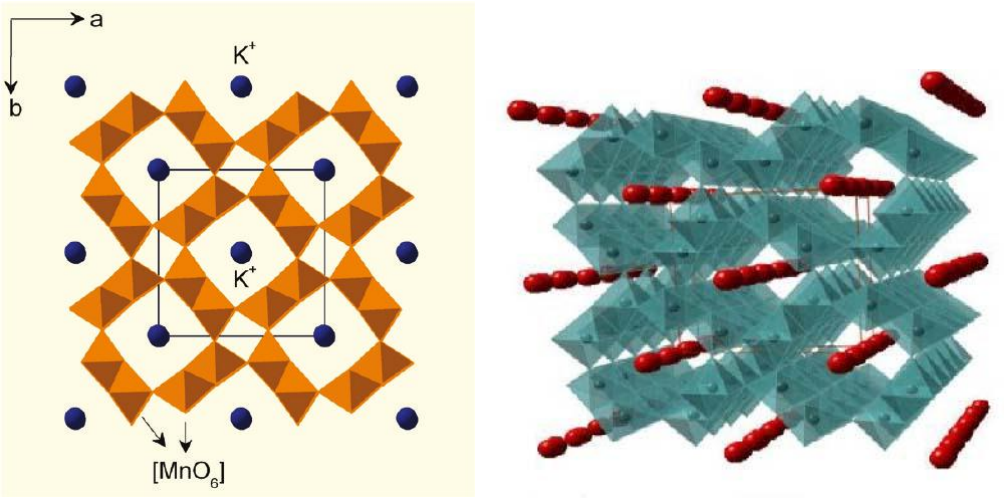

Figure 1.5 Schematic structure of cryptomelane**.**

In order to further improve the electronic and catalytic properties, other metal cations have been introduced inside the tunnels or into the framework, by subsequent ion-exchange [62-64] or by substitution during synthesis [65-67]. It was observed that the introduction of alkali metal into the tunnel can significantly modify the physical and chemical properties of cryptomelane, specially the surface acid-base properties [68]. Liu et al.[68] synthesized for the first time manganese oxides with Li^+, Na^+, Rb^+ as tunnel cations and found that the nature of the cation greatly influences the catalytic properties of OMS-2 towards total oxidation of cyclohexanol. Moreover, octahedral molecular sieves with Co^{2+}, Ag^+ and Cu^{2+} as tunnel cations showed high catalytic activities for CO oxidation at low temperatures [69, 70].

Supported Manganese Oxides/Mixed Oxides with Mn

Manganese oxides are often supported in different carriers in order to enhance catalyst performance [71-74]. The type of support used strongly affects the metal dispersion and the nature of the manganese species present on the support. Trawczynski et al. [72] studied the oxidation of ethanol on manganese oxides supported on different carriers: alumina, titania and yttrium-stabilized zirconia (YSC). It was observed that the presence of the support enhanced reducibility of the MnO_x phase; the reducibility was controlled by the oxide-support interaction; YSC and alumina were considered

the most appropriate supports. Moreover, the nature and characteristics of the supported manganese oxide phase strongly depend on the manganese precursor used and, to a lesser extent, on the support and the manganese loading [75]. Moreover, combinations with other elements can also affect the activity of supported manganese oxides. Álvarez et al. [76] studied the oxidation of formaldehyde over Mn/Al_2O_3 and $Pd\text{-}Mn/Al_2O_3$. It was observed that the presence of palladium enhanced catalyst performance by increasing the reducibility of the catalyst. The presence of PdO species on the catalyst surface not only provides oxygen, but also some metallic sites on which the organic compound becomes decomposed.

Mixed oxides of Mn with Ni, Fe and Cu are also interesting catalysts for the oxidation of VOC. In general, the mobility of bulk and surface oxygen on mixed oxides is significantly higher compared to the single oxides, enhancing catalyst performance. However, the structure and degree of crystallinity of mixed oxides play a key role on their catalysts performance.

Mixed nickel manganese oxides show two different structures: spinel, $NiMn_2O_4$ and ilmenite, $NiMnO_3$. Mehandjiev et al. [77] studied the oxidation of ethyl acetate, benzene and carbon monoxide over mixed nickel manganese oxides. It was observed that ilmenite-type catalysts were significantly more active and more resistant to poisoning than the spinel structure. This effect was explained by the presence of manganese species in a higher oxidation state (Mn(IV)) in the ilmenite structure.

Mn_2O_3- Fe_2O_3 mixed oxides were also used in the oxidation of VOC. The oxidation of propene and propane was studied in the presence of the mixed oxide and compared to the single oxides. It was observed that the mixed oxide showed a better performance in comparison to the single oxides [78].

The oxidation mechanism over the Ni-Mn and Fe-Mn mixed oxides is quite different. The latter involves adsorbed oxygen species (p-type semi-conductor) while the former involves lattice oxygen (n-type semi-conductor) [79].

Mn-Cu is one of the most studied mixed oxides in the oxidation of VOC [45, 80, 81]. The formation of the *hopcalite phase* ($CuMn_2O_4$), which is very active in the amorphous form, is the main reason for the intensive research. The high activity is ascribed to the presence of a redox system in the form of

$Cu^{2+} + Mn^{3+} \Leftrightarrow Cu^{+} + Mn^{4+}$. The main disadvantage of this catalytic system is deactivation at high temperatures, due to the crystallization of the spinel phase. The presence of surface inhibitors [82], a spillover mechanisml with manganese oxide acting as oxygen donator and copper oxide as oxygen acceptor [83] and shifts in the redox couples [82] are some of the reasons for deactivation during the crystallization process. Morales and co-workers [45] studied the oxidation of ethanol over Cu-Mn mixed oxides and they pointed out that the content of copper strongly affects catalyst performance. Small amounts of copper prevent the formation of highly crystalline manganese oxides, improving catalyst performance (due to the higher amount of oxygen vacancies). When the copper content increases, the solid state reaction between Cu and Mn is favoured, and the partial oxidation of ethanol becomes more important. The incorporation of manganese into an incomplete spinel structure diminishes the CO_2 yield.

Manganese oxides can also be mixed with zirconia and cerium. Delimaris and Ioannides [84] found that MnO_x-CeO_2 catalysts, prepared by a urea combustion method, were very active in toluene and ethanol oxidation. Similarly, Mn-Zr mixed oxides have been found to be effective catalysts for the oxidation of chlorinated VOC [85].

1.5.1.2 Noble Metals

The development of noble metal catalysts has been widely reported in the literature. However, according to Bond [86], the use of noble metals other than Pt, Pd, and a few alloys appears to be limited due to their instability in oxygen, high volatility and high cost. In addition, operation problems may occur as a result of sinterization at temperatures above 500 ºC or poisoning.

The general mechanism of oxidation over noble metals is thought to involve the dissociative adsorption of oxygen [21]:

$$O_2 + 2[\ ] \rightarrow 2[O] \qquad (1.1)$$

where [ ] represents an active site. After this step, the organic reactant may follow either a Langmuir-Hinshelwood type of mechanism or an Elley-Rideal mechanism, depending on its nucleophilic character. Nevertheless, some authors considerer the

redox mechanism of the metal surface similar to the mechanism over metal oxide catalysts, namely in the case of gold [28, 87] and Ag [88]. In this case, the noble metal would be oxidized by oxygen and reduced by the hydrocarbon.

Considerable data are available in the literature concerning the oxidation of VOC over supported noble metals [21, 89-94]. Most of these studies involve supported Pt [95, 96] or Pd [97, 98]. TiO_2, CeO_2, Al_2O_3 and ZrO_2 are some of the carriers used. It was observed that the acid-base character of the support plays a key role on catalyst performance. For example, in toluene oxidation over Pd supported on different carriers, the activity of Pd was controlled by the acid-base property of the support via an electronic interaction [99].

Gold is also used in the oxidation of several VOC. However, its performance is strongly dependent of the metal size as well as the type of support. Furthermore, gold can also increase the oxygen mobility of the support, enhancing catalyst performance [28, 100].

The active phase can also be a mixture of noble metals. Some studies show that the combination of platinum and palladium is more efficient that of a single metal [101, 102]. Furthermore, combinations with other metals can also be used. The oxidation of formaldehyde/methanol was enhanced by the use of Pd-Mn/Al_2O_3 catalysts [76].

1.5.2 Catalyst deactivation

In industrial applications, catalyst stability and durability are as important as activity and selectivity. Therefore, catalyst deactivation must be prevented as much as possible. An overview of catalyst deactivation was presented by Butt et al. [103]. Several mechanisms can lead to deactivation: (i) poisoning (ii) volatilization of catalyst species; (iii) thermal degradation and (iv) formation of coke deposits.

Noble metals are frequently poisoned by the presence of chlorinated and sulphur-containing compounds. Moreover, severe operating conditions can also promote sinterization [104]. In the case of metal oxides, chlorinated compounds can also deactivate the catalysts, as chloride atoms may lead to a loss of metal due to the formation of volatile species. Sulphur compounds can also affect the activity of manganese oxides, as it can be incorporated into the support [105].

The formation of carbonaceous deposits (coke) inside the pores or on the outer surface is particularly important during transformation of organic reactants in molecular sieves [106, 107]. When the coke precursors are strongly retained in the porous structure, besides deactivation, the catalyst may also become unstable, showing an oscillatory behaviour. Tsou et al. [36, 37] have studied in detail the origin of this oscillatory behaviour in the oxidation of some VOC compounds over zeolite-based catalysts. Accumulation of adsorbed reactant was found to be at the origin of oscillations; on the other hand, this was found to be related to the adsorption properties of the support. In particular, a support which is capable of retaining the VOC at temperatures higher than the reaction temperature may lead to oscillations in the apparent conversion into CO_2.

The presence of steam can also have a negative effect on the catalyst performance [108, 109], and for this reason, this effect should not be overlooked in the design of industrial plants. The inhibition effect is generally reversible and can be minimized by the use of hydrophobic catalysts [110]. However, the role of water in VOC oxidation is complex, and in some systems it is beneficial. For example, the presence of water vapour could play a positive role in the oxidation of chlorobenzene on VO_x/TiO_2, VO_x-WO_x/TiO_2 and VO_x/MoO_x catalysts, by removing Cl^- from the surface after the oxidation of the aromatic ring [111].

1.5.3 The type of VOC

The reactivity towards oxidation depends on the adsorption strength of the VOC and on its structure. The following reactivity order was assessed in the oxidation of VOC over Pt/Al_2O_3 [112]: alcohols > ethers > aldehydes > alkenes > aromatics > ketones > esters > alkanes.

It is established that C-H bond activation is the determining step in the oxidation of saturated hydrocarbons and oxygenated compounds [113, 114], and for this reason, a single weak bond leads to high reactivity.

Furthermore, the oxidation of VOC is frequently accompanied by the formation of partial oxidation compounds, and it is important to know the reactivity of these by-products. This is particularly important in the oxidation of oxygenated compounds, for

example, in the oxidation of ethanol [96] and ethyl acetate [94, 95], whereas higher amounts of by-product were formed. However, the behaviour of the compounds when present in mixtures may differ from the individual compounds, and this can affect the oxidation efficiency. It is then important to study not only the individual compounds, but also in the presence of mixtures of VOC. The "mixture effect" is very difficult to predict *a priori* [21], as either a common inhibition effect [33, 115, 116] or (more rarely) a promoting effect [117] can be observed when the components of the mixture are oxidised. Besides these possible effects, changes in selectivity to by-products have also been observed [116, 118, 119]. Certain authors have pointed out that the inhibition effect can be due to competition between the molecules for adsorption onto the active sites [33, 95, 119-121]. For example, Tsou et al. [33] observed that the oxidation of methyl-isobutyl-ketone (MIBK) on zeolite supported platinum catalysts was strongly inhibited by the presence of o-xylene, which adsorbs strongly onto the active sites. On the other hand, the oxidation of certain compounds can be also independent of the presence of other VOC. For example, the presence of n-hexane does not affect the oxidation of benzene and toluene over a Pt/Al_2O_3 catalyst [122]. It was concluded that the addition of a compound that is more weakly adsorbed on the catalyst than the original one does not affect the conversion rate significantly [122].

A promoting effect has also been observed in the oxidation of mixtures [117, 123, 124]. Barresi and Baldi [124] state that this effect is, in most cases, a consequence of the higher exothermicity of the process. For example, n-hexane oxidation is enhanced by the presence of toluene [112]. However, in some systems this effect cannot be explained by heat generation during the reaction. For example, the oxidation of chlorobenzene over a $Pt/\gamma\text{-}Al_2O_3$ catalyst [123] is enhanced by the addition of aliphatic hydrocarbons, such as pentane, heptane or decane. It was observed that alkanes have the ability to remove Cl from the Pt surface (at the same time reducing the metal), which otherwise would only be removed at higher temperatures. This phenomenon could explain the promoting effect in this case.

1.6 Aim of this work and thesis outline

The aim of this thesis is the development of active catalysts for the elimination of VOC. Three organic compounds were chosen as a model of VOC: ethyl acetate, ethanol and toluene.

This thesis is divided in five parts. The main core of this text is composed of the Parts II, III and IV.

Parte II consists in the evaluation of several catalysts for the oxidation of ethyl acetate, ethanol and toluene. The most promising catalytic systems were selected for further studies.

Part III describes the preparation, characterization and application of manganese oxides in the oxidation of ethyl acetate, ethanol and toluene. The influence of the redox properties of manganese oxides was evaluated, and possible reaction mechanisms were presented. The effect of the incorporation of cesium cations on the structure of cryptomelane was also evaluated. Stability tests on cryptomelane and study of mixtures were presented in the final part chapters.

Parte IV is dedicated to the application of supported noble metal catalysts on the oxidation of VOC. The effect of the preparation method on the catalyst performance was evaluated. Furthermore, the influence of metal dispersion and type of noble metal was assessed. The oxidation of ethyl acetate over platinum and palladium supported catalysts is presented in the final chapter. The influence of metal dispersion, metal load and electronic state was studied on the most active system.

Part V summarizes and integrates the main conclusions withdrawn from this work. Some suggestions for forthcoming work are also presented.

References

[1] R.J. Heinsohn, R.L. Kabel, *Sources and control of air pollution*, in: Prentice Hall, Upper Saddle River, NJ, 1999.

[2] EU Council Directive 1999/13/EC of 11 March 1999.

[3] EU Council Directive 2001/81/EC of 23 October 2001.

[4] R.E. Hester, R.M. Harrison, *Volatile organic compounds in the atmosphere*, Royal Society of Chemistry 1995.

[5] T.F. Garetto, I. Legorburu, M. Montes, *Eliminación de emisiones atmosféricas de COVs por catálisis y adsorción*, in: CYTED, Argentina, 2008.

[6] K. Mareckova, M. Gager, S. Gottlicher, *Annual european community LRTAP convention emission inventory report 1990–2006*, European Environment Agency, Copenhagem, 2008.

[7] F.I. Khan, A. Kr. Ghoshal, *Removal of volatile organic compounds from polluted air*. J. Loss Prev. Process Ind. 13 (2000) 527-545.

[8] E.C. Moretti, *Reduce VOC and HAP emissions*. Chem. Eng. Prog. 98 (2002) 30-40.

[9] E.C. Moretti, N. Mukhopadhyay, *VOC control - current practices and future-trends*. Chem. Eng. Prog. 89 (1993) 20-26.

[10] G. Finqueneisel, T. Zimny, J.V. Weber, *On the prediction of adsorption isotherms of methanol/water vapour mixtures on microporous activated carbon*. Carbon 43 (2005) 1093-1095.

[11] L. Luo, D. Ramirez, M.J. Rood, G. Grevillot, K.J. Hay, D.L. Thurston, *Adsorption and electrothermal desorption of organic vapors using activated carbon adsorbents with novel morphologies*. Carbon 44 (2006) 2715-2723.

[12] L. Li, P.A. Quinlivan, D.R.U. Knappe, *Effects of activated carbon surface chemistry and pore structure on the adsorption of organic contaminants from aqueous solution. Carbon 40 (2002) 2085-2100*

[13] W.B. Stephen, *Hydrophobic zeolite adsorbent: A proven advancement in solvent separation technology*. Environ. Prog. 12 (1993) 226-230.

[14] T. El Brihi, J.N. Jaubert, D. Barth, L. Perrin, *Determining volatile organic compounds' adsorption isotherms on dealuminated Y zeolite and correlation with different models*. J. Chem. Eng. Data 47 (2002) 1553-1557.

[15] K. Kosuge, S. Kubo, N. Kikukawa, M. Takemori, *Effect of pore structure in mesoporous silicas on VOC dynamic adsorption/desorption performance*. Langmuir 23 (2007) 3095-3102.

[16] S. Kubo, K. Kosuge, *Salt-induced formation of uniform fiberlike SBA-15 mesoporous silica particles and application to toluene adsorption*. Langmuir 23 (2007) 11761-11768.

[17] E. Donley, D. Lewandowski, *Optimized design and operating parameters for minimizing emissions during VOC thermal oxidation*. Metal Finishing. 100 (2002) 505-516.

[18] P.S. Chintawar, H.L. Greene, *Adsorption and catalytic destruction of trichloroethylene in hydrophobic zeolites*. Appl. Catal. B-Environ. 14 (1997) 37-47.

[19] W.B. Li, J.X. Wang, H. Gong, *Catalytic combustion of VOCs on non-noble metal catalysts*. Catal. Today 148 (2009) 81-87.

[20] K. Everaert, J. Baeyens, *Catalytic combustion of volatile organic compounds*. J. Hazard. Mater. 109 (2004) 113-139.

[21] J.J. Spivey, *Complete catalytic-oxidation of volatile organics*. Ind. Eng. Chem. Res. 26 (1987) 2165-2180.

[22] C.N. Satterfield, *Heterogeneous Catalysis in Industrial Practice*, in: 2nd Edition, Mc Graw-Hill, 1991.

[23] H. Arai, T. Yamada, K. Eguchi, T. Seiyama, *Catalytic combustion of methane over various perovskite-type oxides*. Appl. Catal. 26 (1986) 265-276.

[24] M. Baldi, E. Finocchio, F. Milella, G. Busca, *Catalytic combustion of C_3 hydrocarbons and oxygenates over Mn_3O_4*. Appl. Catal. B-Environ. 16 (1998) 43-51.

[25] S.S. Bastos, J.J.M. Órfão, M.M.A. Freitas, M.F.R. Pereira, J.L. Figueiredo, *Manganese oxide catalysts synthesized by exotemplating for the total oxidation of ethanol*. Appl. Catal. B-Environ. 93 (2009) 30-37.

[26] K.M. Parida, A. Samal, *Catalytic combustion of volatile organic compounds on Indian Ocean manganese nodules*. Appl. Catal. A-Gen. 182 (1999) 249-256.

[27] H. Rotter, M.V. Landau, M. Carrera, D. Goldfarb, M. Herskowitz, *High surface area chromia aerogel efficient catalyst and catalyst support for ethylacetate combustion*. Appl. Catal. B-Environ. 47 (2004) 111-126.

[28] S. Scirè, S. Minicò, C. Crisafulli, S. Galvagno, *Catalytic combustion of volatile organic compounds over group IB metal catalysts on Fe_2O_3*. Catal. Commun. 2 (2001) 229-232.

[29] C. Lahousse, A. Bernier, P. Grange, B. Delmon, P. Papaefthimiou, T. Ioannides, X. Verykios, *Evaluation of γ-MnO_2 as a VOC removal catalyst: comparison with a noble metal catalyst*. J. Catal. 178 (1998) 214-225.

[30] B. de Rivas, J.I. Gutierrez-Ortiz, R. Lopez-Fonseca, J.R. Gonzalez-Velasco, *Analysis of the simultaneous catalytic combustion of chlorinated aliphatic pollutants and toluene over ceria-zirconia mixed oxides*. Appl. Catal. A-Gen. 314 (2006) 54-63.

[31] A. Trovarelli, C. de Leitenburg, M. Boaro, G. Dolcetti, *The utilization of ceria in industrial catalysis*. Catal. Today 50 (1999) 353-367.

[32] A.C. Gluhoi, N. Bogdanchikova, B.E. Nieuwenhuys, *The effect of different types of additives on the catalytic activity of Au/Al_2O_3 in propene total oxidation: transition metal oxides and ceria*. J. Catal. 229 (2005) 154-162.

[33] J. Tsou, P. Magnoux, M. Guisnet, J.J.M. Órfão, J.L. Figueiredo, *Catalytic oxidation of methyl-isobutyl-ketone over basic zeolites*. Appl. Catal. B-Environ. 51 (2004) 129-133.

[34] J. Tsou, P. Magnoux, M. Guisnet, J.J.M. Órfão, J.L. Figueiredo, *Catalytic oxidation of volatile organic compounds - oxidation of methyl-isobutyl-ketone over Pt/zeolite catalysts*. Appl. Catal. B-Environ. 57 (2005) 117-123.

[35] J. Tsou, L. Pinard, P. Magnoux, J.L. Figueiredo, M. Guisnet, *Catalytic oxidation of volatile organic compounds (VOCs): Oxidation of o-xylene over Pt/HBEA catalysts*. Appl. Catal. B-Environ. 46 (2003) 371-379.

[36] J. Tsou, P. Magnoux, M. Guisnet, J.J.M. Órfão, J.L. Figueiredo, *Oscillations in the catalytic oxidation of volatile organic compounds*. J. Catal. 225 (2004) 147-154.

[37] J. Tsou, P. Magnoux, M. Guisnet, J.J.M. Órfão, J.L. Figueiredo, *Oscillations in the oxidation of MIBK over a Pt/HFAU catalyst: role of coke combustion*. Catal. Commun. 4 (2003) 651-656.

[38] J. Niu, J. Deng, W. Liu, L. Zhang, G. Wang, H. Dai, H. He, X. Zi, *Nanosized perovskite-type oxides $La_{1-x}Sr_xMO_{3-d}$ (M = Co, Mn; x = 0, 0.4) for the catalytic removal of ethylacetate*. Catal. Today 126 (2007) 420-429.

[39] V. Szabo, M. Bassir, A. Van Neste, S. Kaliaguine, *Perovskite-type oxides synthesized by reactive grinding - Part IV. Catalytic properties of $LaCo_{1-x}Fe_xO_3$ in methane oxidation*. Appl. Catal. B-Environ. 43 (2003) 81-92.

[40] B. Levasseur, S. Kaliaguine, *Effects of iron and cerium in $La_{1-y}Ce_yCo_{1-x}Fe_xO_3$ perovskites as catalysts for VOC oxidation*. Appl. Catal. B-Environ. 88 (2009) 305-314.

[41] G. Pecchi, P. Reyes, R. Zamora, L.E. Cadus, J.L.G. Fierro*, Surface properties and performance for VOCs combustion of $LaFe_{1-y}Ni_yO_3$ perovskite oxides.* J. Solid State Chem 181 (2008) 905.

[42] K. Jiratova, J. Mikulova, J. Klempa, T. Grygar, Z. Bastl, F. Kovanda, *Modification of Co-Mn-Al mixed oxide with potassium and its effect on deep oxidation of VOC*. Appl. Catal. A-Gen. 361 (2009) 106-116.

[43] D. Delimaris, T. Ioannides, *VOC oxidation over $CuO\text{-}CeO_2$ catalysts prepared by a combustion method*. Appl. Catal. B-Environ. 89 (2009) 295-302.

[44] D. Delimaris, T. Ioannides, *VOC oxidation over $MnOx\text{-}CeO_2$ catalysts prepared by a combustion method*. Appl. Catal. B-Environ. 84 (2008) 303-312.

[45] M.R. Morales, B.P. Barbero, L.E. Cadús, *Evaluation and characterization of Mn-Cu mixed oxide catalysts for ethanol total oxidation: Influence of copper content*. Fuel 87 (2008) 1177-1186.

[46] J.I. Gutiérrez-Ortiz, B. de Rivas, R. López-Fonseca, J.R. González-Velasco, *Catalytic purification of waste gases containing VOC mixtures with Ce/Zr solid solutions*. Appl. Catal. B-Environ. 65 (2006) 191-200.

[47] L. Lamaita, M.A. Peluso, J.E. Sambeth, H.J. Thomas, *Synthesis and characterization of manganese oxides employed in VOCs abatement*. Appl. Catal. B-Environ. 61 (2005) 114-119.

[48] M.A. Peluso, J.E. Sambeth, H.J. Thomas, *Complete oxidation of ethanol over MnO_x*. React. Kinet. Catal. Lett. 80 (2003) 241-248.

[49] C. Cellier, V. Ruaux, C. Lahousse, P. Grange, E.M. Gaigneaux, *Extent of the participation of lattice oxygen from γ-MnO_2 in VOCs total oxidation: Influence of the VOCs nature*. Catal. Today 117 (2006) 350-355.

[50] C. Lahousse, A. Bernier, E. Gaigneaux, P. Ruiz, P. Grange, B. Delmon, Activity of manganese dioxides towards VOC total oxidation in relation with their crystallographic characteristics, Stud. Surf. Sci. Catal. 110 (1997) 777.

[51] M.A. Peluso, L.A. Gambaro, E. Pronsato, D. Gazzoli, H.J. Thomas, J.E. Sambeth, *Synthesis and catalytic activity of manganese dioxide (type OMS-2) for the abatement of oxygenated VOCs*. Catal. Today 133-135 (2008) 487-492.

[52] Q. Feng, H. Kanoh, K. Ooi, *Manganese oxide porous crystals*. J. Mater. Chem. 9 (1999) 319-333.

[53] S.L. Suib, *Microporous manganese oxides*. Curr. Opin. Solid State Mat. Sci. 3 (1998) 63-70.

[54] S.L. Suib, *Structure, porosity, and redox in porous manganese oxide octahedral layer and molecular sieve materials*. J. Mater. Chem. 18 (2008) 1623-1631.

[55] S.L. Brock, N.G. Duan, Z.R. Tian, O. Giraldo, H. Zhou, S.L. Suib, *A review of porous manganese oxide materials*. Chem. Mater. 10 (1998) 2619-2628.

[56] M. Pasero, *A short outline of the tunnel oxides*. Micro and Mesoporous Mineral Phases 57 (2005) 291-305.

[57] J. Luo, Q. Zhang, A. Huang, S.L. Suib, *Total oxidation of volatile organic compounds with hydrophobic cryptomelane-type octahedral molecular sieves*. Micropor. Mesopor. Mat. 35-36 (2000) 209-217.

[58] J. Luo, Q. Zhang, J. Garcia-Martinez, S.L. Suib, *Adsorptive and acidic properties, reversible lattice oxygen evolution, and catalytic mechanism of*

cryptomelane-type manganese oxides as oxidation catalysts. J. Am. Chem. Soc. 130 (2008) 3198-3207.

[59] M.I. Dominguez, P. Navarro, F. Romero-Sarria, D. Frias, S.A. Cruz, J.J. Delgado, M.A. Centeno, M. Montes, J.A. Odriozola, *Fibrous mno$_2$ nanoparticles with (2 x 2) tunnel structures. catalytic activity in the total oxidation of volatile organic compounds*. J. Nanosci. Nanotechno. 9 (2009) 3837-3842.

[60] A.R. Gandhe, J.S. Rebello, J.L. Figueiredo, J.B. Fernandes, *Manganese oxide OMS-2 as an effective catalyst for total oxidation of ethyl acetate*. Appl. Catal. B-Environ. 72 (2007) 129-135.

[61] M.A. Peluso, E. Pronsato, J.E. Sambeth, H.J. Thomas, G. Busca, *Catalytic combustion of ethanol on pure and alumina supported K-Mn oxides: an IR and flow reactor study*. Appl. Catal. B-Environ. 78 (2008) 73-79.

[62] J. Cai, J. Liu, W.S. Willis, S.L. Suib, *Framework doping of iron in tunnel structure cryptomelane*. Chem. Mater. 13 (2001) 2413-2422.

[63] Q. Feng, H. Kanoh, Y. Miyai, K. Ooi, *Alkali-metal ions insertion/extraction reactions with hollandite-type manganese oxide in the aqueous-phase*. Chem. Mater. 7 (1995) 148-153.

[64] Y.F. Shen, S.L. Suib, C.L. Oyoung, *Effects of inorganic cation templates on octahedral molecular-sieves of manganese oxide*. J. Am. Chem. Soc. 116 (1994) 11020-11029.

[65] X. Chen, Y.F. Shen, S.L. Suib, C.L. O'Young, *Catalytic decomposition of 2-propanol over different metal-cation-doped OMS-2 materials*. J. Catal. 197 (2001) 292-302.

[66] W. Gac, *The influence of silver on the structural, redox and catalytic properties of the cryptomelane-type manganese oxides in the low-temperature CO oxidation reaction*. Appl. Catal. B-Environ. 75 (2007) 107-117.

[67] J. Liu, Y.C. Son, J. Cai, X.F. Shen, S.L. Suib, M. Aindow, *Size control, metal substitution, and catalytic application of cryptomelane nanomaterials prepared using cross-linking reagents*. Chem. Mater. 16 (2004) 276-285.

[68] J. Liu, V. Makwana, J. Cai, S.L. Suib, M. Aindow, *Effects of alkali metal and ammonium cation templates on nanofibrous cryptomelane-type manganese oxide octahedral molecular sieves (oms-2)*. J. Phys. Chem. B 107 (2003) 9185-9194.

[69] E. Nicolas-Tolentino, Z.R. Tian, H. Zhou, G.G. Xia, S.L. Suib, *Effects of Cu^{2+} ions on the structure and reactivity of todorokite- and cryptomelane-type manganese oxide octahedral molecular sieves*. Chem. Mater. 11 (1999) 1733-1741.

[70] R. Hu, Y. Cheng, L. Xie, D. Wang, *Effect of Doped Ag on Performance of Manganese Oxide Octahedral Molecular Sieve for CO Oxidation*. Chin. J. Catal. 28 (2007) 463-468.

[71] L.M. Gandía, M.A. Vicente, A. Gil, *Complete oxidation of acetone over manganese oxide catalysts supported on alumina- and zirconia-pillared clays*. Appl. Catal. B-Environ. 38 (2002) 295-307.

[72] J. Trawczynski, B. Bielak, W. Mista, *Oxidation of ethanol over supported manganese catalysts--effect of the carrier*. Appl. Catal. B-Environ. 55 (2005) 277-285.

[73] Y. Xi, C. Reed, Y.K. Lee, S.T. Oyama, *Acetone oxidation using ozone on manganese oxide catalysts*. J. Phys. Chem. B 109 (2005) 17587-17596.

[74] F.N. Aguero, A. Scian, B.P. Barbero, L.E. Cadus, *Combustion of volatile organic compounds over supported manganese oxide: Influence of the support, the precursor and the manganese loading*. Catal. Today 133-135 (2008) 493-501.

[75] F.N. Aguero, B.P. Barbero, O. Sanz, F.J.E. Lozano, M. Montes, L.E. Cadus, *Influence of the support on mno_x metallic monoliths for the combustion of volatile organic compounds*. Ind. Eng. Chem. Res. 49 (2008) 1663-1668.

[76] M.C. Álvarez-Galván, V.A. de la Peña O'Shea, J.L.G. Fierro, P.L. Arias, *Alumina-supported manganese- and manganese-palladium oxide catalysts for VOCs combustion*. Catal. Commun. 4 (2003) 223-228.

[77] D. Mehandjiev, E. Zhecheva, G. Ivanov, R. Ioncheva, *Preparation and catalytic activity of nickel-manganese oxide catalysts with an ilmenite-type structure in the reactions of complete oxidation of hydrocarbons*. Appl. Catal. A-Gen. 167 (1998) 277-282.

[78] M. Baldi, V.S. Escribano, J.M.G. Amores, F. Milella, G. Busca, *Characterization of manganese and iron oxides as combustion catalysts for propane and propene*. Appl. Catal. B-Environ. 17 (1998) L175-L182.

[79] M.R. Morales, B.P. Barbero, L.E. Cadús, *Combustion of volatile organic compounds on manganese iron or nickel mixed oxide catalysts*. Appl. Catal. B-Environ. 74 (2007) 1-10.

[80] P.-O. Larsson, A. Andersson, *Oxides of copper, ceria promoted copper, manganese and copper manganese on Al_2O_3 for the combustion of CO, ethyl acetate and ethanol*. Appl. Catal. B-Environ. 24 (2000) 175-192.

[81] V.H. Vu, J. Belkouch, A. Ould-Dris, B. Taouk, *Removal of hazardous chlorinated VOCs over Mn-Cu mixed oxide based catalyst*. J. Hazard. Mater. 169 (2009) 758-765.

[82] G. Fortunato, H.R. Oswald, A. Reller, *Spinel-type oxide catalysts for low temperature CO oxidation generated by use of an ultrasonic aerosol pyrolysis process*. J. Mater. Chem. 11 (2001) 905-911.

[83] F.C. Buciuman, F. Patcas, T. Hahn, *A spillover approach to oxidation catalysis over copper and manganese mixed oxides*. Chem. Eng. Prog. 38 (1999) 563-569.

[84] D. Delimaris, T. Ioannides, *VOC oxidation over MnO_x-CeO_2 catalysts prepared by a combustion method*. Appl. Catal. B-Environ. 84 (2008) 303-312.

[85] J.I. Gutiérrez-Ortiz, B. de Rivas, R. López-Fonseca, S. Martín, J.R. González-Velasco, *Structure of Mn-Zr mixed oxides catalysts and their catalytic performance in the gas-phase oxidation of chlorocarbons*. Chemosphere 68 (2007) 1004-1012.

[86] A. Wilson, "Catalysis by Metals by G. C. Bond", Acta Crystallogr. 16 (1963) 437.

[87] S. Minicò, S. Scirè, C. Crisafulli, R. Maggiore, S. Galvagno, *Catalytic combustion of volatile organic compounds on gold/iron oxide catalysts*. Appl. Catal. B-Environ. 28 (2000) 245-251.

[88] E.M. Cordi, J.L. Falconer, *Oxidation of volatile organic compounds on a Ag/Al_2O_3 catalyst*. Appl. Catal. A-Gen. 151 (1997) 179-191.

[89] T.F. Garetto, C.R. Apesteguia, *Structure sensitivity and in situ activation of benzene combustion on Pt/Al_2O_3 catalysts*. Appl. Catal. B-Environ. 32 (2001) 83-94.

[90] V. Labalme, E. Garbowski, N. Guilhaume, M. Primet, *Modifications of Pt/alumina combustion catalysts by barium addition. Properties of aged catalysts*. Appl. Catal. A-Gen. 138 (1996) 93-108.

[91] C.H. Lee, Y.W. Chen, *Effect of additives on Pd/Al_2O_3 for CO and propylene oxidation at oxygen-deficient conditions*. Appl. Catal. B-Environ. 17 (1998) 279-291.

[92] S. Morales-Torres, A.F. Perez-Cadenas, F. Kapteijn, F. Carrasco-Marin, F.J. Maldonado-Hodar, J.A. Moulijn, *Palladium and platinum catalysts supported on carbon nanofiber coated monoliths for low-temperature combustion of BTX*. Appl. Catal. B-Environ. 89 (2009) 411-419.

[93] P. Papaefthimiou, T. Ioannides, X.E. Verykios, *Combustion of non-halogenated volatile organic compounds over group VIII metal catalysts*. Appl. Catal. B-Environ. 13 (1997) 175-184.

[94] J.E. Sawyer, M.A. Abraham, *Reaction Pathways During the oxidation of ethyl-acetate on a platinum/alumina catalyst*. Ind. Eng. Chem. Res. 33 (1994) 2084-2089.

[95] P. Papaefthimiou, T. Ioannides, X.E. Verykios, *Performance of doped Pt/TiO_2 (W^{6+}) catalysts for combustion of volatile organic compounds (VOCs)*. Appl. Catal. B-Environ. 15 (1998) 75-92.

[96] L.M. Petkovic, S.N. Rashkeev, D.M. Ginosar, *Ethanol oxidation on metal oxide-supported platinum catalysts*. Catal. Today 147 (2009) 107-114.

[97] K. Okumura, T. Kobayashi, H. Tanaka, M. Niwa, *Toluene combustion over palladium supported on various metal oxide supports*. Appl. Catal. B-Environ. 44 (2003) 325-331.

[98] M. Paulis, L.M. Gandia, A. Gil, J. Sambeth, J.A. Odriozola, M. Montes, *Influence of the surface adsorption-desorption processes on the ignition curves of volatile organic compounds (VOCs) complete oxidation over supported catalysts*. Appl. Catal. B-Environ. 26 (2000) 37-46.

[99] K. Okumura, H. Tanaka, M. Niwa, *Influence of acid-base property of support on the toluene combustion activity of palladium*. Catal. Lett. 58 (1999) 43-45.

[100] S. Scirè, S. Minicò, C. Crisafulli, C. Satriano, A. Pistone, *Catalytic combustion of volatile organic compounds on gold/cerium oxide catalysts*. Appl. Catal. B-Environ. 40 (2003) 43-49.

[101] S. Vigneron, P. Deprelle, J. Hermia, *Comparison of precious metals and base metal oxides for catalytic deep oxidation of volatile organic compounds from coating plants: test results on an industrial pilot scale incinerator*. Catal. Today 27 (1996) 229-236.

[102] C. Micheaud, P. Marécot, M. Guérin, J. Barbier, *Preparation of alumina supported palladium-platinum catalysts by surface redox reactions. Activity for complete hydrocarbon oxidation*. Appl. Catal. A-Gen. 171 (1998) 229-239.

[103] J.B. Butt, J.J. Spivey, S.K. Agrawal, Catalyst deactivation in the oxidation of volatile organic-compounds by some metal-oxides, B. Delmon, G.F. Froment (Eds.), 6th International Symposium on Catalyst Deactivation, Oostend, Belgium, 1994, pp 19-31.

[104] J.J. Spivey, J.B. Butt, *Literature review: deactivation of catalysts in the oxidation of volatile organic compounds.* Catal. Today 11 (1992) 465.

[105] J.J. Spivey, J.B. Butt, S.K. Agrawal, *Catalyst Deactivation in the oxidation of volatile organic compounds by some metal oxides*. Stud. Surf. Sci. Catal. 88 (1994) 19.

[106] L. Becker, H. Forster, *Investigations of coke deposits formed during deep oxidation of benzene over Pd and Cu exchanged Y-type zeolites*. Appl. Catal. A-Gen. 153 (1997) 31-41.

[107] A.P. Antunes, M.F. Ribeiro, J.M. Silva, F.R. Ribeiro, P. Magnoux, M. Guisnet, *Catalytic oxidation of toluene over CuNaHY zeolites - coke formation and removal*. Appl. Catal. B-Environ. 33 (2001) 149-164.

[108] S. Kawi, M. Te, *MCM-48 supported chromium catalyst for trichloroethylene oxidation*. Catal. Today 44 (1998) 101-109.

[109] R. López-Fonseca, A. Aranzabal, P. Steltenpohl, J.I. Gutiérrez-Ortiz, J.R. González-Velasco, *Performance of zeolites and product selectivity in the gas-phase oxidation of 1,2-dichloroethane*. Catal. Today 62 (2000) 367-377.

[110] Q.H. Xia, K. Hidajat, S. Kawi, *Improvement of the hydrothermal stability of fluorinated MCM-41 material*. Mater. Lett. 42 (2000) 102-107.

[111] S. Krishnamoorthy, J.A. Rivas, M.D. Amiridis, *Catalytic Oxidation of 1,2-Dichlorobenzene over Supported Transition Metal Oxides*. J. Catal. 193 (2000) 264-272.

[112] J. Hermia, S. Vigneron, *Catalytic incineration for odour abatement and VOC destruction*. Catal. Today 17 (1993) 349-358.

[113] R. Burch, D.J. Crittle, M.J. Hayes, *C-H bond activation in hydrocarbon oxidation on heterogeneous catalysts*. Catal. Today 47 (1999) 229-234.

[114] A. O'Malley, B.K. Hodnett, *The influence of volatile organic compound structure on conditions required for total oxidation*. Catal. Today 54 (1999) 31-38.

[115] A. Musialik-Piotrowska, K. Syczewska, *Catalytic oxidation of trichloroethylene in two-component mixtures with selected volatile organic compounds*. Catal. Today 73 (2002) 333-342.

[116] N. Burgos, M. Paulis, M.M. Antxustegi, M. Montes, *Deep oxidation of VOC mixtures with platinum supported on Al_2O_3/Al monoliths*. Appl. Catal. B-Environ. 38 (2002) 251-258.

[117] S. Irusta, M.P. Pina, M. Menéndez, J. Santamaría, *Catalytic Combustion of Volatile Organic Compounds over La-Based Perovskites*. J. Catal. 179 (1998) 400-412.

[118] F.N. Aguero, B.P. Barbero, L. Gambaro, L.E. Cadus, *Catalytic combustion of volatile organic compounds in binary mixtures over MnO_x/Al_2O_3 catalyst*. Appl. Catal. B-Environ. 91 (2009) 108-112.

[119] A. Musialik-Piotrowska, K. Syczewska, *Combustion of volatile organic compounds in two-component mixtures over monolithic perovskite catalysts*. Catal. Today 59 (2000) 269-278.

[120] V. Blasin-Aubé, J. Belkouch, L. Monceaux, *General study of catalytic oxidation of various VOCs over $La_{0.8}Sr_{0.2}MnO_{3+x}$ perovskite catalyst--influence of mixture*. Appl. Catal. B-Environ. 43 (2003) 175-186.

[121] I. Mazzarino, A.A. Barresi, *Catalytic combustion of voc mixtures in a monolithic reactor*. Catal. Today 17 (1993) 335-347.

[122] S. Ordóñez, L. Bello, H. Sastre, R. Rosal, F.V. Díez, *Kinetics of the deep oxidation of benzene, toluene, n-hexane and their binary mixtures over a platinum on γ-alumina catalyst*. Appl. Catal. B-Environ. 38 (2002) 139-149.

[123] R.W. van den Brink, P. Mulder, R. Louw, *Catalytic combustion of chlorobenzene on Pt/γ-Al_2O_3 in the presence of aliphatic hydrocarbons*. Catal. Today 54 (1999) 101-106.

[124] A.A. Barresi, G. Baldi, *Deep Catalytic Oxidation of Aromatic Hydrocarbon Mixtures: Reciprocal Inhibition Effects and Kinetics*. Ind. Eng. Chem. Res. 33 (1994) 2964-2974.

Part II

Catalyst Screening

In this chapter, several catalysts which were prepared and characterized in the context of Project CYTED PI0269 “Tratamiento de emisiones gaseosas industriales de disolventes para la protección ambiental“, were evaluated in the oxidation of ethyl acetate, ethanol and toluene. These screening tests represent the first step of a systematic investigation of catalysts (supported metal catalysts, base metal oxides and mixed oxides) for the oxidation of volatile organic compounds, and were necessary to select the most promising catalytic systems for further development.

2 Catalytic Oxidation of Volatile Organic Compounds: Catalyst Screening[1]

The oxidation of three organic compounds (ethanol, toluene and ethyl acetate) was studied over Pt/γ-Al_2O_3, Pt/TiO_2, K-OMS-2 (cryptomelane), Pt/K-OMS-2 and CuMn/Al_2O_3. The aim of this work is to select the catalytic systems for further studies.

It was observed that the catalytic performance is affected by the type of VOC. In the case of toluene oxidation, the supported noble metal catalysts were always more active than the metal oxides. Furthermore, K-OMS-2 was found to be more active than CuMn/Al_2O_3.

Generally, the most promising catalysts for the oxygenating organic compounds were Pt/TiO_2, Pt/K-OMS-2 and K-OMS-2.

Based on these results, Pt/TiO_2 and K-OMS-2 were selected for further studies.

2.1 Introduction

Volatile organic compounds (VOC) are an important class of air pollutants and cover a wide ranging class of compounds that differ in their properties and chemistry, but display similar behaviour in the atmosphere. Several abatement technologies have been developed to control the emissions of volatile organic compounds (VOC), including thermal oxidation, catalytic oxidation, adsorption, absorption and condensation [1, 2].

Catalytic oxidation is often considered an effective method for reducing the emissions of VOC from stationary sources. Indeed, the catalytic oxidation of VOC occurs at much lower temperatures than those needed for thermal oxidation, and it does not simply transfer the pollutant from the gas to the solid phase, as in adsorption processes.

[1] VP Santos, JJM Órfão, MFR Pereira, JL Figueiredo, *8º ENCMP*, Outubro 2007, Lamego, Portugal.

Several catalysts have been used for the total oxidation of VOC [3, 4] and it is generally agreed that noble metal supported catalysts are more active for the oxidation of non-oxygenating compounds. Platinum is also considered more active than palladium [5, 6] .

In spite of the extensive research in this area, the development of active catalytic systems still remains a challenge, and further advances have been reported recently in mixed oxides [7, 8], perovskites [9] and gold catalysts [10, 11].

The objective of the present chapter is to study the performance of several catalysts (supported noble metals, mixed oxides and base metal oxides) on the total oxidation of ethyl acetate, ethanol and toluene. The main goal is to select the most promising catalytic systems for further studies.

2.2. Experimental

The catalysts used in this work are summarized in Table 2.1. As can be seen, four supported platinum catalysts were used. Titania, alumina and cryptomelane were chosen as supports. The following sections describe their preparation and characterization.

2.2.1 Supports and catalysts preparation

Titania

The titania support was prepared by a sol gel method, via hydrolysis of titanium alkoxides, under reflux conditions [12]. The gel was aged in air for one week. The resulting xerogel was ground and dried at room temperature. The powder was calcined at 400 ºC for 2 h.

Alumina

Two different supports were used in this study. The first sample was obtained by a sol-gel procedure. The resulting colloidal solution was evaporated to dryness and the gel was calcined in air at 500 ºC for 2 h [13].
The second sample is a commercial product (Alumina Spheralite).

Cryptomelane

Cryptomelane-type manganese oxide (K-OMS-2) was synthesized using the reflux approach in acidic medium [14]. Briefly, 11 g of $Mn(CH_3COO)_2.4H_2O$ (Fluka, 99% purity) were dissolved in 40 mL of water, and the pH was kept constant using a buffer solution (KCH_3COO/CH_3COOH, Fluka, 99% purity). 6.5 g of $KMnO_4$ (Vaz Pereira, 99% purity) were dissolved in 150 mL of water, and this solution was slowly added to the previous one. The black precipitate formed was stirred and refluxed at 100 ºC for 24 h. The solid obtained was filtered and washed with distilled water, dried in an oven and calcined at 450 ºC in air for 4.5 h.

$CuMn/Al_2O_3$

$CuMnAl_2O_3$ was prepared by incipient wetness co-impregnation on alumina (Alumina Spheralite) support, previously dried at 120 ºC for 2 h, with aqueous solutions of $Mn(NO_3)_24H_2O$ and $Cu(NO_3)_2.3H_2O$. The Cu/Mn atomic ratio was 2. The total metal loading on alumina was 10%.The impregnated sample was dried at 120 ºC for 2 h, and calcined at 500 ºC for 4h [13].

Supported platinum catalysts

Platinum supported catalysts (Pt/Al_2O_3; Pt/TiO_2 and Pt/K-OMS-2) were prepared by incipient wetness impregnation using $Pt(NH_3)_4(OH)_2$ as metal precursor, (metal load: 1%). The resulting materials were dried at 110 ºC overnight and calcined at 500 ºC for 2 hours [13].

2.2.2 Catalysts characterization

All samples were characterized by X-ray diffraction (XRD) and nitrogen adsorption at -196 ºC. The metal dispersion was determined by hydrogen chemisorption at room temperature.

2.2.3. Catalytic Experiments

The catalytic oxidation of VOC was performed under atmospheric pressure in a fixed-bed reactor from Autoclave Engineers (BTRS Jr), which consists of a stainless steel tube of 6 mm internal diameter, placed inside a temperature-controlled electric furnace. The catalyst sample (130 mg) was supported in a small plug of glass wool in a vertical steel

tubular reactor. A feed gas with a VOC concentration of 2,000 ppmv and a flow-rate of 150 cm^3/min was used in standard tests. Prior to the reaction, the catalyst was activated under air at 400 ºC for 1 hour.

Conversions were measured over the range 160-350 ºC by incremental steps (10-20 ºC), the temperature being measured by a thermocouple placed in the middle of the catalyst bed. To ensure that steady state data were measured, the reactor was maintained at each temperature for 30 minutes. The conversion of VOC (X) and the conversion into CO_2 (X_{CO_2}) were respectively calculated as $X = 1 - \frac{F_{VOC}}{F_{VOC,in}}$ and $X_{CO_2} = \frac{F_{CO_2}}{\nu F_{VOC,in}}$, where F_{VOC} is the outlet molar flow rate of VOC at steady state, $F_{VOC,in}$ is the inlet molar flow rate of VOC, F_{CO_2} is the outlet molar flow rate of CO_2 at steady state and ν is the number of carbon atoms in the VOC molecule (for ethanol, ethyl acetate and toluene, ν = 2, 4 and 7, respectively).

The analytical system consisted of a gas chromatograph equipped with a flame ionization detector (FID) for the analysis of the organic compounds, and an online non-dispersive infrared (NDIR) analyzer for CO_2 detection and quantification.

2.3 Results and discussion

2.3.1. Characterization

Table 2.1 shows the main properties of the catalysts.

In the case of the supported metal catalysts, it seems that the acid-base properties of the support significantly influence the dispersion of Pt. For instance, highly dispersed noble metals (48%< D_M <72%) were obtained when γ–Al_2O_3 was used as support. Moreover, the source of γ–Al_2O_3 also affects the metal dispersion of Pt, which is higher in the case of the commercial one.

In the case of Pt/K-OMS-2 it was not possible to determine the metal dispersion, which may indicate that platinum atoms were not accessible on the surface.

Table 2.1 Properties of the catalysts: crystalline phase of the support (XRD), metal dispersion (hydrogen chemisorption), surface area and pore volume (nitrogen adsorption).

Catalyst	Phase (support)	D_M (%)	S_{BET} (m^2/g)	V_p (cm^3/g)
1%Pt/Al_2O_3 (A)	-	72	212	0.42
1%Pt/Al_2O_3 (B)	-	42	220	0.45
1%Pt/TiO_2	Anatase	28	67	0.42
K-OMS-2	KMn_8O_{16}	-	102	0.55
1%Pt/K-OMS-2	KMn_8O_{16}	-	80	0.45
10%CuMn/Al_2O_3	-	-	180	0.34

2.3.2. Catalytic performance

The catalytic performance of all samples was evaluated in the oxidation of ethyl acetate, toluene and ethanol. Figure 2.1 shows the results obtained.

As can be observed, the performance trend is a function of the type of VOC. In the oxidation of ethyl acetate (see Figure 2.1a), the following trend was observed: Pt/K-OMS-2 > Pt/TiO_2 > K-OMS-2 ≈ CuMn/Al_2O_3 > Pt/Al_2O_3 (A) ≈ Pt/Al_2O_3 (B). For instance, ethyl acetate is completely oxidised at 240 ºC with the Pt/K-OMS-2 catalyst, which is 40 ºC less than with the conventional Pt catalyst (Pt/Al_2O_3). Moreover, it seems that the metal dispersion does not have a major effect on the performance of Pt/Al_2O_3, since both catalysts (A and B) exhibit almost the same efficiency. These results show that the type of support used has a strong effect on the activity of the corresponding supported platinum catalysts.

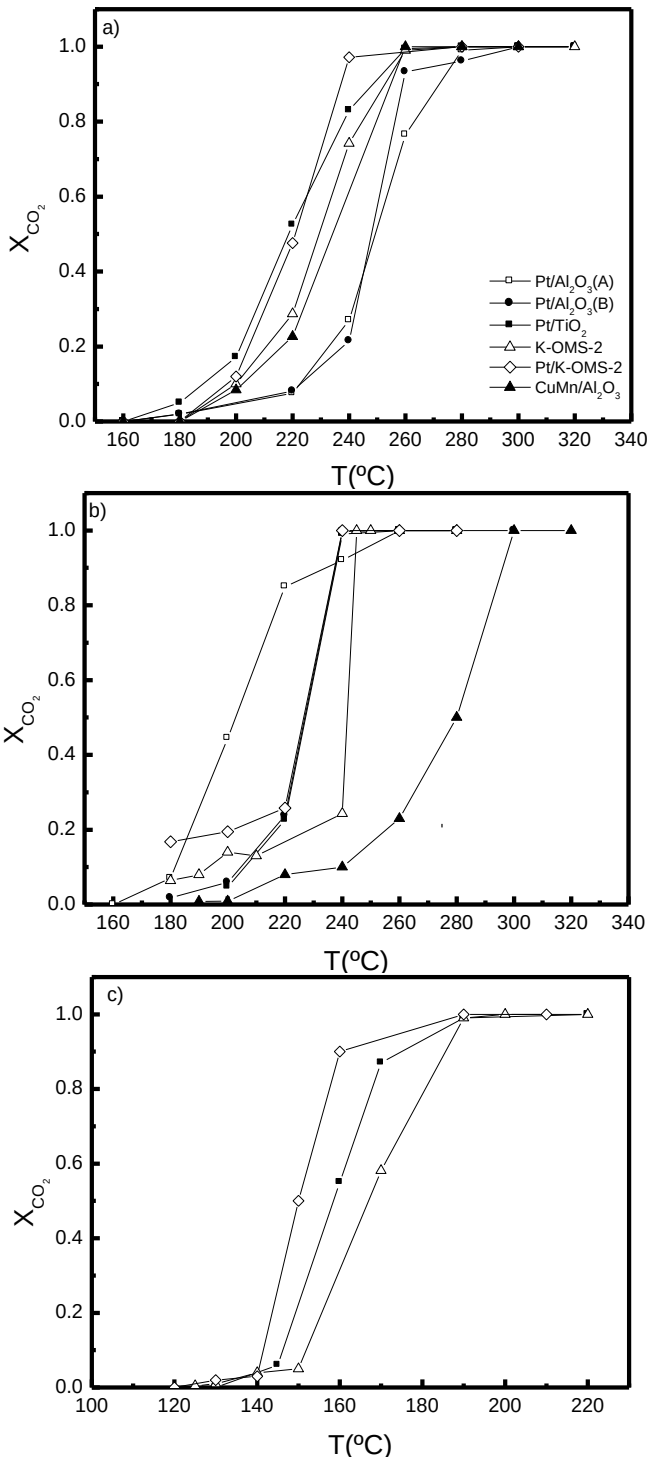

Figure 2.1 Light-off curves for: a) ethyl acetate, b) toluene and c) ethanol oxidation.

On the other hand, a different trend was observed for toluene oxidation (see Figure 2.1b), and the supported metal catalysts were always more active than the metal oxides (K-OMS-2 and $CuMn/Al_2O_3$). For instance, $CuMn/Al_2O_3$ was the worst catalyst of the group, while Pt/K-OMS-2 was the most active. By comparison, toluene is completely oxidized at 240 ºC in the presence of Pt/K-OMS-2, while the oxidation only occurs at 300 ºC over $CuMn/Al_2O_3$. Moreover, the metal dispersion seems to have a slight effect on the performance of the Pt/Al_2O_3 catalyst.

The oxidation of toluene over the K-OMS-2 catalyst shows an unstable behaviour under certain circumstances. Oscillations in the conversion into CO_2 were observed in a restrited temperatures range. These oscillations will be discussed in more detail in chapter 6.

The light-off curves corresponding to ethanol oxidation are shown in Figure 2.1c. In this case, K-OMS-2, Pt/K-OMS-2 and Pt/TiO_2 were the only catalysts tested. The catalytic trend observed is identical to that found in ethyl acetate oxidation, which may indicate that the oxidation mechanism is identical for both compounds. For instance, the conversion into CO_2 is about 50% in the presence of the Pt/K-OMS-2 catalyst at 150 ºC, and 5% over K-OMS-2.

2.4 Conclusions

The performance trend is a function of the type of VOC. For toluene oxidation, supported noble metals are more active than the metal oxides. For the oxidation of oxygenated compounds, Pt/TiO_2, Pt/K-OMS-2 and K-OMS-2 were found to be very active.

Based on these preliminary results, K-OMS-2 and Pt/TiO_2 were selected for further studies.

Acknowledgments

The author acknowledge the Project CYTED PI0269 “Tratamiento de emisiones gaseosas industriales de disolventes para la protección ambiental“.

References

[1] F.I. Khan, A. Kr. Ghoshal, *Removal of volatile organic compounds from polluted air*. J. Loss Prev. Process Ind. **13** (2000) 527-545.

[2] E.C. Moretti, *Reduce VOC and HAP emissions*. Chem. Eng. Prog. **98** (2002) 30-40.

[3] J.J. Spivey, *Complete catalytic-oxidation of volatile organics*. Ind. Eng. Chem. Res. **26** (1987) 2165-2180.

[4] W.B. Li, J.X. Wang, H. Gong, *Catalytic combustion of VOC on non-noble metal catalysts*. Catal. Today **148** (2009) 81-87.

[5] P. Papaefthimiou, T. Ioannides, X.E. Verykios, *Combustion of non-halogenated volatile organic compounds over group VIII metal catalysts*. Appl. Catal. B-Environ. **13** (1997) 175-184.

[6] T. Mitsui, T. Matsui, R. Kikuchi, K. Eguchi, *Low-temperature complete oxidation of ethyl acetate over CeO_2-supported precious metal catalysts*. Top. Catal. **52** (2009) 464-469.

[7] K. Everaert, J. Baeyens, *Catalytic combustion of volatile organic compounds*. J. Hazard. Mater. **109** (2004) 113-139.

[8] K. Jiratova, J. Mikulova, J. Klempa, T. Grygar, Z. Bastl, F. Kovanda, *Modification of Co-Mn-Al mixed oxide with potassium and its effect on deep oxidation of VOC*. Appl. Catal. A-Gen. **361** (2009) 106-116.

[9] B. Levasseur, S. Kaliaguine, *Effects of iron and cerium in $La_{1-y}Ce_yCo_{1-x}Fe_xO_3$ perovskites as catalysts for VOC oxidation*. Appl. Catal. B-Environ. **88** (2009) 305-314.

[10] R. Nedyalkova, L. Ilieva, M.C. Bernard, A.H.L. Goff, D. Andreeva, *Gold supported catalysts on titania and ceria, promoted by vanadia or molybdena for complete benzene oxidation*. Mater. Chem. Phys. **116** (2009) 214-218.

[11] S.M. Yang, D.M. Liu, S.Y. Liu, *Catalytic combustion of benzene over Au supported on ceria and vanadia promoted ceria*. Top. Catal. **47** (2008) 101-108.

[12] D. Bersani, G. Antonioli, P.P. Lottici, T. Lopez, *Raman study of nanosized titania prepared by sol-gel route*. J. Non-Cryst. Solids **232-234** (1998) 175-181.

[13] M. Montes, Acta de la reunión de coordinación 2006 del proyecto CYTED PI0269, México, 2006.

[14] J. Luo, Q. Zhang, A. Huang, S.L. Suib, *Total oxidation of volatile organic compounds with hydrophobic cryptomelane-type octahedral molecular sieves*. Micropor. Mesopor. Mat. **35-36** (2000) 209-217.

Part III

Catalytic Oxidation of Volatile Organic Compounds over Manganese Oxides

Manganese oxides have been extensively studied as catalytic materials in the oxidation of volatile organic compounds. Among them, cryptomelane (K-OMS-2) is considered a very interesting system, due to its open tunnel structure, mixed valence of manganese and high mobility of lattice oxygen.

The preparation, characterization and evaluation of manganese oxides in the oxidation of ethyl acetate, ethanol and toluene are described in the first two chapters of this section. A correlation between the redox properties and the activity of the manganese oxides was proposed and possible reaction mechanism were presented. Cryptomelane was considered one of the most active systems, and selected for further studies.

A cesium modified cryptomelane catalyst was successfully prepared and found to be highly effective in the oxidation of ethyl acetate. The influence of cesium on the catalytic properties of cryptomelane is described in the chapter 4.

The stability of cryptomelane in the oxidation of toluene is presented in chapter 5.

The oxidation of two-component mixtures in the presence of cryptomelane, is described in the final part of this section.

3 Synthesis and Characterization of Manganese Oxides for the Oxidation of Ethyl Acetate[1]

Manganese oxide catalysts were synthesized by direct reaction between manganese acetate and permanganate ions, under acidic and reflux conditions. Parameters such as pH (2.0-4.5) and *template cation* (Na^+, K^+ and Cs^+) were studied. A pure cryptomelane-type manganese oxide was synthesized under specific conditions, and it was found that the template cation plays an important role on the formation of this kind of structure. Cryptomelane was found to be a very active oxidation catalyst, converting ethyl acetate into CO_2 at low temperatures (220 ºC). This catalyst is very stable at least during 90 hours of reaction and its performance is not significantly affected by the presence of water vapour or CO_2 in the feed stream. The catalyst performance can be improved by the presence of small amounts of Mn_3O_4.

3.1 Introduction

In the past decade, manganese oxides have been intensively investigated due to their high economic value and potential applications in heterogeneous catalysis, in particular for oxidation processes [1-3]. Extensive research efforts have been devoted to the synthesis of this kind of material, the so called octahedral molecular sieves (OMS) with layer and tunnel structures [4-10]. The open frameworks of these materials are composed of edge and corner shared MnO_6 octahedra, the internal pores being occupied by cations and water molecules. Cryptomelane-type manganese oxide (K-OMS-2) is one group of the OMS family called hollandite, and has tunnel structures that consist of 2 x 2 arrays of MnO_6 octahedra [7, 11, 12]. Inside the tunnels, potassium cations and small amounts of water stabilize the structure, and can be partially ion-exchanged with other cations with appropriate sizes. The tunnel size is 0.46 nm x 0.46 nm and the average manganese oxidation state is around 3.8, which reflects a vast majority of Mn (IV) with lower amounts of Mn (III). The open tunnel

[1] VP Santos, MFR. Pereira, JJM Órfão, JL. Figueiredo, Top. Catal 52 (2009) 470.

structure and mixed valences of OMS-2 make this material very attractive for oxidation catalysis and, therefore, the synthesis of OMS-2 material with high purities, small particle size, high surface areas, and high yield has been a challenge in recent years. Various synthetic routes have been explored [13], including thermal and hydrothermal treatment of layered birnessite [14], redox precipitation under reflux [7, 15], microwave heating [16], sol-gel methods [17, 18] and a solvent free procedure [19]. The reflux method, involving the oxidation of Mn^{2+} by MnO_4^-, is the most common route. Reaction parameters, such as temperature, pH, concentration of reactants and template cation, are believed to bear a critical impact on the formation of cryptomelane. In spite of the intensive research that has been carried out in this area, the effect of these parameters on the crystallinity, stability and morphologies of OMS-2 material is not yet completely clear.

In this report we use the reflux approach to produce cryptomelane-type manganese oxides, by a direct reaction between manganese acetate and permanganate ions under acidic and reflux conditions. Parameters such as pH and template cation were studied. It is well known that during hydrothermal transformation, cations will stay in the tunnels to stabilize and support the tunnel structures. Therefore, it is expected that the template cation (such as cesium or sodium, alone or mixed with potassium), will have an important effect on the cryptomelane structure obtained. The shapes, crystal forms, average oxidation states and stabilities of these materials were evaluated. The catalytic performance of all materials was tested in the ethyl acetate oxidation.

3.2 Experimental

3.2.1 Synthesis

Manganese oxides were synthesized by the reflux method developed by Luo et al. [15]. 11 g of $Mn(CH_3COO)_2.4H_2O$ (Fluka, 99% purity) were dissolved in 40 mL of water. The pH of this solution was maintained using a buffer solution (KCH_3COO/CH_3COOH, Fluka, 99% purity) or concentrated nitric acid (Panreac, 65 %), in order to ensure different pH values (see Table 1). 6.5 g of $KMnO_4$ (Vaz Pereira, 99% purity) were dissolved in 150 mL of water, and this solution was slowly added to the previous one. The black precipitate formed was stirred and refluxed at 100 ºC for

24 h. The solid obtained was filtered and washed with distilled water, dried in an oven and calcined at 450 ºC in air for 4.5 h. To study the effect of the template cation on the products obtained, two procedures were used: in the first one $NaMnO_4$ or $CsMnO_4$ were used in the presence of the buffer solution and in the second nitric acid was used to control the pH (pH=4.5), as summarized in Table 3.1.

Table 3.1 Synthesis parameters of the prepared oxides.

Sample	Oxidant agent	pH control	Initial pH
Mn1	$KMnO_4$	CH_3COOH/KCH_3COO	4.5
Mn2	$KMnO_4$	HNO_3	3.5
Mn3	$KMnO_4$	HNO_3	3
Mn4	$KMnO_4$	HNO_3	2
Mn5	$NaMnO_4$	CH_3COOH/KCH_3COO	4.5
Mn6	$CsMnO_4$	CH_3COOH/KCH_3COO	4.5
Mn7	$NaMnO_4$	HNO_3	4.5
Mn8	$CsMnO_4$	HNO_3	4.5

3.2.2 Characterization

All samples were characterized by X-ray diffraction (XRD), X-ray photoelectron spectroscopy (XPS), scanning electron microscopy/energy dispersive X-ray spectroscopy (SEM/EDS), N_2 adsorption at 77 K, thermogravimetric analysis (TGA) and temperature programmed desorption (TPD).

3.2.2.1. Structure and morphology

The structure and phase purity of the prepared materials were analysed by X-ray diffraction using a PANalytical X´Pert PRO diffractometer with Cu K_α radiation source (λ=1.54 nm) and with a beam voltage of 50 kV and 40 mA of beam current. The data were collected in the 2θ range of 10º-100º with a scanning rate of 0.017 º/s. The morphology of the materials was studied by field emission scanning electron microscopy (FEG-ESEM) on a FEI Quanta 400FEG / EDAX Genesis X4M with a Schottky Emitter at an accelerating voltage of 10 kV.

3.2.2.2. Average oxidation state

The average oxidation state of manganese in all materials was obtained by XPS. XPS analysis was performed with a VG Scientific ESCALAB 200A spectrometer using Al K_α radiation (1486.6 eV). Charging effects were corrected by adjusting the binding energy of C 1s to 284.6 eV.

3.2.2.3. N_2 adsorption at 77 K

Nitrogen adsorption isotherms were obtained with a Quantachrome Instruments Nova 4200e. The samples were pre-degassed at 300 ºC for 3 h. Nitrogen was used as adsorbate at liquid nitrogen temperature.

3.2.2.4. Thermal stability

Thermogravimetric analysis (TGA) was done on a Mettler TA 4000 system under air or nitrogen atmospheres. About 10 mg of sample were loaded into a ceramic sample holder and the temperature was raised to 900ºC at 10 ºC/min. Thermal stability of the materials was also studied by temperature programmed desorption combined with a mass spectrometer (TPD-MS). These experiments were conducted on an Altamira Instruments (AMI 200) apparatus. 100 mg of the sample was loaded in the reactor and placed inside the furnace. The sample was purged with helium for 1 hour at room temperature followed by heating to 900 ºC at 5 ºC/min in the same atmosphere.

3.2.3 Catalytic experiments

The catalytic oxidation of VOC was performed under atmospheric pressure in a fixed-bed reactor from Autoclave Engineers (BTRS Jr), which consists of a stainless steel tube of 6 mm internal diameter, placed inside a temperature-controlled electric furnace. A feed gas with a VOC concentration of 4,000 mgC/m^3 and a space velocity of 16,000 h^{-1} was used in standard tests. The catalyst sample (50 mg) was diluted with glass spheres of the same size as the catalyst particles (0.2-0.5 mm), in order to minimize temperature gradients. Prior to the reaction the catalyst was activated under air at 400 ºC for 1 hour. A feed gas with 4,000 mgC/m^3 of ethyl acetate and a space velocity of 16,000 h^{-1} was used in the standard conditions. The space velocity quoted was defined in terms of the total bed volume (catalyst + inert).

The reaction temperature was raised from 160 to 260 ºC by steps of 10 ºC. The reactor was maintained at each temperature for 30 minutes in order to obtain experimental values at steady state. The ethyl acetate conversion (X) and the conversion into CO_2 (X_{CO_2}) were respectively calculated as $X = 1 - \frac{F_{VOC}}{F_{VOC,in}}$ and $X_{CO_2} = \frac{F_{CO_2}}{\nu F_{VOC,in}}$, where F_{VOC} is the outlet molar flow rate of VOC at steady state, $F_{VOC,in}$ is the inlet molar flow rate of VOC, F_{CO_2} is the outlet molar flow rate of CO_2 at steady state and ν is the number of carbon atoms in the VOC molecule (for ethyl acetate, $\nu = 4$).

The analytical system consisted of a gas chromatograph equipped with a flame ionization detector (FID) for the analysis of the organic compounds, and an online non-dispersive infrared (NDIR) analyzer for CO_2 detection and quantification.

3.3 Results and discussion

3.3.1 Characterization

3.3.1.1 Structure and morphology

Cryptomelane is synthesized by the reaction between Mn^{2+} and MnO_4^- in acid medium, in which an amorphous phase of manganese oxide is formed according to the equation:

$$2MnO_4^- + 3Mn^{2+} + 2H_2O \rightarrow 5MnO_2 + 4H^+ \quad (3.1)$$

Subsequently, the mixture is maintained in reflux during 24 h at 100 ºC to obtain the nanostructured oxide.This synthesis mainly depends on three factors: temperature, pH and the template cation. In order to understand the effect of pH and template cation on OMS-2 formation, three types of procedures were used (see Table 3.1). In the first one, $KMnO_4$ was used as oxidant, and the initial pH was adjusted at 3.5, 3.0 and 2.0 using nitric acid, and 4.5 using a buffer solution of KCH_3COO/CH_3COOH. In the second and third procedures, $NaMnO_4$ or $CsMnO_4$ were used as oxidants, and the pH was adjusted by using the same buffer solution, or nitric acid, respectively (in the last case, there was no source of potassium).

XRD allowed to study the effect of pH and template cation on the crystallization process of OMS-2 (see Figure 3.1). Figure 3.1a shows the XRD patterns for all

materials prepared with $KMnO_4$. All positions of the diffractions lines in the XRD patterns of OMS-2 materials produced at pH 4.5, 3.5 and 3.0 are in good agreement with the standard pattern of the pure tetragonal cryptomelane Q-phase with lattice parameters a=b=0.9917 nm and c=0.22738 nm (KMn_8O_{16}, JCPDS 42-1348), although the relative intensities do not exactly match the theoretical data. This fact may result from defects in the lattice (primarily O defects), small crystal size, preferential ordering (anisotropic crystallite morphology) or different quantities of potassium cations [6]. At the lowest pH, α-Mn_2O_3 was detected as impurity. Additionally, it may be observed that the widths of the peaks of OMS-2 materials produced with nitric acid are larger than those produced with the buffer solution, which indicates small crystallite sizes. The calculation of the crystallite sizes from Scherrer's equation at 2θ = 37.5 and 2θ = 28.7 suggest a range between 30 and 16 nm.

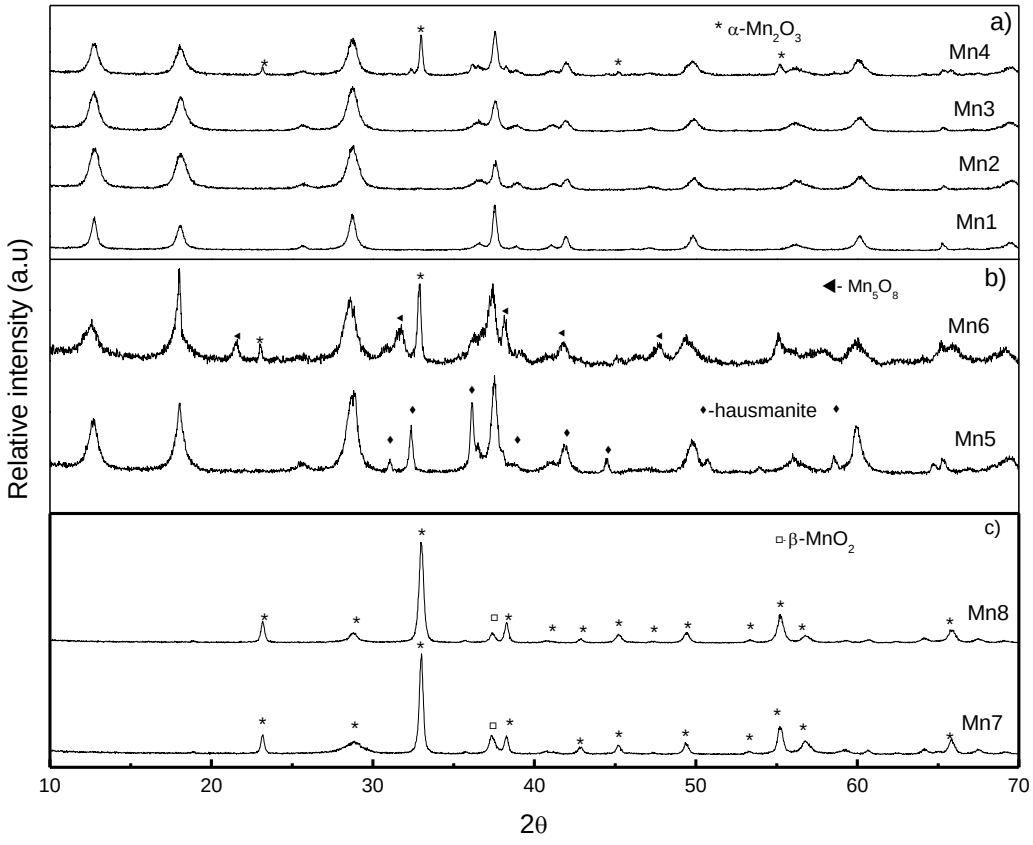

Figure 3.1 XRD spectra of the synthesized materials: a) Mn1 to Mn4; b) Mn5 to Mn6; c) Mn7 to Mn8. The samples are identified in Table 3.1.

Figures 3.1b and 3.1c show the effect of the template cation on the structure of manganese oxide materials. When $KMnO_4$ was replaced by $NaMnO_4$ or $CsMnO_4$, using the buffer solution to control the pH (source of potassium cations in the medium), no pure cryptomelane phase was observed. In the first case (Mn5), small amounts of Mn_3O_4 were detected, while in the second case (Mn6) a more complex spectrum was obtained: α-Mn_2O_3 was identified as the major impurity and residual amounts of Mn_5O_8 might be present. When potassium cations were completely removed from the reactant mixture (Figure 3.1c), no cryptomelane structure was attained, but instead a mixture of α-Mn_2O_3 and β–MnO_2 (small amounts). This result shows that potassium cations in the reactant medium play an important role for the formation of the tunnel structure and the incorporation of monovalent cations such as Na^+ and Cs^+ in the manganese structure was unsuccessful. Table 3.2 summarises these results.

Table 3.2 Manganese oxides detected by XRD in the prepared samples.

Sample	pH	Dopant cation	K/Mn	X/Mn	Product
Mn1	4.5	K^+	2:1	-	KMn_8O_{16}
Mn2	3.5	K^+	1:1	-	KMn_8O_{16}
Mn3	3.0	K^+	1:1	-	KMn_8O_{16}
Mn4	2.0	K^+	1:1	-	KMn_8O_{16}; α-Mn_2O_3
Mn5	4.5	K^+, Na^+	1.1:1	0.91:1	KMn_8O_{16}; Mn_3O_4
Mn6	4.5	K^+, Cs^+	1.1:1	0.91:1	KMn_8O_{16}, α-Mn_2O_3, (Mn_5O_8)
Mn7	4.5	Na^+	-	0.91:1	α-Mn_2O_3, β-MnO_2
Mn8	4.5	Cs^+	-	0.91:1	α-Mn_2O_3, β-MnO_2

Figure 3.2 shows SEM micrographs of the prepared materials. Fibers or needle-like particles, typical of cryptomelane [11, 20], are observed in samples synthesized under different pH with $KMnO_4$ (samples Mn1 to Mn4). In all cases considered, the nanofibers have very long lengths that vary from a few hundred nanometers to a few micrometers, and widths in the middle varying from 10 to 30 nm, characteristic of the method used [19]. However, it seems that the materials prepared with nitric acid have small fiber widths compared with the buffer solution, which is consistent with the XRD results. EDS analysis confirms the presence of K, Mn and O and there is a gradual decrease in the K/Mn ratio as the pH decreases, except for the lowest pH as can be seen in Table 3.3. The atomic ratios of potassium to manganese cations on the surface are relatively lower than the ideal ratio of K/Mn (0.25) in cryptomelane [11], which may indicate the presence of more vacancies in octahedral sites of manganese.

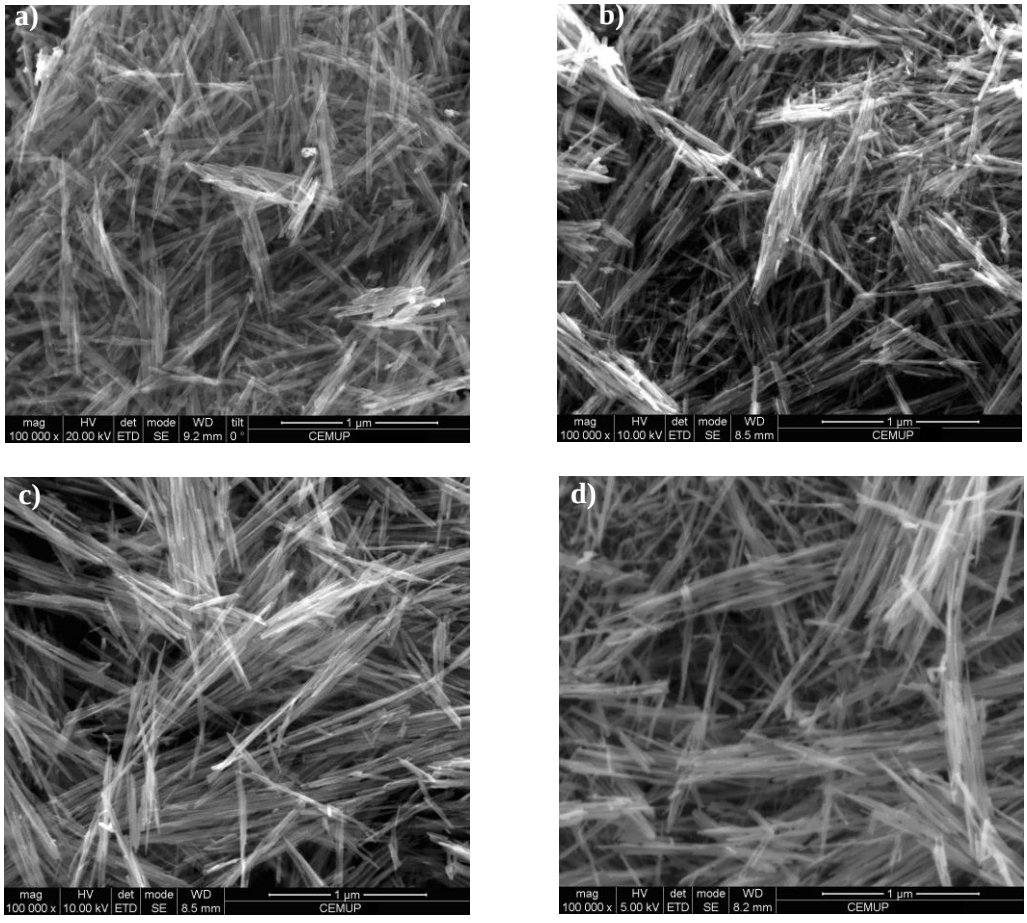

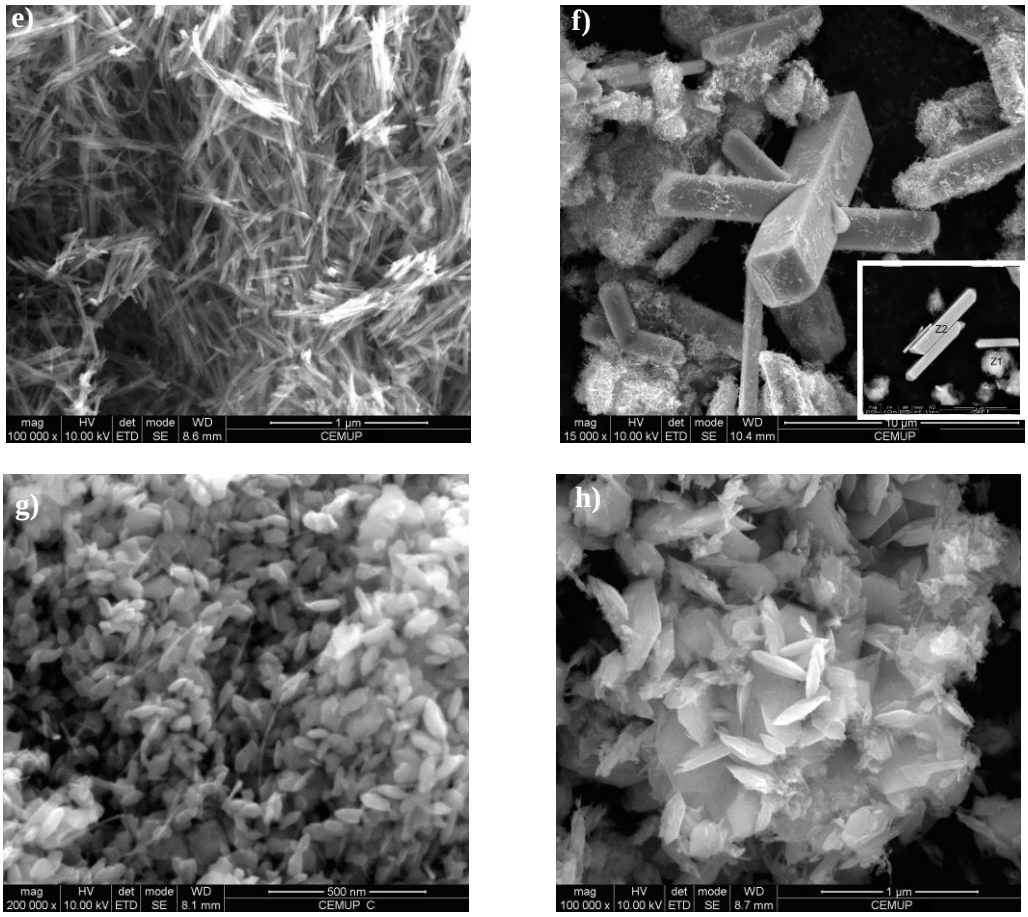

Figure 3.2 FESEM images of the materials: a) Mn1, b) Mn2, c) Mn3, d) Mn4, e) Mn5 f) Mn6 g) Mn7, h) Mn8.

Figure 3.2e shows that the replacement of $KMnO_4$ for $NaMnO_4$ does not promote a significant change in morphology, while the use of $CsMnO_4$ creates two different microstructures (Figure 3.2f): the first one corresponds to cryptomelane with the typical nanofibrous appearance and the second is MnO_x which has a quadrangular prism shape. In order to confirm the composition of the two single phases, EDS experiments were performed in zones identified by Z1 and Z2 (Figure 3.2f inset). Z2

contains only Mn and O, while the Z1 zone contains K, Mn and O, which supports the presence of MnO_x and cryptomelane, respectively.

Figure 3.2g and 3.2h show that a MnO_x structure was formed in the absence of potassium cations, with a shape that depends on the kind of template cation present. When $CsMnO_4$ was used, a typical sheetlike morphology and, to a lower extent, thin fibers, were obtained. Similar morphologies were reported when refluxing the aqueous solution containing $Mn(ClO_4)_2$, $(C_2H_5)_4NOH$, and $CsMnO_4$ at 100 ºC for 11 days [21]. In the case of $NaMnO_4$, irregularly shaped globules and thin fibers were obtained. The presence of Mn and O was confirmed by EDS analysis in both samples.

3.3.1.2 Manganese valence

The average oxidation state of manganese (AOS) in all samples was obtained by XPS. Table 3.3 displays the binding energies of Mn $2p_{1/2}$ and Mn $2p_{3/2}$. As can be seen, those values do not change significantly. It is well known that Mn(II), Mn(III) and Mn(IV) have essentially the same binding energy in the perovskite sample, so it is difficult to identify the oxidation state only by the binding energy shift of Mn 2p [22]. Galakhov et al. [23] proposed that the XPS of Mn 3s is more promising for identifying the manganese oxidation state. Mn 3s exhibits an exchange splitting in its X-ray photoelectron spectrum, promoted by the exchange coupling between the 3s holes and the 3d electrons [23, 24]. The magnitude of the 3s splitting is proportional to (2S+1) where S is the value of the local spin of the 3d electrons in the ground state. Since the splitting depends on the d configuration, the manganese valency can be estimated.

According to this and to the relationship between ΔEs and the average oxidation state (AOS) reported by Galakhov et al. [23], the AOS of all materials were calculated using the following equation:

$$AOS = 8.956 - 1.126\ \Delta E_s\,(eV). \qquad (3.1)$$

Table 3.3 shows that all cryptomelane materials prepared at pH 4.5, 3.5 and 3.0 have an AOS between 3.8 and 3.9, which is in agreement with the mixed state of manganese in the framework of cryptomelane (coexistence of Mn(IV) and a minor amount of Mn(III)) [6, 19]. The AOS of cryptomelane obtained at pH 2.0 is lower, due to the presence of the α-Mn_2O_3 phase, increasing the amount of Mn(III) species. These

results support the XRD analysis. The manganese AOS of the other samples are similar (values between 3.72 and 3.78), due to the presence of Mn(IV) and Mn(III) species (in the case of the Mn5 sample, Mn(IV), Mn(III) and Mn(II)).

3.3.1.3 BET surface area

The BET surface areas of manganese oxides prepared with different pH and template cation are listed in Table 3. As can be seen, the manganese oxide materials have surface areas that range from 25 to 84 m^2/g. However, we must refer that N_2 adsorption at 77 K is not suitable for the characterization of the micropores in this kind of tunnel structured manganese oxides [25]. There is no apparent correlation between the pH and the surface areas obtained. The highest surface area was obtained for the Mn5 sample, which has the cryptomelane structure and small amounts of Mn_3O_4.

Table 3.3 Catalyst characterization by XPS, EDS and nitrogen adsorption

Sample	E [Mn 2p] (eV)		ΔE_s[Mn3s]	AOS	K/Mn (atomic ratio)		S_{BET}
	$2p_{1/2}$	$2p_{3/2}$	(eV)		bulk	surface	(m^2/g)
Mn1	642.2	653.8	4.50	+3.89	0.13	0.21	45
Mn2	642.3	653.9	4.50	+3.89	0.11	0.17	71
Mn3	642.2	653.9	4.56	+3.82	0.09	0.14	65
Mn4	642.3	653.9	4.63	+3.74	0.11	0.17	45
Mn5	642.1	653.9	4.65	+3.72	0.14	0.23	84
Mn6	642.1	653.8	4.63	+3.74	0.10	0.14	59
Mn7	642.0	653.6	4.60	+3.78	0	0	46
Mn8	641.9	653.6	4.64	+3.73	0	0	25

3.3.1.4 Thermal stability

The thermal stability of manganese oxides was studied by TGA in air and nitrogen atmospheres (Figure 3.3) and TPD in a helium atmosphere (Figure 3.4). From TGA experiments, it can be seen that for all materials the weight loss under air is lower than

in nitrogen atmosphere, due to the reduction of manganese species. Comparing the thermal stability of Mn1, Mn2, Mn3 and Mn4 samples, it seems that the pH used in the synthesis does not affect significantly the TGA profile of the samples (total weight loss ≈ 10-12%). Figure 3.3 shows that cryptomelane materials have three zones of weight loss under nitrogen. The first occurs at temperatures lower than 200 ºC (0.7-1.4%) and is due to the release of water physically adsorbed on the surface of the material, which is consistent with the H_2O profile in TPD (Figure 3.4). The amount of water adsorbed is very low, which supports the hydrophobic character of cryptomelane [12]. The second weight loss zone occurs in the range 200-550 ºC (1.9-3.4%), and is due to the evolution of chemically adsorbed water and oxygen species from the material (mainly oxygen near the surface) [26]. The last weight loss has been attributed to the evolution of structural oxygen in the framework of the tunnels and occurs in the temperature range 550-900 ºC (≈ 6.7-8.1%). At temperatures higher than 500 ºC and under nitrogen atmosphere, the oxygen released from cryptomelane usually leads to the formation of oxygen deficient products such as Mn_2O_3 (≈ 600 ºC) and Mn_3O_4 (≈ 750-800 ºC), and consequently the collapse of the tunnel structure [27]. In summary, the following weight losses were observed: Mn1 (11.4%) > Mn3 (10.9%) > Mn2 (10.3%) > Mn4 (10.0%). These results were expected, since the AOS and the amount of oxygen released are related with each other; justifying the highest and the lowest weight losses observed with Mn1 and Mn4, respectively.

The TGA profiles of the Mn5, Mn6, Mn7 and Mn8 samples are also shown in Figure 3.3 The thermal behaviour of Mn5 and Mn6 under nitrogen atmosphere is similar to that of the Mn1 - Mn4 samples, although the weight loss is relatively lower (8.1 and 8.5%, respectively) due to the lower average oxidation state. Mn7 and Mn8 also show a smaller weight loss in comparison to Mn1 - Mn4, and a gradual weight loss till 700 ºC was observed, where all the Mn(III) species are reduced to a lower oxidation state.

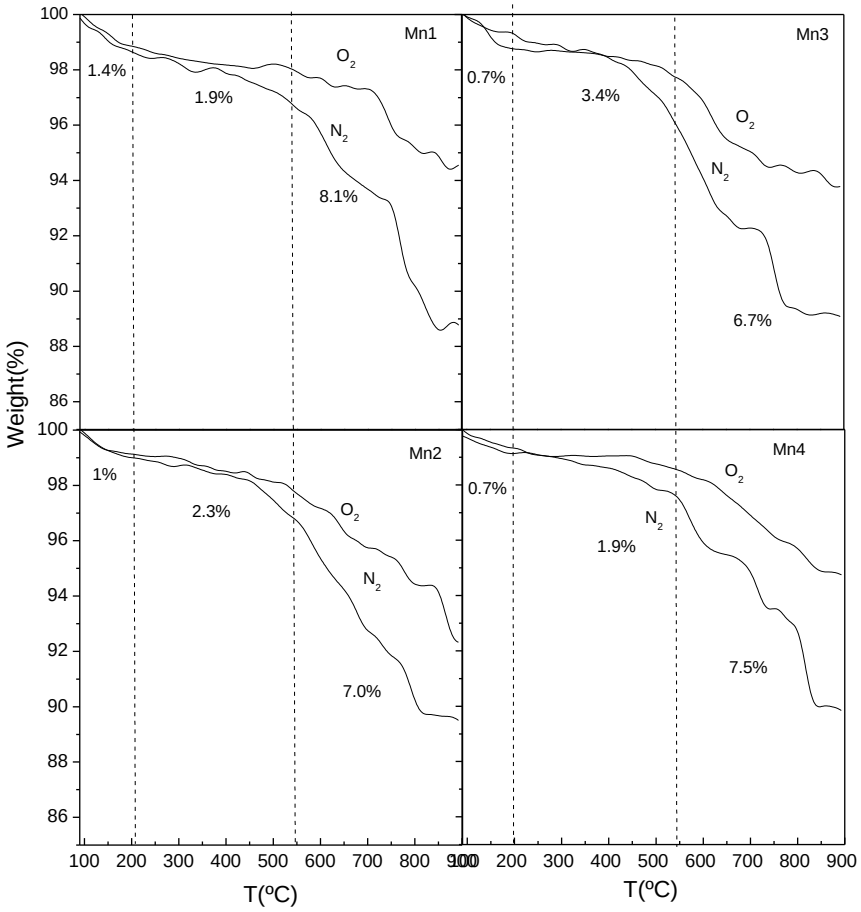
Mn1
Mn3
Mn2
Mn4
O2
N2
1.4%
1.9%
8.1%
0.7%
3.4%
6.7%
1%
2.3%
7.0%
0.7%
1.9%
7.5%
Weight(%)
T(ºC)
T(ºC)

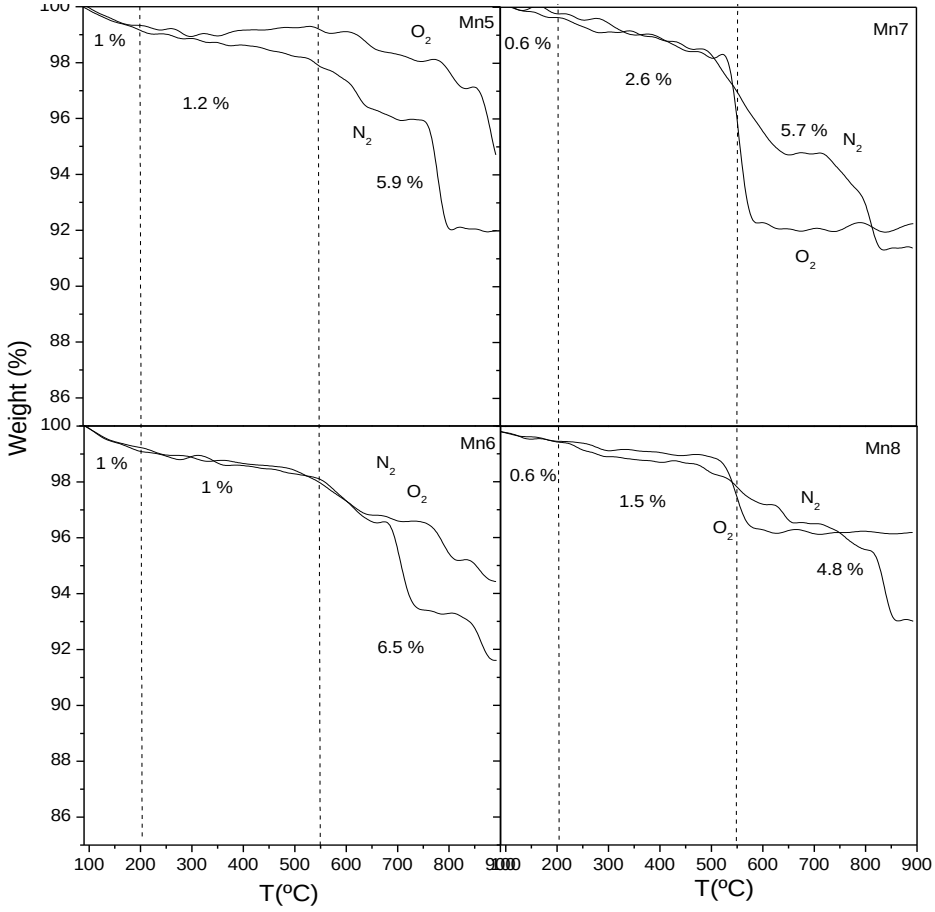

Figure 3.3 TGA experiments under nitrogen and air atmospheres. Heating rate: 10 ºC/min.

The oxygen spectra obtained by TPD are consistent with the TGA results. As can be seen in Figure 3.4a, the spectra of Mn1-Mn4 show three peaks: one broad peak in the range 450-550 ºC, and two intense and sharp peaks around 600 ºC and 800 ºC. Yin et al. [26, 28] have studied the oxygen species in tunnel structured manganese oxides and they suggest that there are three types of oxygen species corresponding to oxygen released in lower temperature regions (LT 250-400 ºC), intermediate regions (MT 400-650 ºC) and higher temperature regions (HT higher than 650 ºC). The α-species

(LT peak) was assigned to chemisorbed oxygen species. The β and γ (MT and HT peaks, respectively) species were believed to be due to different structural oxygen species bound to manganese cations: lower manganese valency, and Mn(IV), respectively. Accordingly, it can be seen that in all samples most of the oxygen species can be ascribed to structural oxygen. The evolution of oxygen from the samples prepared at different pH is quite similar, except in the case of lowest pH where the MT peak shifts to lower temperatures. This behaviour indicates that this sample has different Mn-O bond strengths.

Figure 3.4b shows the TPD spectra of Mn5, Mn6, Mn7 and Mn8. The Mn5 sample shows a small peak at medium temperatures and an intense peak at higher temperatures. The Mn6 sample shows three peaks in the temperature range of 400-900 ºC, which indicate three different strengths of Mn-O bonds associated to different manganese valence. Mn7 and Mn8 show only two strong peaks at 525-550 ºC and 850 ºC, suggesting two different strengths of Mn-O bonds. This is supported by XRD analysis, which shows the presence of Mn(III) and Mn(IV) species.

During TPD analysis, traces of CO_2 have been detected. Two main broad peaks at 250 ºC and 600 ºC were observed, suggesting that CO_2 molecules are adsorbed on different sites.

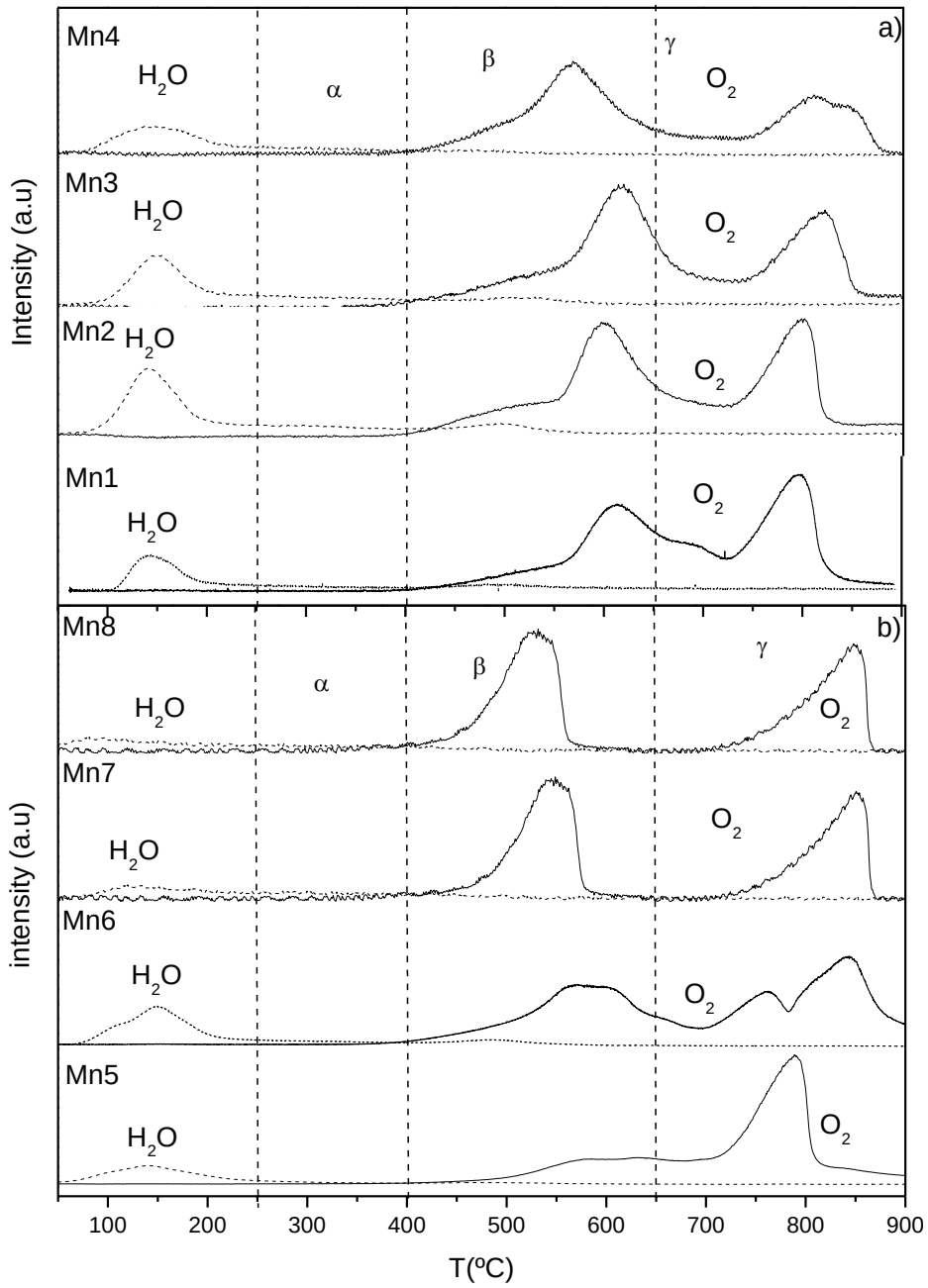

Figure 3.4 TPD of O_2 and H_2O of all materials synthesized: a) Mn1 to Mn4; b) Mn5 to Mn8. Heating rate: 5 ºC/min.

3.3.2 Catalytic activities

The catalytic activities of all materials for the total oxidation of ethyl acetate were evaluated. This study was carried out in order to determine the effect of the physical and chemical properties of the materials, such as structure, surface area and manganese average oxidation state.

The light-off curves of ethyl acetate on the manganese based catalysts are shown in Figure 3.5. As can be seen in Figures 3.5a and 3.5b, no significant change in the catalytic behaviour was observed when the pH used in the preparation was varied from 3.5 to 4.5 and complete oxidation into CO_2 occurs at 215-220 ºC. With the Mn3 sample, the catalytic activity is slightly lower at low temperatures (200-215 ºC), but complete oxidation to CO_2 occurs at almost the same temperature. The sample prepared at the lowest pH (sample Mn4) presents a significantly lower activity, since the temperature for complete oxidation into CO_2 is approximately 20 ºC higher than with the other materials. The main by-product detected in all these experiments is acetaldehyde.

According to these results, it can be stated that the catalytic activity of these materials cannot be correlated with the surfaces areas (see Table 3.3), as Mn1 has practically the same activity as Mn2 and Mn3, in spite of their different surface areas. Therefore, it is probable that the catalytic activity may be related to the structure and the manganese species on the catalyst surface (and consequently with the AOS).

This assumption seems reasonable because it has been suggested that the oxidation of organic molecules with manganese oxide catalysts at low temperatures may involve a Mars and van Krevelen (MVK) mechanism which includes a redox cycle on the catalyst surface with the participation of the lattice oxygen from the oxide [25,29,30]. Following the MVK concept, it could thus be predicted that oxides with the highest oxidation state would have the highest oxidation activities, because they have more oxygen atoms that can be used for the VOC oxidation. However, the activity of an oxide is also related to the energy needed to transfer their lattice oxygen atoms to the hydrocarbon, as this energy depends on the global oxidation state of the catalyst. Therefore, the most efficient catalyst for promoting oxidation reactions might not be the fully oxidised one.

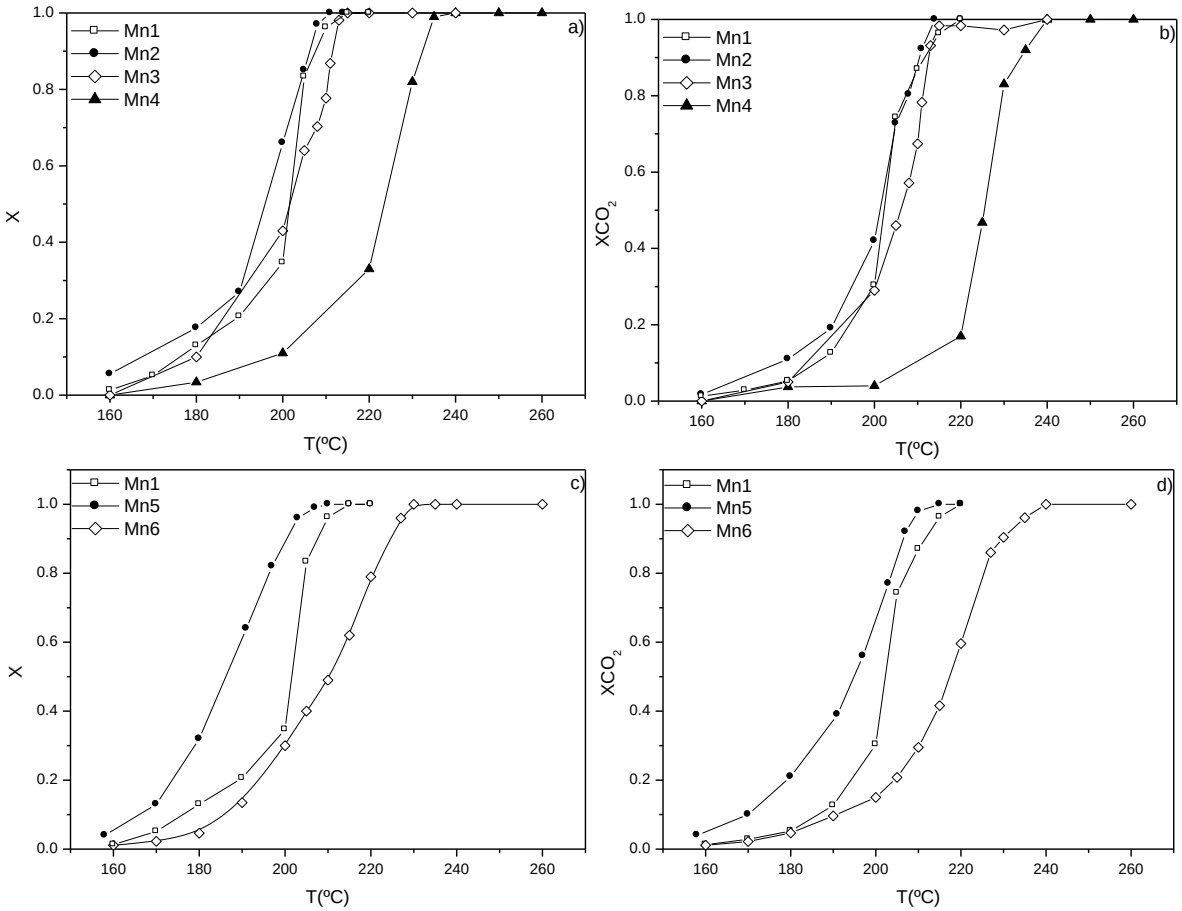
a)
Mn1
Mn2
Mn3
Mn4
X
T(ºC)
b)
Mn1
Mn2
Mn3
Mn4
XCO2
T(ºC)
c)
Mn1
Mn5
Mn6
X
T(ºC)
d)
Mn1
Mn5
Mn6
XCO2
T(ºC)

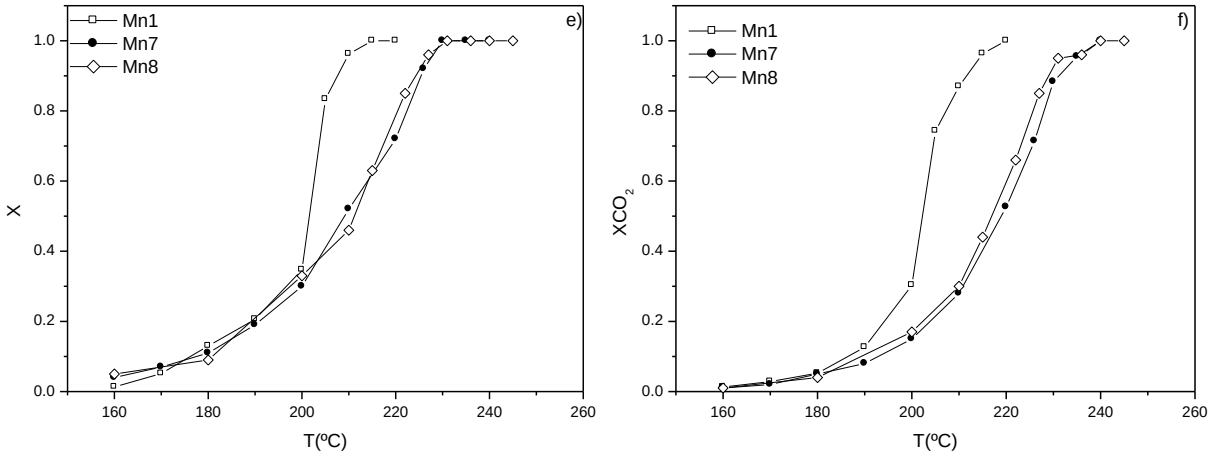

Figure 3.5 Performance of manganese oxide catalysts on the total oxidation of ethyl acetate.

It can be observed from Table 3.3 that AOS and catalytic activities are correlated with each other. Indeed, samples Mn1 and Mn2, with the highest AOS, are the most active, followed by sample Mn3, with a lower AOS. Sample Mn4 has the lowest AOS and is much less active; however, in this case, we do not have a pure cryptomelane phase (see Table 3.2). Xia et al. [31] have also observed that the performances of Cu-OMS-2, Co-OMS-2 and Ag-OMS-2 catalysts for the oxidation of CO were also related to the manganese average oxidation state.

Figures 3.5c and 3.5d show the light-off curves for Mn1, Mn5 and Mn6 samples. The following activity sequence was obtained: Mn5 (100% X_{CO2} at 215 ºC) > Mn1 (100% X_{CO2} at 220 ºC) > Mn6 (100% X_{CO2} at 240 ºC). This activity sequence was not expected since the manganese average oxidation state of Mn5 is lower than of Mn1. However, the catalytic performance of the Mn5 sample may be correlated with the presence of small amounts of Mn_3O_4, detected by XRD analysis. Therefore, the presence of the manganese redox pair Mn(II)/Mn(III) in Mn_3O_4 should improve the performance of the catalyst. In fact, the presence of Mn(II) species can make this catalyst more active, as it can exchange oxygen more easily (the Mn(II)-O bond is weaker, which leads to the formation of more active oxygen species) [32]. Chen et al. [33] also observed this effect in the decomposition of 2-propanol over a series of metal doped OMS-2 materials. They observed that during the reaction over Cu-OMS-2 there was a gradual phase transition from cryptomelane to Mn_3O_4, and the presence of the two phases improved the performance of the catalyst.

The manganese oxidation state of the Mn6 sample is quite similar to that of Mn4, and the complete oxidation of ethyl acetate occurs at the same temperature. At low temperatures, this catalyst has an activity a little higher than the Mn4 sample. The catalytic activities of Mn7 and Mn8 are similar to the Mn6 sample, in spite of their different surface areas, promoting the complete oxidation of ethyl acetate into CO_2 at 240 ºC (Figure 3.5e and 3.5f).

These results show that cryptomelane type manganese oxides are very active and selective. The Mn1 sample was selected for further studies.

3.3.3 Stability tests

In order to analyse the stability of the catalyst, long duration experiments were made on the Mn1 sample. The conversion into CO_2 at 210ºC as a function of time on stream (TOS) is shown in Figure 3.6. The reaction temperature was selected in order to achieve a high initial ethyl acetate conversion (about 96 %). After a period of about 20 hours, the conversion reached an almost constant value. The conversion history during the first 2.5 hours is similar to those obtained by the light-off curves; the presence of an initial stabilization period has been reported for the catalytic oxidation of ethyl acetate, n-hexane and benzene on γ-MnO_2 [34] . It can be considered that the stabilization period of about 16 hours represents the time needed to obtain a constant coverage of the catalyst surface by the reactants and products, especially water [24]. The slight activity decrease which occurs during this period was attributed to a competition of the reactants and water for specific sites [35]. Other authors explain this deactivation by the accumulation of heavy products on the surface, blocking the active sites [36]. In order to understand the activity decay in our system (9.6%), TPO experiments were made after stopping the reaction at different TOS. The total amount of coke does not increase with TOS, its value being very low (0.05% wt), as can be seen in Table 3.4. In order to confirm this result, another stability test was made at lower temperature (180 ºC), and TPO experiments were carried out after 1 and 20 h of the reaction. Similar results were obtained (see Table 3.4), ie, coke does not accumulate on the catalyst.

Table 3.4 Amount of coke on the Mn1 sample as a function of time on stream (TOS).

T (ºC)	TOS (h)	g coque/100 gcat
210	1	0.05
210	90	0.05
180	1	0.27
180	20	0.29

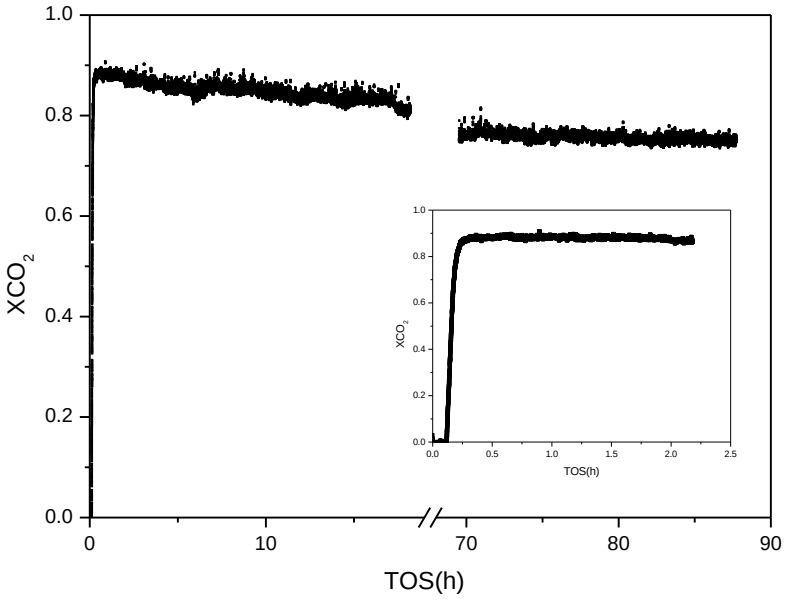

Figure 3.6 Evolution of the conversion into CO_2 with time on stream on the Mn1 sample at 210 ºC.

3.3.4 Influence of water vapour or CO_2 in the feed stream

The performance of catalyst Mn1 was also tested in the standard conditions with water vapour or CO_2 added to the inlet stream. In industrial applications, humidity and CO_2 will be present in the effluents to be treated, so it is important to know the performance of cryptomelane in these conditions. Therefore, 2% of water vapour or 2 % of CO_2 were individually introduced in the feed. The light-off curves are compared in Figure 3.7. In the presence of 2% of H_2O, there is no significant difference in the temperature for total oxidation of ethyl acetate, but at lower temperatures slightly lower conversions were observed. This behaviour is quite different from supported platinum catalysts (namely Pt/TiO_2), where the presence of water vapour increases the global conversion but decreases the CO_2 yield [34]. At 210 ºC, the conversion into CO_2 changes from 0.85 to 0.65 in the presence of water vapour. Nevertheless, this catalyst can still oxidise completely ethyl acetate into CO_2 at the same temperature of 220 ºC. In order to understand this behaviour, TPO experiments were conducted at 180 ºC in the presence and in the absence of water vapour. It was observed that there

were no significant differences in the coke content. In addition to the results described above, the behaviour of catalyst Mn1 in the presence of 2% CO_2 was also investigated. As can be seen in Figure 3.7, no significant effect was observed when CO_2 was present, in the temperature range studied. This behaviour shows that there is no competition between the reactants and CO_2 for the active sites involved in the reaction mechanism.

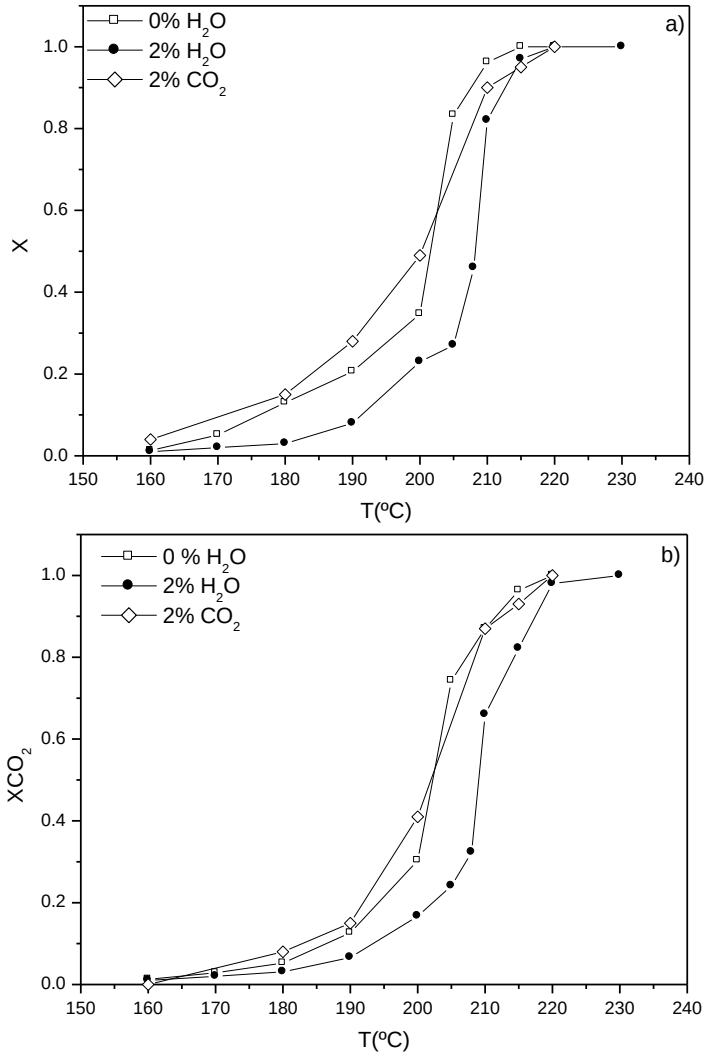

Figure 3.7 Influence of water vapour or CO_2 on the performance of the cryptomelane catalyst (Mn1 sample): a) ethyl acetate conversion; b) conversion into CO_2.

3.4 Conclusions

Cryptomelane type manganese oxide was synthesized using a reflux method. The synthesis parameters studied were the acidity of the solution and the template cation.

At very low pH (pH=2) no pure cryptomelane phase was obtained, but instead a mixture of α-Mn_2O_3 and cryptomelane. In the pH range 4.5-3.0 a pure cryptomelane phase was produced, and there are no significant differences between the use of buffer solution or nitric acid for pH control, except in the fibers width.

During the reflux treatment the presence of potassium cations is necessary to support and stabilize the tunnel structure of cryptomelane. When no source of potassium cations was used in the reactant mixture, no cryptomelane phase was obtained, but instead a mixture of β-MnO_2 and α-Mn_2O_3. The morphology of the materials depends on the source of permanganate.

All the manganese oxides synthesised in this study were active for the total oxidation of ethyl acetate into CO_2. All the catalysts oxidize ethyl acetate into CO_2 at temperatures below 250 ºC.

The activity of the catalysts seems to be correlated mainly with the average oxidation state of the manganese oxides.

The highest activity was obtained for the cryptomelane-type manganese oxide catalyst. Small amounts of Mn_3O_4 increase the performance of this catalyst.

Long duration experiments show that there is a slight deactivation of the catalyst in the first 20 hours of reaction, being stable afterwards. This deactivation is not due to the accumulation of coke.

The presence of water vapour and CO_2 in the feed does not have a major influence on the performance of cryptomelane for the total oxidation of ethyl acetate conversion, although the catalytic performance is slightly affected at low temperatures in the presence of water vapour.

References

[1] J.E. Post, *Improvement of the hydrothermal stability of fluorinated MCM-41 material.* Proc. Natl. Acad. Sci. U. S. A. 96 (1999) 3447.

[2] S.L. Suib, *Microporous manganese oxides.* Curr. Opin. Solid State Mat. Sci. 3 (1998) 63.

[3] S.L. Brock, N.G. Duan, Z.R. Tian, O. Giraldo, H. Zhou and S.L. Suib, A *review of porous manganese oxide materials*. Chem. Mat. 10 (1998) 2619.

[4] Y.F. Shen, R.P. Zerger, R.N. Deguzman, S.L. Suib, L. McCurdy, D.I. Potter and C.L. Oyoung, *Manganese oxide octahedral molecular-sieves - preparation, characterization, and applications*. Science 260 (1993) 511.

[5] D. Frias, S. Nousir, I. Barrio, M. Montes, T. Lopez, M.A. Centeno and J.A. Odriozola, *Synthesis and characterization of cryptomelane- and birnessite-type oxides: Precursor effect*. Mater. Charact. 58 (2007) 776.

[6] R.N. DeGuzman, Y.F. Shen, E.J. Neth, S.L. Suib, C.L. Oyoung, S. Levine and J.M. Newsam, *Synthesis and characterization of octahedral molecular-sieves (oms-2) having the hollandite structure*. Chem. Mater. 6 (1994) 815.

[7] J.C. Villegas, L.J. Garces, S. Gomez, J.P. Durand and S.L. Suib, *Particle size control of cryptomelane nanomaterials by use of H_2O_2 in acidic conditions*. Chem. Mater. 17 (2005) 1910.

[8] S. Ching and S.L. Suib, *Synthetic routes to microporous manganese oxides*. Comments Inorganic Chem. 9 (1997) 263.

[9] L. Lamaita, M.A. Peluso, J.E. Sambeth and H.J. Thomas, *Synthesis and characterization of manganese oxides employed in VOCs abatement*. Appl. Catal. B-Environ. 61 (2005) 114.

[10] K.M. Parida and A. Samal, *Catalytic combustion of volatile organic compounds on Indian Ocean manganese nodules*. Appl. Catal. A-Gen. 182 (1999) 249.

[11] J. Liu, V. Makwana, J. Cai, S.L. Suib and M. Aindow, *effects of alkali metal and ammonium cation templates on nanofibrous cryptomelane-type manganese oxide octahedral molecular sieves (OMS-2)*. J. Phys. Chem. B 107 (2003) 9185.

[12] S.L. Suib, *Structure, porosity, and redox in porous manganese oxide octahedral layer and molecular sieve materials*. J. Mater. Chem. 18 (2008) 1623.

[13] Q. Feng, H. Kanoh and K. Ooi, *Manganese oxide porous crystals*. J. Mater. Chem. 9 (1999) 319.

[14] Q. Feng, K. Yanagisawa and N. Yamasaki, *Hydrothermal soft chemical process for synthesis of manganese oxides with tunnel structures*. J. Porous Mat. 5 (1998) 153.

[15] J. Luo, Q. Zhang, A. Huang and S.L. Suib, *Total oxidation of volatile organic compounds with hydrophobic cryptomelane-type octahedral molecular sieves*. Micropor. Mesopor. Mat. 35-36 (2000) 209.

[16] K.A. Malinger, Y.S. Ding, S. Sithambaram, L. Espinal, S. Gomez and S.L. Suib, *Microwave frequency effects on synthesis of cryptomelane-type manganese oxide and catalytic activity of cryptomelane precursor*. J. Catal. 239 (2006) 290.

[17] S. Ching, J.L. Roark, N. Duan and S.L. Suib, *Sol-gel route to the tunneled manganese oxide cryptomelane*. Chem. Mat. 9 (1997) 750.

[18] E. Welch, A. Bahadoor, S. Hughes and S. Ching, *Nonaqueous sol-gel routes to microporous manganese oxides*. Abstr. Pap. Am. Chem. Soc. 221 (2001) U159.

[19] Y.S. Ding, X.F. Shen, S. Sithambaram, S. Gomez, R. Kumar, V.M.B. Crisostomo, S.L. Suib and M. Aindow, *Synthesis and catalytic activity of cryptomelane-type manganese dioxide nanomaterials produced by a novel solvent-free method.* Chem. Mater. 17 (2005) 5382.

[20] Y.F. Shen, R.P. Zerger, S.L. Suib, L. McCurdy, D.I. Potter and C.L. Oyoung, *Octahedral molecular-sieves - preparation, characterization and applications*. J. Chem. Soc.-Chem. Commun. (1992) 1213.

[21] L.X. Yang, Y.J. Zhu, W.W. Wang, H. Tong and M.L. Ruan, *Synthesis and formation mechanism of nanoneedles and nanorods of manganese oxide octahedral molecular sieve using an ionic liquid*. J. Phys. Chem. B 110 (2006) 6609.

[22] M.L. Rojas, J.L.G. Fierro, L.G. Tejuca and A.T. Bell, *Preparation and characterization of $LaMn_{1-x}Cu_xO_3$ Perovskite oxides*. J. Catal. 124 (1990) 41.

[23] V.R. Galakhov, M. Demeter, S. Bartkowski, M. Neumann, N.A. Ovechkina, E.Z. Kurmaev, N.I. Logachevskaya, Y.M. Mukovskii, J. Mitchell and D.L. Ederer, *Mn 3s exchange splitting in mixed-valence manganites.* Phys. Rev. B 65 (2002) 4.

[24] X. Wang, Q.L. Cui, Y.W. Pan and G.T. Zou, *X-Ray photoelectron and infrared transmission spectra of manganite system* $La_{0.5-x}Bi_xCa_{0.5}MnO_3$ *(0 ≤ x ≤ 0.25)* .J. Alloy. Compd. 354 (2003) 91.

[25] J. Luo, Q. Zhang, J. Garcia-Martinez and S.L. Suib, *Adsorptive and acidic properties, reversible lattice oxygen evolution, and catalytic mechanism of cryptomelane-type manganese oxides as oxidation Catalysts*. J. Am. Chem. Soc. 130 (2008) 3198.

[26] Y.G. Yin, W.Q. Xu, Y.F. Shen, S.L. Suib and C.L. Oyoung, *Studies of oxygen species in synthetic todorokite-like manganese oxide octahedral molecular-sieves.* Chem. Mat. 6 (1994) 1803.

[27] D.L. Bish and J.E. Post, *Thermal-behavior of complex, tunnel-structure manganese oxides.* Am. Miner. 74 (1989) 177.

[28] Y.G. Yin, W.Q. Xu, S.L. Suib and C.L. Oyoung, *Studies of stability and reactivity of synthetic cryptomelane-like manganese oxide octahedral molecular-sieves*. Inorg. Chem. 34 (1995) 4187.

[29] M. Baldi, E. Finocchio, F. Milella and G. Busca, *Catalytic combustion of C3 hydrocarbons and oxygenates over* Mn_3O_4. Appl. Catal. B-Environ. 16 (1998) 43.

[30] C. Cellier, V. Ruaux, C. Lahousse, P. Grange and E.M. Gaigneaux, *Extent of the participation of lattice oxygen from* γ*-*MnO_2 *in VOCs total oxidation: Influence of the VOCs nature*. Catal. Today 117 (2006) 350.

[31] G.G. Xia, Y.G. Yin, W.S. Willis, J.Y. Wang and S.L. Suib, *Efficient stable catalysts for low temperature carbon monoxide oxidation*. J. Catal. 185 (1999) 91.

[32] M.A. Peluso, L.A. Gambaro, E. Pronsato, D. Gazzoli, H.J. Thomas and J.E. Sambeth, *Synthesis and catalytic activity of manganese dioxide (type OMS-2) for the abatement of oxygenated VOCs*. Catal. Today 133-135 (2008) 487.

[33] X. Chen, Y.F. Shen, S.L. Suib and C.L. O'Young, *Catalytic decomposition of 2-propanol over different metal-cation-doped OMS-2 materials*. J. Catal. 197 (2001) 292.

[34] C. Lahousse, A. Bernier, P. Grange, B. Delmon, P. Papaefthimiou, T. Ioannides and X. Verykios, *Evaluation of* γ*–*MnO_2 *as a VOC removal catalyst: comparison with a noble metal catalyst*. J. Catal. 178 (1998) 214.

[35] L.M. Gandia, A. Gil and S.A. Korili, *Effects of various alkali-acid additives on the activity of a manganese oxide in the catalytic combustion of ketones*. Appl. Catal. B-Environ. 33 (2001) 1.

[36] M. Paulis, L.M. Gandia, A. Gil, J. Sambeth, J.A. Odriozola and M. Montes, *Influence of the surface adsorption-desorption processes on the ignition curves of volatile organic compounds (VOCs) complete oxidation over supported catalysts*. Appl. Catal. B-Environ. 26 (2000) 37.

4 The Role of Lattice Oxygen on the Activity of Manganese Oxides towards the Oxidation of Volatile Organic Compounds[1]

A series of manganese oxides differing in the structure, composition, average manganese oxidation state and specific surface area have been used in the total oxidation of volatile organic compounds (VOC). Ethanol, ethyl acetate and toluene were chosen as models of VOC.

Among the manganese oxides tested, cryptomelane (KMn_8O_{16}) was found to be very active in the oxidation of VOC. It was observed that the performance of cryptomelane was significantly affected by the presence of other phases, namely, Mn_2O_3 and Mn_3O_4. Temperature-programmed experiments combined with X-ray photoelectron spectroscopy (XPS) show that the mobility and reactivity of the oxygen species were significantly affected, explaining the catalytic performances of those samples. Mn_3O_4 improves the catalytic performance due to the increase of the reactivity and mobility of lattice oxygen, while Mn_2O_3 has the opposite effect. These results show that there is a correlation between the redox properties and the activity of the manganese oxides.

Temperature programmed surface reactions (TPSR) after adsorption of toluene or ethanol, in addition to reactions performed without oxygen in the feed, show that lattice oxygen is involved in the VOC oxidation mechanism. The conversion level was found to be influenced by the type of VOC, the reactivity into CO_2 increasing in the following order: Toluene<Ethanol<Ethyl Acetate. The type of VOC is particularly important, as it dictates the reduction of the catalyst and, consequently, the incorporation rate of oxygen from the gas phase. It is suggested that toluene decreases the oxygen mobility, so there is a slower incorporation rate of oxygen in the lattice, which explains the lower conversions observed.

[1] VP Santos, MFR Pereira, JJM Órfão, JL Figueiredo, submitted (2010)

4.1 Introduction

Tunnel structured manganese oxides are promising catalysts for the total oxidation of volatile organic compounds (VOC) [1-6]. Their high activity is ascribed to the open tunnel structure, the mixed valence character of manganese, and the high mobility of lattice oxygen [7-11].

The synthesis and properties of bulk cryptomelane (KMn_8O_{16}) materials have been intensively studied in the past [12-14]. Synthesis methods include thermal and hydrothermal treatment of layered birnessite [15], redox precipitation under reflux [1, 16], microwave heating [17], sol-gel methods [18] and a solvent-free procedure [19]. Among them, the reflux method, involving the oxidation of Mn^{2+} by MnO_4^-, is the most common route.

In a previous report [4], our group studied the influence of pH and the template cation on the formation of this kind of structure. The reflux method was the procedure adopted. It was found that the crystallinity and the microstruture of cryptomelane largely depended on the nature of the template, while the template concentration was found to be an important parameter to prevent the formation of Mn_3O_4, Mn_5O_8 and Mn_2O_3 as by-products. Several manganese oxides, differing in their crystallinity, structure, average oxidation state and surface area were obtained. The activity of these materials was tested in the total oxidation of ethyl acetate, and it was found that all samples were able to oxidise this VOC into CO_2 at low temperatures. Cryptomelane doped with small amounts of Mn_3O_4 showed the best performance.

The aim of the present paper is to study the oxidation of ethanol and toluene over the same catalysts, and to provide a better understanding of the VOC oxidation mechanism over manganese oxides. The oxidation of organic molecules over this type of catalyst usually proceeds according to the Mars and van Krevelen (MVK) mechanism, where the organic molecule is oxidised by the lattice oxygen of the oxide, the latter being re-oxidised by gas phase oxygen. Therefore, the availability and reactivity of surface oxygen species provide a method for the identification of the most active catalyst. The oxygen species in manganese oxides were studied in detail

by temperature programmed experiments in combination with X-ray photoelectron spectroscopy (XPS), in order to correlate catalysts activities with their properties.

4.2 Experimental

4.2.1 Catalysts synthesis and characterization

Five manganese oxides with different structures, surface areas and manganese average oxidation states were prepared as described in a previous work [4]. The structure, morphology, composition, manganese average oxidation state (AOS), texture and stability of the prepared samples were fully characterized by X-ray diffraction (XRD), scanning electron microscopy/energy dispersive X-ray spectroscopy (SEM/EDS), XPS, N_2 adsorption at -196 ºC, thermogravimetric analysis (TGA) and temperature programmed desorption (TPD). A summary of the catalysts properties is presented in Table 4.1. It should be noticed that the nomenclature used here is the same as in the chapter 3.

This paper is focused on the study of the oxygen species in the tunnel structured manganese oxides by TPD and temperature programmed reduction (TPR), combined with XPS. The fractions of Mn(II), Mn(III) and Mn(IV) species, for each sample, were obtained by XPS.

Table 4.1 Properties of the catalysts: average oxidation states (obtained by XPS), surface areas (obtained by nitrogen adsorption) and crystalline phases (obtained by XRD).

Sample	AOS	S_{BET} (m^2/g)	Phases
Mn2	3.89	71	KMn_8O_{16}
Mn4	3.74	45	KMn_8O_{16} ; α-Mn_2O_3
Mn5	3.72	84	KMn_8O_{16}; Mn_3O_4
Mn6	3.74	59	KMn_8O_{16}; α-Mn_2O_3; Mn_5O_8
Mn7	3.78	46	α-Mn_2O_3; β-MnO_2

4.2.1.1 Temperature programmed experiments (TPD and TPR)

These experiments were carried out in an Altamira Instruments (AMI 200) apparatus.

For TPD, 100 mg of each sample were loaded into the sample holder and placed inside the furnace. The sample was purged with helium for 1 hour at room temperature followed by heating to 900 ºC at 5 ºC/min in the same atmosphere. Evolution of oxygen from the sample was monitored with a mass spectrometer (MS).

A mixture of 10 vol.% H_2/He was used for TPR experiments, at a total flow rate of 30 cm^3/min, with 50 mg of catalyst. The temperature was increased at a rate of 10ºC/min from room temperature to 600 ºC, while the hydrogen consumption was monitored.

4.2.2.2 X-ray photoelectron spectroscopy

XPS analysis was performed with a VG Scientific ESCALAB 200A spectrometer using Al K_α radiation (1486.6 eV). Charge effects were corrected by adjusting the binding energy of C 1s to 284.6 eV.

4.2.3 Catalytic experiments

The catalytic oxidation of VOC was performed under atmospheric pressure in a fixed-bed reactor from Autoclave Engineers (BTRS Jr), which consists of a stainless steel tube of 6 mm internal diameter, placed inside a temperature-controlled electric furnace. A feed gas with a VOC concentration of 4,000 mgC/m^3 and a space velocity of 16,000 h^{-1} was used in standard tests. The catalyst sample (50 mg) was diluted with glass spheres of the same size as the catalyst particles (0.2-0.5 mm), in order to minimize temperature gradients.

Conversions were measured over the range 100-350 ºC by incremental steps (10-20 ºC), the temperature being measured by a thermocouple placed in the middle of the catalyst bed. To ensure that steady state data were measured, the reactor was maintained at each temperature for 30 minutes. The conversion of VOC (X) and the conversion into CO_2 (X_{CO2}) were respectively calculated as as $X = 1 - \frac{F_{VOC}}{F_{VOC,in}}$ and

$X_{CO_2} = \frac{F_{CO_2}}{\nu F_{VOC,in}}$, where F_{VOC} is the outlet molar flow rate of VOC at steady state, $F_{VOC,in}$ is the inlet molar flow rate of VOC, F_{CO_2} is the outlet molar flow rate of CO_2 at steady state and ν is the number of carbon atoms in the VOC molecule (for ethanol, ethyl acetate and toluene, ν = 2, 4 and 7, respectively).

4.2.4 Temperature Surface reactions (TPSR) and reactions without oxygen in the feed

TPSR experiments were conducted in an Altamira Instruments (AMI 200) apparatus. 100 mg of each sample were loaded into the sample holder and placed inside the furnace. The adsorption of VOC (ethanol or toluene) was carried out at room temperature, using a concentration of 4,000 mgC/m^3. After saturation, the system was purged with helium and the experiment started. The temperature was increased at 10 ºC/min to 600 ºC. The products were analysed by MS.

Reactions without oxygen in the feed were carried out in a fixed-bed reactor from Autoclave Engineers (BTRS Jr). The experimental conditions used here were the same as described in section 4.2 (4,000 mgC/m^3 and 16,000 h^{-1}). Prior to the reaction the catalyst was activated in air at selected reaction temperatures (210 ºC or 270 ºC, for ethanol or toluene, respectively). The reactor was then purged with nitrogen in order to remove physisorbed oxygen, and the experiment started. Additional experiments were carried out with a selected sample (Mn5) varying the activation time, which was 10 minutes in the first cycle, and 5, 2 and 1 min in the following cycles.

4.3 Results and discussion

4.3.1 Catalysts characterization

The oxygen species present in the MnO_x materials were completely characterized by temperature programmed studies (TPD and TPR) and XPS.

4.3.1.1 Temperature Programmed studies

TPD and TPR techniques have proved to be very useful to investigate oxygen species of single and mixed oxides, throwing light on the type of oxygen species and their properties, such as reactivities [20-23]. According to Yin et al. [20], three types of oxygen species can be identified in the tunnel structured manganese oxides, according to their peak positions in TPD/TPR spectra: the α-species, which are weakly bound to the surface (usually O_2^- and O^-surface oxygen species), and the β and γ species, assigned to lattice oxygen. The β and γ species are differentiated by the binding strengths between manganese and oxygen. Oxygen atoms in the framework bound to Mn(III) have a weaker interaction, and are released in the middle temperature range during TPD, while the oxygen atoms bound to Mn(IV) are released at higher temperatures, and are assigned as γ species.

Temperature programmed desorption

The TPD-O_2 profiles of the MnO_x materials are presented in Figure 4.1. It is apparent that the great majority of oxygen species in all samples can be ascribed to lattice oxygen. This result is in agreement with other authors [20, 22].

The O_2 pattern of Mn2 is characterized by two peaks at about 600 and 800 ºC. The first peak exhibits a clear shoulder that can result from desorption of surface oxygen species (O^- and O_2^-) and/or the presence of labile oxygen species (β species), with different Mn-O bond strengths. According to the literature [3, 24] and confirmed by TGA [4], the first peak is assigned to the transformation of cryptomelane to Mn_2O_3 (responsible for a weight loss of 7%), while the second peak corresponds to the subsequent reduction to Mn_3O_4 (2.6 % weight loss).

A similar pattern was obtained for the Mn4 sample, but the temperature of the first peak is shifted to lower temperatures (≈550 ºC), showing lower stability. The differences in the stability between Mn2 and Mn4 samples can be explained by the structural changes caused by the presence of the Mn_2O_3 phase. Moreover, the higher temperature peak (800 ºC) is wider and less intense in comparison to that obtained with the Mn2 sample. A shoulder is also present in the lower temperature peak, although not so evident as in the case of the Mn2 sample.

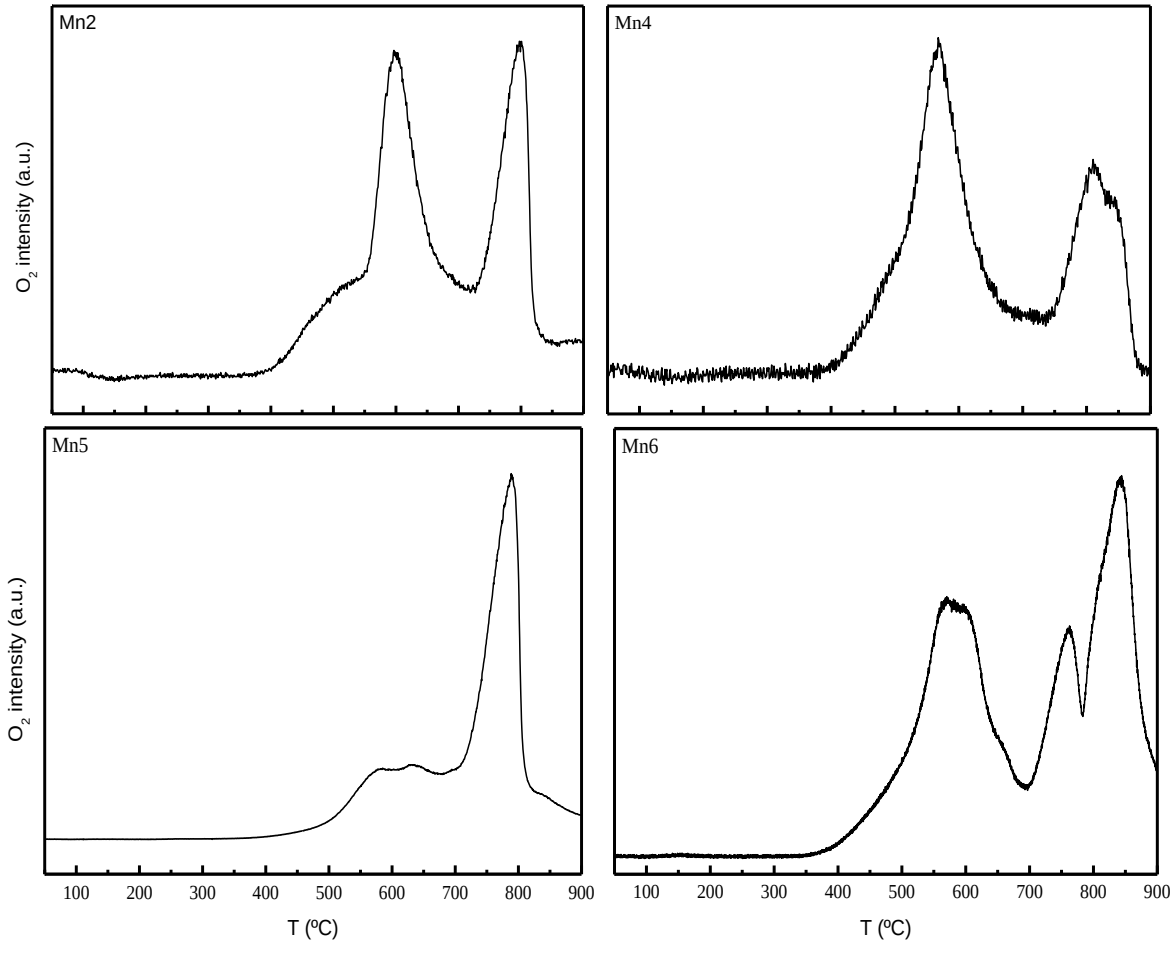
Mn2
Mn4
Mn5
Mn6
O2 intensity (a.u.)
O2 intensity (a.u.)
100
200
300
400
500
600
700
800
900
T (ºC)
T (ºC)

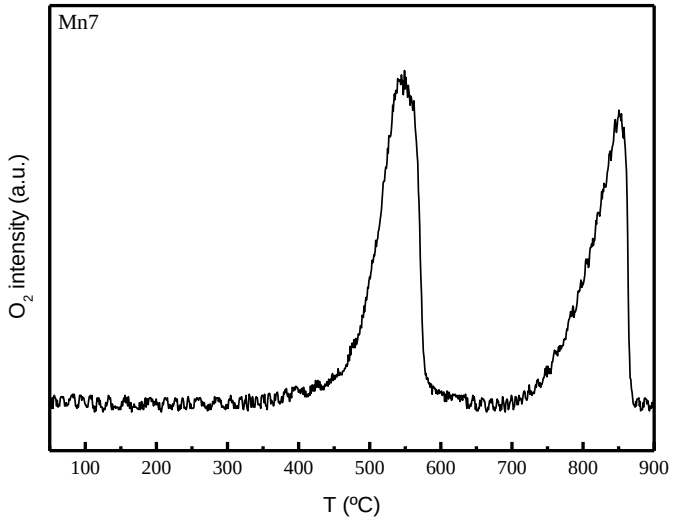

Figure 4.1 Oxygen TPD spectra of the MnO_x catalysts. Heating rate: 5ºC/min.

The O_2 profile of the Mn5 sample is quite different from the Mn2 and Mn4 samples. The lower temperature peak (maximum near 600 ºC) is less intense, and is also ascribed to desorption of α and β species. In this case, the transformation of cryptomelane to Mn_2O_3 does not occur, possibly due to the presence of Mn_3O_4. The higher temperature peak is also ascribed to the transformation of cryptomelane to Mn_3O_4. Compared to the pure cryptomelane sample (Mn2), Mn5 has a higher stability (the first peak is shifted to higher temperatures), which means that the presence of Mn_3O_4 has a pronounced effect on the stability of the oxygen species.

The oxygen spectrum of Mn6 is more complex, showing three peaks between 400 and 900 ºC, assigned to three intermediate transformations.

The last sample shows a different behaviour as a result of its different structure and composition. Two major peaks at 550 and 850 ºC are observed, as a result of the successive transformations to Mn_2O_3 and Mn_3O_4.

In summary, it can be concluded that the structural changes caused by the presence of Mn_2O_3, Mn_3O_4 and Mn_5O_8 phases in cryptomelane play a decisive role on the stability of the materials, affecting the mobility of lattice oxygen. The different shapes of the oxygen TPD profiles resulted also from the presence of different manganese species (Mn(II), Mn(III), Mn(IV)).

Temperature programmed reduction

The reactivity of the oxygen species was studied by TPR. According to Kapteijn et al [25], the reduction of manganese oxides can be described by the successive processes:

$$MnO_2 \rightarrow Mn_2O_3 \rightarrow Mn_3O_4 \rightarrow MnO$$

However, the peaks on the TPR curves may also result from reduction of species in different local environments [26]. Figure 4.2 shows the reduction profiles of the MnO_x samples. Each profile was decomposed into three or four components, depending on the sample, and the corresponding positions are summarized in Table 4.2.

The TPR spectrum of the Mn2 sample is characterized by a large peak with a maximum at about 350 ºC. A shoulder clearly appears at the end of the peak, which may indicate that the reduction proceeds in two steps:

$$KMn_8O_{16} \rightarrow Mn_3O_4 \rightarrow MnO$$

This result is in agreement with other authors [27]. Moreover, the shoulder at low temperatures reveals the presence of labile species with different Mn-O strengths, in agreement with the TPD results. Those species are not strongly stabilized within the oxide lattice, and can be regarded as the surface reactive species.

A similar reduction pattern is obtained for the Mn4 sample, but the temperature of the main peak is shifted to higher temperatures, showing lower reducibility (see also Table 4.2). Moreover, the low temperature shoulder is larger in comparison to the Mn2 sample, due to the lower AOS (and consequently higher relative amounts of Mn(III) species).

The reduction profiles of Mn5 and Mn6 are different from those observed on the two previous samples. The spectra are characterized by the presence of two overlapping components with maxima around 335 ºC and 380 ºC, suggesting that an intermediate reduction into Mn_2O_3 takes place. Shoulders also appear at the beginning and at the end of the mentioned peaks. The main difference between the Mn5 and Mn6 samples is the intensity of the component peaks II_β and III (which are much larger in the Mn6 sample) and the position of component I. In fact, the reduction of Mn5 starts at lower temperatures, having higher reducibility.

The TPR spectrum of the Mn7 sample differs greatly from the others, as a result of its different structure and composition, in agreement with TPD results. Two major peaks at about 360 ºC and 480 ºC can be observed, the intensity of the peaks being quite similar. We propose that the low temperature peak corresponds to the reduction of MnO_2 to Mn_3O_4, whereas the high temperature peak represents the reduction of Mn_3O_4 to MnO, in agreement with [25].

Using the temperatures of the first component (peak I, see Figure 4.2 and Table 4.2), it is possible to compare the reducibility of all samples. The following trend was obtained: $T_{Mn5} < T_{Mn2} \approx T_{Mn6} < T_{Mn7} < T_{Mn4}$.

As a conclusion, the TPR profiles clearly indicate the major effect of other phases on the reducibility of cryptomelane. The presence of Mn_2O_3 (sample Mn4) decreases the reducibility, while the presence of Mn_3O_4 (sample Mn5) has the opposite effect.

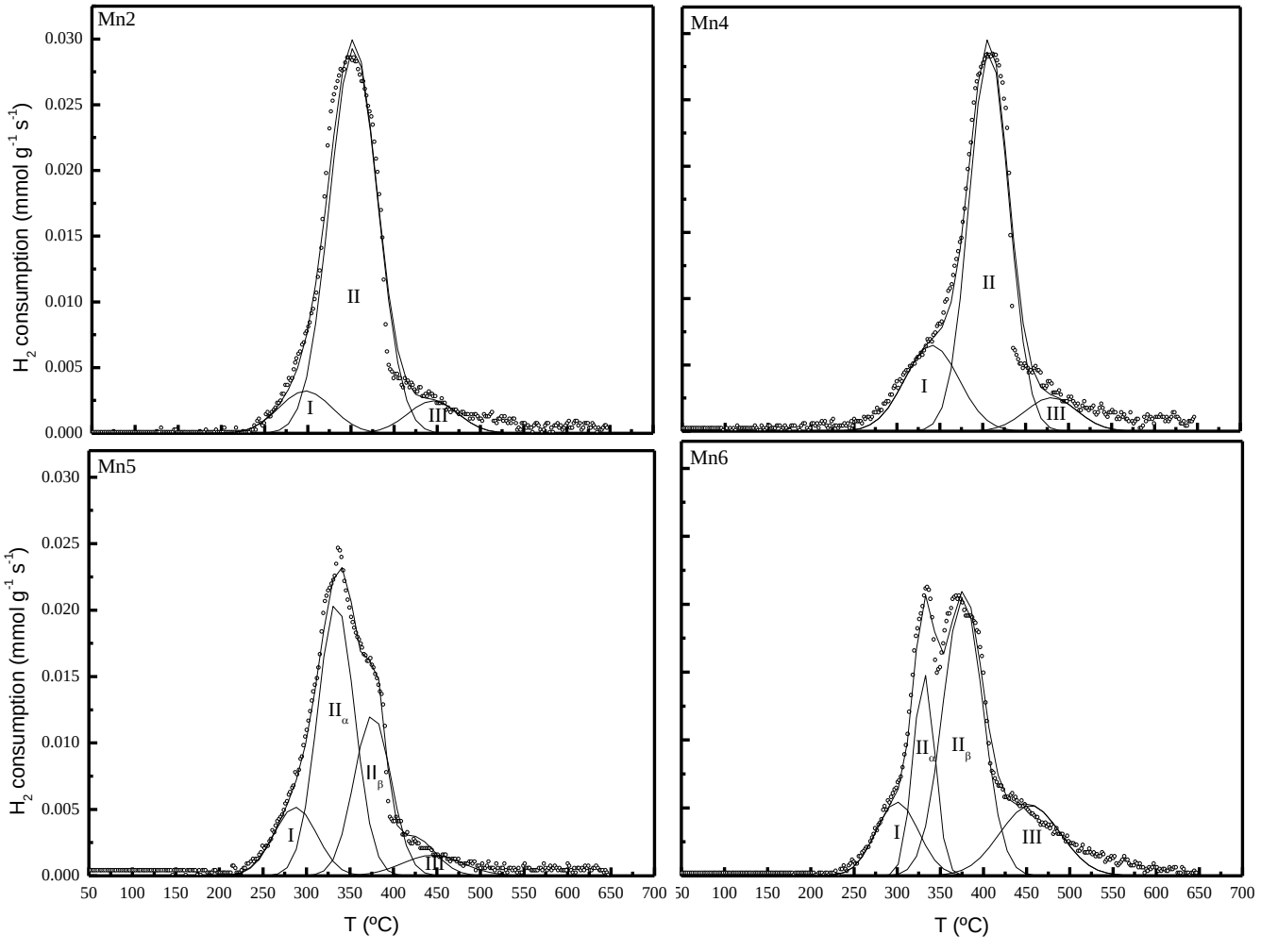
Mn2
Mn4
Mn5
Mn6
H2 consumption (mmol g-1 s-1)
T (ºC)
I
II
III
IIα
IIβ

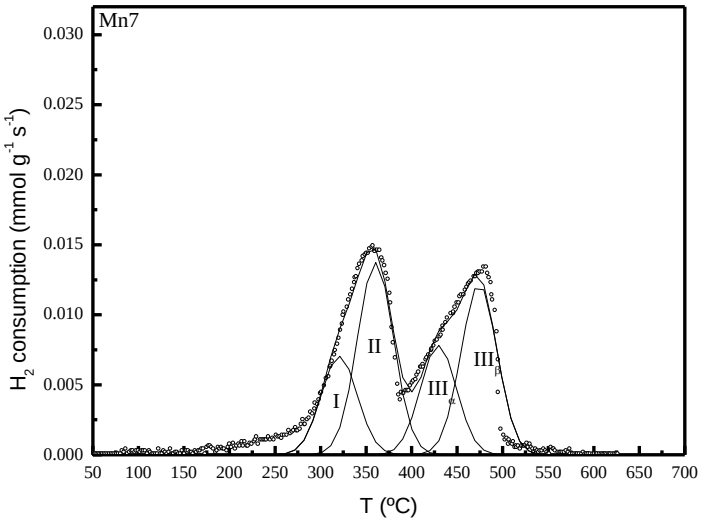

Figure 4.2 TPR profiles of the MnO_x catalysts. Heating rate: 10 ºC/min

Table 4.2 Position of the TPR components (ºC) for the MnO_x catalysts.

Sample	Peak I	Peak II		Peak III	
		Peak II_α	Peak II_β	Peak III_α	Peak III_β
Mn2	296	352		445	
Mn4	340	407		488	
Mn5	284	339	383	425	
Mn6	300	333	374	456	
Mn7	320	360		430	480

X-ray Photoelectron spectroscopy

XPS is a powerful technique for the characterization of surface oxygen species and the determination of surface chemical compositions. In this study, XPS was used for both purposes.

O1s spectra

The manner by which oxygen is bound to metals, in metal oxide catalysts, is most important for their catalytic properties. The O1s spectrum is frequently used to identify the types of surface oxygen species present in a particular oxide. According to the peak positions, three types of oxygen species can be identified: the low binding energy peak (O_I: 529.8-530.1 eV), which is ascribed to lattice oxygen (O_2^{2-}), the medium binding energy peak (O_{II}: 531.3 eV), assigned to surface adsorbed oxygen (O_2^- or O^-), OH groups and oxygen vacancies; and finally the high binding energy peak (533.0 eV), likely to be associated with adsorbed molecular water [28]. The relative surface oxygen composition plays a key role on the catalytic activity. For example, it is well established that O_{II} species have a higher mobility than lattice oxygen, and some authors correlate the higher activity of a particular catalyst with the higher amount of HO groups and oxygen vacancies [9, 29]. Figure 4.3 shows the O1s spectra of all samples. The spectra were fitted using the three peaks mentioned above,

considering a mixture of Lorentzian and Gaussian curves (all curves have the same shape). The relative abundances of O_I and O_{II} species are listed in Table 4.3. As expected, the most abundant component in all samples is lattice oxygen (see Table 4.3), varying between 76% and 72% for Mn5 and Mn6, respectively. On the other hand, the abundance of the O_{II} species ranges between 24 % (Mn6) and 20% (Mn4).

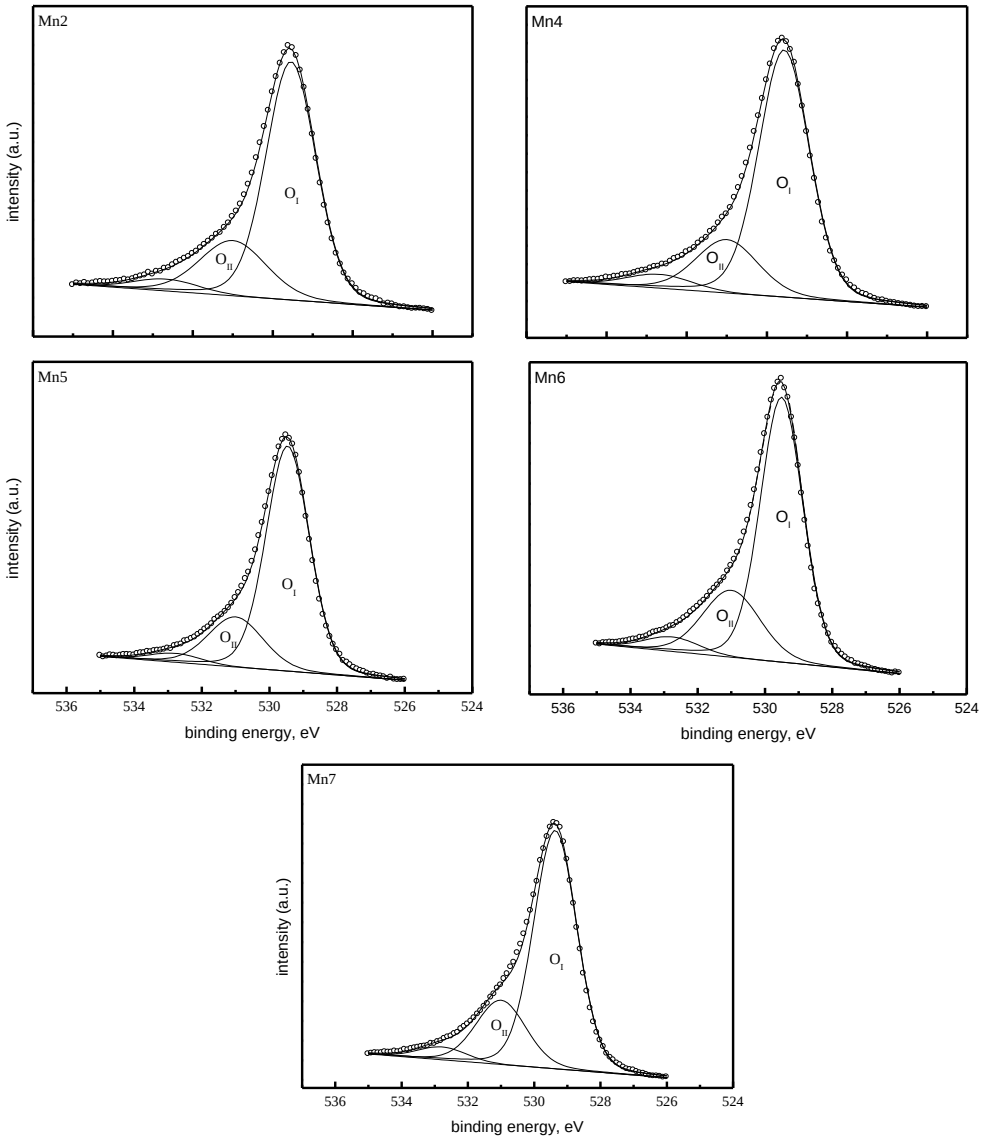

Figure 4.3 O 1s XPS spectra of the MnO_x catalyst

Table 4.3 XPS results for the MnO_x catalysts.

Sample	O1s				Mn2p$_{3/2}$					
	O_I		O_{II}		Mn(II)		Mn(III)		Mn(IV)	
	Peak Position (eV)	at. (%)	Peak Position (eV)	at. (%)	Peak Position (eV)	at. (%)	Peak Position (eV)	at. (%)	Peak Position (eV)	at. (%)
Mn2	529.5	73	531.0	23	-	-	641.4	17	642.3	83
Mn4	529.6	75	531.0	20	-	-	641.9	23	642.2	77
Mn5	529.5	76	531.0	22	640.3	11	641.9	55	643.3	34
Mn6	529.5	72	531.1	24	640.4	12	642.0	57	643.4	31
Mn7	529.4	73	531.0	23	-	-	642.1	18	643.0	82

$Mn2p_{3/2}$ spectra

One of the major problems in the chemistry of non-stoichiometric transition metal oxides is the determination of the oxidation states and the amounts of the different species. This is particularly problematic in the case of manganese oxides, owing to their multiple oxidation states, Mn(II), Mn(III) and Mn(IV), and the overlap of energy ranges for the various oxidation states of manganese. In a previous study [4], the AOS of manganese was determined by XPS, based on a correlation between the binding energies of the doublet separation of Mn3s (ΔEs) and the AOS, proposed by Galakhov et al. [30]; the corresponding values are presented in Table 4.1. Here, the relative abundance of Mn(II), Mn(III) and Mn(IV) species for each sample was obtained by studying the $Mn2p_{3/2}$ spectra [31]. The spectra of all samples (not shown) were decomposed into three components corresponding to Mn(II), Mn(III) and Mn(IV) species. Table 4.3 shows the results obtained. It can be observed that for Mn2, Mn4 and Mn7 samples, Mn(II) is not detected, in agreement with the X-ray diffraction results. For these samples, the relative abundances obtained by this method are roughly in agreement with the average oxidation states (see Table 4.1).

4.3.2 Catalytic activities

The catalytic performance of all samples was evaluated in the oxidation of ethanol and toluene. In a previous study [4], the same samples were tested in the oxidation of ethyl acetate, and selected results are also included here, for comparison.

The ethanol conversion and the conversion into CO_2 as a function of the temperature are presented in Figure 4.4. The conversion into acetaldehyde (see Figure 4.4b) is also shown, as this compound is the major intermediate in the oxidation of ethanol. For comparative purposes, the temperatures corresponding to 50, 90 and 100% conversion into CO_2 are summarized in Table 4.4.

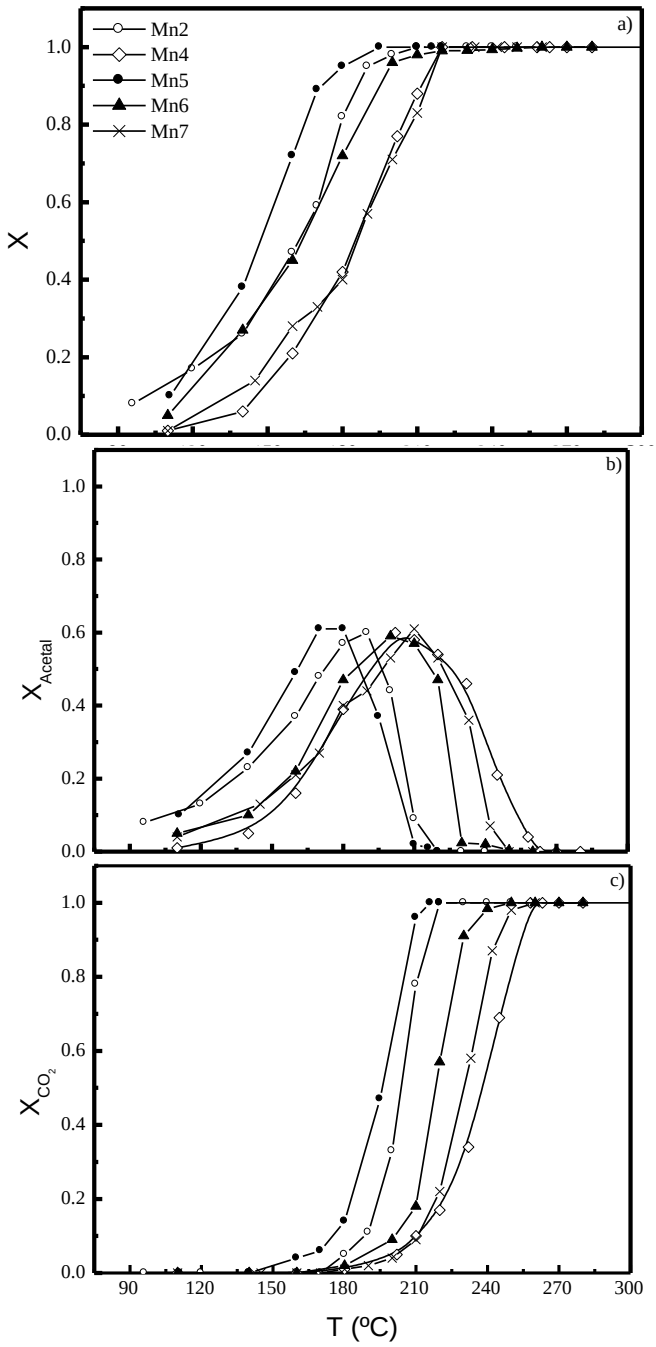

Figure 4.4 Light-off curves for ethanol oxidation over the MnO_x catalysts: a) Ethanol conversion (X); b) Conversion into acetaldehyde (X_{Acetal}); c) Conversion into CO_2

(X_{CO2}). Conversion into acetaldehyde is defined as: $X_{Acetal} = \frac{F_{Acetal}}{F_{Ethanol,in}}$, where F_{Acetal} is the outlet molar flow rate of acetaldehyde at steady state.

Table 4.4 Catalytic performances expressed as T_{50} (ºC), T_{90} (ºC) and T_{100} (ºC) (temperatures at which 50%, 90% and 100% conversions into CO_2 are obtained).

Sample	Ethanol			Ethyl acetate [4]			Toluene		
	T_{50}	T_{90}	T_{100}	T_{50}	T_{90}	T_{100}	T_{50}	T_{90}	T_{100}
Mn2	204	216	220	200	211	213	252	260	283
Mn4	238	254	263	225	233	240	278	295	300
Mn5	196	208	215	195	206	213	245	258	283
Mn6	219	230	250	217	230	240	272	287	290
Mn7	230	244	258	219	231	240	268	280	300

Generally, all the catalysts tested reveal high activity towards the oxidation of ethanol, which is completely converted into CO_2 at temperatures lower than 265 ºC. In terms of ethanol conversion, the following performance trend was observed: Mn5>Mn2>Mn6>Mn7≈Mn4. However, the performance of a catalyst should take into account the CO_2 yield and not the global conversion, as the by-products formed could be more toxic than the original reactant. In terms of the temperatures corresponding to 50, 90 and 100% conversion into CO_2 (see Table 4.4), the catalysts follow the sequence Mn5>Mn2>Mn6>Mn7>Mn4. For example, in the presence of the Mn5 catalyst, ethanol achieves full conversion at 215 ºC, which is ≈ 50ºC less than with the Mn4 catalyst. The observed product distribution is clearly indicative of a series reaction scheme, i.e. ethanol is oxidised to acetaldehyde, and acetaldehyde is further oxidised to CO_2. The contribution of an intermediate step involving the oxidation of acetaldehyde (probably into acetic acid) also seems to occur, especially in the case of Mn6 and Mn4 (this may account for as much as 30% of the total conversion, depending on the temperature).

The corresponding results referring to ethyl acetate [4] are also presented in Table 4.4. In terms of conversion into CO_2, the following performance trend was observed: Mn5>Mn2>Mn6≈Mn7>Mn4. In this case, the differences between the catalysts are less evident: ethyl acetate is completely oxidised to CO_2 at 213 ºC over Mn5, while the complete oxidation occurs at 240 ºC in the presence of Mn4. Comparing the VOC conversions, ethanol is slightly more reactive than ethyl acetate [4]. However, the complete oxidation into CO_2 occurs at lower temperatures in the case of ethyl acetate, which may indicate that the by-products formed in the partial oxidation of ethanol (namely acetaldehyde and/or acetic acid) are less reactive than ethyl acetate. Acetaldehyde was also found to be an intermediate product during ethyl acetate oxidation, but its amount is significantly lower than that detected during ethanol oxidation.

In the case of toluene oxidation (see Figure 4.5 and Table 4.4), the catalyst trend is identical to that of ethyl acetate oxidation, although the differences between the catalysts were even less evident in this case. For instance, toluene is completely oxidised into CO_2 at 283 ºC over the Mn5 sample, while this oxidation occurs at 300 ºC with Mn4. It was found that CO_2 is the only product detected from toluene oxidation, at all conversion levels.

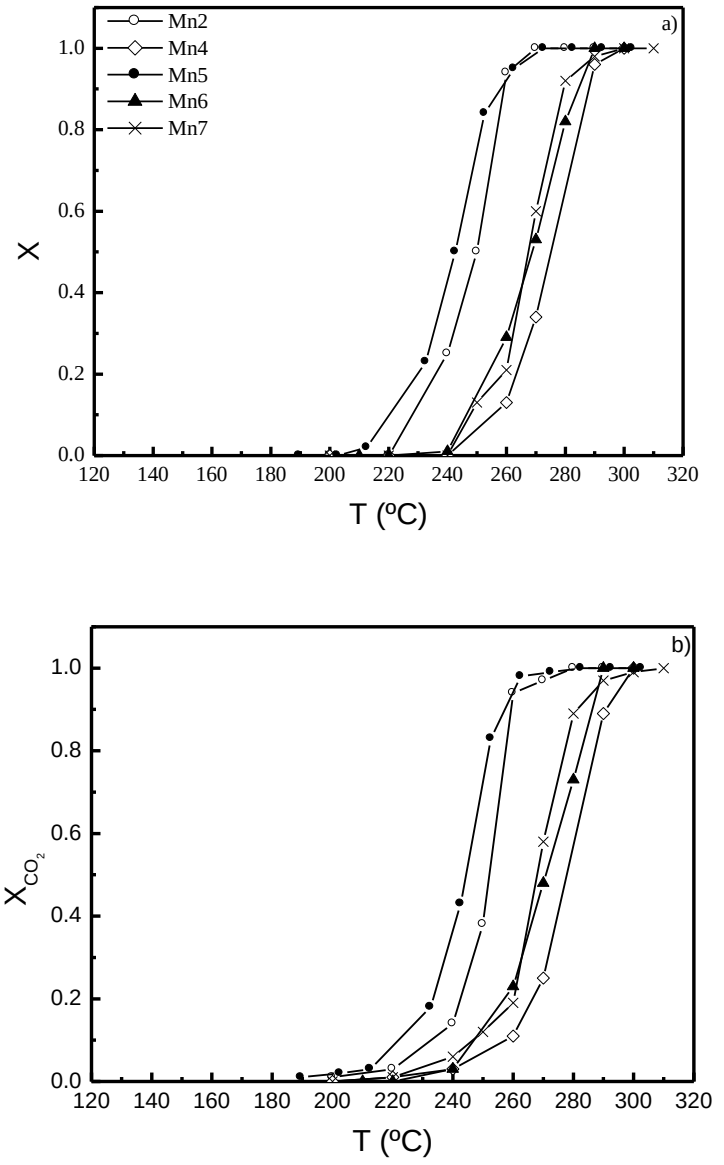

Figure 4.5 Light-off curves for toluene oxidation over the MnO_x catalysts: a) Toluene conversion (X); b) Conversion into CO_2 (X_{CO_2})

Comparing the three VOC studied, it seems that toluene is the most resistant to oxidation, requiring temperatures 37-68 ºC higher than ethanol for 100% conversion into CO_2. In summary, it can be stated that, for all VOC studied, Mn5 and Mn2 are the most efficient catalysts, while Mn4 is the worst catalyst of the group. It was observed that, in general, Mn6 and Mn7 have similar performances. Taking into account the characterization results (namely the TPR results), it can be observed that the efficiency of Mn5, Mn2, Mn7 and Mn4 is in close agreement with the reducibility of the samples (see correlation lines in Figure 4.6), revealing the catalytic role of oxygen species from the catalysts. This result is consistent with the oxidation mechanism proposed in the literature for this type of catalysts (MVK mechanism) [3, 5, 8, 10, 29].

In the case of Mn6, it seems that this sample has lower efficiency (see Figure 4.6) than what might be expected from the TPR results, so other properties should be taken into account to explain its activity, namely its structure and composition.

The XPS results can also shed some light on the mobility of oxygen species. It has been established that oxygen vacancies and HO^- groups (O_{II}) play an important role in this context, as they allow the diffusion of lattice oxygen [29]. As can be seen in Table 4.3, there are no major differences between the relative abundances of O_{II} species in the MnO_x samples, and no correlation can be established. However, it can be observed that Mn4 has the lowest percentage of oxygen vacancies (20%), which can also justify the lowest activity in VOC oxidation.

In order to provide a better understanding of the VOC oxidation mechanism over manganese oxides, some additional experiments were performed, namely TPSR after adsorption of toluene or ethanol, as well as reactions without oxygen in the feed.

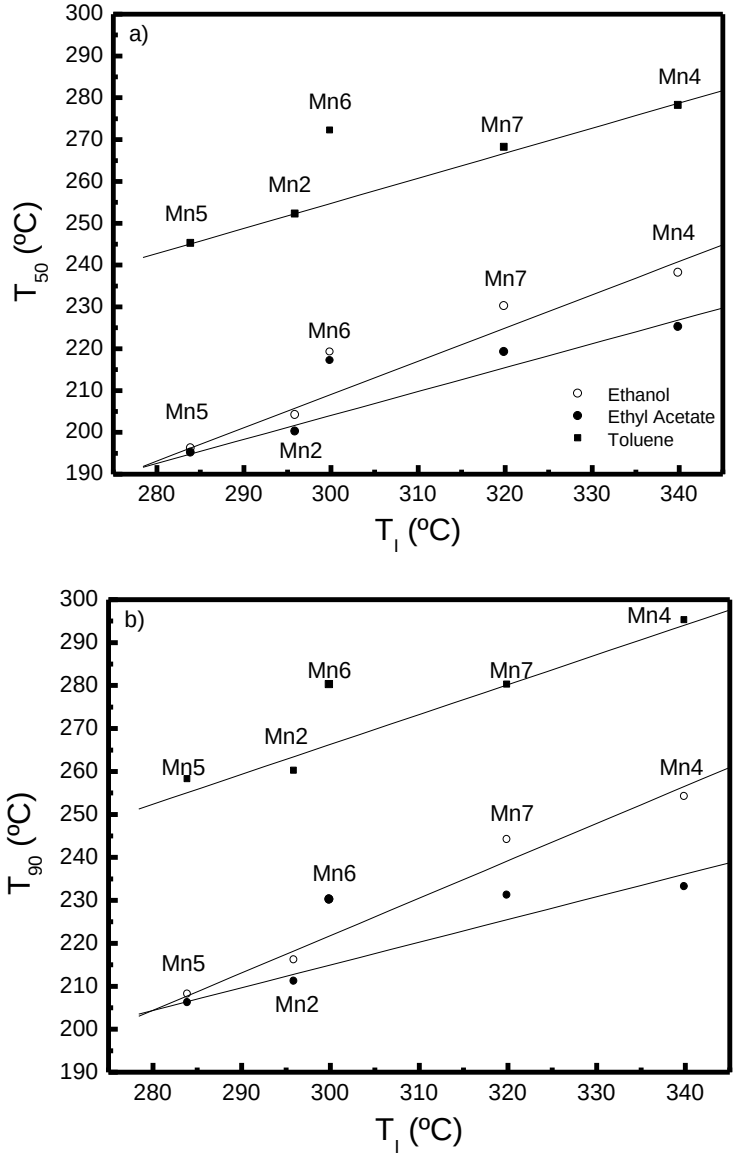

Figure 4.6 T_{50} (a) and T_{90} (b) determined for toluene, ethanol and ethyl acetate oxidation as a function of the reducibility of the catalysts, expressed as the temperature of the first peak in TPR spectra (T_I (ºC)).

4.3.3 Temperature Programmed surface reaction

4.3.3.1 Ethanol

TPSR experiments were performed after adsorption of ethanol at room temperature, in order to analyse the nature of the active sites involved in the oxidation of ethanol over the manganese oxides. The signals of CO_2 (44), water (18), ethanol (31) and acetaldehyde (29) were continuously monitored during the TPSR experiment. CO_2 and water were the only products detected, confirming that lattice oxygen is involved in ethanol oxidation (MVK mechanism). A similar experiment was carried out after adsorption of ethyl acetate in a previous study [5], and the same conclusions were reached.

Figure 4.7 shows the CO_2 evolution for all samples. Generally, two significant peaks (components II and III) with a low temperature shoulder (component I) are clearly observed, suggesting the presence of different adsorption-reaction sites. Moreover, in some cases (Mn4 and Mn6), an additional peak at higher temperatures (around 450 ^{o}C) was also found, which shows the presence of different adsorbed species.

The adsorption of ethanol over manganese oxides has already been studied by some authors [8, 9, 11]. Peluso et al. [9] studied the adsorption of ethanol over cryptomelane catalysts, and they pointed out that there are two different adsorption sites, which is in agreement with our own findings. Moreover, infrared studies after adsorption of ethanol at 70 ^{o}C [8, 11], reveal that the adsorption of ethanol occurs mainly in the form of ethoxides ($H_3C\text{-}CH_2\text{-}O^-$). As the temperature rises, these ethoxides are converted into acetates, showing different stabilities depending on the structure and composition of the particular manganese oxide. Accordingly, the different component peaks observed in Figure 4.7 are the result of the different interactions between ethanol and the catalyst surface, as well as the interactions of some intermediate species involved in the adsorption-reaction pathway of ethanol, namely acetaldehyde and acetic acid. The different surface reactive species involved in the VOC oxidation could be lattice oxygen (O^{2-}) and HO^- groups [7-9, 11]. According to the characterization results, the catalyst surface composition (Mn(II), Mn(III), Mn(IV)) plays a key role on the reactivity of lattice oxygen. As a result, the area and intensity of these component peaks differ greatly from sample to sample.

Another important feature related with the TPSR experiment is the amount of CO_2 produced (see Table 4.5). This value is a measure of the availability to release oxygen and, according to the MVK mechanism, plays a key role on the catalytic activity of manganese oxides. Figure 4.8 shows that, as expected, there is a clear correlation between the amount of CO_2 produced and the catalytic performance for the total oxidation of ethanol.

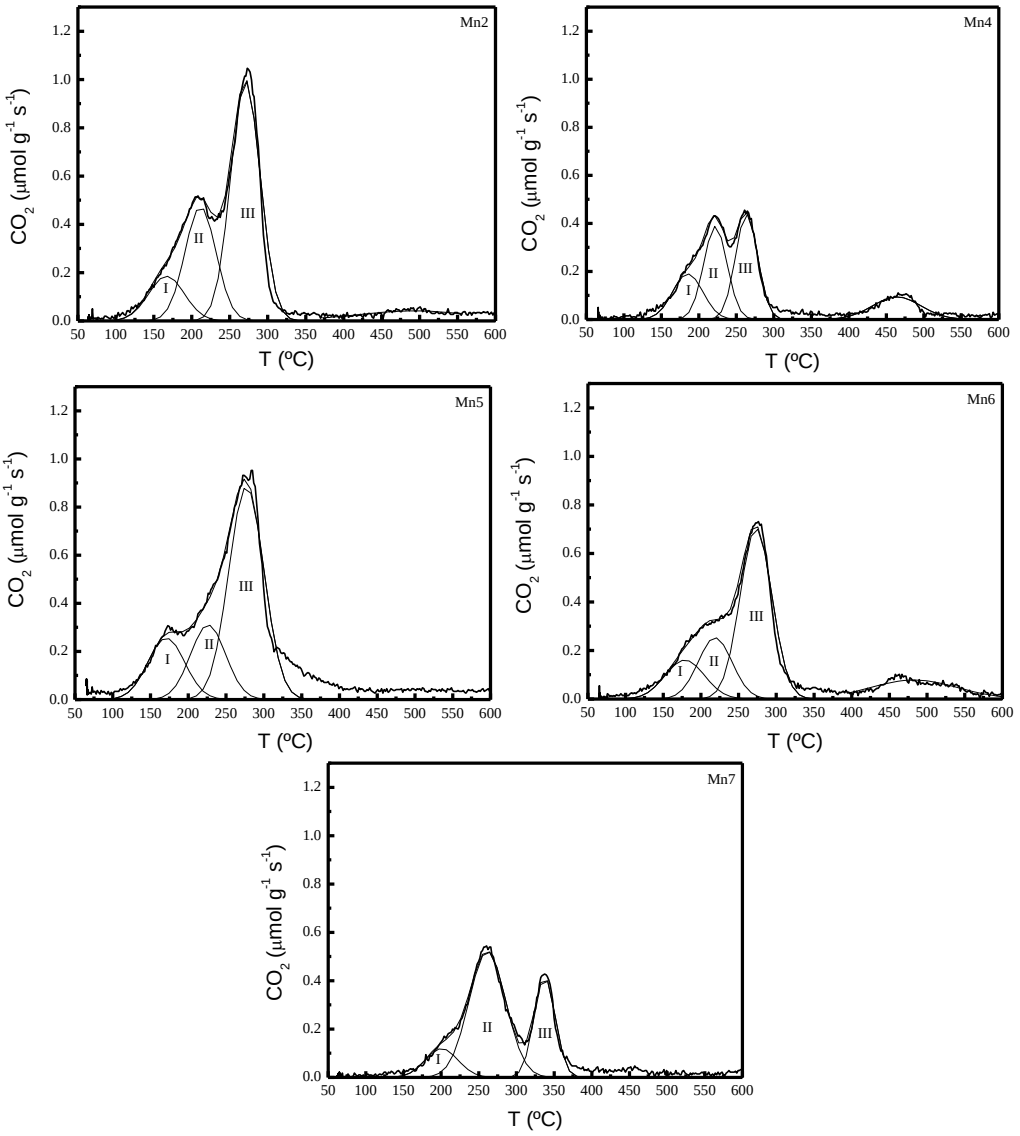

Figure 4.7 TPSR experiments (in helium) after adsorption of ethanol at room temperature over the MnO_x catalysts.

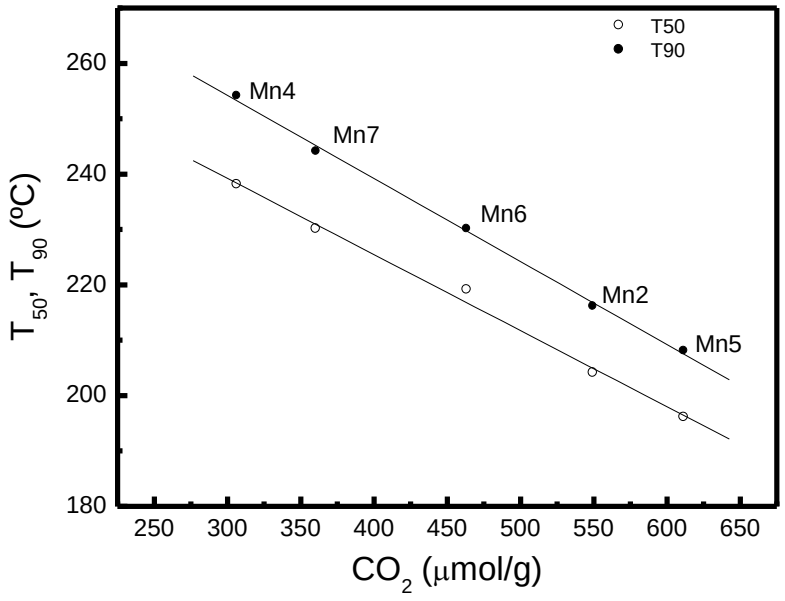

Figure 4.8 T_{50} and T_{90} determined for ethanol oxidation as a function of the amount of CO_2 measured during TPSR experiments.

4.3.3.2 Toluene

TPSR experiments were also done after adsorption of toluene at room temperature. The signal associated to toluene was also not detected in TPSR, CO_2 and water being the only products detected. However, there are several differences between these results and those obtained with ethanol. The first main difference is related to the shape of the CO_2 evolution curves. One peak (instead of two) was observed in all samples, suggesting that the adsorption/reaction of toluene involves just one type of active site. Furthermore, a much lower amount of CO_2 was measured (see Table 4.5), and in this case, there is no correlation between that amount and the catalytic performance. This result suggests that adsorbed toluene affects the mobility of the oxygen species, making them less reactive. In a recent report [32], we studied the stability of manganese oxides in the oxidation of toluene, and it was shown that cryptomelane is able to retain toluene at high temperatures (suggesting a strong adsorption).

4.3.4 Reaction without oxygen in the feed

Reactions without oxygen in the feed were also performed for ethanol and toluene, at 210 and 270 ºC, respectively. As expected, the oxidation of both VOC takes place in the absence of any gaseous oxygen, which is in agreement with the TPSR experiments. The amounts of CO_2 obtained during ethanol and toluene oxidation are summarized in Table 4.5, and were correlated with the catalytic performances of all samples (expressed as T_{50} and T_{90}). Figure 4.9 shows the results obtained. As can be seen, a significant correlation occurs for both VOC studied, which is consistent with the proposed mechanism.

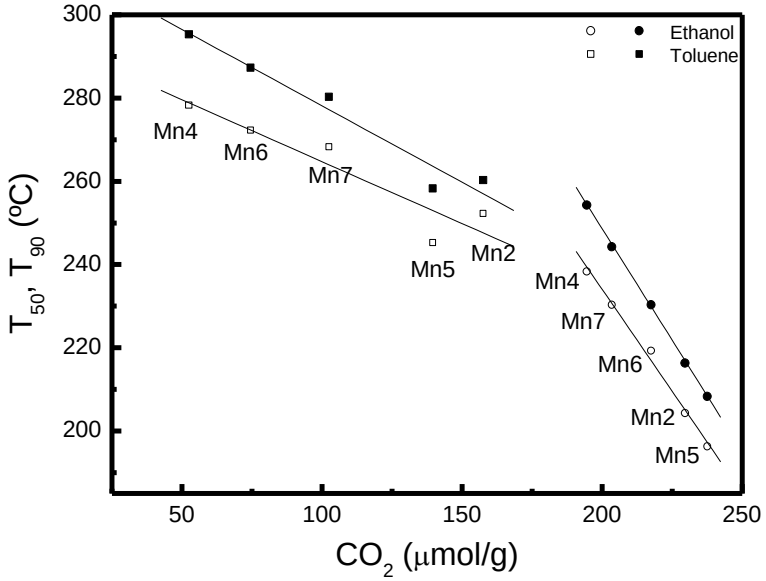

Figure 4.9 T_{50} (open symbols) and T_{90} (filled symbols) determined for ethanol and toluene oxidation as a function of the amount of CO_2 obtained in the reactions without oxygen in the feed.

Table 4.5 Amounts of CO_2 obtained in the TPSR experiments (a) and in reactions without oxygen in the feed (b).

Sample	CO_2 (μmol/gcat)[a]		CO_2 (μmol/gcat)[b]	
	Ethanol	Toluene	Ethanol	Toluene
Mn2	550	83	230	158
Mn4	307	48	195	53
Mn5	612	57	238	140
Mn6	464	64	218	100
Mn7	361	103	204	75

Following the MVK concept, the re-oxidation of the catalysts is a very important step. Cellier et al. [33] studied the extent of participation of lattice oxygen in the oxidation of n-hexane and trimethylamine over γ-MnO_2. They pointed out that the polarizability of the VOC molecule plays a role in the diffusion of gaseous oxygen and, consequently, in the incorporation of oxygen in the lattice.

In order to study the influence of the type of VOC on the rate of incorporation of oxygen from the gas phase, additional experiments were carried out with the Mn5 sample. In each cycle, prior to the reaction, the catalyst was activated in air at the reaction temperature. The activation time was 10 minutes in the first cycle, and 5, 2 and 1 min, in the subsequent cycles. The results obtained are summarized in Figure 4.10. In the case of ethanol (see Figure 4.10a), it can be observed that the molar flow rate of CO_2 produced sharply increases, reaching a maximum value, and then decreasing rapidly. In the last cycle, the total amount of CO_2 produced is significantly lower. It can be stated that, during ethanol oxidation, the incorporation of oxygen from the gas phase is very fast, and only 2 minutes of treatment are enough to re-oxidise the active sites. In the case of toluene (see Figure 4.10b), it seems that the re-oxidation of the catalyst is more difficult, and 5 minutes are not enough to activate the catalyst. The shapes of the curves differ greatly from those obtained in the case of ethanol, the molar flow rate of CO_2 measured decreasing at a very slow rate for an extended period

of time. The slow incorporation of oxygen on the active sites is assumed to explain the lower conversions.

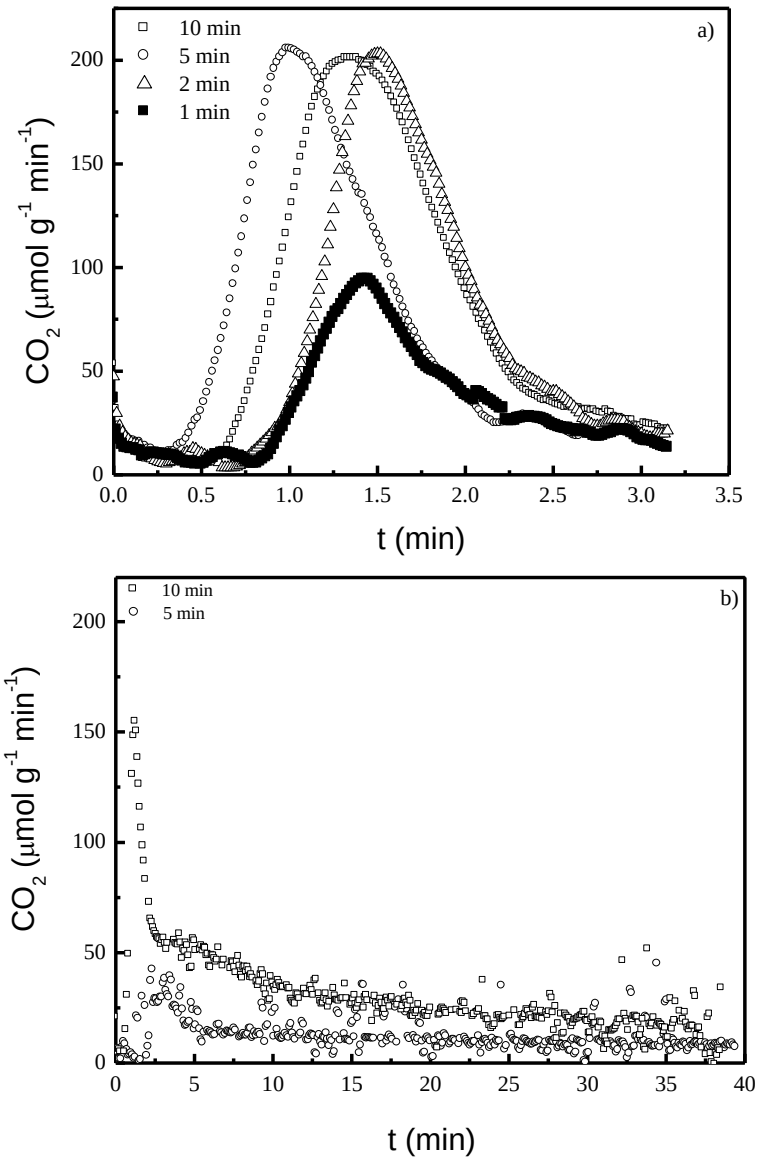

Figure 4.10 Influence of the activation time on the conversion into CO_2 over Mn5 without oxygen in the feed: a) Ethanol at 220 ºC; b) Toluene at 270 ºC.

4.5 Conclusions

Characterization results by XPS, TPD and TPR show that the oxygen species present in MnO_x samples have different mobility and reactivity, as a result of their different structure and composition.

All samples were very active for the total oxidation of ethanol, ethyl acetate and toluene. The following reactivity trend was observed: Ethyl Acetate> Ethanol>Toluene.

Cryptomelane was found to be very active in VOC oxidation. Its performance is significantly affected by the presence of other phases, namely, Mn_2O_3 and Mn_3O_4. Mn_3O_4 improves the catalytic activity due to the increase of the reactivity and mobility of lattice oxygen, while Mn_2O_3 has the opposite effect. These results show that the reducibility and reactivity of lattice oxygen play a key role on the activity of manganese oxides.

Temperature programmed surface reaction studies after adsorption of ethanol or toluene over MnO_x samples show that the interaction of these molecules with the catalyst surface is quite different. In the case of ethanol, two types of adsorption/reaction sites are involved, while in the case of toluene just one type of active site is evident. Moreover, in the case of ethanol, the amounts of CO_2 obtained during these experiments are correlated with the catalytic performances.

Reactions without oxygen in the feed, after different activation conditions, suggest that the incorporation rate of oxygen is slower in the case of toluene. This may explain its lower reactivity. Strong correlations between catalytic performance (measured by T_{50} or T_{90}) and CO_2 produced in these experiments were observed, both for ethanol and toluene, in agreement with a Mars and van Krevelen mechanism.

References

[1] J. Luo, Q. Zhang, A. Huang, S.L. Suib, *Total oxidation of volatile organic compounds with hydrophobic cryptomelane-type octahedral molecular sieves*. Micropor. Mesopor. Mat. **35-36** (2000) 209-217.

[2] J. Cai, J. Liu, W.S. Willis, S.L. Suib, *Framework doping of iron in tunnel structure cryptomelane*. Chem. Mater. **13** (2001) 2413-2422.

[3] J. Luo, Q. Zhang, J. Garcia-Martinez, S.L. Suib, *Adsorptive and acidic properties, reversible lattice oxygen evolution, and catalytic mechanism of cryptomelane-type manganese oxides as oxidation catalysts*. J. Am. Chem. Soc. 130 (2008) 3198-3207.

[4] V.P. Santos, M.F.R. Pereira, J.J.M. Órfão, J.L. Figueiredo, *Synthesis and characterization of manganese oxide catalysts for the total oxidation of ethyl acetate*. Top. Catal. **52** (2009) 470-481.

[5] V.P. Santos, M.F.R. Pereira, J.J.M. Órfão, J.L. Figueiredo, *Catalytic oxidation of ethyl acetate over a cesium modified cryptomelane catalyst*. Appl. Catal. B-Environ. **88** (2009) 550-556.

[6] M.I. Dominguez, P. Navarro, F. Romero-Sarria, D. Frias, S.A. Cruz, J.J. Delgado, M.A. Centeno, M. Montes, J.A. Odriozola, *Fibrous mno_2 nanoparticles with (2 x 2) tunnel structures. catalytic activity in the total oxidation of volatile organic compounds*. J. Nanosci. Nanotechnol. **9** (2009) 3837-3842.

[7] L. Lamaita, M.A. Peluso, J.E. Sambeth, H. Thomas, G. Mineli, P. Porta, *A theoretical and experimental study of manganese oxides used as catalysts for VOCs emission reduction*. Catal. Today **107-08** (2005) 133-138.

[8] L. Lamaita, M.A. Peluso, J.E. Sambeth, H.J. Thomas, *Synthesis and characterization of manganese oxides employed in VOCs abatement*. Appl. Catal. B-Environ. **61** (2005) 114-119.

[9] M.A. Peluso, L.A. Gambaro, E. Pronsato, D. Gazzoli, H.J. Thomas, J.E. Sambeth, *Synthesis and catalytic activity of manganese dioxide (type OMS-2) for the abatement of oxygenated VOCs*. Catal. Today **133-135** (2008) 487-492.

[10] S.L. Suib, *Structure, porosity, and redox in porous manganese oxide octahedral layer and molecular sieve materials*. J. Mater. Chem. **18** (2008) 1623-1631.

[11] M.A. Peluso, E. Pronsato, J.E. Sambeth, H.J. Thomas, G. Busca, *Catalytic combustion of ethanol on pure and alumina supported K-Mn oxides: An IR and flow reactor study*. Appl. Catal. B-Environ. **78** (2008) 70.

[12] Y.F. Shen, R.P. Zerger, R.N. Deguzman, S.L. Suib, L. McCurdy, D.I. Potter, C.L. Oyoung, *Manganese oxide octahedral molecular-sieves - Preparation, characterization, and applications*. Science **260** (1993) 511-515.

[13] S. Ching, S.L. Suib, *Synthetic routes to microporous manganese oxides*. Comments Inorganic Chem. **19** (1997) 263-282.

[14] S.L. Brock, N.G. Duan, Z.R. Tian, O. Giraldo, H. Zhou, S.L. Suib, *A review of porous manganese oxide materials*. Chem. Mater. **10** (1998) 2619-2628.

[15] Q. Feng, K. Yanagisawa, N. Yamasaki, *Hydrothermal soft chemical process for synthesis of manganese oxides with tunnel structures*. J. Porous Mat. **5** (1998) 153-161.

[16] R.N. Deguzman, Y.F. Shen, E.J. Neth, S.L. Suib, C.L. Oyoung, S. Levine, J.M. Newsam, *Synthesis and characterization of octahedral molecular-sieves (OMS-2) having the hollandite structure*. Chem. Mater. **6** (1994) 815-821.

[17] K.A. Malinger, Y.S. Ding, S. Sithambaram, L. Espinal, S. Gomez, S.L. Suib, *Microwave frequency effects on synthesis of cryptomelane-type manganese oxide and catalytic activity of cryptomelane precursor*. J. Catal. **239** (2006) 290-298.

[18] S. Ching, J.L. Roark, N. Duan, S.L. Suib, *Sol-gel route to the tunneled manganese oxide cryptomelane*. Chem. Mater. **9** (1997) 750-754.

[19] Y.S. Ding, X.F. Shen, S. Sithambaram, S. Gomez, R. Kumar, V.M.B. Crisostomo, S.L. Suib, M. Aindow, *Synthesis and catalytic activity of cryptomelane-type manganese dioxide nanomaterials produced by a novel solvent-free method*. Chem. Mater. **17** (2005) 5382-5389.

[20] Y.G. Yin, W.Q. Xu, R. Deguzman, S.L. Suib, C.L. Oyoung, *Studies of stability and reactivity of synthetic cryptomelane-like manganese oxide octahedral molecular-sieves*. Inorg. Chem. **33** (1994) 4384-4389.

[21] Y.G. Yin, W.Q. Xu, Y.F. Shen, S.L. Suib, C.L. Oyoung, *Studies of oxygen species in synthetic todorokite-like manganese oxide octahedral molecular-sieves*. Chem. Mater. **6** (1994) 1803-1808.

[22] Y.G. Yin, W.Q. Xu, S.L. Suib, C.L. Oyoung, *Lattice oxygen mobility and structural stability of ni and cu octahedral molecular-sieves having the cryptomelane structure*. Inorg. Chem. **34** (1995) 4187-4193.

[23] B. Levasseur, S. Kaliaguine, *Effects of iron and cerium in $La_{1-y}Ce_yCo_{1-x}Fe_xO_3$ perovskites as catalysts for VOC oxidation*. Appl. Catal. B-Environ. **88** (2009) 305-314.

[24] D.L. Bish, J.E. Post, *Thermal-behavior of complex, tunnel-structure manganese oxides*. Am. Miner. **74** (1989) 177-186.

[25] F. Kapteijn, L. Singoredjo, A. Andreini, J.A. Moulijn, *Activity and selectivity of pure manganese oxides in the selective catalytic reduction of nitric-oxide with ammonia*. Appl. Catal. B-Environ. **3** (1994) 173-189.

[26] W. Gac, *The influence of silver on the structural, redox and catalytic properties of the cryptomelane-type manganese oxides in the low-temperature CO oxidation reaction*. Appl. Catal. B-Environ. **75** (2007) 107-117.

[27] R. Xu, X. Wang, D.S. Wang, K.B. Zhou, Y.D. Li, *Surface structure effects in nanocrystal MnO_2 and Ag/MnO_2 catalytic oxidation of CO*. J. Catal. **237** (2006) 426-430.

[28] K. Jiratova, J. Mikulova, J. Klempa, T. Grygar, Z. Bastl, F. Kovanda, *Modification of Co-Mn-Al mixed oxide with potassium and its effect on deep oxidation of VOC*. Appl. Catal. A-Gen. **361** (2009) 106-116.

[29] H. Chen, A. Sayari, A. Adnot, F. Larachi, *Composition-activity effects of Mn-Ce-O composites on phenol catalytic wet oxidation*. Appl. Catal. B-Environ. **32** (2001) 195-204.

[30] V.R. Galakhov, M. Demeter, S. Bartkowski, M. Neumann, N.A. Ovechkina, E.Z. Kurmaev, N.I. Logachevskaya, Y.M. Mukovskii, J. Mitchell, D.L. Ederer, *Mn 3s exchange splitting in mixed-valence manganites*. Phys. Rev. B **65** (2002) 4.

[31] Y.J. Wei, L.Y. Yan, C.Z. Wang, X.G. Xu, F. Wu, G. Chen, *Effects of Ni Doping on MnO_6 Octahedron in $LiMn_2O_4$*. J. Phys. Chem. B **108** (2004) 18547-18551.

[32] V.P. Santos, S.S.T. Bastos, M.F.R. Pereira, J.J.M. Órfão, J.L. Figueiredo, *Stability of a cryptomelane catalyst in the oxidation of toluene*. Catal. Today (2010) doi:10.1016/j.cattod.2009.1012.1005.

[33] C. Cellier, V. Ruaux, C. Lahousse, P. Grange, E.M. Gaigneaux, *Extent of the participation of lattice oxygen from γ-MnO_2 in VOCs total oxidation: Influence of the VOCs nature*. Catal. Today **117** (2006) 350-355.

5 Catalytic Oxidation of Ethyl Acetate over a Cesium modified Cryptomelane Catalyst[1]

Cryptomelane-type manganese oxide was synthesised by redox reaction under acid and reflux conditions. Cesium was incorporated into the tunnel structure by the ion-exchange technique. The catalytic oxidation of ethyl acetate in low concentration was used to test the performance of the catalysts prepared. The presence of small amounts of cesium was found to improve the catalytic performance of cryptomelane. This behaviour was correlated with the basic properties of the catalyst. Temperature programmed experiments, and tests without oxygen in the feed, suggest that lattice oxygen atoms can react with ethyl acetate at low temperatures and are involved in the mechanism of ethyl acetate oxidation.

5.1 Introduction

Increasing concern about environmental and health effects resulting from emission of volatile organic compounds (VOC) has led to more stringent regulation standards, which require efficient and economic methods for VOC abatement [1]. Among the various methods that can be applied to efficiently control VOC emissions, catalytic oxidation seems to be the most efficient and cost-effective technology [2-4]. Catalyst formulation plays a key role towards the performance of the process.

Manganese oxides (β-MnO_2, γ-MnO_2, Mn_2O_3, Mn_3O_4) have been extensively studied as catalytic materials in the oxidation of many pollutants such as ethanol, acetone, propane and propene, ethyl acetate and CO [5-9]. Although the nature of the active sites for catalytic oxidation is not well established, several authors attribute their high catalytic activity to the mixed valence of framework manganese, and to the high mobility of oxygen species, implying the participation of the lattice oxygen in the reaction [10, 11]. Among the various manganese oxides studied, microporous manganese oxides with hollandite structure (cryptomelane, OMS-2) have received appreciable attention for over 50 years, due their exceptional catalytic properties and

[1] VP Santos, MFR Pereira, JJM Órfão, JL Figueiredo, Appl. Catal. B-Environ. 52 (2009) 470.

their shape-selective character [11-13]. Cryptomelane is a type of manganese oxide composed of 2 x 2 edge shared MnO_6 octahedral chains, which are corner connected to form one dimensional tunnels (0.46 nm x 0.46 nm). Manganese in the octahedra is mainly present as Mn(IV) and Mn(III), and cations such as K^+ and small amounts of water partially occupy the tunnel to provide charge balance and stabilize the tunnel structure [14, 15]. In order to further improve the electronic and catalytic properties, other metal cations have been introduced inside the tunnels or into the framework, by subsequent ion-exchange [16-20] or by substitution during synthesis [21-23]. The introduction of alkali metal into the tunnel can significantly modify the physical and chemical properties of cryptomelane, specially the surface acid-base properties [16]. Liu et al. [20] synthesized for the first time manganese oxides with Li^+, Na^+, Rb^+ as tunnel cations and found that the nature of the cation greatly influences the catalytic properties of OMS-2 towards total oxidation of cyclohexanol. Moreover, octahedral molecular sieves with Co^{2+}, Ag^+ and Cu^{2+} as tunnel cations showed high catalytic activities for CO oxidation at low temperatures [24, 25].

The effect of cesium cations on the catalytic activitiy of cryptomelane for the oxidation of ethyl acetate was the subject of this study. It was expected that the presence of cesium into the tunnel structure of crytpomelane would changes the surface acid-base properties and improve catalytic performance. A positive effect of alkali doping has been observed by several researchers in various systems [19, 26, 27] and has been related to the basic and acid surface properties of the catalyst and with the possible creation of new reaction pathways.

5.2 Experimental

5.2.1 Synthesis

Cryptomelane-type manganese oxide (K-OMS-2) was synthesized using the reflux approach in acidic medium [12]. Cesium was incorporated into the tunnel structure by ion-exchange (sample Cs,K-OMS-2): 1 g of cryptomelane was stirred with 30 mL of 0.5 M solution of $CsNO_3$ (Aldrich) for 24 hours. Every 4 hours a fresh solution was added to improve the ion-exchange process. The solid obtained was filtered and

washed with distilled water, followed by drying at 100 ºC and calcination at 450 ºC in air for 4.5 hours.

5.2.2 Characterization

The structure, morphology, composition and texture of all samples were characterized by X-ray diffraction (XRD), scanning electron microscopy (SEM), inductively coupled plasma atomic emission spectroscopy (ICP-AES) and nitrogen adsorption, respectively. The thermal stability was studied by thermogravimetric analysis (TGA) under nitrogen atmosphere and temperature programmed desorption / mass spectroscopy (TPD/MS) under helium atmosphere. The average oxidation state of manganese and the basicity of O_2^- sites were determined by X-ray photoelectron spectroscopy (XPS).

5.2.2.1 Structure and morphology

The structure and phase purity of the prepared materials were analysed by X-ray diffraction using a PANalytical X´Pert PRO diffractometer with Cu K_α radiation source (λ=1.54 nm) and with a beam voltage of 50 kV and 40 mA of beam current. The data were collected in the 2θ range of 10º-100º with a scanning rate of 0.017 º/s. The morphology of the materials was studied by field emission scanning electron microscopy (FEG-ESEM) on a FEI Quanta 400FEG / EDAX Genesis X4M with a Schottky Emitter at an accelerating voltage of 10 kV.

5.2.2.2 Chemical Composition

Manganese analyses were performed by inductively coupled plasma spectroscopy on a Plasma Perkin–Elmer Optima 2000 DV, while the potassium and cesium analyses were performed by atomic emission spectroscopy on a Perkin-Elmer AAnalyst 300. Prior to the analysis about 20 mg of sample were dissolved into an acqua regia solution, and the mixture was then diluted with water.

5.2.2.3 Nitrogen Adsorption

Nitrogen adsorption isotherms at liquid nitrogen temperature were obtained with a Quantachrome Instruments Nova 4200e. The samples were previously degassed at 300 ºC for 3 h.

5.2.2.4 Thermal Stability

Thermogravimetric analysis (TGA) was done on a Mettler TA 4000 system under air or nitrogen atmosphere. About 10 mg of sample were loaded into a ceramic sample holder and the temperature was raised to 900ºC at 10 ºC/min. Thermal stability of the materials was also studied by temperature programmed desorption combined with a mass spectrometer (TPD-MS). These experiments were conducted on an Altamira Instruments (AMI 200) apparatus. 100 mg of sample were loaded in the reactor and placed inside the furnace. The sample was purged with helium for 1 hour at room temperature followed by heating to 900 ºC at 5 ºC/min in the same atmosphere.

5.2.2.5 Average oxidation state and basicity of O_2^- sites

The average oxidation state of manganese in all materials was obtained by XPS. XPS analysis was performed with a VG Scientific ESCALAB 200A spectrometer using Al $K_{\square}$ radiation (1486.6 eV). Charging effects were corrected by adjusting the binding energy of C 1s to 284.6 eV.

5.2.3 Catalytic Experiments

The catalytic oxidation of ethyl acetate was performed under atmospheric pressure in a fixed-bed reactor from Autoclave Engineers (BTRS Jr), which consists of a stainless steel tube of 6 mm internal diameter, placed inside a temperature-controlled electric furnace. A feed gas with a VOC concentration of 4,000 mgC/m^3 and a space velocity of 16,000 h^{-1} was used in standard tests. The catalyst sample (50 mg) was diluted with glass spheres of the same size as the catalyst particles (0.2-0.5 mm), in order to minimize temperature gradients.

The reaction temperature was raised by steps of 10 ºC, from 160 to 220 ºC. The reactor was maintained at each temperature for 30 minutes in order to obtain

experimental values at steady state. The conversion of ethyl acetate (X) and the conversion into CO_2 (X_{CO_2}) were respectively calculated as $X = 1 - \frac{F_{VOC}}{F_{VOC,in}}$ and $X_{CO_2} = \frac{F_{CO_2}}{\nu F_{VOC,in}}$, where F_{VOC} is the outlet molar flow rate of VOC at steady state, $F_{VOC,in}$ is the inlet molar flow rate of VOC, F_{CO_2} is the outlet molar flow rate of CO_2 at steady state and ν is the number of carbon atoms in the VOC molecule (ν = 4).

The analytical system consisted of a gas chromatograph equipped with a flame ionization detector (FID) for the analysis of the organic compounds, and an online non-dispersive infrared (NDIR) analyzer for CO_2.

The carbonaceous compounds retained in the catalyst ("coke") were quantified by temperature programmed oxidation (TPO) and temperature programmed desorption (TPD) techniques.

Temperature programmed experiments were also conducted after adsorption of ethyl acetate at 40 ºC from a nitrogen stream. After saturation, the catalyst was purged with helium and the experiment started. The temperature was increased at 10 ºC/min to 500 ºC. The products were analysed by MS.

5.3 Results and discussion

5.3.1 Catalysts characterization

Figure 5.1 shows the XRD patterns for K-OMS-2 and Cs,K-OMS-2 materials. All the diffraction peaks correspond to the pure cryptomelane phase [28]. It was expected that the incorporation of cesium would increase the unit cell volume, due the higher ionic radius of cesium compared to potassium cations, as reported by Nur et al. [29] for the incorporation of Ti^{4+}. The unit cell volumes were obtained by calculation of the cell parameters (a, b and c) assuming tetragonal geometry:

$$\frac{1}{(d_{hkl})^2} = \frac{h^2 + k^2}{a^2} + \frac{l^2}{c^2} \qquad (5.1)$$

where d_{hkl} is the interplanar distance and hkl are the Miller indices. The lattice parameters were determined by selecting two diffractogram lines (θ = 12.7 º

(110) and θ = 37.5 º (211)) and solving the equations. The unit cell volumes obtained for K-OMS-2 (274 $Å^3$) and Cs,K-OMS-2 (277 $Å^3$), confirm the incorporation of cesium.

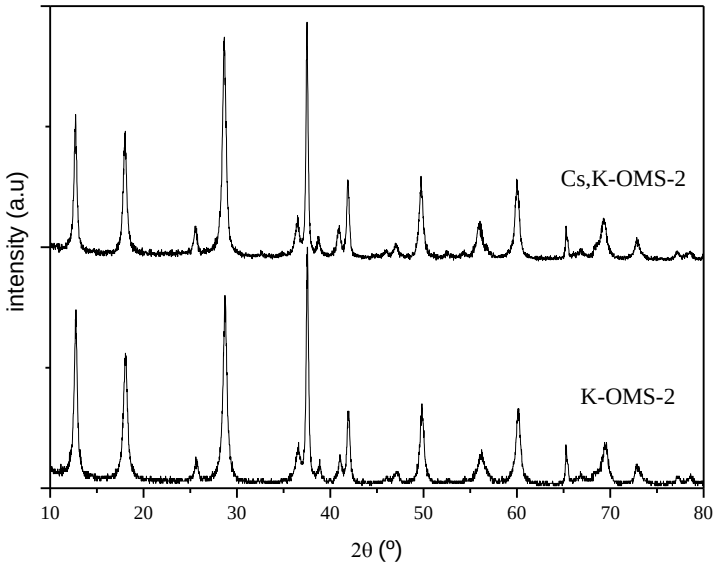

Figure 5.1 X-ray diffraction patterns of the K-OMS-2 and Cs,K-OMS-2 materials.

The presence of cesium does not change the characteristic morphology of cryptomelane, showing very long nanofibers with diameters in the range 10-20 nm (Figure 5.2).

The stability of the materials was evaluated by TGA and TPD/MS experiments; as can be observed in Figure 5.3, the incorporation of cesium into the tunnel structure does not significantly affect the cryptomelane stability (both materials show a weight loss of about 11%). The first weight loss occurs in the range of 90-200 ºC (about 1%, for both materials), and is due to physically adsorbed water, as shown by TPD/MS analysis. Weight losses at higher temperatures (about 10 %) are due to the evolution of oxygen species from the lattice, as confirmed by TPD/MS [30-32]. In nitrogen flow, the evolution of oxygen at temperatures higher than 500 ºC promotes the decomposition of cryptomelane into Mn_2O_3 and then into Mn_3O_4 [33].

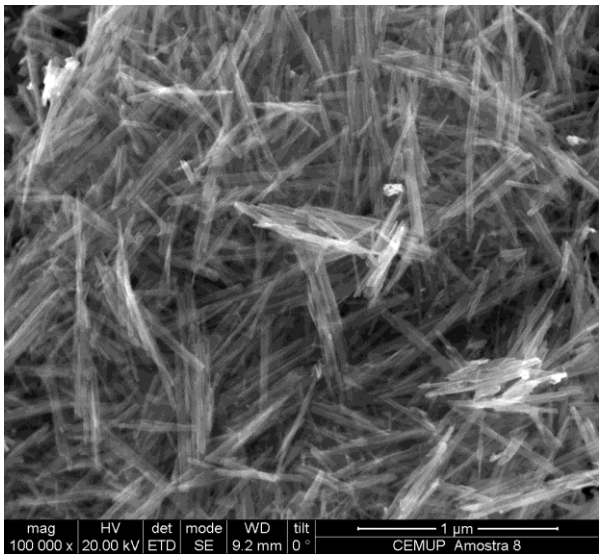

Figure 5.2 SEM image of the K-OMS-2 material.

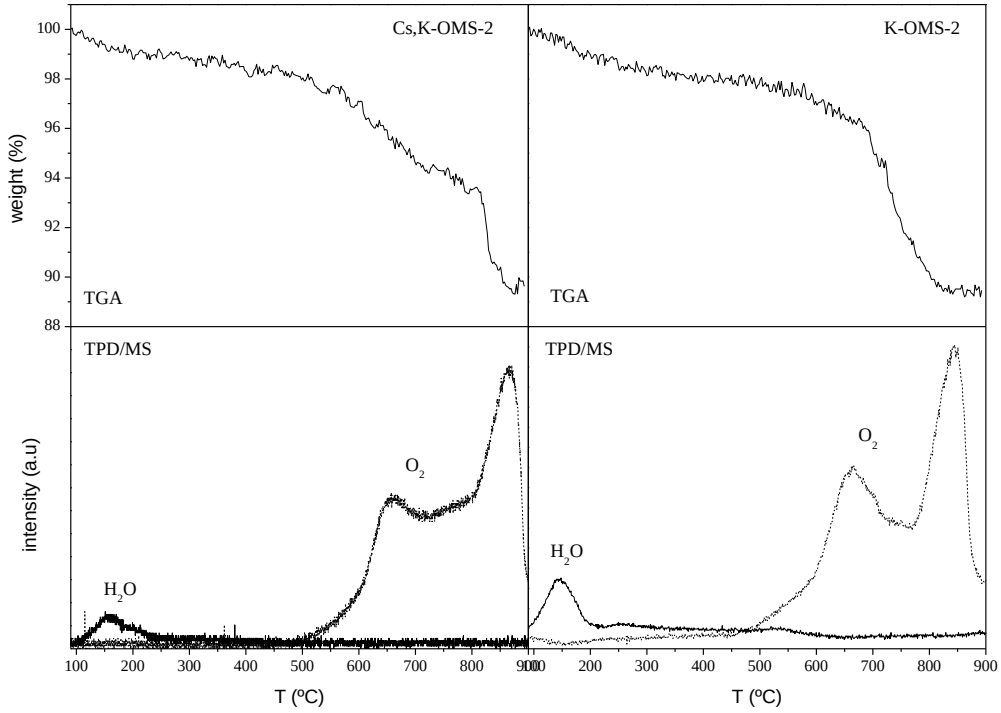

Figure 5.3 TGA and TPD/MS experiments under nitrogen and helium, respectively.

The average oxidation state of manganese (AOS) was obtained from the difference of binding energies between the Mn 3s peak and its satellite [34, 35]. It is well known that for manganese oxides it is insufficient to employ the BE shifts of the Mn $2p_{3/2}$ to clearly distinguish the various manganese species (Mn(II), Mn(III) and Mn(IV)) [36]. As an alternative, Galakov et al. [34] showed that it is possible to obtain the manganese valence by studying the Mn 3s x-ray photoelectron spectra. The splitting of the 3*s* core-level x-ray photoemission spectra in transition metals and their compounds results from the exchange coupling between the 3*s* hole and the 3*d* electrons. The magnitude of the splitting is proportional to (2*S*+1), where *S* is the local spin of the 3*d* electrons in the ground state. This means that the binding energy for the 3s multiplet splitting of the manganese ion depends on the number of 3d electrons [34]. The same authors show that the energy difference (ΔEs) between the main peak and its satellite decreases monotically with the increase of the average oxidation state (AOS) of the manganese ions (except the region from Mn^{3+} to $Mn^{3.3+}$). The following relationship was obtained from the data in reference [34], which was used in the present work to calculate the AOS for both materials:

$$AOS = 8.956 - 1.126\Delta E_s(eV) \tag{5.1}$$

As can be seen in Table 5.1, the AOS of both materials is 3.9, which is in agreement with other authors [28]. This result suggests that Mn (IV) is dominant in both materials, and the influence of cesium incorporation on the average oxidation state of manganese is not significant.

The basic strength of the framework oxygen in all materials was also studied by XPS (Figure 5.4). It is well known that there is a relationship between the O1s binding energy determined by XPS and the intermediate electronegativities (S_{int}) [37]. The lower the O1s BE, the lower is S_{int} (and the higher the basic strength) [38]. As can be seen in Figure 5.4, the presence of cesium shifts the O1s peak from 529.6 to 529.4 eV. This might indicate an increase of the catalyst surface basic strength. However, it should be mentioned that this difference is in the limit of the experimental error (± 0.2).

The bulk chemical compositions of both materials were determined by ICP/AES and are listed in Table 5.1. It may be observed that the bulk K/Mn atomic ratio in Cs,K-OMS-2 is lower than that of K-OMS-2, indicating a partial exchange with the cesium cations.

Relatively to the texture of the materials, it seems that the incorporation of cesium into the tunnel structure does not have a major influence in the surface area of the materials (see S_{BET} in Table 5.1).

Table 5.1 Properties of the catalysts.

Sample	Mn 3s ΔE_s (eV)	AOS	S_{BET} (m^2/g)	Chemical Composition (ICP/AES)
K-OMS-2	4.50	3.89	45	$K_{0.12}MnO_2$
Cs,K-OMS-2	4.49	3.90	43	$K_{0.09}Cs_{0.03}MnO_2$

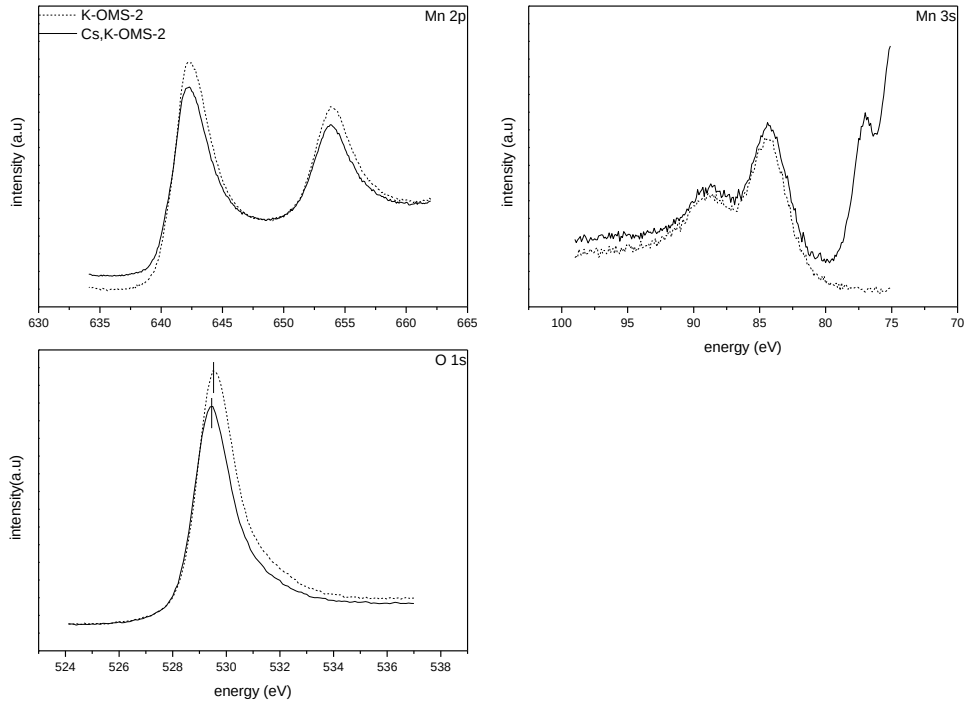

Figure 5.4 Mn 2p, Mn 3s and O 1s XPS of the K-OMS-2 and Cs,K-OMS-2 samples.

5.3.2 Catalytic activities

The catalytic oxidation of ethyl acetate was studied over K-OMS-2 and Cs,K-OMS-2 catalysts. The ethyl acetate conversion (X) and the conversion into CO_2 (X_{CO2}), as a function of the reaction temperature, are shown in Figure 5.5 for both catalysts.

Over the Cs,K-OMS-2 catalyst, the oxidation of ethyl acetate starts near 160 ºC, reaching 100 % conversion into CO_2 at 200 ºC. With the K-OMS-2 catalyst, ethyl acetate oxidation starts at the same temperature, but complete oxidation into CO_2 and H_2O only occurs at a temperature 20 ºC higher than that of the cesium dopped catalyst. The CO_2 selectivity (defined as X_{CO2}/X) is not significantly affected by the presence of cesium. In both systems, the CO_2 selectivity was not 100% due to the formation of some oxygenated products: acetaldehyde was the major by-product detected, together with minor amounts of acetone. CO was never produced. Acetic acid, which could also be produced, could not be detected under the experimental conditions used.

In summary, it can be stated that the incorporation of cesium into the tunnel structure of cryptomelane improves the catalytic performance of this material.

The positive effect of alkali doping has also been observed by other authors in various reactions systems [19, 26, 27, 39]. This effect has been ascribed to the basic and acid surface properties of the catalysts and with the possible creation of new reaction pathways. Gandía et al. [19] studied the catalytic oxidation of acetone and methyl-ethyl-ketone over Mn_2O_3 catalysts. They found that when this oxide is modified by alkali additives, like Na or Cs, the conversion is shifted to lower temperatures. They attributed this behaviour to the formation of strongly bound enolic species that can also undergo aldol condensation, producing compounds that remain adsorbed on the catalyst. The presence of Cs and Na favours the oxidation of these adsorbed species on the catalyst surface, reducing the combustion temperatures. The characterization results, namely the O 1s XPS spectrum of the two catalysts, might support this theory. As can be seen from Figure 5.4, the presence of cesium shifts the binding energy to lower values, suggesting an increase in the surface basicity of the catalyst [27]. In order to analyse the effect of cesium on the oxidation of adsorbed species, TPO and TPD analyses were performed.

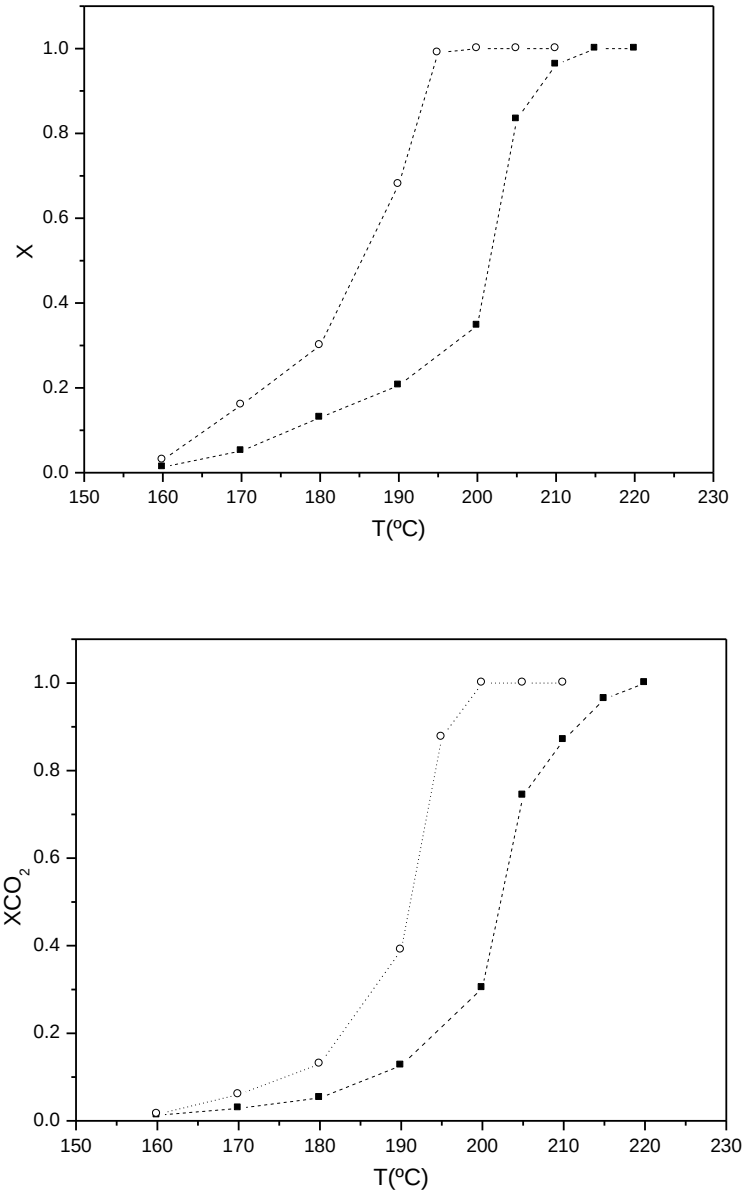

Figure 5.5 Conversion of ethyl acetate (X) and conversion into CO_2 (XCO_2) as a function of reaction temperature over catalysts K-OMS-2 (filled symbols) and Cs,K-OMS-2 (open symbols).

5.3.3 Temperature programmed experiments

The amount of adsorbed species deposited on the catalyst surface during the oxidation of ethyl acetate (generally designated as "coke") was measured by temperature programmed oxidation in air (TPO).

Figure 5.6a shows the TPO profiles after 1 h reaction at 160 ºC for K-OMS-2 and Cs,K-OMS-2 catalysts. A single peak was observed, with maximum at 214 ºC and 180 ºC, for K-OMS-2 and Cs,K-OMS-2, respectively. This result suggests that the presence of cesium renders the adsorbed products more reactive towards oxidation. Similar TPO profiles were obtained at 180 and 200 ºC, only CO_2 being detected, in all cases.

Figure 5.6b shows the carbon content after 1 hour reaction at different temperatures (160, 180 and 200 ºC), determined by integration of the TPO curves. It may be observed that the amount of adsorbed species in both catalysts decreases as the temperature increases.

Some TPO experiments were also performed in the K-OMS-2 catalyst, after stopping the reaction (180 ºC) at different times: 5, 30, 60 minutes and 15 hours, in order to analyse the evolution of the adsorbed species. It was observed that the carbon content remained constant after 30 minutes of reaction. This means that the net amount of retained compounds at steady state is negligible, suggesting that the major part of it consists of adsorbed reactant. This behaviour is essential to promote the stability of manganese oxide for long duration runs.

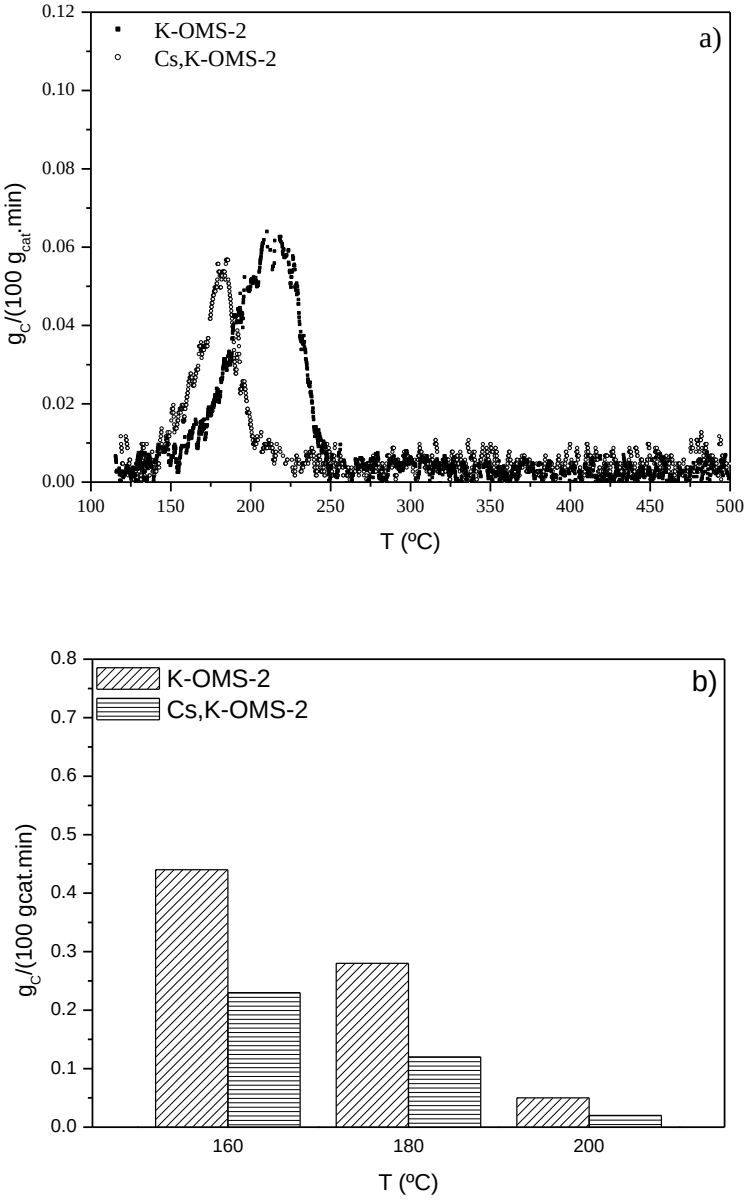

Figure 5.6 a) TPO curve after ethyl acetate oxidation at 160 ºC over catalysts K-OMS-2 and Cs,K-OMS-2. b) "Coke" content obtained by TPO after ethyl acetate oxidation at 160, 180 and 200 ºC over catalysts K-OMS-2 and Cs,K-OMS-2.

Figure 5.7 shows two profiles obtained after 1 hour reaction at 180 ºC with K-OMS-2, one in air (TPO) and the other in helium (TPD). Surprisingly, there was no desorption of ethyl acetate in the TPD experiment, only CO_2 being detected, with a peak at 300 ºC; the corresponding TPO shows a peak at 245 ºC. This suggests that lattice oxygen is involved in the total oxidation of ethyl acetate. A similar behaviour was also observed in the oxidation of benzene and CO over cryptomelane [15].

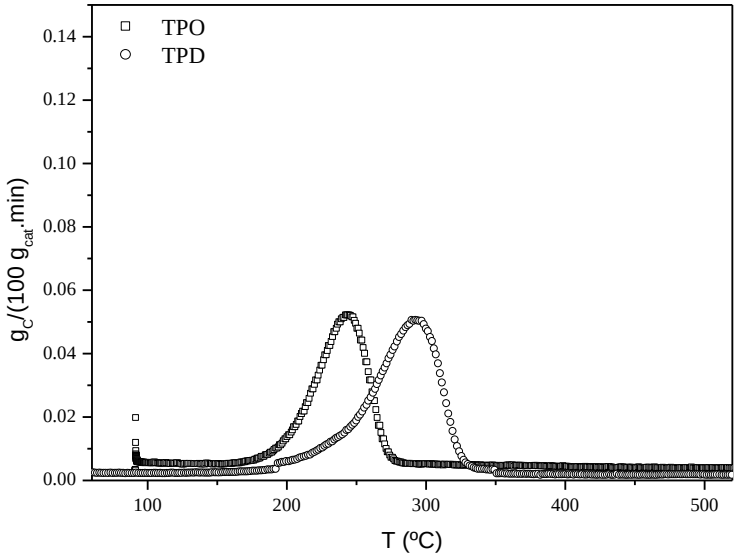

Figure 5.7 Temperature programmed oxidation (TPO) and temperature programmed desorption (TPD) after reaction at 180 ºC over the K-OMS-2 catalyst.

In order to support this hypothesis, additional experiments in the absence of oxygen were made in both systems, namely, a temperature programmed experiment (in helium) after adsorption of ethyl acetate at room temperature. The results obtained over both catalysts can be observed in Figure 5.8. Desorption of ethyl acetate or other oxygenated products (such as ethanol, acetaldehyde, acetic acid and acetone) was not observed in this experiment, even at lower temperatures, which may indicate the absence of strong acid sites. The only products detected were H_2O and CO_2, probably formed during the oxidation of adsorbed ethyl acetate by lattice oxygen. Moreover, two peaks of CO_2 were detected in both systems, (237 ºC and 304 ºC, for K-OMS-2 catalyst and 209 ºC and 290 ºC for Cs,K-OMS-2 catalyst) which may indicate the

presence of two types of adsorption sites. As can be observed, with the cesium modified catalyst the two CO_2 peaks were shifted to 209 ºC and 290 ºC, confirming that cesium facilitates the oxidation of the adsorbed compounds.

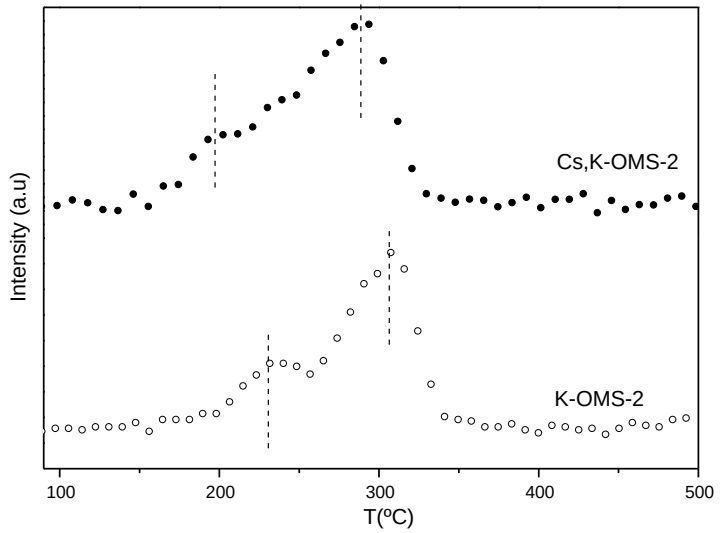

Figure 5.8 Temperature programmed experiment (in helium) after adsorption of ethyl acetate at 40 ºC over the K-OMS-2 and Cs,K-OMS-2 catalysts. The m/z = 44 signal is **represented**.

5.3.4 Reaction without oxygen in the feed

In order to study the effect of the lattice oxygen on the mechanism of ethyl acetate oxidation, successive tests over K-OMS-2 without oxygen in the feed were performed at 220 ºC. In each cycle, prior to the reaction, the catalyst was activated in air at the reaction temperature. The activation time was 1 hour in the first and second cycles, and 30 minutes in the third. The reactor was then purged with nitrogen in order to remove any oxygen physisorbed on the catalyst.

Figure 5.9 shows the results of this experiment. It can be observed that the conversion into CO_2 sharply increases, reaching a maximum value and then decreases. The behaviour is the same in the first two cycles. In the third cycle, deactivation is faster.

These results show that lattice oxygen species are involved in the mechanism of ethyl acetate oxidation, and that during the activation period there is an incorporation of oxygen into the catalyst lattice, which explains why the catalytic activity is recovered.

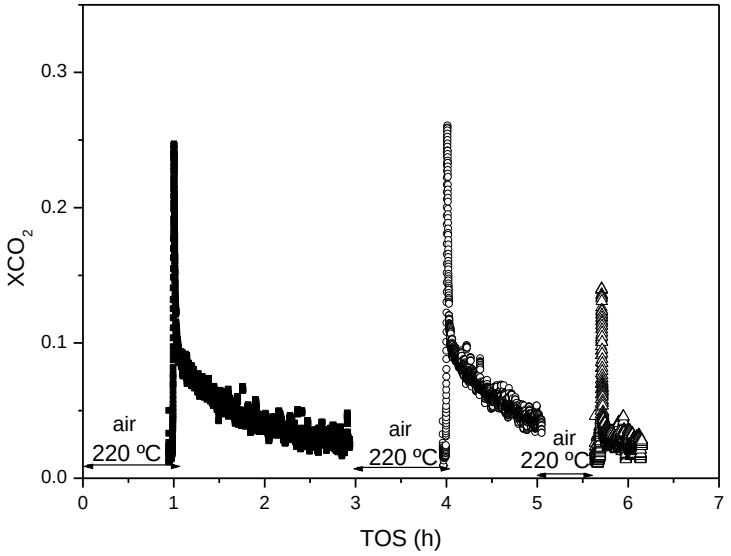

Figure 5.9 Influence of the activation conditions on the conversion into CO_2 over catalyst K-OMS-2 at 220 ºC without oxygen in the feed.

5.3.5 Stability experiments

The stability of the cesium modified catalyst was evaluated in long duration experiments. The conversion into CO_2 at 195 and 210 ºC as a function of time on stream (TOS) is shown in Figure 5.10. The histories of conversion into CO_2 are similar to those obtained by the light-off curves (XCO_2 = 0.87 and XCO_2 = 1.0 at 195 and 210 ºC, respectively). It seems that there is no stabilization period and the conversion into CO_2 remains constant during the experiment. This result shows that cesium modified catalyst is stable.

Some tests were also made in order to evaluate the performance of the catalyst after being used and treated in air up to 500 ºC. It was observed that there was no deactivation after the regeneration treatments.

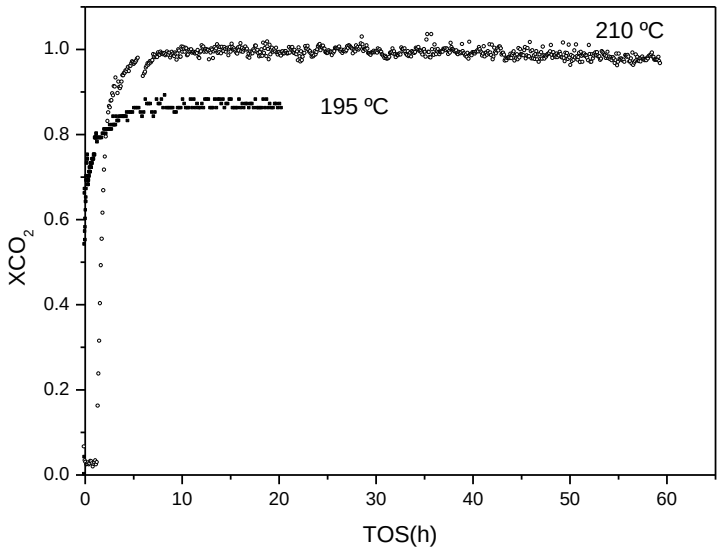

Figure 5.10 Influence of time on stream (TOS) on the conversion into CO_2 over Cs,K-OMS-2 at 195 and 210 ºC.

5.4 Conclusions

K-OMS-2 is active for the oxidation of ethyl acetate into CO_2.

The incorporation of cesium into the tunnel structure improves the performance of K-OMS-2 catalyst in the oxidation of ethyl acetate. This improvement may be correlated to the enhanced basic properties of the catalyst.

Both catalysts are relatively stable during long duration experiments, but the addition of cesium further enhances the stability of the catalyst.

Lattice oxygen atoms are involved in the mechanism of ethyl acetate oxidation.

References

[1] R. Atkinson, *Atmospheric chemistry of VOCs and NO_x.* Atmos. Environ. 34 (2000) 2063-2101.

[2] E.C. Moretti, N. Mukhopadhyay, *VOC control: current practices and future trends.* Chem. Eng. Prog. 89 (1993) 20-26.

[3] E.N. Ruddy, L.A. Carroll, *Select the best VOC control strategy.* Chem. Eng. Prog. 89 (1993) 28-35.

[4] K. Everaert, J. Baeyens, *Catalytic combustion of volatile organic compounds.* J. Hazard. Mater. 109 (2004) 113-139.

[5] C. Lahousse, A. Bernier, P. Grange, B. Delmon, P. Papaefthimiou, T. Ioannides, X. Verykios, *Evaluation of γ-mno$_2$ as a voc removal catalyst: comparison with a noble metal catalyst.* J. Catal. 178 (1998) 214-225.

[6] K.M. Parida, A. Samal, *Catalytic combustion of volatile organic compounds on Indian Ocean manganese nodules.* Appl. Catal. A-Gen. 182 (1999) 249-256.

[7] E. Finocchio, G. Busca, *Characterization and hydrocarbon oxidation activity of coprecipitated mixed oxides Mn_3O_4/Al_2O_3.* Catal. Today 70 (2001) 213-225.

[8] L. Lamaita, M.A. Peluso, J.E. Sambeth, H. Thomas, G. Mineli, P. Porta, *A theoretical and experimental study of manganese oxides used as catalysts for VOCs emission reduction*. Catal. Today 107-08 (2005) 133-138.

[9] L. Lamaita, M.A. Peluso, J.E. Sambeth, H.J. Thomas, *Synthesis and characterization of manganese oxides employed in VOCs abatement.* Appl. Catal. B-Environ. 61 (2005) 114-119.

[10] C. Cellier, V. Ruaux, C. Lahousse, P. Grange, E.M. Gaigneaux, *Extent of the participation of lattice oxygen from γ-MnO_2 in VOCs total oxidation: Influence of the VOCs nature*. Catal. Today 117 (2006) 350-355.

[11] J. Luo, Q. Zhang, J. Garcia-Martinez, S.L. Suib, *Adsorptive and acidic properties, reversible lattice oxygen evolution and catalytic mechanism of cryptomelane-type manganese oxides as oxidation catalysts*. J. Am. Chem. Soc. 130 (2008) 3198-3207.

[12] J. Luo, Q. Zhang, A. Huang, S.L. Suib, *Total oxidation of volatile organic compounds with hydrophobic cryptomelane-type octahedral molecular sieves*. Micropor. Mesopor. Mat. **35-36** (2000) 209-217.

[13] F.N. Aguero, A. Scian, B.P. Barbero, L.E. Cadus, *Combustion of volatile organic compounds over supported manganese oxide: Influence of the support, the precursor and the manganese loading.* Catal. Today 133-135 (2008) 493-501.

[14] S.L. Suib, *Microporous manganese oxides.* Curr. Opin. Solid State Mat. Sci. 3 (1998) 63-70.

[15] S.L. Suib, *Structure, porosity, and redox in porous manganese oxide octahedral layer and molecular sieve materials*. J. Mater. Chem 18 (2008) 1623-1631.

[16] Y.F. Shen, S.L. Suib, C.L. Oyoung, *Effects of inorganic cation templates on octahedral molecular sieves of manganese oxide.* J. Am. Chem. Soc. 116 (1994) 11020-11029.

[17] Q. Feng, H. Kanoh, Y. Miyai, K. Ooi, *Alkali metal Ions insertion/extraction reactions with hollandite-type manganese oxide in the aqueous phase.* Chem. Mater. 7 (1995) 148-153.

[18] J. Cai, J. Liu, W.S. Willis, S.L. Suib, *Framework doping of iron in tunnel structure cryptomelane.* Chem. Mater. 13 (2001) 2413-2422.

[19] L.M. Gandia, A. Gil, S.A. Korili, *Effects of various alkali–acid additives on the activity of a manganese oxide in the catalytic combustion of ketones.* Appl. Catal. B-Environ. 33 (2001) 1-8.

[20] J. Liu, V. Makwana, J. Cai, S.L. Suib, M. Aindow, *Effects of alkali metal and ammonium cation templates on nanofibrous cryptomelane-type manganese oxide octahedral molecular sieves (OMS-2*). J. Phys. Chem. B 107 (2003) 9185-9194.

[21] X. Chen, Y.F. Shen, S.L. Suib, C.L. O'Young, *Catalytic decomposition of 2-propanol over different metal-cation-doped OMS-2 materials.* J. Catal. 197 (2001) 292-302.

[22] J. Liu, Y.C. Son, J. Cai, X.F. Shen, S.L. Suib, M. Aindow, Size control, *metal substitution, and catalytic application of cryptomelane nanomaterials prepared using cross-linking reagents.* Chem. Mater. 16 (2004) 276-285.

[23] W. Gac, *The influence of silver on the structural, redox and catalytic properties of the cryptomelane-type manganese oxides in the low-temperature CO oxidation reaction.* Appl. Catal. B-Environ. 75 (2007) 107-117.

[24] E. Nicolas-Tolentino, Z.R. Tian, H. Zhou, G.G. Xia, S.L. Suib, *Effects of Cu^{2+} Ions on the structure and reactivity of todorokite- and cryptomelane-type manganese oxide octahedral molecular sieves.* Chem. Mater. 11 (1999) 1733-1741.

[25] R. Hu, Y. Cheng, L. Xie, D. Wang, *Effect of doped Ag on performance of manganese oxide octahedral molecular sieve for CO Oxidation.* Chin. J. Catal. 28 (2007) 463-468.

[26] C.H. Lee, Y.W. Chen, *Effect of additives on Pd/Al_2O_3 for CO and propylene oxidation at oxygen-deficient conditions.* Appl. Catal. B-Environ. 17 (1998) 279-291.

[27] J. Tsou, P. Magnoux, M. Guisnet, J.J.M. Órfão, J.L. Figueiredo, *Catalytic oxidation of methyl-isobutyl-ketone over basic zeolites.* Appl. Catal. B-Environ. 51 (2004) 129-133.

[28] R.N. Deguzman, Y.F. Shen, E.J. Neth, S.L. Suib, C.L. Oyoung, S. Levine, J.M. Newsam, Synthesis and characterization of octahedral molecular sieves (OMS-2) having the hollandite structure. Chem. Mater. 6 (1994) 815-821.

[29] H. Nur, F. Hayati, H. Hamdan, *On the location of different titanium sites in Ti–OMS-2 and their catalytic role in oxidation of styrene.* Catal. Commun. 8 (2007) 2007-2011.

[30] Y.G. Yin, W.Q. Xu, R. Deguzman, S.L. Suib, C.L. Oyoung, *Studies of stability and reactivity of synthetic cryptomelane-like manganese oxide octahedral molecular-sieves*. Inorg. Chem. **33** (1994) 4384-4389.

[31] Y.G. Yin, W.Q. Xu, Y.F. Shen, S.L. Suib, C.L. Oyoung, *Studies of oxygen species in synthetic todorokite-like manganese oxide octahedral molecular-sieves*. Chem. Mater. **6** (1994) 1803-1808.

[32] Y.G. Yin, W.Q. Xu, S.L. Suib, C.L. Oyoung, *Lattice oxygen mobility and structural stability of ni and cu octahedral molecular-sieves having the cryptomelane structure*. Inorg. Chem. **34** (1995) 4187-4193.

[33] D.L. Bish, J.E. Post, *Thermal-behavior of complex, tunnel-structure manganese oxides*. Am. Miner. **74** (1989) 177-186.

[34] V.R. Galakhov, M. Demeter, S. Bartkowski, M. Neumann, N.A. Ovechkina, E.Z. Kurmaev, N.I. Logachevskaya, Y.M. Mukovskii, J. Mitchell, D.L. Ederer, *Mn 3s exchange splitting in mixed-valence manganites*. Phys. Rev. B **65** (2002) 4.

[35] I. Barrio, I. Legorburu, M. Montes, M.I. Dominguez, M.A. Centeno, J.A. Odriozola, *New redox deposition-precipitation method for preparation of supported manganese oxide catalysts.* Catal. Lett. 101 (2005) 151-157.

[36] M.L. Rojas, J.L.G. Fierro, L.G. Tejuca and A.T. Bell, *Preparation and characterization of $LaMn_{1-x}Cu_xO_3$ Perovskite oxides*. J. Catal. 124 (1990) 41.

[37] J. Weitkamp, M. Hunger, U. Rymsa, *Base catalysis on microporous and mesoporous materials: recent progress and perspectives*. Micropor. Mesopor. Mat. 48 (2001) 255-270.

[38] Y. Okamoto, M. Ogawa, A. Maezawa, T. Imanaka, *Electronic structure of zeolites studied by X-Ray photoelectron spectroscopy*. J. Catal. 112 (1988) 427-436.

[39] C.A. Querini, L.M. Cornaglia, M.A. Ulla, E.E. Miro, *Catalytic combustion of diesel soot on Co,K/MgO catalysts. Effect of the potassium loading on activity and stability.* Appl. Catal. B-Environ. 20 (1999) 165-177.

6 Stability of a Cryptomelane catalyst in the Oxidation of Toluene[1]

The oxidation of toluene over a cryptomelane (K-OMS-2) catalyst was investigated at temperatures between 100 and 300 ºC. The catalyst was tested both in temperature-programmed experiments (light-off curves) and in isothermal tests.

The carbonaceous deposits retained in the porous structure after the isothermal tests were evaluated by temperature programmed oxidation. The results show that gradual deactivation occurs at temperatures below 268 ºC (which corresponds to the peak maximum in the TPO curves). Besides deactivation, the catalyst also shows an oscillatory behaviour in the conversion into CO_2 in a restricted temperature range (252-258 ºC).

TPD experiments after adsorption of toluene at room temperature show that this compound is strongly retained in the porous structure up to high temperatures, which can explain the deactivation and the unstable behaviour. For comparative purposes, TPD after adsorption of ethyl acetate was also carried out, and it was observed that this compound was not retained as much as toluene, no oscillations being detected.

6.1 Introduction

Manganese oxides with octahedral molecular sieve structure (OMS-2) are considered very active catalysts for the oxidation of volatile organic compounds [1-4]. Their catalytic properties are related to the mixed valence of manganese into the framework of the catalyst and to the high mobility of oxygen species [4,5].

In industrial applications, catalyst stability and durability are as important as activity and selectivity. Therefore, catalyst deactivation must be prevented as much as possible. An overview of catalyst deactivation was presented by Butt et al. [6]. In the case of catalytic oxidation, several mechanisms can lead to deactivation: (i)

[1] VP Santos, SST Bastos, MFR. Pereira, JJM. Órfão, JL Figueiredo, Catal. Today, (2010) doi: 10.1016/j.cattod.2009.12.005.

volatilization of catalyst species; (ii) poisoning; (iii) formation of coke deposits and (iv) thermal degradation.

The formation of carbonaceous deposits (coke) inside the pores or on the outer surface is the main cause of deactivation during transformation of organic reactants in molecular sieves [7,8]. When the coke precursors are strongly retained in the porous structure, besides deactivation, the catalyst may also become unstable, showing an oscillatory behaviour. Tsou et al. [9,10] have studied in detail the origin of this oscillatory behaviour in the oxidation of some VOC compounds over zeolite-based catalysts. Accumulation of coke was found to be at the origin of oscillations; on the other hand, this was found to be related to the adsorption properties of the support. In particular, a support which is capable of retaining the VOC at temperatures higher than the reaction temperature may lead to oscillations in the apparent conversion into CO_2. In this context, it is also interesting to refer the work of Paulis et al. [11]. These authors studied the influence of adsorption and desorption processes in the oxidation of toluene and acetone over Pd/Al_2O_3, Mn_2O_3/Al_2O_3 and Mn_2O_3/SiO_2 catalysts. The corresponding light-off curves show apparent conversions into CO_2 which are higher than 100 %. These results were also explained in terms of the accumulation of coke at low temperatures. It may be concluded that the oscillations observed in isothermal tests and the CO_2 peak (conversions higher than 100%) in the light-off curves are different manifestations of the same phenomenon.

The aim of the present report is to study the stability of the cryptomelane catalyst in the oxidation of toluene. For that purpose, isothermal tests at selected temperatures were carried out. TPD and TPO after adsorption of toluene were also performed in order to assess the strength of the adsorption. For comparative purposes, similar experiments were carried out with ethyl acetate.

6.2 Experimental

6.2.1 Catalyst preparation and characterization

Cryptomelane-type manganese oxide (K-OMS-2) was synthesized by the reflux method developed by Luo et al. [3]. The structure, morphology, composition and

texture were characterized by X-ray diffraction (XRD), scanning electron microscopy (SEM), inductively coupled plasma/atomic emission spectroscopy (ICP-AES) and nitrogen adsorption, respectively. The average oxidation state (AOS) of manganese was determined by X-ray photoelectron spectroscopy (XPS) based on a correlation between the binding energies of the doublet separation of Mn3s (ΔEs) and the AOS proposed by Galakhov et al. [12]. Catalyst synthesis and characterization are explained in detail elsewhere [2].

A summary of the catalyst characterization results is presented in Table 6.1.

Table 6.1 Properties of K-OMS-2

Sample	AOS	S (m^2/g) [a]	V_p (cm^3/g)[a]	Chemical Composition (ICP/AES)
K-OMS-2	3.89	50	0.141	$K_{0.13}MnO_2$

[a] Calculated by the BJH method;

6.2.2 Catalytic experiments

The catalytic oxidation of toluene was performed under atmospheric pressure, using a VOC concentration of 2,000 ppmv. The catalyst sample (130 mg) was diluted with glass spheres of the same size as the catalyst particles (0.2-0.5 mm), in order to minimize temperature gradients. The space velocity of all experiments was fixed to 10,000h^{-1}. Prior to the reaction the catalyst was activated under air at 400 ºC for 1 hour.

The light-off curves were obtained in a fixed-bed reactor, consisting of an U-shaped quartz tube of 6 mm internal diameter, placed inside a temperature controlled electrical furnace. The temperature in the reactor zone was measured by a thermocouple placed in the middle of the catalyst bed. The gas mixture at the reactor outlet was analysed by a CO_2 non-dispersive infrared (NDIR) sensor and a total volatile organic compounds analyser. In these experiments, the temperature was increased at 2.5 ºC/min between room temperature and 300 ºC. In order to test the

stability of the catalyst, the reaction was performed in two cycles of increasing and decreasing temperature.

The isothermal experiments were carried out in a fixed bed reactor (BTRS Jr Autoclave Engineers) at atmospheric pressure. The catalyst was supported in a small plug of glass wool in a vertical stainless steel tubular reactor. The reactor was placed into an oven, and the temperature controlled by a thermocouple that was inserted into the middle of the catalyst bed. The analytical system consisted of a gas chromatograph equipped with a flame ionization detector (FID) for the analysis of the organic compounds, and an online non-dispersive infrared (NDIR) analyzer for CO_2.

The conversion of toluene (X) and the conversion into CO_2 (X_{CO_2}) were respectively calculated as $X = 1 - \frac{F_{VOC}}{F_{VOC,in}}$ and $X_{CO_2} = \frac{F_{CO_2}}{\nu \, F_{VOC,in}}$, where F_{VOC} is the outlet molar flow rate of VOC, $F_{VOC,in}$ is the inlet molar flow rate of VOC, F_{CO_2} is the outlet molar flow rate of CO_2 and ν is the number of carbon atoms in the VOC molecule (for toluene, $\nu = 7$).

The total amount of carbon retained in the porous structure of the catalyst after reaction was measured by temperature programmed oxidation in air (TPO). After the reaction, the catalyst was cooled in nitrogen to 100 ºC. Then, a stream of air was passed and the temperature increased at 10 ºC .min^{-1} up to 450 ºC.

Temperature programmed desorption (TPD) was also studied after pre-adsorption of the VOC at room temperature. The reactant was adsorbed on the catalysts from an air stream, using the same concentration as in the reaction study. After saturation, the lines were purged with nitrogen and the TPD started. The reactant was analysed using a total volatile organic compounds analyser.

6.3 Results and discussion

6.3.1 Light−off curves

The light-off curves for complete oxidation of toluene over K-OMS-2 are shown in Figure 6.1. A large hysteresis was observed both in the conversion of toluene and in the conversion into CO_2 when performing heating (1) and cooling (2) cycles. In the heating ramp, the toluene conversion starts to increase at 220 ºC, reaching 100% at about 270 ºC. Decreasing the temperature to 205 ºC resulted in a small drop in toluene conversion to 98%. When the temperature was further decreased to 190 ºC, the catalyst became inactive. The hysteresis and the characteristic steep increase in the conversion can be in part attributed to the increase of the bed temperature during the highly exothermic oxidation of toluene ($\Delta H^{o}_{298\ K}$ = - 4163 kJ/mol). Furthermore, the gap between these two curves may also be a function of the amount and strength of the adsorbed molecules (reactant and products) on the catalyst surface. The reactant remains adsorbed when the temperature is increased up to 260ºC. As the temperature increases, below the ignition point, there is no desorption of VOC and products, and a considerable amount of molecules can be retained by the catalyst. On the other hand, during cooling, in the temperature range mentioned, the catalyst surface is clean and toluene is oxidised at lower temperatures. Our results suggest that retained toluene and eventually some of its oxidation products could deactivate the catalyst.

Another aspect, which is related to these processes, is the observation of a CO_2 peak with 196% of conversion in the light-off curve at about 235 ºC. Furthermore, below this temperature an important disagreement was found between the conversion of VOC and the CO_2 released. This phenomenon was observed in the oxidation of many VOC in several catalytic systems and according to some authors is the result of adsorption/desorption processes on the catalyst surface [11]. The catalyst adsorbs the VOC and, as the reaction temperature increases, CO_2 starts to be produced, and part of the VOC can also stay adsorbed on the catalyst surface. Since the oxidation reaction is highly exothermic, the bed temperature increases rapidly and the VOC is oxidised into CO_2, leading to instantaneous CO_2 conversions higher than 100%. The CO_2 peak appears in the ignition curves whenever the activity of the catalyst is high enough to

start the oxidation of VOC at low temperatures, which are close to the temperatures for which the adsorption-desorption of the VOC take place [11].

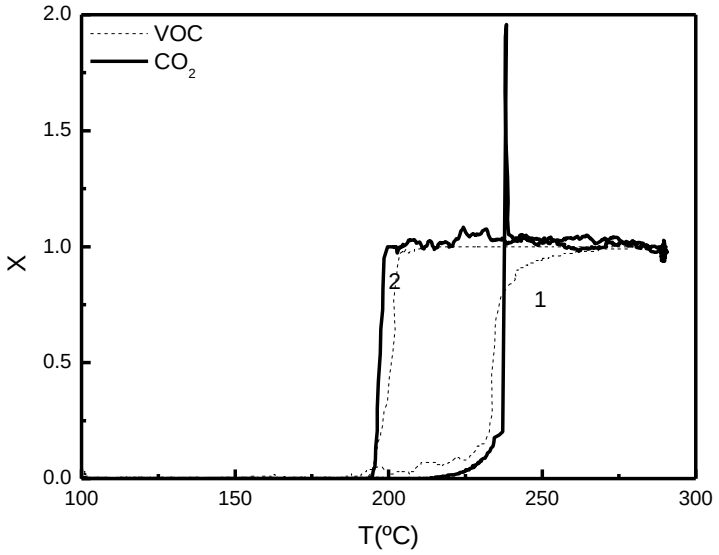

Figure 6.1 Light-off curves for toluene oxidation over K-OMS-2 (1: heating ; 2: cooling).

6.3.2 Isothermal tests

To get a closer insight into the effect of adsorption/desorption processes in the stability and activity of the catalyst, isothermal experiments were performed at selected temperatures. The conversions into CO_2 obtained over K-OMS-2 catalyst at 240, 250, 264, 270 and 280 ºC as a function of time on stream (TOS) are compared in Figure 6.2a. The catalytic behaviour at temperatures between 250 and 264 ºC will be further discussed.

At temperatures below 270 ºC the conversion increases to a maximum and decreases afterwards. The strong adsorption of toluene and other high molecular weight carbonaceous compounds on the catalyst surface could be responsible for deactivation. To elucidate this question, TPO analyses were carried out after reaction at selected temperatures (see Figure 6.2b). It was observed that at temperatures higher than 268 ºC (peak maximum in the TPO curves), deactivation does not occur, in agreement with smaller amounts of "coke". Moreover, TPD experiments after pre-adsorption of

toluene at 30 ºC (see Figure 6.3a) were also carried out. For comparative purposes, the adsorption strength of ethyl acetate was also studied in the same conditions, because in a previous study it was shown that there is no deactivation at low temperatures [2]. In both experiments, there is no desorption of VOC and only CO_2 is detected, which suggests that lattice oxygen is involved in the oxidation mechanism of ethyl acetate and toluene. This result is in agreement with previous studies [13,14]. However, lattice oxygen was not able to oxidise all adsorbed toluene. For this reason, a TPO experiment after TPD (see Figure 6.3b) shows a CO_2 peak at 250 ºC, which is absent in the case of ethyl acetate.

The TPD experiments show that there is a large difference in the adsorption strength of toluene and ethyl acetate on the cryptomelane catalyst. In the case of toluene, CO_2 starts to appear at 246 ºC and presents a broad peak with a maximum at around 300 ºC. So, if the reaction takes place at temperatures below 300 ºC, the oxidation reaction will be coupled with adsorption processes, and the catalyst will keep the reactant adsorbed at higher temperatures. On the contrary, in the case of ethyl acetate, CO_2 is evolved at much lower temperatures and presents two peaks with maxima at 180 and 240 ºC. It is then clear that ethyl acetate is less strongly adsorbed on cryptomelane than toluene, and that cryptomelane is able to keep the reactant adsorbed up to higher temperatures

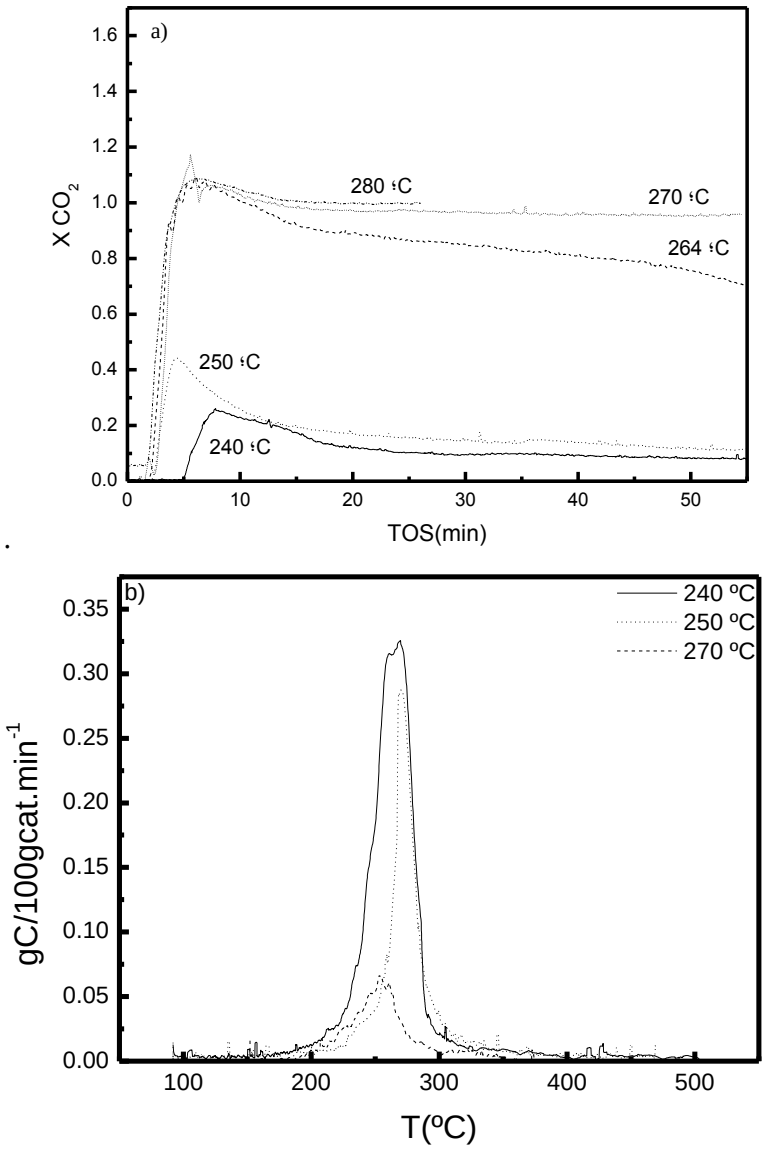

Figure 6.2 Isothermal tests at selected temperatures as a function of time on stream (TOS) (a) and some of the corresponding TPO curves (b).

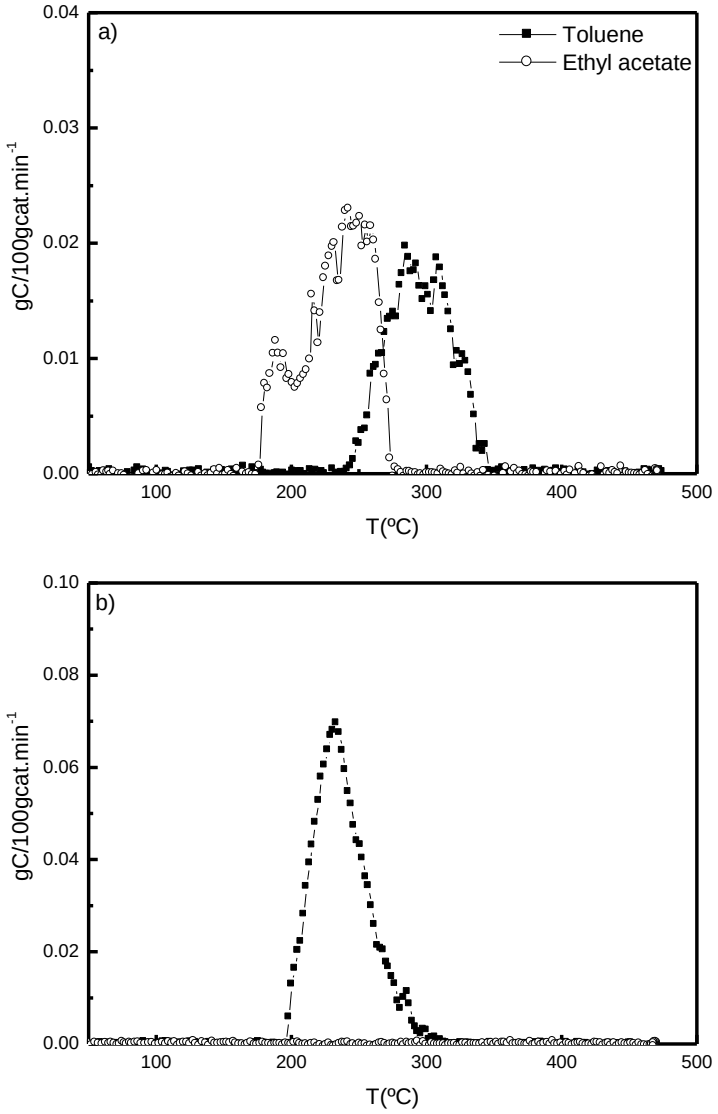

Figure 6.3 TPD after pre-adsorption of toluene or ethyl acetate at room temperature (a) and TPO of toluene and ethyl acetate after TPD (b).

6.3.3 Oscillatory behaviour

At temperatures between 250 and 264 ºC, oscillations in the CO_2 conversion were observed. Tsou et al. [9,10] studied in detail the oscillatory behaviour in the oxidation of methyl-isobutyl-ketone and xylene, and found that the oscillations result from

cycles of accumulation and oxidation of the so called “reactive coke”, which includes adsorbed VOC and heavier products. The accumulation of reactive coke was found to be related to the adsorption properties of the catalyst. In particular, the catalyst must be able to retain the VOC at temperatures higher than the reaction temperature. As demonstrated by TPD experiments, cryptomelane is able to retain toluene at higher temperatures, explaining why there are oscillations in this system and not in the case of ethyl acetate oxidation.

The effect of TOS on the oscillatory behaviour at 252 ºC and 258 ºC is shown in Figure 6.4. It was observed that at temperatures near 250 ºC, the amplitude and frequency of the oscillations are not constant with time (Figure 6.4a), and after 30 minutes of reaction the system stops to oscillate and deactivation occurs. The measured temperature follows the same cyclic behaviour as the conversion into CO_2: it increases initially up to about 260 ºC, and then it starts to oscillate between 252 ºC and 268 ºC during the first 10 minutes; then there is a period up to about 30 minutes where the amplitude is higher; afterwards, the temperature stabilizes at 249 ºC, and the system stops to oscillate. At higher temperatures (e.g. 258 ºC) the frequency and amplitude of oscillations are constant with time (the temperature ranges between 258 and 262 ºC), and deactivation does not occur (Figure 6.4b). It is important to notice that the frequency of oscillations increases with rising temperature, while the amplitude was larger at low temperatures. In both cases, there was a clear synchronization between the oscillations in X_{CO2} and the temperatures measured in the catalyst bed.

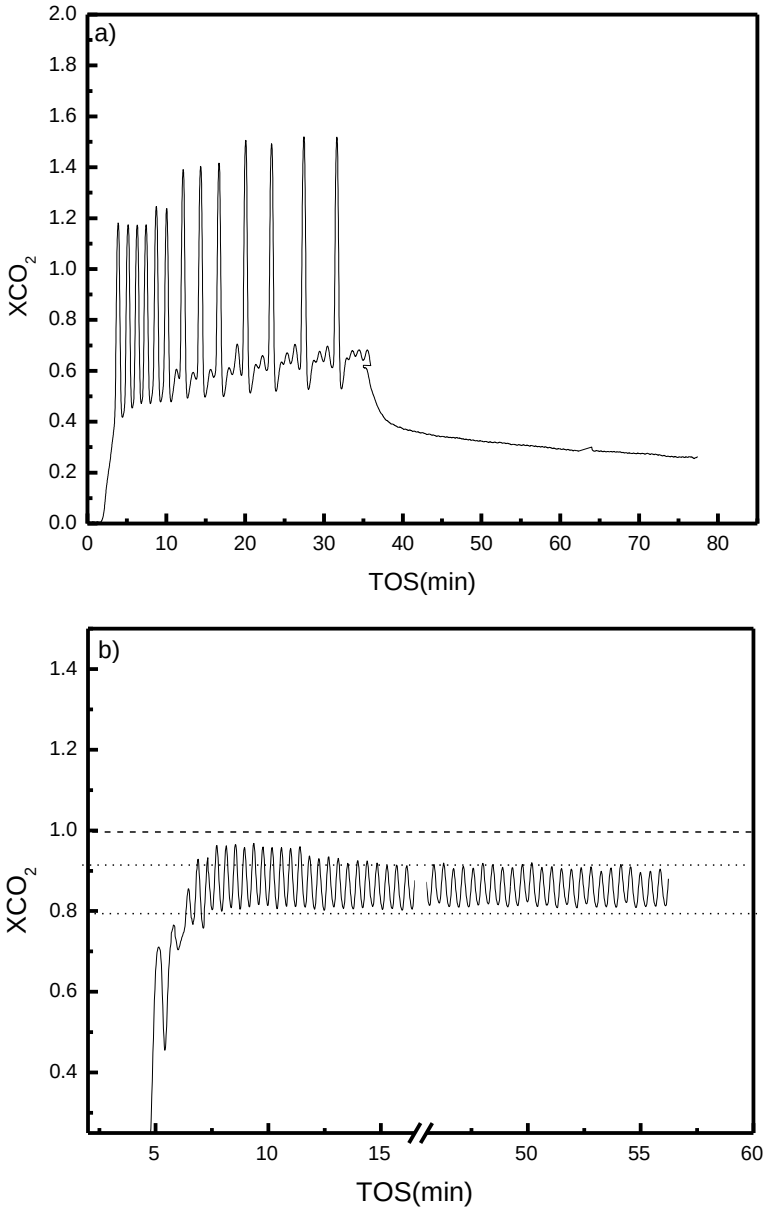

Figure 6.4 Effect of TOS and temperature on the oscillatory behaviour: a) 252 ºC; b) 258 ºC.

6.4 Conclusions

The effect of the adsorption/desorption processes on the activity and stability of the catalyst were evaluated in this study. The following conclusions can be drawn:

Cryptomelane is able to retain toluene up to high temperatures (until 300 ºC).

At lower temperatures (T< 270 ºC) accumulation of toluene and products occurs, and the activity of cryptomelane decays.

In a restricted temperature range (252-258 ºC), oscillations in the apparent conversion into CO_2 occur, which result from cycles of accumulation and oxidation of adsorbed reactant and products. The frequency and amplitude of the oscillations are synchronized with the measured temperatures.

References

[1] J. Cai, J. Liu, W.S. Willis, S.L. Suib, *Synthesis and characterization of octahedral molecular sieves (OMS-2) having the hollandite structure.* Chem. Mater. 13 (2001) 2413-2422.

[2] V.P. Santos, M.F.R. Pereira, J.J.M. Órfao, J.L. Figueiredo, *Synthesis and characterization of manganese oxides for the total oxidation of ethyl acetate.* Top. Catal. 52 (2009) 470-481.

[3] J. Luo, Q. Zhang, A. Huang, S.L. Suib, *Total oxidation of volatile organic compounds with hydrophobic cryptomelane-type octahedral molecular sieves*. Micropor. Mesopor. Mat. **35-36** (2000) 209-217.

[4] J. Luo, Q. Zhang, J. Garcia-Martinez, S.L. Suib, *Adsorptive and acidic properties, reversible lattice oxygen evolution, and catalytic mechanism of cryptomelane-type manganese oxides as oxidation catalysts*. J. Am. Chem. Soc. 130 (2008) 3198-3207.

[5] S.L. Suib, *Structure, porosity, and redox in porous manganese oxide octahedral layer and molecular sieve materials*. J. Mater. Chem 18 (2008) 1623-1631.

[6] J.J. Spivey, J.B. Butt, *Literature review: deactivation of catalysts in the oxidation of volatile organic compounds.* Catal. Today 11 (1992) 465-500.

[7] A.P. Antunes, M.F. Ribeiro, J.M. Silva, F.R. Ribeiro, P. Magnoux, M. Guisnet, *Catalytic oxidation of toluene over CuNaHY zeolites: coke formation and removal.* Appl. Catal. B-Environ. 33 (2001) 149-164.

[8] L. Becker, H. Forster, *Investigations of coke deposits formed during deep oxidation of benzene over Pd and Cu exchanged Y-type zeolites.* Appl. Catal. A-Gen. 153 (1997) 31-41.

[9] J. Tsou, P. Magnoux, M. Guisnet, J.J.M. Órfao, J.L. Figueiredo, *Oscillations in the oxidation of MIBK over a Pt/HFAU catalyst: role of coke combustion.* Catal. Commun. 4 (2003) 651-656.

[10] J. Tsou, P. Magnoux, M. Guisnet, J.J.M. Órfao, J.L. Figueiredo, *Oscillations in the catalytic oxidation of volatile organic compounds.* J. Catal. 225 (2004) 147-154.

[11] M. Paulis, L.M. Gandia, A. Gil, J. Sambeth, J.A. Odriozola, M. Montes, *Influence of the surface adsorption–desorption processes on the ignition curves of volatile organic compounds (VOCs) complete oxidation over supported catalysts.* Appl. Catal. B-Environ. 26 (2000) 37-46.

[12] V.R. Galakhov, M. Demeter, S. Bartkowski, M. Neumann, N.A. Ovechkina, E.Z. Kurmaev, N.I. Logachevskaya, Y.M. Mukovskii, J. Mitchell, D.L. Ederer, *Mn 3s exchange splitting in mixed-valence manganites*. Phys. Rev. B **65** (2002) 4.

[13] V.P. Santos, M.F.R. Pereira, J.J.M. Órfao, J.L. Figueiredo, *Catalytic oxidation of ethyl acetate over a cesium modified cryptomelane catalyst.* Appl. Catal. B-Environ. 88 (2009) 550-556.

[14] S.S. Bastos, J.J.M. Órfão, M.M.A. Freitas, M.F.R. Pereira, J.L. Figueiredo, *Manganese oxide catalysts synthesized by exotemplating for the total oxidation of ethanol.* Appl. Catal. B-Environ. 93 (2009) 30-37.

7 Mixture effects during the oxidation of toluene, ethyl acetate and ethanol over cryptomelane catalyst[1]

The catalytic oxidation of two-component VOC mixtures (ethanol, ethyl acetate and toluene) was studied over cryptomelane.

Remarkable mixture effects were observed on the activity and the selectivity. Toluene was found to inhibit both ethyl acetate and ethanol oxidation, this effect being more evident in the case of ethyl acetate. On the contrary, toluene oxidation is slightly inhibited by the presence of ethyl acetate, while the presence of ethanol exerts a promoting effect.

Concerning the mixtures of ethyl acetate and ethanol, it was observed that both molecules have a mutual inhibitory effect, which is more evident in the case of ethyl acetate.

7.1 Introduction

Catalytic oxidation is a promising technology to control the emissions of volatile organic compounds (VOC) [1]. The key parameter of this process is the type of catalyst used, which is always a function of the VOC type and its concentration, the presence of poisons or/and inhibitors and any inlet temperature constraints.

Industrial emissions usually contain a mixture of VOC with variable composition. The "mixture effect" is very difficult to predict *a priori* [2], as either an inhibition effect [3-5] or (more rarely) a promoting effect [6] can be observed when the components of

[1] VP Santos, MFR. Pereira, JJM. Órfão, JL Figueiredo, to be submited (2010).

the mixture are oxidised. Besides these possible effects, changes in selectivity to by-products have also been observed [4, 7, 8].

Certain authors have pointed out that the inhibition effect can be due to competition between the molecules for adsorption onto the active sites [5, 8-11]. For example, Tsou et al. [5] observed that the oxidation of methyl-isobutyl-ketone (MIBK) on zeolite supported platinum catalysts was strongly inhibited by the presence of o-xylene, which adsorbs strongly onto the active sites. Moreover, the oxidation of 2-propanol over platinum supported on a monolith was negatively affected by the presence of toluene and methyl-ethyl-ketone (MEK) [4]. This inhibition effect was found to be related to the competition for the oxygen atoms chemisorbed on Pt, and not due to competition for the adsorption sites on the support.

On the other hand, the oxidation of certain compounds can be also independent of the presence of other VOC. For example, the presence of n-hexane does not affect the oxidation of benzene and toluene over a Pt/Al_2O_3 catalyst [12]. It was concluded that the addition of a compound that is more weakly adsorbed on the catalyst than the original one does not affect the conversion rate significantly.

A promoting effect has also been observed in the oxidation of mixtures [6, 13, 14]. Barresi and Baldi [14] state that this effect is, in the most cases, a consequence of the higher exothermicity of the process. For example, n-hexane oxidation is enhanced by the presence of toluene [15]. However, in some systems this effect cannot be explained by heat generation during the reaction. For example, the oxidation of chlorobenzene over a $Pt/\gamma\text{-}Al_2O_3$ catalyst [13] is enhanced by the addition of aliphatic hydrocarbons, such as pentane, heptane or decane. It was observed that alkanes have the ability to remove Cl from the Pt surface (at the same time reducing the metal), which otherwise would only be removed at higher temperatures. This phenomenon could explain the promoting effect in this case.

The aim of the present work is to study the performance of cryptomelane (KMn_8O_{16}) in the oxidation of VOC binary mixtures. Three binary mixtures are studied: ethyl acetate/toluene, ethyl acetate/ethanol and ethanol/toluene.

7.2 Experimental

7.2.1 Catalysis synthesis and characterization

Cryptomelane was prepared as described in section 3.2.1. The structure, morphology, composition, manganese average oxidation state (AOS), texture and stability of the prepared samples were fully characterized in previous papers [16, 17], by X-ray diffraction (XRD), scanning electron microscopy/energy dispersive X-ray spectroscopy (SEM/EDS), X-ray photoelectron spectroscopy (XPS), N_2 adsorption at -196 ºC, thermogravimetric analysis (TGA) and temperature programmed desorption (TPD). A summary of the main catalyst properties is presented in Table 7.1 [16, 17].

Table 7.1 Properties of the catalyst: structure (obtained by XRD), surface area (obtained by nitrogen adsorption), average oxidation state and relative amount of Mn(III) surface species (obtained by XPS)

Phase	S_{BET} (m^2/g)	AOS	% Mn(III)
KMn_8O_{16}	71	3.89	17

7.2.2 Catalytic experiments

The catalytic oxidation of VOC was performed under atmospheric pressure in a fixed-bed reactor from Autoclave Engineers (BTRS Jr), which consists of a stainless steel tube of 6 mm internal diameter, placed inside a temperature-controlled electric furnace. A feed gas with selected VOC inlet concentrations and a space velocity of 16,000 h^{-1} was used. The catalyst sample (50 mg) was diluted with glass spheres of the same size as the catalyst particles (0.2-0.5 mm) in order to minimize temperature gradients.

Conversions were measured over the range 100-350 ºC by incremental steps (10-20 ºC), the temperature being measured by a thermocouple placed in the middle of the

catalyst bed. To ensure that steady state data were measured, the reactor was maintained at each temperature for 30 minutes. The conversion of VOC (X) and the conversion into CO_2 (X_{CO_2}) were respectively calculated as $X = 1 - \frac{F_{VOC}}{F_{VOC,in}}$ and $X_{CO_2} = \frac{F_{CO_2}}{\nu F_{VOC,in}}$ where F_{VOC} is the outlet molar flow rate of VOC at steady state, $F_{VOC,in}$ is the inlet molar flow rate of VOC, F_{CO_2} is the outlet molar flow rate of CO_2 at steady state and ν is the number of carbon atoms in the VOC molecule (for ethanol, ethyl acetate and toluene, ν = 2, 4 and 7, respectively). Further details can be found in section 3.2.3. [16].

7.3 Results and discussion

The catalytic performance of cryptomelane in the single oxidation of ethanol, ethyl acetate and toluene was previously studied [16-19]. Cryptomelane was found to be very active, oxidising all of these VOC at relatively low temperatures. The conversion level was influenced by the type of VOC, the reactivity into CO_2 increasing in the following order: Toluene < Ethanol < Ethyl acetate.

The oxidation process of the oxy-derivative compounds was found to be more complex than toluene, yielding not only CO_2 and H_2O, but also partially oxidised intermediates (namely acetaldehyde). On the other hand, it was established that lattice oxygen is involved in the oxidation process of all VOC studied, suggesting a Mars and van Krevelen mechanism. In this context, the type of VOC is particularly important, as it dictates the reduction of the catalyst and, consequently, the incorporation rate of oxygen in the lattice, which explains the lower reactivity observed with toluene.

In the present work, the performance of cryptomelane in the oxidation of three binary mixtures was evaluated.

7.3.1 Ethyl acetate/ toluene mixture

The activity of cryptomelane in the oxidation of ethyl acetate/toluene mixtures was evaluated by performing two sets of experiments. In the first one, the concentration of one of the components was kept constant, while the concentration of the other

component was changed within a pre-established range (see Figures 7.1 and 7.2). The second type of experiment was carried out by changing the relative proportions of toluene and ethyl acetate in the mixture, while keeping the concentration of carbon in the feed constant (see Figure 7.3).

Figure 7.1 shows the effect of toluene on ethyl acetate oxidation. It can be observed that the presence of toluene strongly inhibits the oxidation of ethyl acetate, and this effect increases with the toluene concentration. For instance, the temperature for 100% conversion is about 210 ºC when ethyl acetate is oxidised alone, and 250 ºC or higher, when it is oxidised in mixtures with toluene.

On the other hand, it can be observed (see Figure 7.2) that ethyl acetate does not have a significant effect in the oxidation of toluene. This result was already expected, since ethyl acetate is almost completely oxidised before toluene conversion starts.

Figure 7.3 shows the results obtained in the second set of experiments, as well as the corresponding theoretical curves (obtained by averaging the oxidation temperatures of the individual compounds). As can be seen, the light-off curves of the mixtures have an intermediate behaviour in comparison to the two compounds alone. However, these curves do not follow the theoretical ones (particularly in the range of temperatures where toluene is converted), showing an inhibition effect, in agreement with the previous results. Moreover, it can be observed that the temperature necessary for the total conversion into CO_2 is determined by the corresponding temperature of the less reactive compound.

Similar conclusions were reported by other authors [3, 7, 8]. In general, the inhibition effects can be a result of the competition between the molecules for the adsorption sites [5, 8-11], or/and the competition for oxygen atoms [4, 7]. In a previous work [17], it was shown that the interaction of the oxy-derivative compounds on cryptomelane differs greatly from toluene. Toluene has a strong affinity with the catalyst surface, being retained at high temperatures (temperatures higher than the reaction temperature). The accumulation of these molecules on the catalyst structure was found to be at the origin of an unstable behaviour (oscillations) [18]. On the other hand, cryptomelane was not able to retain ethyl acetate at high temperatures. These results suggest that toluene is more strongly adsorbed than ethyl acetate, and the

inhibition effect can result from the competition of both molecules for the active sites. It should be noticed that the inhibition effect observed for ethyl acetate oxidation (in the first set of experiments) cannot be explained by the presence of higher amounts of H_2O and CO_2. It was established in a previous work [16] that the oxidation of ethyl acetate is not affected by the presence of these compounds.

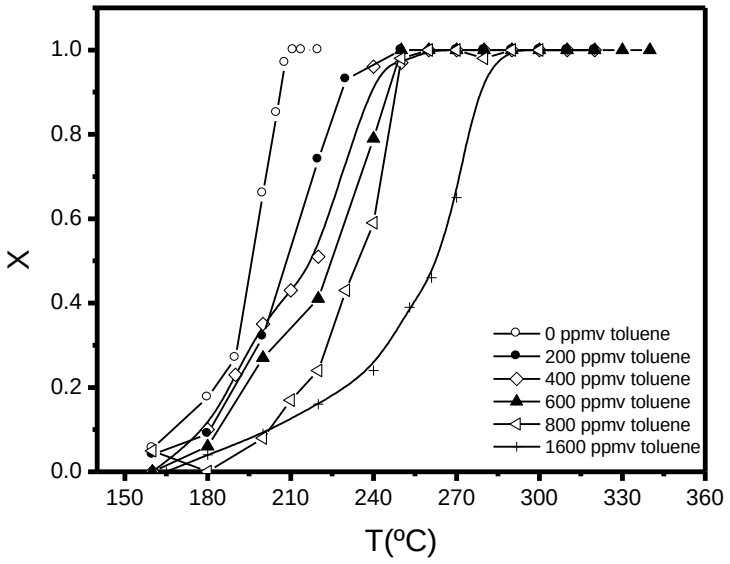

Figure 7.1 Conversion of ethyl acetate alone (1,600 ppmv), and in binary mixtures with toluene.

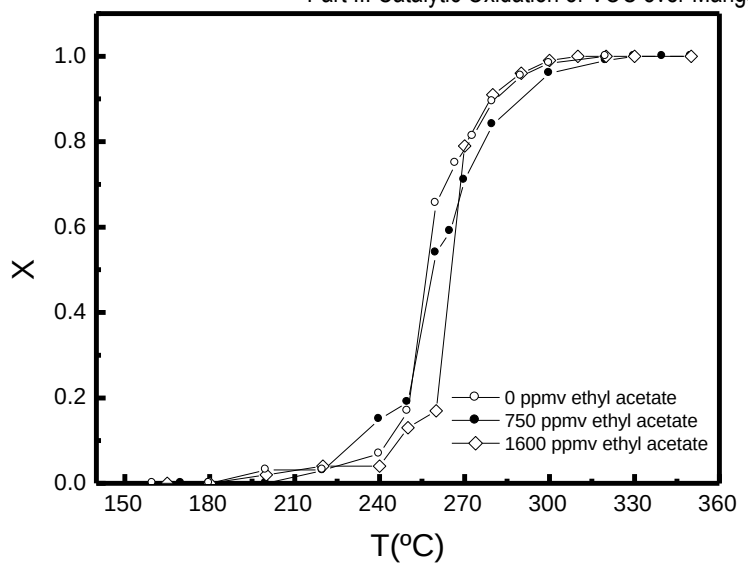

Figure 7.2 Conversion of toluene alone (1,600 ppmv), and in binary mixtures with ethyl acetate.

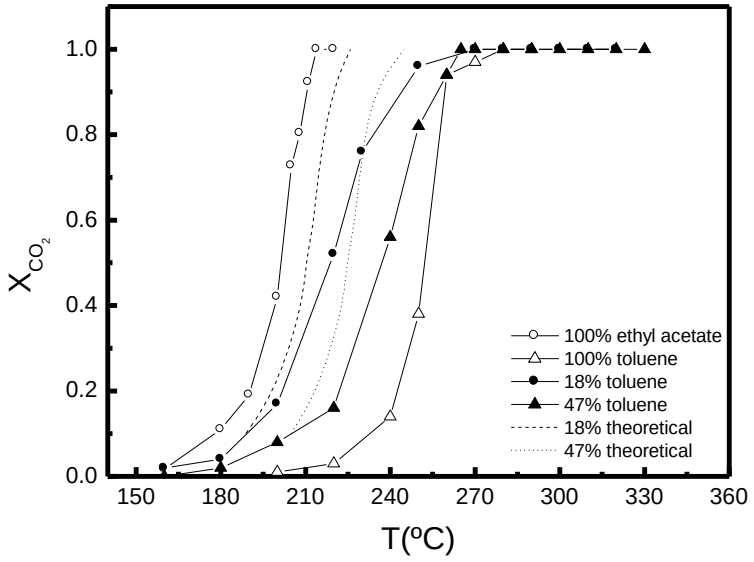

Figure 7.3 Conversion into CO_2 (X_{CO2}) of the individual compounds and ethyl acetate/toluene mixtures. (Concentration of carbon in the feed is 4,000 ppm). The theoretical curves for the mixtures (obtained by averaging the oxidation temperatures of the individual compounds) are also represented.

7.3.2 Ethanol/ toluene mixture

The results concerning ethanol/toluene mixtures are shown in Figures 7.4 and 7.5. It can be observed (see Figure 7.4a) that ethanol conversion is also inhibited by the presence of toluene, but to a lesser extent comparatively with ethyl acetate. Concerning acetaldehyde production (see Figure 7.4b), it was observed that the presence of toluene slows down the partial oxidation of ethanol to acetaldehyde, shifting the curve to higher temperatures. However, the maximum amount of acetaldehyde produced in the individual oxidation of ethanol is lower than that produced in the oxidation of the mixture. This effect was also observed by other authors [4, 7].

The effect of ethanol on the conversion of toluene is shown in Figure 7.5. A slight promoting effect was observed, since the light-off curve is shifted to lower temperatures at high conversions. This effect increases with the concentration of ethanol. For instance, the temperature for 100% conversion is about 300 ºC when toluene is oxidised alone, and lower than 280 ºC when it is oxidised in mixtures with ethanol. This effect is most probably a consequence of the higher exothermicity of the process when the mixtures are considered.

It should be noticed that when toluene starts to oxidise, ethanol has already been transformed into acetaldehyde and CO_2 (minor amounts), so significant amounts of this intermediate compound are present. For this reason, the behaviour of this mixture should be the same as the acetaldehyde/toluene mixture.

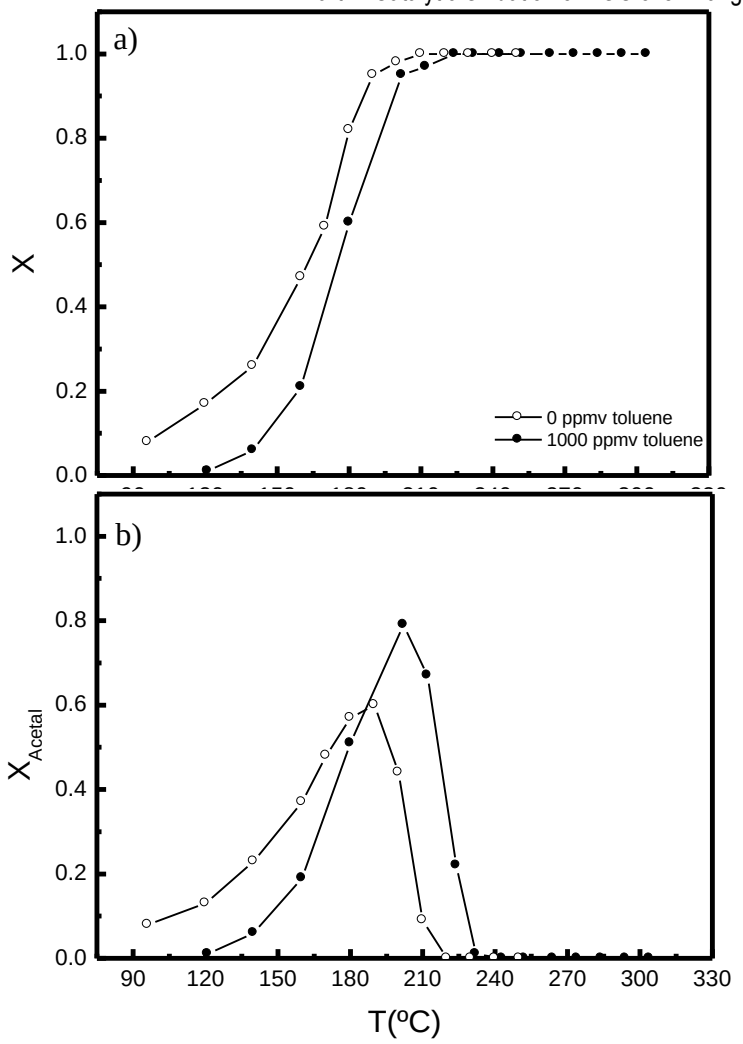

Figure 7.4 a) Conversion of ethanol alone (3,700 ppmv) and in a binary mixture with toluene. b) Corresponding conversion into acetaldehyde, defined as: $X_{Acetal} = \frac{F_{Acetal}}{F_{Ethanol,in}}$, where F_{Acetal} is the outlet molar flow rate of acetaldehyde at steady state.

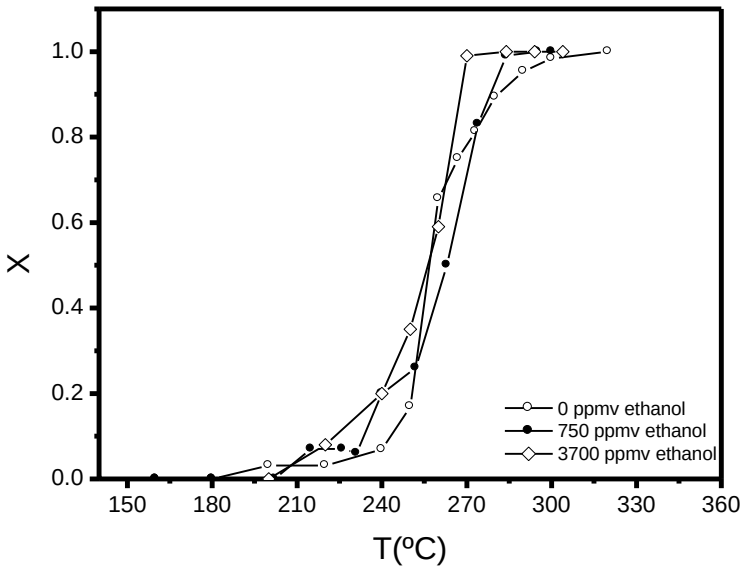

Figure 7.5 Conversion of toluene alone (1,600 ppmv) and in binary mixtures with ethanol.

7.3.3 Ethyl acetate/Ethanol

The mutual influence of the components of a binary mixture is more interesting when the oxidation reactions of both molecules alone take place in the same temperature range, such as in the case of the ethyl acetate/ethanol mixture (Figures 7.6 and 7.7).

Regarding the effect of ethanol concentration on ethyl acetate oxidation (see Figure 7.6), it can be seen that the presence of ethanol inhibits the oxidation of ethyl acetate, shifting the light-off curve to higher temperatures. The temperature for 100% conversion is about 45 ºC higher.

Figure 7.7 shows the effect of the presence of ethyl acetate on ethanol oxidation. It can be observed that the presence of ethyl acetate also inhibits the partial combustion of ethanol, decreasing the conversion into acetaldehyde. However, this effect is not as evident as with the addition of ethanol to ethyl acetate.

In summary, it can be observed that there is a mutual inhibition effect between ethanol and ethyl acetate, although this effect is much more evident in ethyl acetate combustion. These results can be explained by the competition between both molecules for the adsorption sites, because they are both polar, which results in a similar interaction between the molecules and the catalyst surface. Moreover, a similar mechanism can take place in the oxidation of both molecules.

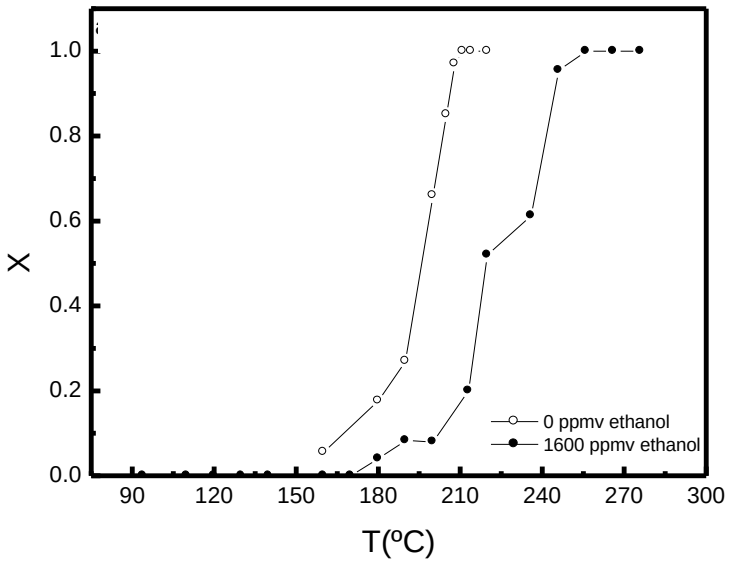

Figure 7.6 Conversion of ethyl acetate alone (1,600 ppmv) and in a binary mixture with ethanol.

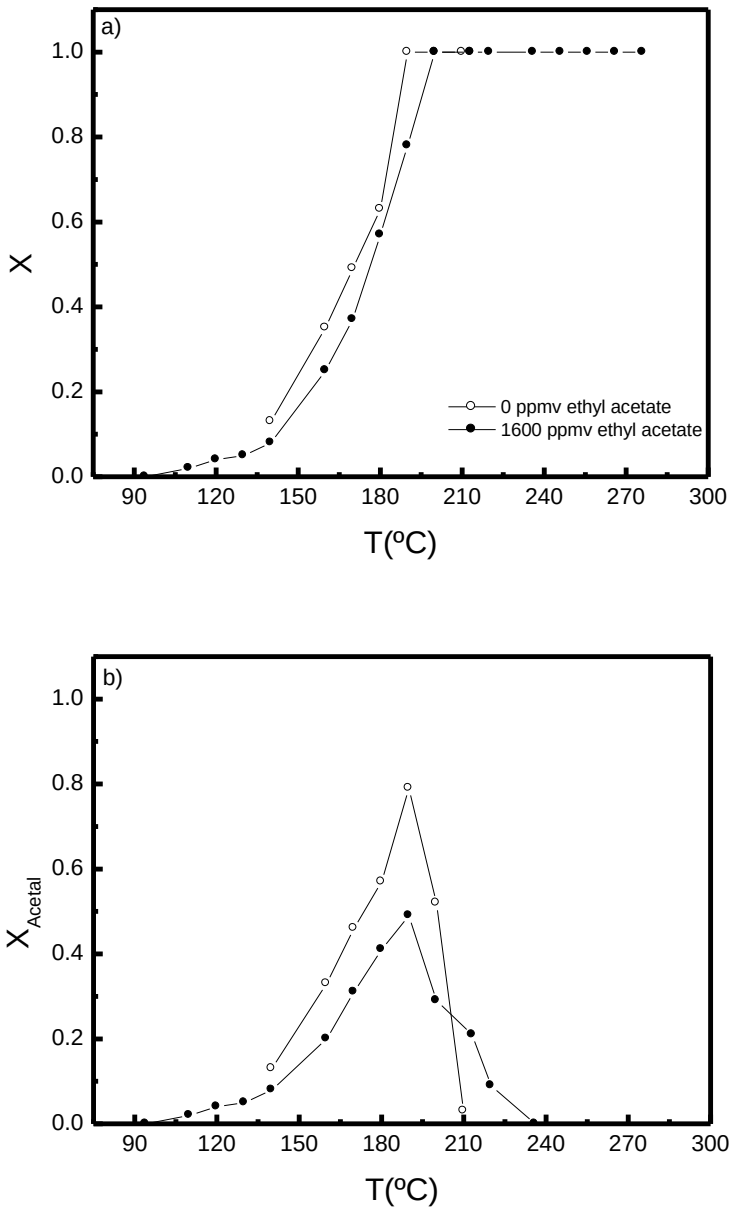

Figure 7.7 a) Conversion of ethanol alone (1,600 ppmv) and in a binary mixture with ethyl acetate. b) Corresponding conversions into acetaldehyde

7.4 Conclusions

Remarkable mixture effects were observed on the activity and selectivity.

Toluene affects both ethyl acetate and ethanol oxidation, this effect being much more evident in the case of ethyl acetate. The inhibition effect was explained by a competition between the molecules for the adsorption sites.

Toluene oxidation is slightly inhibited by the presence of ethyl acetate, while the presence of ethanol has a slight promotion effect (mainly due the oxidation of acetaldehyde), which was attributed to a local heating effect.

Concerning ethyl acetate and ethanol mixtures, it was observed that both molecules have a mutual inhibitory effect. However, this effect is much more evident in the case of ethyl acetate oxidation.

References

[1] E.C. Moretti, N. Mukhopadhyay, *VOC control: current practices and future-trends*. Chem. Eng. Prog. **89** (1993) 20-26.

[2] J.J. Spivey, *Complete catalytic-oxidation of volatile organics*. Ind. Eng. Chem. Res. **26** (1987) 2165-2180.

[3] A. Musialik-Piotrowska, K. Syczewska, *Catalytic oxidation of trichloroethylene in two-component mixtures with selected volatile organic compounds*. Catal. Today **73** (2002) 333-342.

[4] N. Burgos, M. Paulis, M.M. Antxustegi, M. Montes, *Deep oxidation of VOC mixtures with platinum supported on Al_2O_3/Al monoliths*. Appl. Catal. B-Environ. **38** (2002) 251-258.

[5] J. Tsou, P. Magnoux, M. Guisnet, J.J.M. Órfão, J.L. Figueiredo, *Catalytic oxidation of methyl-isobutyl-ketone over basic zeolites*. Appl. Catal. B-Environ. **51** (2004) 129-133.

[6] S. Irusta, M.P. Pina, M. Menéndez, J. Santamaría, *Catalytic combustion of volatile organic compounds over la-based perovskites*. J. Catal. **179** (1998) 400-412.

[7] F.N. Aguero, B.P. Barbero, L. Gambaro, L.E. Cadus, *Catalytic combustion of volatile organic compounds in binary mixtures over MnO_x/Al_2O_3 catalyst*. Appl. Catal. B-Environ. **91** (2009) 108-112.

[8] A. Musialik-Piotrowska, K. Syczewska, *Combustion of volatile organic compounds in two-component mixtures over monolithic perovskite catalysts*. Catal. Today **59** (2000) 269-278.

[9] V. Blasin-Aubé, J. Belkouch, L. Monceaux, *General study of catalytic oxidation of various VOCs over $La_{0.8}Sr_{0.2}MnO_3$ perovskite catalyst--influence of mixture*. Appl. Catal. B-Environ. **43** (2003) 175-186.

[10] I. Mazzarino, A.A. Barresi, *Catalytic combustion of VOC mixtures in a monolithic reactor*. Catal. Today **17** (1993) 335-347.

[11] P. Papaefthimiou, T. Ioannides, X.E. Verykios, *Performance of doped Pt/TiO2 (W^{6+}) catalysts for combustion of volatile organic compounds (VOCs)*. Appl. Catal. B-Environ. **15** (1998) 75-92.

[12] S. Ordóñez, L. Bello, H. Sastre, R. Rosal, F.V. Díez, *Kinetics of the deep oxidation of benzene, toluene, n-hexane and their binary mixtures over a platinum on γ-alumina catalyst*. Appl. Catal. B-Environ. **38** (2002) 139-149.

[13] R.W. van den Brink, P. Mulder, R. Louw, *Catalytic combustion of chlorobenzene on Pt/γ-Al_2O_3 in the presence of aliphatic hydrocarbons*. Catal. Today **54** (1999) 101-106.

[14] A.A. Barresi, G. Baldi, *Deep catalytic oxidation of aromatic hydrocarbon mixtures: reciprocal inhibition effects and kinetics*. Ind. Eng. Chem. Res. **33** (1994) 2964-2974.

[15] J. Hermia, S. Vigneron, *Catalytic incineration for odour abatement and VOC destruction*. Catal. Today **17** (1993) 349-358.

[16] V.P. Santos, M.F.R. Pereira, J.J.M. Órfão, J.L. Figueiredo, *Synthesis and characterization of manganese oxide catalysts for the total oxidation of ethyl acetate*. Top. Catal. **52** (2009) 470-481.

[17] V.P. Santos, M.F.R. Pereira, J.J.M. Órfão, J.L. Figueiredo, *The role of lattice oxygen on the activity of manganese oxides towards the oxidation of VOC*. (2010) submitted.

[18] V.P. Santos, S.S.T. Bastos, M.F.R. Pereira, J.J.M. Órfão, J.L. Figueiredo, *Stability of a cryptomelane catalyst in the oxidation of toluene*. Catal. Today (2010) doi:10.1016/j.cattod.2009.1012.1005.

[19] V.P. Santos, M.F.R. Pereira, J.J.M. Órfão, J.L. Figueiredo, *Catalytic oxidation of ethyl acetate over a cesium modified cryptomelane catalyst*. Appl. Catal. B-Environ. **88** (2009) 550-556.

[20] J. Tsou, P. Magnoux, M. Guisnet, J.J.M. Órfão, J.L. Figueiredo, *Catalytic oxidation of volatile organic compounds - Oxidation of methyl-isobutyl-ketone over Pt/zeolite catalysts*. Appl. Catal. B-Environ. **57** (2005) 117-123.

Part IV

Catalytic Oxidation of VOC over Supported Noble metal Catalysts

Supported noble metals are frequently used in the oxidation of VOC. In this section, several noble metals (Au, Pt, Pd, Ir, Rh) supported on titania were tested in the oxidation of VOC. The catalysts were prepared by incipient wetness impregnation and liquid phase reduction deposition. The effect of the metal particle size on catalyst performance was assessed. The effects of the crystalline phase of the support, the amount of platinum and the activation conditions were also studied in the case of ethyl acetate oxidation.

The most promissing system was tested in the oxidation of ethanol/toluene mixtures.

8 Oxidation of CO, ethanol and toluene over TiO_2 supported noble metal catalysts [1]

The oxidation of CO, ethanol and toluene was investigated on noble metal catalysts (Pt, Pd, Ir, Rh and Au) supported on TiO_2. The catalysts were prepared by liquid phase reduction deposition (LPRD) and by incipient wetness impregnation (IMP). It was observed that the preparation method can have a significant effect on the dispersion of the metallic phase, and subsequently on the performance of the catalysts towards total oxidation of CO or VOC.

For CO oxidation, Au IMP was the worst catalyst, while Au LPRD was the most active. This can be explained in terms of different Au particle sizes, well known to be related with catalytic activity. For all the other metals, LPRD also produces better results, although the differences are not so marked as with gold. Iridium seems to be the only exception since results were very similar.

In VOC oxidation, the following performance trend was observed: $Pt/TiO_2 > Pd/TiO_2 >> Rh/TiO_2 \approx Ir/TiO_2 >> Au/TiO_2$, for both preparation methods. Ethanol and toluene oxidation over Pt and Pd catalysts were found to be structure sensitive reactions.

Some experiments with ethanol/toluene mixtures were performed using the best catalyst (Pt/TiO_2). It was observed that toluene inhibits the combustion of ethanol, namely by slowing down the partial oxidation of ethanol towards acetaldehyde. Ethanol also has a slight inhibition effect on the total oxidation of toluene.

8.1 Introduction

The design of catalytic systems for the reduction of polluting emissions is an important tool for environmental protection. Supported noble metal catalysts are well

[1] VP Santos, SSC Carabineiro, P Tavares, MFR Pereira, JJM Órfão, JL Figueiredo, submitted (2010).

known for their high activity in oxidation reactions [1-13]. It has been established for a long time that the catalytic activity and/or the selectivity of noble metals (especially gold) strongly depends on the particle size and this parameter is a function of several factors, including the preparation method. For example, gold is only active when it is deposited as ultrafine particles with high dispersion on metal oxide supports, which is not accomplished by the conventional preparation methods, such as traditional impregnation [9, 12, 13]. The problem of these methods is that they generally lead to poorly active systems due to the presence of chloride, which is well known to cause sinterization of gold particles, thus turning them inactive [9, 12-14].

There is an extensive work concerning the oxidation of VOC and CO over supported noble metal catalysts [1, 3, 7, 9, 12, 13, 15]. Most of these studies involve supported Pt, Pd or Au [9, 12, 13, 15-19], titania being one of the most widely used carriers.

As CO is a possible by-product in VOC oxidation (as not always complete oxidation of the pollutant to CO_2 takes place), the study of CO oxidation is also important in this context. As documented in the literature, this reaction follows a Langmuir-Hinshelwood mechanism, over noble metal catalysts (Pt, Pd), and the surface reaction occurs between adsorbed CO and dissociatively adsorbed oxygen. On supported Au catalysts the reaction mechanism is more complex, and it is widely accepted that a CO molecule is chemisorbed on a gold atom, while an hydroxyl ion moves from the support to an Au(III) ion, creating an anion vacancy. They react to form a carboxylate group, and an oxygen molecule occupies the anion vacancy as O_2^-. This oxidizes the carboxylate group by extracting a hydrogen atom, forming carbon dioxide, and the resulting hydroperoxide ion HO_2^- then oxidizes a further carboxylate species forming another carbon dioxide and restoring two hydroxide ions on the support surface, completing the catalytic cycle. This mechanism was proposed in 2000 by Bond and Thompson [9], and has been substantiated by subsequent results [20].

On the other hand, it is generally accepted that the oxidation of VOC over noble metals involves the dissociative adsorption of oxygen, followed by a Langmuir-Hinshelwood mechanism (reaction with chemisorbed reactant) or a Rideal-Eley mechanism (reaction with gaseous reactant), depending on the nucleophilic character of the particular organic reactant [1]. In some metals, such as Ag, oxygen

chemisorption is too strong, which implies a Mars-van Krevelen mechanism similar to metal oxides (with formation of surface oxygen vacancies as the key step and their successive replenishment by gas-phase oxygen) [1].

Another important aspect concerning the oxidation of VOC over noble metal catalysts is that the reaction is generally recognized to be structure sensitive. The effect of the Pt particle size on the catalytic combustion of different hydrocarbons has been extensively studied [21-23]. Nevertheless, the results obtained are conflicting, probably due to the fact that the correlation between catalytic activity and metal dispersion depends on the type of VOC. Very few papers deal with the structure sensitivity of aromatic hydrocarbons combustion on Pt-based catalysts. Papaefthimiou et al. [3] studied the oxidation of benzene over Pt-based catalysts. They found that, in the presence of Pt-Al_2O_3, turnover rates strongly increase with increasing Pt particle size.

It is well known that the preparation method is crucial to obtain catalysts with small particle sizes, especially for gold supported catalysts [9, 12, 13]. The liquid phase reduction deposition (LPRD) method was used by Sunagawa et al. [24] to prepare Pt and Au catalysts supported on Fe_2O_3, FeOOH, ZrO_2 and TiO_2, and by our group for the preparation of Au/ceria catalysts for CO oxidation [14]. This technique is based on the adsorption of metal ions or complexes on the surface followed by reduction. The initial adsorption of metal or complexes is thus the key point of this method. Highly dispersed particles on the support can be produced, overcoming the limitations of the conventional methods (incipient wetness impregnation and ion exchange) [24].

In the present work, several noble metals (Pt, Pd, Rh, Ir and Au) were supported on commercial titania by LPRD and by traditional incipient wetness impregnation (IMP). The materials were characterized by transmission electron microscopy (TEM) and pulse chemisorption of hydrogen, and used as catalysts for the oxidation of CO, ethanol, toluene and mixtures of these two VOC. The influence of the preparation method and the type of metal on the catalytic activity was assessed.

To the best of our knowledge, there are no reports in the literature dealing with catalytic oxidation of toluene and ethanol, where a comparison of several noble metals supported on titania prepared by the two different methods mentioned above is made.

Particularly, we found no reference to studies concerning titania supported Ir or Rh catalysts for VOC oxidation.

8.2 Experimental

8.2.1 Catalysis synthesis and characterization

Commercial TiO_2 (Degussa P 25) was used as support. Supported noble metal (Pt, Pd, Ir, Rh and Au) catalysts were prepared by incipient wetness impregnation (IMP) and liquid phase reduction deposition (LPRD) with 1% metal load (nominal). These catalysts are referred to in subsequent text as M IMP and M LPRD, where M defines the noble metal.

In the first method, an appropriate volume of the corresponding precursor (see Table 8.1) was added to the support. The resultant materials were dried at 110 ºC overnight and calcined at 500 ºC for 2 hours.

The second method (LPRD) consists of mixing a solution of the precursor with a solution of NaOH with stirring at room temperature. The resulting solution is aged for 24 h, in the dark, at room temperature to complete the hydroxylation. Then the appropriate amount of support is added to the solution and, after ultrasonic dispersion for 30 min, the suspension is aged in the oven at 100ºC overnight. The resulting solid is washed repeatedly with distilled water for chloride removal, and dried in the oven at 100ºC overnight.

The metal dispersion was determined by hydrogen chemisorption with an Altamira instrument (AMI 200). The samples were pre-reduced at 400 ºC in a stream of hydrogen and then cooled to room temperature, in order to proceed with the pulse chemisorption of hydrogen. For palladium catalysts, metal dispersions were obtained by chemisorption at 70 ºC, in order to avoid the formation of β-Pd hydride phase by diffusion of hydrogen into the palladium [25]. In fact, measurements carried out with Pd samples at room temperature gave lower dispersions, as will be discussed ahead.

The average metal particle sizes were determined also by Transmission Electron Microscopy (TEM) using a Leo 906 E apparatus, at 100 kV. Samples were prepared by ultrasonic dispersion in ethanol and placed on a copper grid for TEM analysis.

The noble metal loading of the samples was determined by inductively coupled plasma - optical emission spectroscopy (ICP/OES) in an external laboratory.

8.2.2 Catalytic Experiments

8.2.2.1 CO oxidation

CO oxidation experiments were performed using a continuous flow reactor. The catalyst sample weight was 200 mg and the feed gas (5% CO, 10% O_2 in He) was passed through the catalytic bed at a total flow rate of 50 Ncm^3 min^{-1}. The reaction temperature was raised from room temperature until full conversion was obtained, by steps of 25 ºC. The reactor was maintained at each temperature for 20 min in order to obtain experimental values at steady state. The composition of the outgoing gas stream was determined by gas chromatography. Further details can be found elsewhere [14].

8.2.2.1 VOC oxidation

A different catalytic reactor was used for VOC oxidation. The catalytic oxidation of ethanol and toluene was carried under atmospheric pressure in a 6 mm stainless steel reactor (BTRS Jr Autoclave Engineers). A feed gas with a VOC concentration of 4,000 mgC/m^3 and a space velocity of 16,000 h^{-1} was used in standard tests. The catalyst sample (50 mg) was diluted with glass spheres of the same size as the catalyst particles (0.2-0.5 mm), in order to minimize temperature gradients. Prior to the reaction the catalyst was activated under air at 400 ºC for 1 hour.

Conversions were measured over the range 100-300 ºC in incremental steps (10 – 20 ºC) and temperatures were measured by a thermocouple placed in the middle of the catalysts bed. To ensure the measurement of steady state data, the reactor was maintained at each temperature for 30 minutes. The conversion of VOC (X) and the conversion into CO_2 (X_{CO_2}) were respectively calculated as $X = 1 - \frac{F_{VOC}}{F_{VOC,in}}$ and

$X_{CO_2} = \frac{F_{CO_2}}{\nu F_{VOC,in}}$, where F_{VOC} is the outlet molar flow rate of VOC at steady state, $F_{VOC,in}$ is the inlet molar flow rate of VOC, F_{CO_2} is the outlet molar flow rate of CO_2 at steady state and ν is the number of carbon atoms in the VOC molecule (ν = 2 or 7, for ethanol or toluene, respectively). Further details can be found in section 3.2.3 [26].

The intrinsic activity (γ) was used in this work in order to compare the activity of the catalysts with different metal dispersions. γ was calculated as: $\gamma = \frac{F_{CO_2}}{wD_M / M}$, where w is the metal weight, D_M is the metal dispersion and M is the molar mass of the noble metal.

8.3 Results and discussion

8.3.1 Catalyst characterization

The characteristics of the different catalysts are summarized in Table 8.1. As can be seen, the catalysts obtained by the two methods described above display very different metal particle sizes. When the metal is introduced by IMP, the average metal particle size ranges from 5-9 nm in all samples prepared. The size is reduced to 3-4 nm when the metal is deposited by LPRD. As expected, highly dispersed noble metal catalysts were produced by this method (see Table 8.1), with values ranging from about 30% (for Pt, Pd, Rh and Au) to 39% (for Ir). IMP samples have lower dispersion, ranging from 13 to 21%. As mentioned in Section 8.2.1, the values for Pd dispersion were obtained by chemisorption at 70 ºC, in order to avoid the formation of β-Pd hydrides. In fact, measurements carried out for the Pd LPRD sample at room temperature gave a lower dispersion (15%).

Figure 8.1 shows selected TEM images of the titania supported catalysts prepared by both methods. It was not possible to obtain metal dispersions by TEM for Pt, Ir and Rh catalysts (prepared by LPRD), since no metal particles could be seen in the micrographs. This might be due to their very low sizes (most likely below detection limit of 2-3 nm). In fact, Table 8.1 shows that these catalysts present low average particle sizes (~2-4 nm) determined by chemisorption (the experimental limitations imposed by the low metal loadings of about 1 wt % must be considered for this kind

of technique). However, Pd particles can be seen very well (Figure 8.1b). Catalysts prepared by IMP are also well visible, since they show larger metal particle sizes (Figure 8.1a is shown as an example). In general, there is a large difference between the particle sizes of catalysts prepared by IMP and LPRD methods, the latter producing much smaller particles (Figure 8.1c, referring to Au LPRD catalyst, is shown as an example).

In the cases where comparison is possible, dispersions and particle sizes obtained by TEM and by hydrogen chemisorption are generally in agreement (although the latter method gives higher values of dispersion), which implies that the majority of the metal particles are exposed on the titania surface.

Table 8.1 Properties of TiO_2 supported catalysts (D_M- metal dispersion, d_M – average diameter of the metal particles)

Catalyst	Precursor	Metal loading (%)	D_M (%)[a]	d_M (nm)[a]	D_M (%)[b]	d_M (nm)[b]
Pt IMP	$H_2PtCl_6 \cdot 6H_2O$	0.8	19	5.4	16	6.3
Pd IMP	$PdCl_2$	0.9	16[c]	7.2[c]	14	8.0
Ir IMP	$H_2IrCl_6 \cdot H_2O$	1.0	18	6.1	14	7.9
Rh IMP	$RhCl_3$ $3H_2O$	0.8	21	5.2	14	7.9
Au IMP	$HAuCl_4 \cdot 3H_2O$	0.9	-	-	13	9.1
Pt LPRD	$H_2PtCl_6 \cdot 6H_2O$	1.1	28	3.6	-	-
Pd LPRD	$PdCl_2$	1.1	28[c]	4.0[c]	38	3.0
Ir LPRD	$H_2IrCl_6 \cdot H_2O$	1.5	39	2.9	-	-
Rh LPRD	$RhCl_3 \cdot 3H_2O$	1.1	29	3.8	-	-
Au LPRD	$HAuCl_4 \cdot 3H_2O$	0.5	-	-	29	4.0

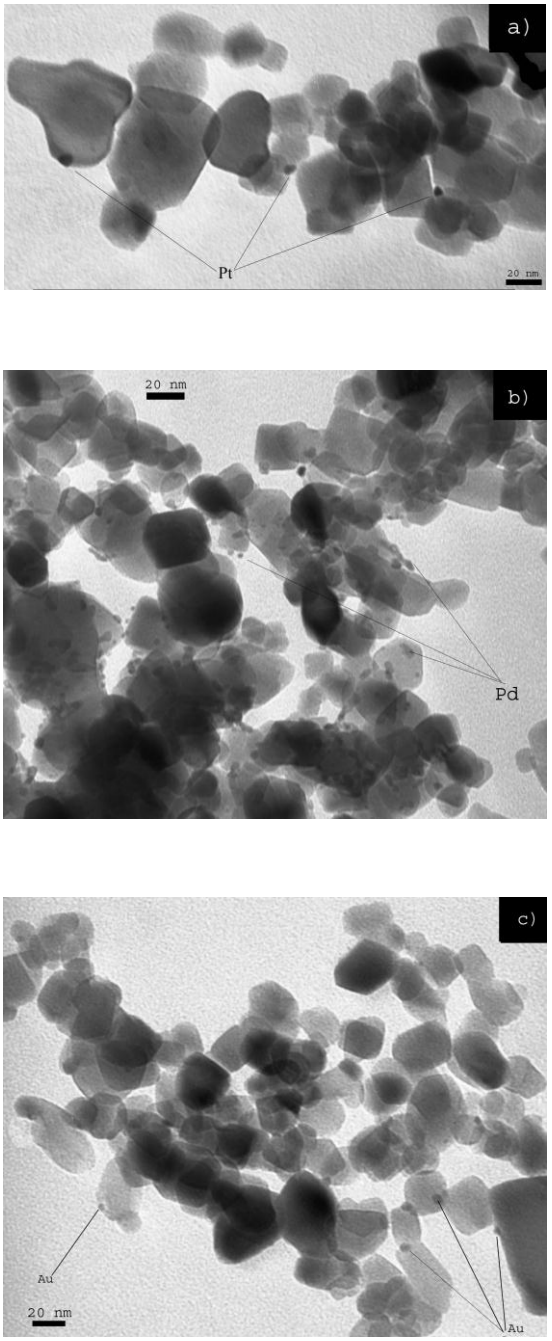

Figure 8.1 TEM images of catalysts: a) Pt IMP; b) Pd LPRD; c) Au LPRD.

The metal loading of the samples is also shown in Table 8.1. It can be observed that the Au contents resulting from the two preparation methods are quite different, ranging from 0.5% for LPRD to 0.9% for IMP. This result indicates that gold present in solution cannot be totally deposited on the support. It has been established that the preparation method has a strong influence on the metal loading. In fact, this is a common problem, as the gold loading depends on the way the metal is deposited on the surface, either in the form of a complex or in the reduced state [27-29].

8.3.2 Catalytic activities

All the catalysts studied in this work were tested in the oxidation of VOC (ethanol and toluene) and CO.

8.3.2.1 CO oxidation

Figure 8.2 shows the light-off curves for CO oxidation with the titania supported catalysts, prepared by both methods, and with the support itself, for comparison. It can be observed that Au IMP is the worst catalyst of the group, while Au LPRD is by far the most active. This can be explained in terms of the particle sizes, well known to be dependant of the preparation method [9, 12, 13]. In fact, the IMP method, since it does not remove chloride, produces larger gold particles, which are much less active than the smaller produced by LPRD, as already shown with Au/ceria materials [14].

For all the remaining metals, LPRD still produces better results, although the difference is not so marked as with gold. Iridium seems to be the only exception, since both curves are very similar. The performance trend for LPRD samples is Au>>Pt>Pd>Rh>Ir, while for IMP samples the order Rh>Ir>Pd≈Pt>Au is observed. Particle sizes and metal dispersions alone are not enough to explain these differences; therefore they must be related with the metal itself. Thus, it should be interesting to plot the intrinsic activity of each noble metal at a selected temperature as a function of the dissociative chemisorption energies of oxygen [30], assuming that dissociative adsorption of oxygen takes place. Figure 8.3 shows the results obtained. If we disregard Au, since it presents a unique mechanism [9] (described in Section 8.1), a typical volcano plot occurs, explaining the catalytic trend observed.

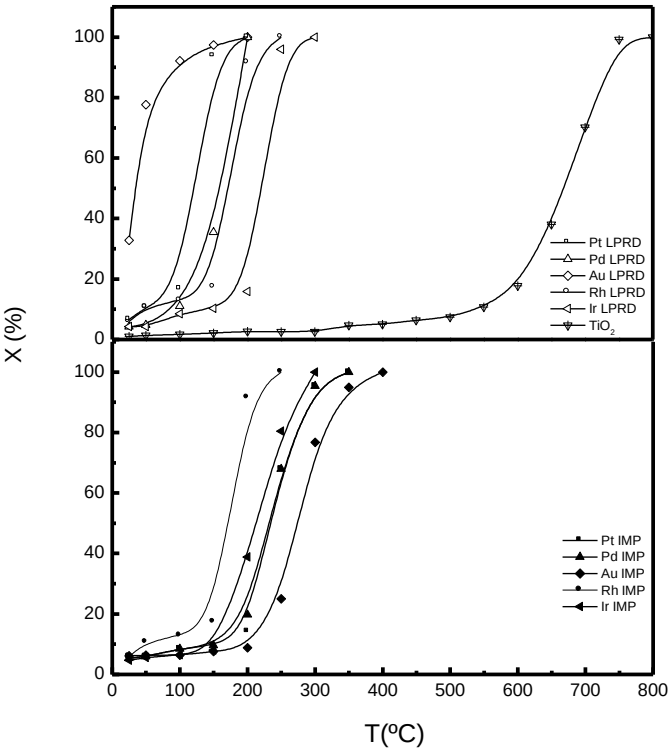

Figure 8.2 Light-off curves for CO oxidation over supported noble metal catalysts.

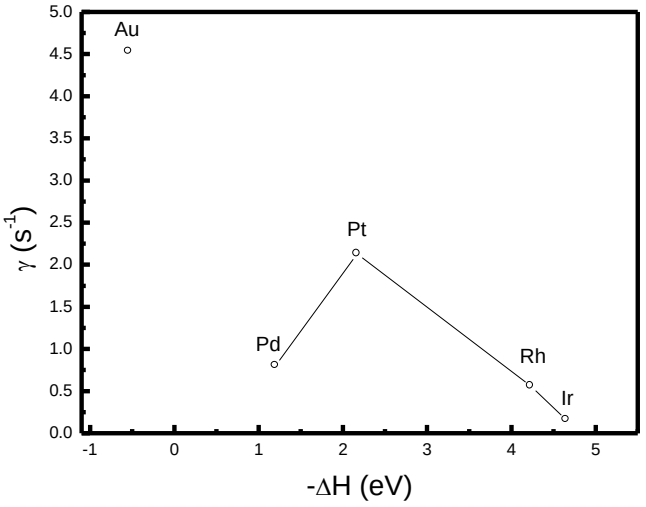

Figure 8.3 Volcano-type plot indicating the specific activity at 175 ºC in CO oxidation for catalysts prepared by LPRD, as a function of oxygen dissociative chemisorption energies on metals.

8.3.2.2 VOC oxidation

Figures 8.4 and 8.5 show the light-off curves for ethanol and toluene oxidation, respectively. For comparative purposes, the light-off curve of the support was also included. The temperatures corresponding to 50, 90 and 100% of conversion into CO_2 are summarized in Table 8.2. Accordingly, it can be observed that the temperature required for a certain level of conversion into CO_2 (higher than 50%), for both VOC studied, is always higher for the catalysts prepared by IMP, like the results obtained for CO oxidation. For example, with the Pt LPRD catalyst, ethanol and toluene are completely oxidized to CO_2 at 260 and 210 ºC, respectively, which is ~20 ºC less than with the Pt conventional catalyst (IMP). However, according to Table 8.1, the samples prepared by the two methods display very different metal dispersions, so their catalytic performance should be compared taking into account the particle size effect. The effect of the average metal particle size on the intrinsic activity (γ) of each catalyst is presented in Table 8.3. For each type of noble metal, the intrinsic activity (γ) was determined at selected temperatures (between 210ºC and 300ºC). For the oxidation of both VOC, the intrinsic activities of Pt/TiO_2 and Pd/TiO_2 were found to increase with the metal particle size. In fact, the activity doubles as the average particle size varies from 3.6 to 5.4 nm (for Pt), or from 4.0 to 7.2 nm (for Pd). These results show that the oxidation of ethanol and toluene over Pt and Pd catalysts is structure-sensitive. Considering the Rh and Au catalysts in the oxidation of ethanol, it can be observed that the intrinsic activity slightly decreases with the increase of the average particle size of Rh, while in the case of Au the influence is rather weak, taking into consideration the errors involved

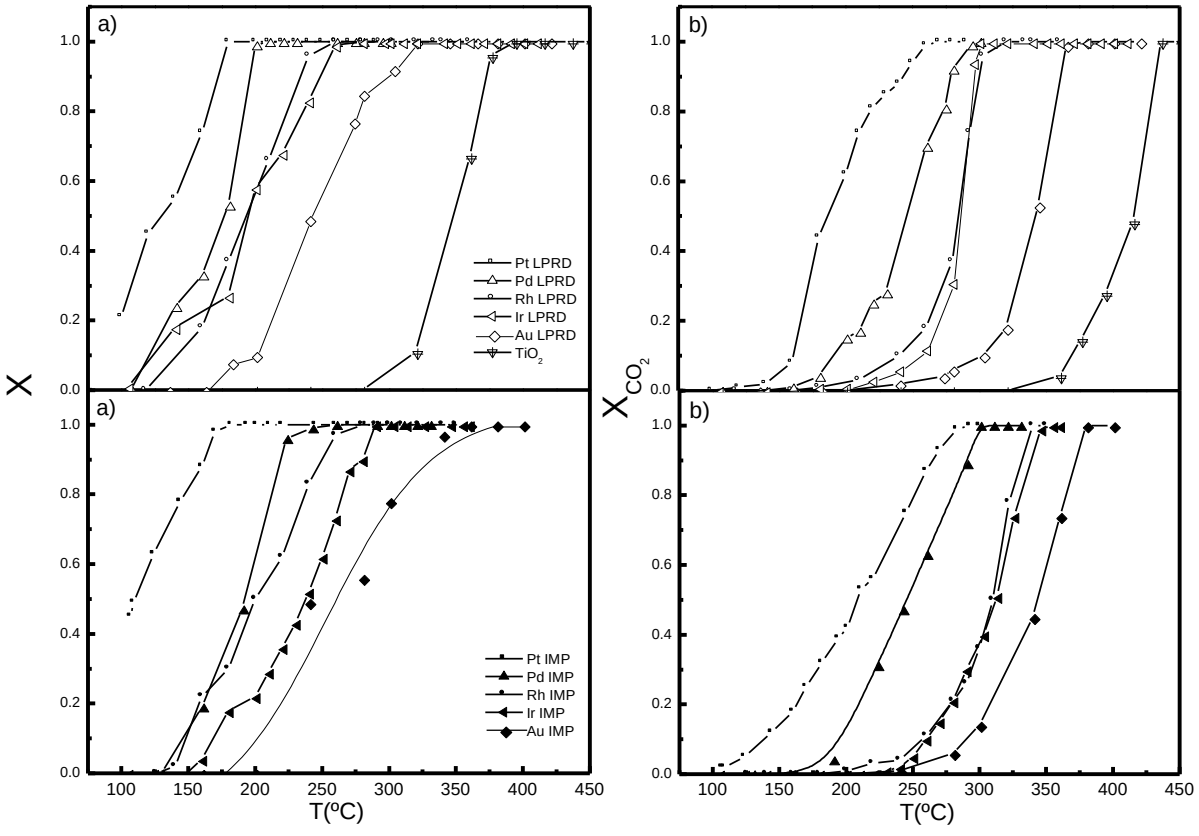

Figure 8.4 Light-off curves for ethanol oxidation over supported noble metal catalysts: a) Ethanol conversion (X); b) Conversion into CO_2 (X_{CO2}).

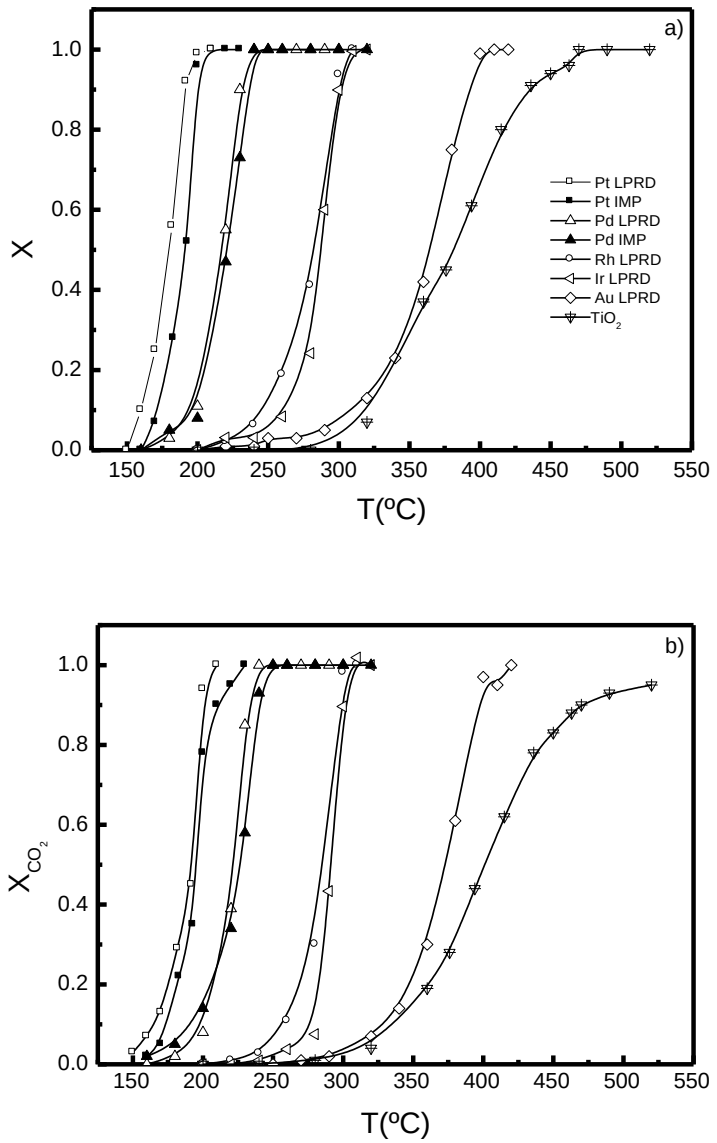

Figure 8.5 Light-off curves for toluene oxidation over supported noble metal catalysts: a) Toluene conversion (X); b) Conversion into CO_2 (X_{CO2}).

Table 8.2 Catalytic activity data expressed as T_{50} (ºC), T_{90} (ºC) and T_{100} (ºC) (temperatures at which 50%, 90% and 100% conversion into CO_2 are obtained).

Catalysts	Ethanol			Toluene		
	T_{50}	T_{90}	T_{100}	T_{50}	T_{90}	T_{100}
Pt IMP	208	265	283	196	212	230
Pt LPRD	187	243	260	191	201	210
Pd IMP	245	290	300	226	242	250
Pd LPRD	245	279	294	221	234	240
Ir IMP	312	340	346	-	-	-
Ir LPRD	283	296	300	292	302	313
Rh IMP	310	332	340	-	-	-
Rh LPRD	283	300	316	284	300	310
Au IMP	341	373	380	-	-	-
Au LPRD	341	363	370	372	398	420
TiO_2	413	432	436	403	470	>520

There are some studies in the literature concerning the effect of the metal particle size on the catalytic combustion of VOC (hydrocarbons, ethyl acetate and benzene) [3, 21-23, 31]. To the best of our knowledge, no study has been reported on the influence of particle size in the oxidation of toluene and ethanol using these catalysts; particularly, we found no reference to studies concerning titania supported Ir or Rh catalysts. It was observed that the correlation between the catalytic activity and the metal dispersion depends on the type of VOC, the noble metal and the support. Usually, the oxidation of VOC over Pt supported catalysts is recognized to be structure sensitive [31]. The enhancement of activity on larger crystallites was ascribed to the differences in the nature of the supported active phase. Papaefthimiou et al. [3] studied the oxidation of benzene and ethyl acetate over Pt based catalysts and they found that the turnover frequency (TOF) strongly increases with the particle size on Pt/Al_2O_3; on a Pt/TiO_2

catalyst this correlation was found to be rather weak compared to the Pt/Al_2O_3 catalyst.

In both systems (ethanol and toluene), the presence of noble metal decreases the formation of by-products (namely acetaldehyde and acetic acid in ethanol oxidation and CO in toluene oxidation), and increases the CO_2 yield. For example, in the presence of the Pt LPRD catalyst, ethanol is completely oxidized into CO_2 at 260 ºC, while no CO_2 was formed at this temperature in the presence of titania only. The CO oxidation experiments (Figure 8.2) confirmed these results, since the support is almost unable to convert CO below 350 ºC, while in the presence of a noble metal full conversions are already achieved at that temperature, or even below.

By comparing the temperatures for 50%, 90% and 100% conversion into CO_2, the following performance trend was observed in the oxidation of both VOC (independently of the preparation method): Pt > Pd >> Rh ≈ Ir >> Au >>support (see Table 8.2). For example, with Pt LPRD, the oxidation of ethanol and toluene into CO_2 starts at about 150 ºC (Figures 8.4 and 8.5) and complete conversion into CO_2 occurs at 260 and 210 ºC, respectively (see Table 8.2). In the presence of Au LPRD, the complete oxidations of ethanol and toluene were achieved at 370 and 420 ºC, respectively. This catalytic trend can be explained in terms of the oxidation mechanism. In the literature, it was suggested that the oxidation of VOC over supported noble metal catalysts usually involves the dissociative adsorption of oxygen. Accordingly, the intrinsic activity of each noble metal at a selected temperature was plotted as a function of the dissociative chemisorption energies of oxygen [30], as it was done for CO oxidation (see Section 8.3.2.1). Figure 8.6 shows the results thus obtained. As can be seen, typical volcano plots occur, explaining the catalytic trend observed. In particular, it explains the relatively lower performance of gold catalysts in comparison to the other noble metals.

Table 8.3 Specific activities as a function of the catalysts average metal particle size

Catalyst	d_M[a](nm)	Ethanol		Toluene	
		T(ºC)[c]	γ (s^{-1})	T (ºC)[c]	γ (s^{-1})
Pt LPRD	3.6	260	1.05	210	1.05
Pt IMP	5.4		1.89		1.95
Pd LPRD	4.0	294	0.57	240	0.57
Pd IMP	7.2		1.25		1.05
Ir LPRD	2.9	300	0.54	300	0.49
Ir IMP	6.1		0.64		-
Rh LPRD	3.8	300	0.51	300	0.52
Rh IMP	5.2		0.36		-
Au LPRD	4.0[b]	285	0.12	300	0.12
Au IMP	9.1[b]		0.14		-

a obtained by hydrogen chemisorption
b obtained by TEM
c selected temperatures for the determination of the intrinsic activities

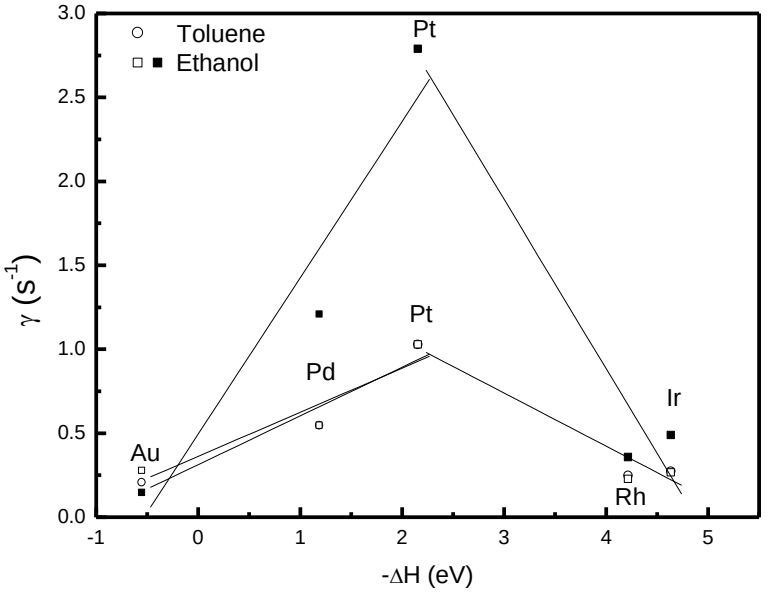

Figure 8.6 Volcano-type plot indicating the specific activity at 285 ºC in VOC oxidation as a function of oxygen dissociative chemisorption energies on metals. The filled symbols represent the catalysts prepared by IMP, while the empty symbols represent the catalysts prepared by LPRD.

8.3.3 Oxidation of VOC mixtures

Industrial emissions usually contain a mixture of VOC, and not just one single component. Moreover, it has been reported that the oxidation of a VOC in a mixture is different from its single oxidation, due to the interaction of the different species with the catalyst. The mixture effect is very difficult to predict a priori, as either a common inhibition effect or a rare promoting effect could be observed, when the components of the mixture are oxidized [32-38]. Apart from the possible inhibitory or promoting effects, some changes in the selectivity to by-products have also been reported when mixtures of VOC are oxidized [34].

The aim of this section is to study the performance of Pt/TiO_2 (LPRD) in the oxidation of binary mixtures. We will first consider in more detail the complete oxidation of single organic compounds.

Single oxidation of ethanol and toluene over titania supported Pt catalyst

The catalytic performance of the Pt/TiO_2 catalyst in the single oxidation of toluene and ethanol is shown in Figures 8.5 and 8.7, respectively.

Regarding ethanol oxidation (see Figure 8.7), it can be seen that acetaldehyde, formed by the partial oxidation of ethanol according to the equation :

$$C_2H_5OH + \tfrac{1}{2}O_2 \rightarrow CH_3CHO + H_2O \qquad (8.1)$$

is the primary product below 170 ºC. Its production reaches a maximum at ~160 ºC, and starts to decrease with temperature increase, down to 0% at 230 ºC. On the other hand, the conversion into CO_2 continuously increases with reaction temperature, reaching 100% at 260 ºC. During toluene oxidation, no significant amounts of by-products were detected, and $X_{CO2} \approx X$ (see Figure 8.5).

Comparing Figures 8.5 and 8.7, it can be observed that ethanol is slightly more reactive than toluene. These two VOC are completely oxidised at 200 ºC and 210 ºC, respectively. However, the complete oxidation into CO_2 occurs at a lower temperature in the case of toluene (see Table 8.3), which may indicate that the by-products formed in the partial oxidation of ethanol (namely acetaldehyde) are less reactive than toluene.

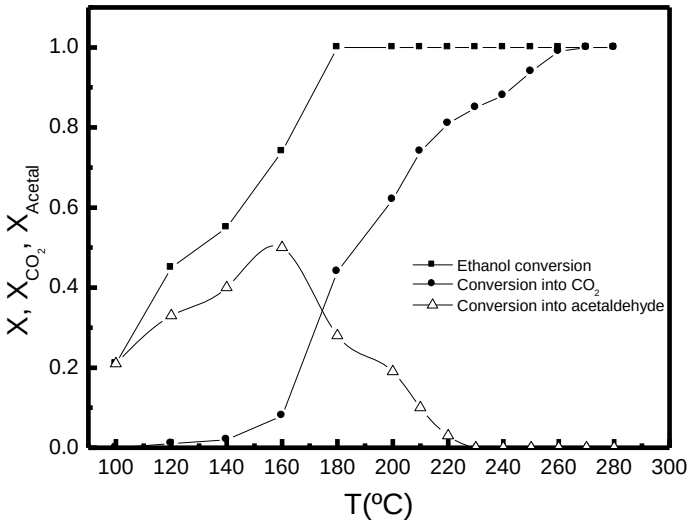

Figure 8.7 Light-off curves corresponding to ethanol oxidation on titania supported Pt catalyst (LPRD). Conversion into acetaldehyde (X_{Acetal}) is defined as: $X_{Acetal} = \frac{F_{Acetal}}{F_{Ethanol,in}}$, where F_{Acetal} is the outlet molar flow rate of acetaldehyde at steady state.

The results obtained for the oxidation of ethanol and toluene mixtures in the presence of Pt/TiO_2 are shown in Figures 8.8 and 8.9. Regarding the effect of toluene on ethanol oxidation (Figure 8.8), it can be seen that the presence of toluene inhibits the partial combustion of ethanol (especially at low temperatures), decreasing the acetaldehyde yield. The curves corresponding to the conversion of ethanol and its conversion to acetaldehyde are shifted to higher temperatures as toluene concentration increases. The amount of acetaldehyde formed is smaller when toluene is added to ethanol.

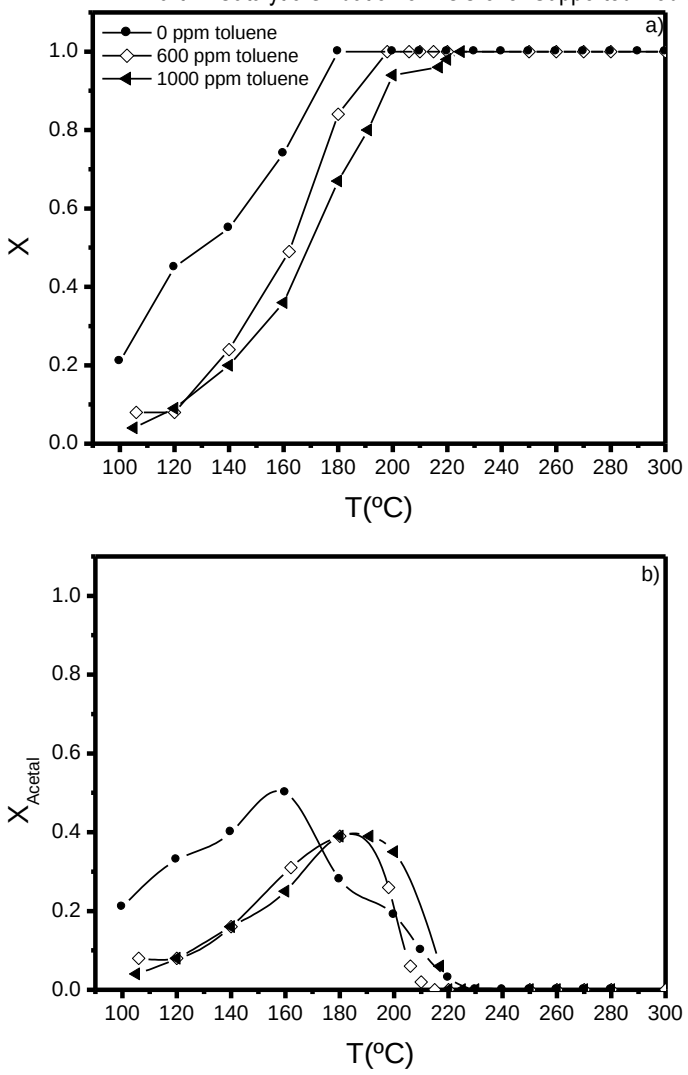

Figure 8.8 a) Ethanol conversion curves alone and in binary mixtures with toluene, in the presence of titania supported Pt catalyst (LPRD). b) Conversion into acetaldehyde $X_{Acetal} = \frac{F_{Acetal}}{F_{Ethanol,in}}$, where F_{Acetal} is the outlet molar flow rate of acetaldehyde at steady state.

Figure 8.9 shows the effect of ethanol concentration on toluene oxidation. It can be observed that the presence of ethanol slightly inhibits toluene combustion, although the effect is not as pronounced as with the addition of toluene to ethanol. Similar results were reported by Burgos et al. [36] for the simultaneous oxidation of toluene and isopropanol over a Pt/Al_2O_3 catalyst. They found out that toluene inhibits the conversion of 2-propanol to acetone, shifting the light-off curves to higher temperatures, while 2-propanol does not have any significant effect on toluene oxidation. In order to explain these results, adsorption studies of both compounds and subsequent temperature programmed desorption (TPD) and temperature programmed surface oxidation (TPSO) experiments were performed by the same authors. They showed that both VOC adsorb on the support, and the adsorption preference is related to the polarity of the VOC. From this result, those authors deduced that toluene reacts mainly in the gas phase with oxygen chemisorbed on the metal surface (Rideal-Eley mechanism). On the other hand, iso-propanol is oxidized via acetone formation over the catalyst surface, by a two-centre mechanism involving alcohol chemisorbed on alumina and oxygen chemisorbed on Pt. In summary, the reactivity is mainly affected by the competition for the oxygen atoms chemisorbed on the Pt particles. Although the support used in our work is different (TiO_2) from that reported by Burgos et al. (Al_2O_3) [31], we believe that the results obtained by these authors can help us to interpret our own findings. Moreover, isopropanol is not that much different from ethanol in terms of polarity (authors report the formation of acetone instead of acetaldehyde as we found in our own work) and toluene was also used in the mentioned work. Therefore, we believe that a similar mechanism can take place in the present case.

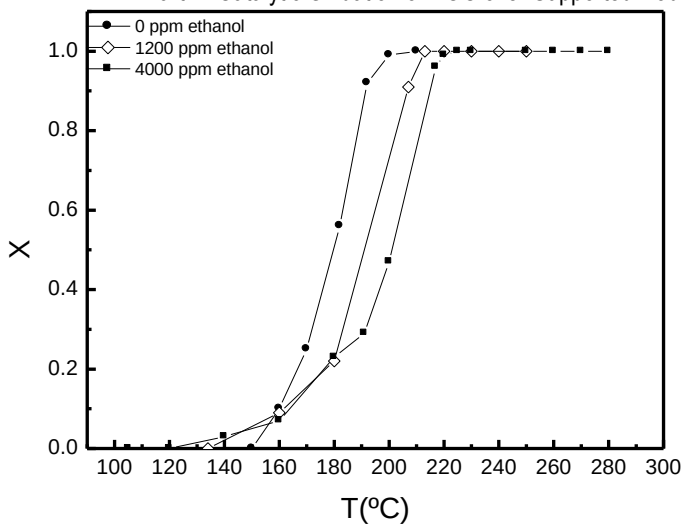

Figure 8.9 Toluene conversion curves alone and in binary mixtures with ethanol, in the presence of titania supported Pt catalyst (LPRD).

8.4 Conclusions

LPRD is a suitable method for the preparation of highly dispersed supported noble metal catalysts, which are very active for the total oxidation of CO and VOC.

The preparation method does not change the catalytic trend in VOC oxidation, but it does in CO oxidation. The following performance trend was observed for VOC oxidation for both preparation methods: Pt > Pd >> Rh ≈ Ir >> Au >>support. For CO oxidation, the trend for the catalysts prepared by LPRD is Au>>Pt>Pd>Rh>Ir, while for IMP samples is Rh>Ir>Pd≈ Pt>Au.

The dispersion of the metal phase has an important effect on the performance of the catalysts towards total oxidation of CO and VOC (especially in the case of Au in CO oxidation).

The oxidation reactions of ethanol and toluene in the presence of Pt or Pd catalysts are structure sensitive.

In the catalytic oxidation of mixtures over Pt/TiO_2 it was observed that toluene and ethanol have a mutual inhibitory effect. However, this effect is much more evident in the case of ethanol.

References

[1] J.J. Spivey, *Complete catalytic-oxidation of volatile organics*. Ind. Eng. Chem. Res. 26 (1987) 2165-2180.

[2] J.E. Sawyer, M.A. Abraham, *Reaction pathways during the oxidation of ethyl-acetate on a Pt/Al_2O_3 catalyst*. Ind. Eng. Chem. Res. 33 (1994) 2084-2089.

[3] P. Papaefthimiou, T. Ioannides, X.E. Verykios, *Performance of doped Pt/TiO_2 (W^{6+}) catalysts for combustion of volatile organic compounds (VOCs)*. Appl. Catal. B-Environ. 15 (1998) 75-92.

[4] E.M. Cordi, J.L. Falconer, *Oxidation of volatile organic compounds on a Ag/Al_2O_3 catalyst*. Appl. Catal. A-Gen. 151 (1997) 179-191.

[5] G.L. Dong, J.G. Wang, Y.B. Gao, S.Y. Chen, *A novel catalyst for CO oxidation at low temperature*. Catal. Lett. 58 (1999) 37-41.

[6] T. Mitsui, T. Matsui, R. Kikuchi, K. Eguchi, *Low-temperature complete oxidation of ethyl acetate over CeO_2-supported precious metal catalysts*. Top. Catal. 52 (2009) 464-469.

[7] W.B. Li, J.X. Wang, H. Gong, *Catalytic combustion of VOCs on non-noble metal catalysts*. Catal. Today 148 (2009) 81-87.

[8] N. Bion, F. Epron, M. Moreno, F. Marino, D. Duprez, *Preferential oxidation of carbon monoxide in the presence of hydrogen (PROX) over noble metals and transition metal oxides: advantages and drawbacks*. Top. Catal. 51 (2008) 76-88.

[9] G.C. Bond, D.T. Thompson, *Gold-catalysed oxidation of carbon monoxide*. Gold Bull. 33 (2000) 41-51.

[10] E.D. Park, D. Lee, H.C. Lee, *Recent progress in selective CO removal in a H_2 rich stream*. Catal. Today 139 (2009) 280-290.

[11] M. Skoglundh, E. Fridell, *Strategies for enhancing low-temperature activity*. Top. Catal. 28 (2004) 79-87.

[12] S.A.C. Carabineiro, D.T. Thompson, *Catalytic applications for gold nanotechnology*, in: Nanocatalysis, Eds. U. Heiz and U. Landman, Springer-Verlag, Berlin, Heidelberg, New York, pp. 377-489.

[13] S.A.C. Carabineiro, D.T. Thompson, *Gold catalysis* in: Gold: Science and applications, Eds. C. Corti, R. Holliday, CRC Press, Taylor and Francis Group, Boca Raton, London, New York, Chapter 6, pp.89-122.

[14] S.A.C. Carabineiro, A.M.T. Silva, G. Dražić, P.B. Tavares, J.L. Figueiredo, *Effect of chloride on the sinterization of Au/CeO_2 catalysts*. Catal. Today (2010), doi:10.1016/j.cattod.2009.12.017.

[15] P. Papaefthimiou, T. Ioannides, X.E. Verykios, *VOC removal: investigation of ethylacetate oxidation over supported Pt catalysts*. Catal. Today 54 (1999) 81-92.

[16] C. Della Pina, N. Dimitratos, E. Falletta, M. Rossi, A. Siani, *Catalytic performance of gold catalysts in the total oxidation of VOCs*. Gold Bull. 40 (2007) 67-72.

[17] M.I. Dominguez, M. Sanchez, M.A. Centeno, M. Montes, J.A. Odriozola, *2-propanol oxidation over gold supported catalysts coated ceramic foams prepared from stainless steel wastes*. J. Mol. Catal. A-Chem. 277 (2007) 145-154.

[18] C. Gennequin, M. Lamallem, R. Cousin, S. Siffert, F. Aissi, A. Aboukais, *Catalytic oxidation of VOCs on Au/Ce-Ti-O*. Catal. Today 122 (2007) 301-306.

[19] S.Y. Liu, S.M. Yang, *Complete oxidation of 2-propanol over gold-based catalysts supported on metal oxides*. Appl. Catal. A-Gen. 334 (2008) 92-99.

[20] G. Bond, D. Thompson, *Formulation of mechanisms for gold-catalysed reactions*. Gold Bull. 42 (2009) 247-259.

[21] P. Briot, A. Auroux, D. Jones, M. Primet, *Effect of particle-size on the reactivity of oxygen-adsorbed platinum supported on alumina*. Appl. Catal. 59 (1990) 141-152.

[22] V. Labalme, E. Garbowski, N. Guilhaume, M. Primet, *Modifications of Pt/alumina combustion catalysts by barium addition. Properties of aged catalysts*. Appl. Catal. A-Gen. 138 (1996) 93-108.

[23] K. Otto, *Methane oxidation over Pt/Al_2O_3 - kinetics and structure sensitivity*. Langmuir 5 (1989) 1364-1369.

[24] Y. Sunagawa, K. Yamamoto, H. Takahashi, A. Muramatsu, *Liquid-phase reductive deposition as a novel nanoparticle synthesis method and its application to supported noble metal catalyst preparation*. Catal. Today 132 (2008) 81-87.

[25] P.C. Aben, *Palladium areas in supported catalysts - determination of palladium surface areas in supported catalysts by means of hydrogen chemisorption*. J. Catal. 10 (1968) 224-&.

[26] V.P. Santos, M.F.R. Pereira, J.J.M. Órfão, J.L. Figueiredo, *Synthesis and characterization of manganese oxide catalysts for the total oxidation of ethyl acetate*. Top. Catal. 52 (2009) 470-481.

[27] M. Lamallem, H. El Ayadi, C. Gennequin, R. Cousin, S. Siffert, F. Aissi, A. Aboukais, *Effect of the preparation method on Au/Ce-Ti-O catalysts activity for VOCs oxidation*. Catal. Today 137 (2008) 367-372.

[28] S. Ivanova, W. Pitchon, Y. Zimmermann, C. Petit, *Preparation of alumina supported gold catalysts: Influence of washing procedures, mechanism of particles size growth*. Appl. Catal. A-Gen. 298 (2006) 57-64.

[29] R. Zanella, L. Delannoy, C. Louis, *Mechanism of deposition of gold precursors onto TiO_2 during the preparation by cation adsorption and deposition-precipitation with NaOH and urea*. Appl. Catal. A-Gen. 291 (2005) 62-72.

[30] T. Bligaard, J.K. Norskov, S. Dahl, J. Matthiesen, C.H. Christensen, J. Sehested, *The Bronsted-Evans-Polanyi relation and the volcano curve in heterogeneous catalysis*. J. Catal. 224 (2004) 206-217.

[31] T.F. Garetto, C.R. Apesteguia, *Structure sensitivity and in situ activation of benzene combustion on Pt/Al_2O_3 catalysts*. Appl. Catal. B-Environ. 32 (2001) 83-94.

[32] J. Hermia, S. Vigneron, *Catalytic incineration for odour abatement and VOC destruction*. Catal. Today 17 (1993) 349-358.

[33] J. Tsou, P. Magnoux, M. Guisnet, J.J.M. Órfão, J.L. Figueiredo, *Catalytic oxidation of volatile organic compounds - Oxidation of methyl-isobutyl-ketone over Pt/zeolite catalysts*. Appl. Catal. B-Environ. 57 (2005) 117-123.

[34] F.N. Aguero, B.P. Barbero, L. Gambaro, L.E. Cadus, *Catalytic combustion of volatile organic compounds in binary mixtures over MnO_x/Al_2O_3 catalyst*. Appl. Catal. B-Environ. 91 (2009) 108-112.

[35] V. Blasin-Aubé, J. Belkouch, L. Monceaux, *General study of catalytic oxidation of various VOCs over $La_{0.8}Sr_{0.2}MnO_{3+x}$ perovskite catalyst-influence of mixture*. Appl. Catal. B-Environ. 43 (2003) 175-186.

[36] N. Burgos, M. Paulis, M.M. Antxustegi, M. Montes, *Deep oxidation of VOC mixtures with platinum supported on Al_2O_3/Al monoliths*. Appl. Catal. B-Environ. 38 (2002) 251-258.

[37] J.I. Gutierrez-Ortiz, B. de Rivas, R. Lopez-Fonseca, J.R. Gonzalez-Velasco, *Catalytic purification of waste gases containing VOC mixtures with Ce/Zr solid solutions*. Appl. Catal. B-Environ. 65 (2006) 191-200.

[38] P.-O. Larsson, A. Andersson, *Oxides of copper, ceria promoted copper, manganese and copper manganese on Al_2O_3 for the combustion of CO, ethyl acetate and ethanol*. Appl. Catal. B-Environ. 24 (2000) 175-192.

9 Oxidation of Ethyl Acetate over TiO_2 supported Pt and Pd Catalysts[1]

The catalytic oxidation of ethyl acetate in low concentration was investigated over noble metal catalysts (palladium or platinum) supported on titania. The influence of several parameters was investigated, such as the crystalline phase of the support, the nature and amount of noble metal, the metal dispersion and the activation conditions.

The crystalline phase of titania was found to have a slight effect on its performance, anatase being the most active phase.

In comparison to titania alone, the presence of noble metal enhances the activity and decreases the amount of by-products produced. Platinum was found to be more active and selective to CO_2 than palladium. The activation conditions influence the activity of the Pt/TiO_2 catalyst, the highest activities being obtained when the catalyst was activated under hydrogen.

The presence of water vapour in the feed enhances the global conversion and decreases CO_2 selectivity. On the other hand, the presence of CO_2 in the feed does not affect the performance of the catalyst.

9.1 Introduction

Volatile organic compounds (VOC) are considered an important class of air pollutants, not only due to their toxic nature, but also because they are precursors of ground level ozone and smog [1]. VOC are emitted into the atmosphere from a variety of sources, such as industrial processes (stationary sources ≈ 40 %) and vehicle exhaust (mobile sources ≈ 60 %). Among the different methods that can be applied to efficiently control the emissions of VOC, catalytic oxidation seems to be the most efficient and cost-effective technology for emissions containing low concentrations [2, 3]. In this

[1] Part of this chapter was published in: VP Santos, MFR Pereira, JJM Órfão, JL Figueiredo, Chempor 2008, Setembro, Braga, Portugal.

process, high elimination efficiency can be achieved at relatively low temperatures, although the performance of the process critically depends on the type of the catalyst used, operating temperature, VOC type and concentration, space velocity and O_2 concentration.

Extensive studies have been carried out in recent years in order to develop more active catalysts and to understand the factors that determine VOC reactivity [4-8].

The choice of catalyst (metal oxide or noble metal catalyst) depends on several factors, including the nature of the stream to be treated and/or the presence of contaminants; however, it is generally accepted that noble metals are more active than metal oxides [9].

In a previous work [10], the activity of several noble metals (Pt, Pd, Ir, Rh and Au) supported on titania was evaluated in the oxidation of ethanol and toluene. Platinum and palladium catalysts were found to be the most active catalysts. Furthermore, the oxidations of ethanol and toluene over the same catalysts (Pt and Pd) were found to be structure sensitive reactions, intrinsic activities increasing with the average metal particle size.

The main goal of the present work is to study the oxidation of ethyl acetate over noble metal catalysts supported on titania. Several parameters were investigated, such as the crystalline phase of the support and the nature of the noble metal (platinum or palladium). The best catalytic system was chosen for further studies, namely the effects of the load of noble metal, pre-treatment conditions, stability and the presence of other species in the performance of the catalyst.

9.2 Experimental

9.2.1 Catalysts synthesis and characterization

Three TiO_2 samples with different amounts of anatase and rutile phases were used in this work. The first sample was synthesized by an acid-catalysed sol-gel method from an alkoxide precursor [11]. The gel was aged in air for one week. The resulting xerogel was ground and dried at room temperature. The powder was calcined at 400 ºC for 2 hours. The second sample is a commercial product (Degussa P-25) containing

80% anatase. The third sample (P-25, air, 700 ºC) was obtained by submitting P-25 to a thermal treatment at 700 ºC under air, in order to reduce the content of anatase.

Platinum and palladium supported catalysts were prepared by incipient wetness impregnation on Degussa P-25 using as metal precursors, H_2PtCl_6 and $PdCl_2$, respectively (metal load: 1% or 2%). The resulting materials were dried at 110 ºC overnight and calcined at 500 ºC for 2 hours.

An additional titania supported platinum catalyst (Cyted Pt 5) was used in this work, in order to study the effect of the metal particle size on the catalyst performance. Cyted Pt 5 was prepared by incipient wetness impregnation on Millenium DT5, using $Pt(NH_3)_4(OH)_2$ as metal precursor (metal load 1%). Millenium DT5 is a comercial product containing 100% anatase.

The crystalline structure of titania samples was studied by X-ray diffraction (XRD). The metal dispersion was obtained by hydrogen chemisorption at room temperature. Chemical analyses were performed in selected samples by inductive coupled plasma (ICP/AOS). BET surface areas were calculated from nitrogen adsorption at -196 ºC. The characterization results are shown in Table 9.1.

9.2.2 Catalytic Experiments

The catalytic oxidation of ethyl acetate was performed under atmospheric pressure in a fixed-bed reactor from Autoclave Engineers (BTRS Jr), consisting of a stainless steel tube of 6 mm internal diameter, placed inside a temperature-controlled electric furnace. A feed gas with a VOC concentration of 4,000 mgC/m^3 and a space velocity of 16,000 h^{-1} was used in standard tests. The catalyst sample (50 mg) was diluted with glass spheres of the same size as the catalyst particles (0.2-0.5 mm), in order to minimize temperature gradients. Usually, the catalyst is pre-treated in air at 400 ºC for 1 hour, prior to the reaction.

Conversions were measured over the range 100-350 ºC by incremental steps (10-20 ºC), the temperature being measured by a thermocouple placed in the middle of the catalyst bed. To ensure that steady state data were measured, the reactor was maintained at each temperature for 30 minutes. The conversion of VOC (X) and the

conversion into CO_2 (X_{CO_2}) were respectively calculated as $X = 1 - \frac{F_{VOC}}{F_{VOC,in}}$ and $X_{CO_2} = \frac{F_{CO_2}}{\nu F_{VOC,in}}$, where F_{VOC} is the outlet molar flow rate of VOC at steady state, $F_{VOC,in}$ is the inlet molar flow rate of VOC, F_{CO_2} is the outlet molar flow rate of CO_2 at steady state and ν is the number of carbon atoms in the VOC molecule (for ethyl acetate ν = 4). Further details can be found elsewhere [12].

9.3 Results and discussion

9.3.1 Characterization

The crystalline structure of the titania samples was studied by XRD. Figure 9.1 shows the XRD patterns of the three samples. Anatase was the only phase detected in the TiO_2 (sol-gel) sample; the diffraction peaks are relatively broad, which indicates small crystallite sizes.

In the other samples there is a mixture of anatase and rutile phases, as expected. The third sample shows a clear conversion from anatase to rutile phase after the heat treatment. The corresponding anatase content was determined from the equation [13]:

$$x = \left(1 + 1.26\frac{I_R}{I_A}\right)^{-1} \tag{9.1}$$

where x is the anatase fraction and I_R and I_A are the integral intensities of the (110) and (101) peaks of rutile and anatase, respectively.

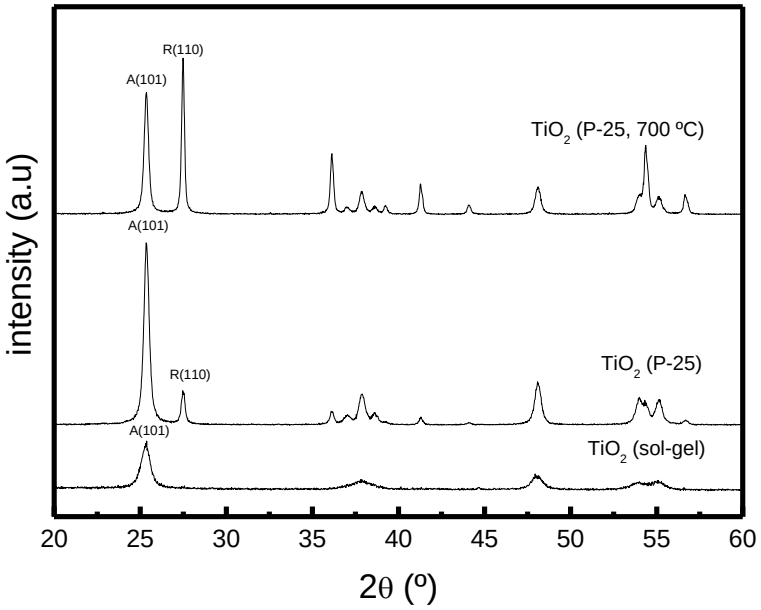

Figure 9.1 XRD patterns of the TiO_2 samples (the samples are identified in Table 9.1).

Table 9.1 Properties of the catalysts: crystalline phase (XRD), metal load (ICP/OES), metal dispersion (hydrogen chemisorption), surface area (nitrogen adsorption).

Sample	Phases	%M	D_M (%)	S_{BET} (m^2/g)
TiO_2 (sol-gel)	100% anatase	-	-	50
TiO_2 (P-25)	80% anatase	-	-	50
TiO_2 (P-25, 700 ºC)	47 % anatase	-	-	50
1% Pd/TiO_2	80% anatase	0.9	14	50
1% Pt/TiO_2	80% anatase	0.8	15	50
Cyted Pt 5	100% anatase	1.0	3	68
2% Pt/TiO_2	80% anatase	n.d	18	50

9.3.2 Catalytic activities

All the catalysts used in this work were tested in the oxidation of ethyl acetate, in order to obtain the best catalytic system with respect to: a) crystalline structure of the support, comparing three samples with different amounts of anatase; b) nature of the noble metal (palladium or platinum). The results are presented in Figure 9.2. The temperatures corresponding to 50, 90 and 100% conversion and conversion into CO_2 are summarized in Table 9.2.

Table 9.2 Performance of the catalysts used in this work expressed as T_{50}, T_{90} and T_{100} (temperatures in ºC at which 50%, 90% and 100% conversion and conversion into CO_2 are obtained).

Catalysts	T_{50}		T_{90}		T_{100}	
	X	X_{CO2}	X	X_{CO2}	X	X_{CO2}
TiO_2 (sol-gel)	283	331	305	353	330	370
TiO_2 (P-25)	280	339	320	358	345	370
TiO_2 (P-25, 700 ºC)	300	343	331	377	340	389
1% Pd/TiO_2	253	279	282	309	300	330
1% Pt/TiO_2	249	265	270	278	280	290
1% Pt/TiO_2 (pre-reduced)	227	246	258	267	275	276
Cyted Pt 5	239	255	268	278	279	300
2% Pt/TiO_2	236	250	256	268	270	280

Generally, large amounts of by-products were formed in the presence of the support (see differences between X and X_{CO2} in Figure 9.2 and Table 9.2), namely acetic acid, acetaldehyde and acetone, due to the presence of a large number of acidic sites on titania. Considering these by-products, it is possible to assume that the oxidation of ethyl acetate can proceed through different pathways, as depicted in the scheme of Figure 9.3. The oxidation process proposed is also supported by other authors [14, 15]. Furthermore, it can be observed that the crystalline phase of titania has a slight effect on its performance, anatase being the most active phase. For example, over the TiO_2 (sol-gel) sample (corresponding to pure anatase) ethyl acetate is completely oxidised

at 370 ºC (see Table 9.2), which is about 20 ºC lower than with the sample that contains only 47% of anatase.

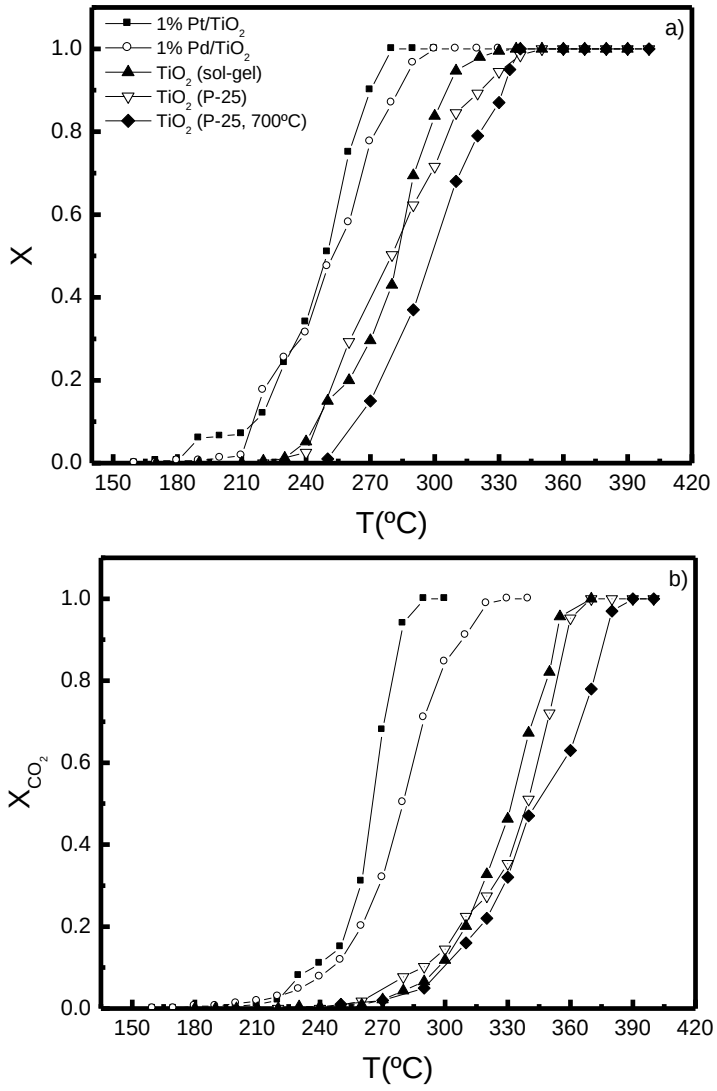

Figure 9.2 Catalytic performance of 1% Pt/TiO_2, 1% Pd/TiO_2 and TiO_2 for the oxidation of ethyl acetate: a) Ethyl acetate conversion (X), b) Conversion into CO_2 (X_{CO2}).

Supporting palladium or platinum on TiO_2 considerably reduces the amount of by-products formed (namely acetaldehyde) and enhances the activity, decreasing the temperature at which ethyl acetate is completely converted into CO_2 to 330 and 290 ºC, respectively. This effect is less evident for the palladium catalyst, where higher amounts of by-products were detected in the temperature range studied. Thus, the Pt/TiO_2 catalyst was selected for further studies. In a previous work [10], platinum was also found to be more active than palladium in the oxidation of ethanol and toluene.

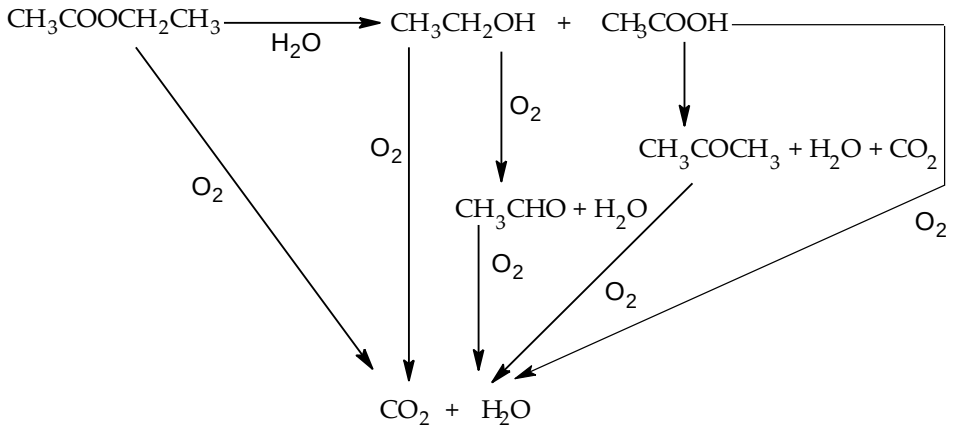

Figure 9.3 Reaction pathways for ethyl acetate

9.3.2.1 Effect of the electronic state of platinum

There are some studies in the literature concerning the effect of the initial electronic state of platinum on its catalytic activity [16, 17]. It was established that metallic platinum species are very active for VOC oxidation. In order to check for the activity of these species on the oxidation of ethyl acetate, the $1\%Pt/TiO_2$ catalyst was reduced before reaction at 350 ºC under hydrogen flow for 2 hours (pre-reduced catalyst). The performances of both samples (pre-reduced and standard) are compared in Figure 9.4.

As can be seen, the pre-reduced catalyst is more active in the oxidation than the calcined one. At 276 ºC, ethyl acetate is fully converted into CO_2 on the pre-reduced catalyst (see Table 9.2), while only 76% conversion into CO_2 can be obtained with the catalyst activated under air. This latter catalyst can only oxidise all the ethyl acetate into CO_2 at temperatures higher than 290 ºC. As a result, it can be concluded that metallic platinum species are the most active for ethyl acetate oxidation.

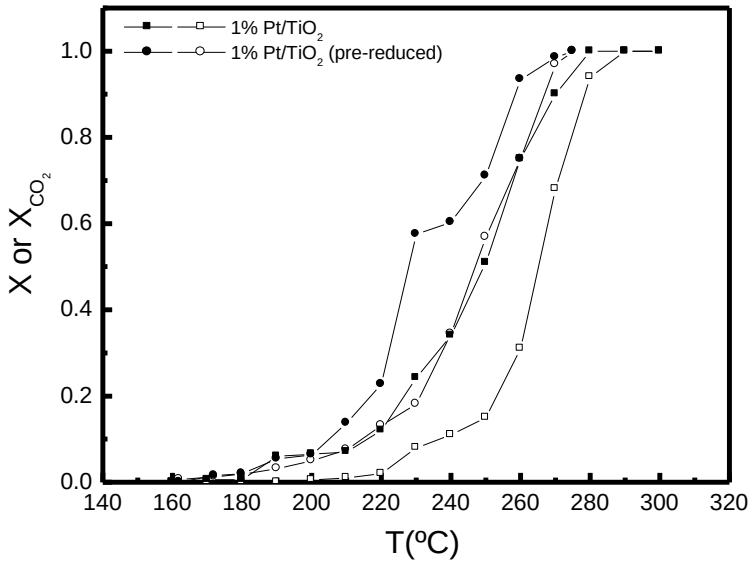

Figure 9.4 Effect of the activation conditions on the performance of titania supported Pt catalyst (filled symbols: ethyl acetate conversion; open symbols: conversion into CO_2.

9.3.2.2 Effect of the metal particle size

The metal particle size can also be an important parameter in oxidation reactions. The oxidation of VOC over Pt supported catalysts is usually considered to be structure sensitive [10, 17-20]. The enhanced activity on larger crystallites has been ascribed to the increased concentration of more reactive surface oxygen species [19]. On the other hand, metal-support interactions can also play a key role. For instance, Papaefthimiou et al. [4] studied the oxidation of benzene and ethyl acetate over Pt based catalysts and they found that the turnover frequency (TOF) strongly increases with the particle size

on Pt/Al_2O_3; on the other hand, in the presence of a Pt/TiO_2 catalyst this correlation was found to be rather weak.

In the present study, the influence of the metal particle size was assessed by comparing the performance of two samples with different metal dispersions (1% Pt/TiO_2 and Cyted Pt 5).

Figure 9.5 and Table 9.2 show the results obtained. It can be observed that the performance was better with the low dispersion catalyst. It is worthwhile to mention that the activities of the two supports (TiO_2 P-25 and TiO_2 Millenium DT) are comparable, which implies that the observed enhancement is due to the higher metal particle size, showing that the ethyl acetate oxidation over Pt/TiO_2 is structure sensitive. This effect was also observed in the oxidation of ethanol and toluene over the same catalyst [10]. However, it seems that the correlation between the intrinsic activity and the metal particle size is stronger in this case.

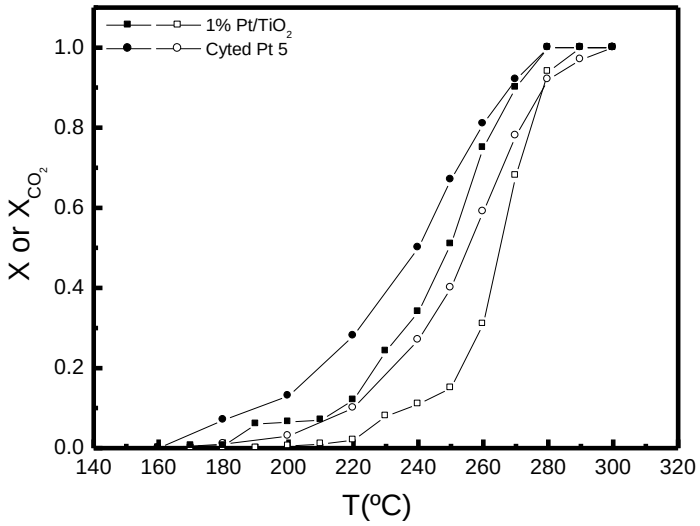

Figure 9.5 Effect of the metal dispersion on the performance of titania supported Pt catalyst (filled symbols: ethyl acetate conversion; open symbols: conversion into CO_2).

9.3.2.3 Influence of platinum content

The influence of platinum load on the catalytic activity was investigated by varying the platinum level from 1 to 2%. The results are presented in Figure 9.6 and Table 9.2. For a similar metal dispersion (see Table 9.1), the higher the platinum content, the higher the global conversion and the CO_2 yield. For example, complete oxidation of ethyl acetate into CO_2 is obtained at 290 ºC for a Pt content of 1% and at 280 ºC for 2%.

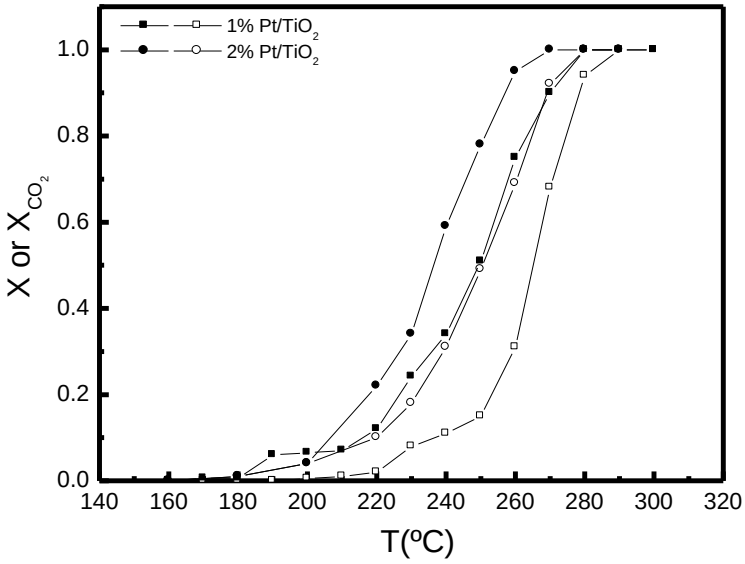

Figure 9.6 Effect of the metal load on the performance of titania supported Pt catalyst (filled symbols: ethyl acetate conversion; open symbols: conversion into CO_2).

9.3.2.4 Stability of the catalyst

In order to analyze the stability of the materials, light-off experiments were made with a fresh catalyst and with a sample previously used in a long duration experiment at 450 ºC for 24 hours. Figure 9.7 shows the results obtained. As can be seen, the conversion into CO_2 was 100% for the whole duration of the experiment. Furthermore, the light-off curves obtained for the fresh and used catalyst show that platinum supported catalyst is stable and does not show any kind of deactivation.

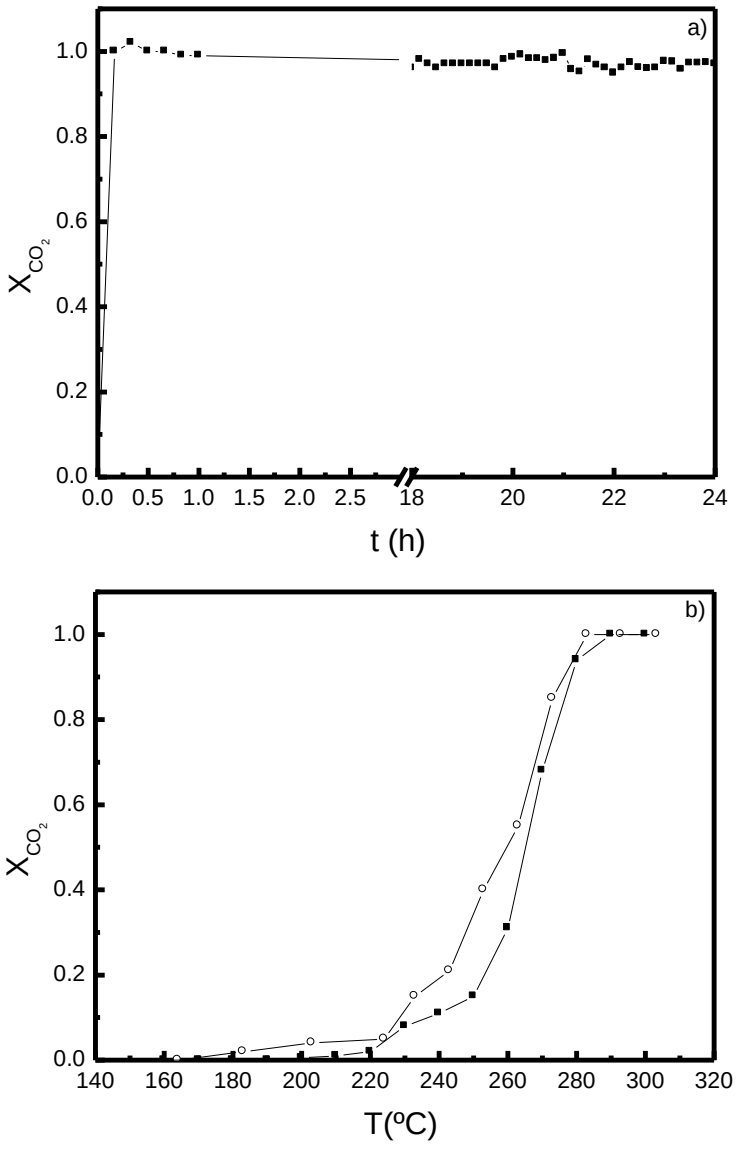

Figure 9.7 Stability of the 1%Pt/TiO_2: a) Long-duration experiment at 450 ºC. b) Light-off curves: fresh catalyst (filled symbols) and used catalyst (open symbols).

9.3.2.5 Effect of the presence of water vapour, CO_2 and ethanol in the feed

In practical situations, the conditions for the oxidation of VOC will not be the same as the standard conditions used in this work. Moisture, CO_2 and other VOC will be present in the feed to be treated. In order to study the effect of these parameters on the performance of the catalyst, kinetic studies were carried out by introducing CO_2, water or ethanol in the feed.

Figure 9.8 shows the effect of CO_2 and water on the performance of Pt/TiO_2. As can be observed, CO_2 does not have a major effect on the performance of the catalyst, suggesting that CO_2 has no affinity for the support (mainly due the absence of basic sites). On the other hand, the presence of water vapour enhances the conversion of ethyl acetate and decreases the CO_2 selectivity. Larger amounts of by-products are formed, such as acetaldehyde, ethylene, acetone, acetic acid and ethanol. Water promotes the decomposition of ethyl acetate into ethanol and acetic acid, which are further converted into acetaldehyde and acetone, or oxidized completely into CO_2 and H_2O. This result supports the oxidation scheme proposed in section 9.3.2., presented in Figure 9.3.

In addition to the results described above, the performance of Pt/TiO_2 in the oxidation of ethyl acetate/ethanol mixtures was also investigated. Kinetic experiments were carried out at different temperatures in the standard conditions described previously (4,000 mgC/m^3 of each VOC). Figure 9.9 shows the results obtained. As can be observed, the oxidation of ethyl acetate is not affected by the presence of ethanol. This result was not expected, since the oxidation of both molecules alone takes place in the same temperature range. On the other hand, ethyl acetate and ethanol are both polar molecules, which results in a similar interaction with the catalyst surface; consequently, they both compete for adsorption onto the active sites. However, this result can be explained by the presence of larger amounts of H_2O, which promote the decomposition of ethyl acetate into ethanol and acetic acid (see Figure 9.3). In this way, it is probable that mutual inhibition effects exist when these two components are oxidised in mixtures, but this effect is minimized by the presence of larger amounts of water vapour.

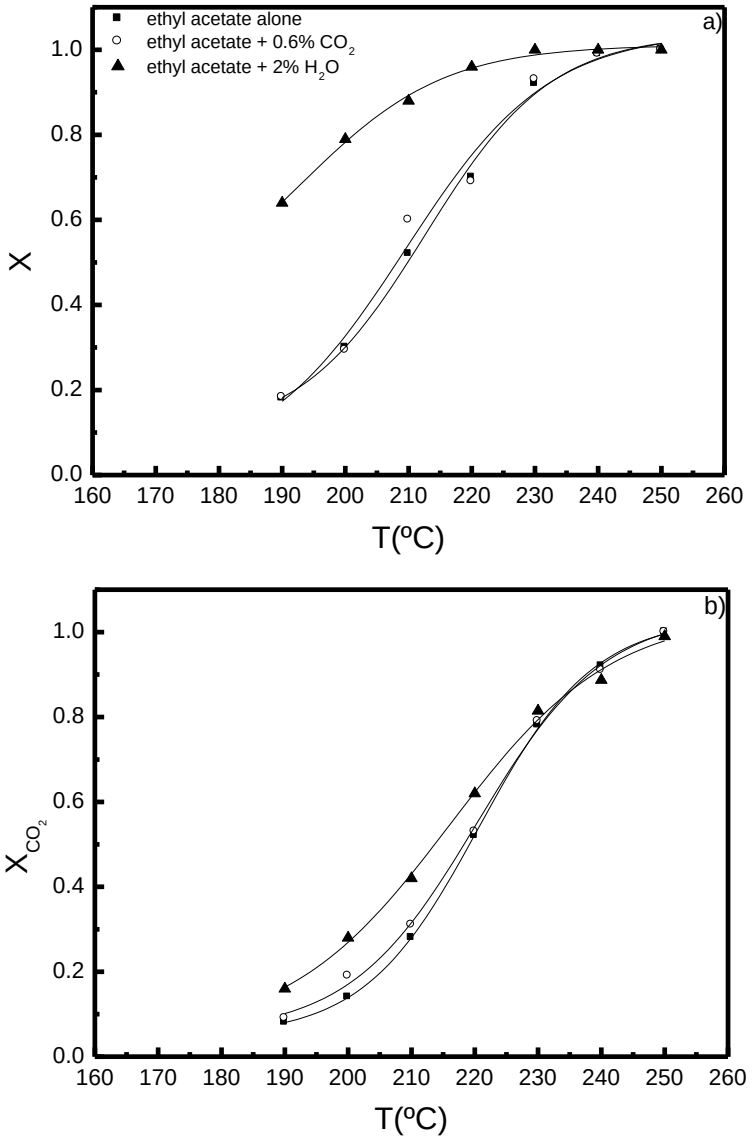

Figure 9.8 Ethyl acetate conversion (a) and conversion into CO_2 (b) as a function of temperature for ethyl acetate oxidation alone and with water vapour or CO_2. Experimental conditions: catalyst weight = 150 mg, space velocity = 16000 h^{-1}, inlet VOC concentration = 4,000 mgC/m^3.

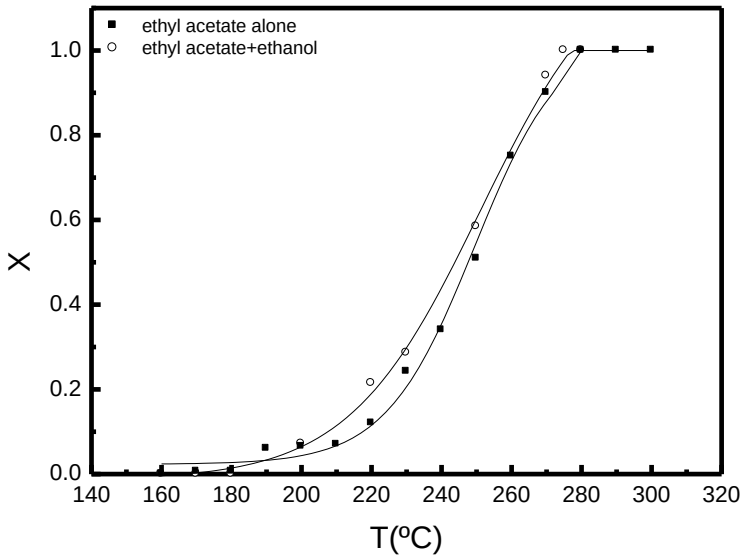

Figure 9.9 Conversion of ethyl acetate alone and in binary mixtures with ethanol (4,000 mgC/m^3) over titania supported Pt catalyst.

9.4 Conclusions

The following conclusions can be drawn from this study:

The TiO_2 phase slight affects its catalytic activity, anatase being more active than the rutile phase.

The presence of a noble metal is essential to increase both the activity and the selectivity into CO_2.

Platinum is more active and selective than palladium.

The pre-reduced catalyst is more active than the pre-calcined one.

The oxidation of ethyl acetate over Pt/TiO_2 is a structure sensitive reaction.

The higher the platinum content, the lower the temperature necessary to completely convert ethyl acetate into CO_2.

Long duration experiments show that the platinum supported catalyst is very stable during the reaction.

The presence of water vapour in the feed stream increases the global conversion but decreases the CO_2 selectivity. On the contrary, CO_2 has no significant influence on those parameters.

References

[1] R.J. Heinsohn, R.L. Kabel, Sources and control of air pollution, in: Prentice Hall, Upper Saddle River, NJ, 1999.

[2] E.C. Moretti, *Reduce VOC and HAP emissions*. Chem. Eng. Prog. **98** (2002) 30-40.

[3] F.I. Khan, A. Kr. Ghoshal, *Removal of Volatile Organic Compounds from polluted air*. J. Loss Prev. Process Ind. **13** (2000) 527-545.

[4] P. Papaefthimiou, T. Ioannides, X.E. Verykios, *Performance of doped Pt/TiO_2 (W^{6+}) catalysts for combustion of volatile organic compounds (VOCs)*. Appl. Catal. B-Environ. **15** (1998) 75-92.

[5] A. O'Malley, B.K. Hodnett, *The influence of volatile organic compound structure on conditions required for total oxidation*. Catal. Today **54** (1999) 31-38.

[6] J. Tsou, P. Magnoux, M. Guisnet, J.J.M. Órfão, J.L. Figueiredo, *Catalytic oxidation of methyl-isobutyl-ketone over basic zeolites*. Appl. Catal. B-Environ. **51** (2004) 129-133.

[7] W.B. Li, J.X. Wang, H. Gong, *Catalytic combustion of VOCs on non-noble metal catalysts*. Catalysis Today **148** (2009) 81-87.

[8] K. Everaert, J. Baeyens, *Catalytic combustion of volatile organic compounds*. J. Hazard. Mater. **109** (2004) 113-139.

[9] S. Vigneron, P. Deprelle, J. Hermia, *Comparison of precious metals and base metal oxides for catalytic deep oxidation of volatile organic compounds from coating plants: test results on an industrial pilot scale incinerator*. Catal. Today **27** (1996) 229-236.

[10] V.P. Santos, S.S. Carabineiro, M.F.R. Pereira, J.J.M. Órfão, J.L. Figueiredo, *Total oxidation of CO, ethanol and toluene over TiO_2 supported noble metal catalysts* (2010).

[11] C.S.C.G. Silva, Synthesis, *Spectroscopy and Characterization of Titanium Dioxide Based Photocatalysts for the Degradative Oxidation of Organic Pollutants*, Ph. D. Thesis, Faculdade de Engenharia, Universidade do Porto, Porto, Portugal (2008).

[12] V.P. Santos, M.F.R. Pereira, J.J.M. Órfão, J.L. Figueiredo, *Synthesis and characterization of manganese oxide catalysts for the total oxidation of ethyl acetate*. Top. Catal. **52** (2009) 470-481.

[13] R.A. Spurr, H. Myers, *Quantitative analysis of anatase-rutile mixtures with an X-Ray diffractometer*. Anal. Chem. **29** (1957) 760-762.

[14] P. Papaefthimiou, T. Ioannides, X.E. Verykios, *VOC removal: investigation of ethylacetate oxidation over supported Pt catalysts*. Catal. Today **54** (1999) 81-92.

[15] J.E. Sawyer, M.A. Abraham, *Reaction pathways during the oxidation of ethyl-acetate on a platinum/alumina catalyst*. Ind. Eng. Chem. Res. **33** (1994) 2084-2089.

[16] J. Tsou, L. Pinard, P. Magnoux, J.L. Figueiredo, M. Guisnet, *Catalytic oxidation of volatile organic compounds (VOCs): oxidation of o-xylene over Pt/HBEA catalysts*. Appl. Catal. B-Environ. **46** (2003) 371-379.

[17] J. Völter, G. Lietz, H. Spindler, H. Lieske, *Role of metallic and oxidic platinum in the catalytic combustion of n-heptane*. J. Catal. **104** (1987) 375-380.

[18] P. Briot, A. Auroux, D. Jones, M. Primet, *Effect of particle-size on the reactivity of oxygen-adsorbed platinum supported on alumina*. Appl. Catal. **59** (1990) 141-152.

[19] T.F. Garetto, C.R. Apesteguia, *Structure sensitivity and in situ activation of benzene combustion on Pt/Al2O3 catalysts*. Appl. Catal. B-Environ. **32** (2001) 83-94.

[20] P. Papaefthimiou, T. Ioannides, X.E. Verykios, *Combustion of non-halogenated volatile organic compounds over group VIII metal catalysts*. Appl. Catal. B-Environ. **13** (1997) 175-184.

Part V

Conclusions and Forthcoming Work

A general overview of the main results is presented in the final part of this thesis, along with the most relevant conclusions. Some ideas for forthcoming work are suggested in the last chapter.

10 General Overview and Concluding Remarks

Volatile organic compounds are an important class of air pollutants. Among the treatment techniques, none has emerged as a simple, cost-effective and universally applicable method to control the emission of VOC. However, from an environmental point of view, oxidative rather than separation methods should preferably be used for the treatment of VOC.

Catalytic oxidation is considered a promising technology to control the emissions of VOC. The performance of this process critically depends on the type of catalyst, which is a function of the type of VOC to be treated. From a practical point of view, this process should not be feasible in the oxidation of large flow rate streams with very low concentrations. In this context, a dual function adsorbent/catalyst system, which integrates the adsorption and catalytic combustion into a single control unit, should be preferable.

The main goal of this thesis was the development of efficient catalysts for the elimination of VOC. Based on the preliminary results obtained in the context of Project CYTED 305PI0269 "Tratamento de emisiones gaseosas industriales de disolventes para la protección ambiental", this work was mainly focused on the application of manganese oxides, with different structures and chemical compositions, in the oxidation of volatile organic compounds. Additionally, supported noble metal catalysts were also evaluated.

10.1 Catalytic oxidation of VOC over manganese oxides

A number of conclusions have been reached in the course of this research regarding the preparation, characterization and catalytic activities of manganese oxides for the oxidation of ethyl acetate, ethanol and toluene and their mixtures.

The manganese oxides used in this work were prepared by the direct reaction between manganese acetate and permanganate ions under acidic and reflux conditions. By controlling the pH of the medium and the nature of the template cation, it is possible to tailor the shape, crystalline phase and chemical composition of the manganese oxides.

A pure cryptomelane phase was obtained in a restricted pH range using potassium as a template cation. The size of the template cation plays an important role on the stabilization of the cryptomelane structure. The incorporation of other cations, namely Na^+ and Cs^+ during the synthesis was unsuccessful. The template concentration was also considered an important parameter in order to prevent the formation of Mn_3O_4, Mn_5O_8 and Mn_2O_3 as by-products.

These materials were further characterized and it was observed that the structural changes caused by the presence of other phases in cryptomelane play a decisive role on their stability, affecting the mobility of lattice oxygen. Moreover, the reactivity of lattice oxygen was also affected; the presence of Mn_2O_3 in cryptomelane decreasing its reducibility, while the presence of Mn_3O_4 has the opposite effect.

The manganese oxides were tested as catalysts for the oxidation of ethyl acetate, ethanol and toluene, and the following reactivity trend (in terms of conversion into CO_2) was observed: Toluene< ethanol < ethyl acetate. Pure-cryptomelane type manganese oxide was found very active and selective into CO_2, and its performance was significantly affected by the presence of other phases, namely Mn_2O_3 and Mn_3O_4. The latter improves the catalytic performance, while the former has the opposite effect. It was observed that the catalytic performances of manganese oxides are strongly related with their redox properties, revealing the catalytic role of oxygen species from the catalysts.

In order to provide a better understanding of the VOC oxidation mechanism over manganese oxides, some additional experiments were performed, namely temperature programmed surface reaction after adsorption of ethyl acetate, ethanol and toluene, as well as reactions without oxygen in the feed.

CO_2 and water were the only products detected during the temperature programmed reaction experiments, confirming that lattice oxygen is involved in the VOC oxidation, and that a Mars and van Krevelen mechanism is operative. Moreover, these experiments also show that the interaction of oxygenated compounds with the catalyst surface is quite different from that observed in the case toluene.

Reactions without oxygen in the feed also show the role of lattice oxygen in the oxidation of VOC, supporting the TPSR experiments. Strong correlations between catalytic performance and CO_2 produced in these experiments were observed. Moreover, reactions at different activation conditions suggest that oxygen incorporation is slower in the case of toluene, explaining its lower reactivity.

In order to further enhance the electronic and catalytic properties of cryptomelane, cesium was introduced into the tunnel structure by the ion-exchange technique. This was found to improve the performance of the catalyst in the oxidation of ethyl acetate, which was correlated with the basic properties of the catalyst.

The stability of the cryptomelane catalyst in the oxidation of toluene was also studied. A gradual deactivation was observed at low temperatures, as a result of the formation of carbonaceous deposits strongly retained on the catalyst surface. Besides deactivation, the catalyst also shows an oscillatory behaviour in a restrited range of temperatures, which results from cycles of accumulation and oxidation of adsorbed reactant and reaction products. However, it is possible to work in conditions where deactivation does not occur.

The final part of this section was dedicated to the study of the catalytic oxidation of two-component VOC mixtures on cryptomelane. Remarkable mixture effects on the activity and the selectivity were observed. Toluene was found to inhibit both ethyl acetate and ethanol oxidation, this effect being more evident in the case of ethyl acetate. The inhibition effect was explained by a competition between the reactant molecules for the adsorption sites. Toluene oxidation is slightly inhibited by the

presence of ethyl acetate, while the presence of ethanol has a slight promotion effect (mainly due the oxidation of acetaldehyde), which was attributed to a local heating effect. Concerning ethyl acetate and ethanol mixtures, it was observed that both compounds have a mutual inhibitory effect. However, this effect is much more evident in the case of ethyl acetate oxidation.

10.2 Catalytic oxidation of VOC over supporte noble metals

The final part of this thesis was dedicated to the catalytic oxidation of VOC over supported noble metal catalysts.

Several noble metals (Pt, Pd, Rh, Ir and Au) were supported on titania by liquid phase reduction deposition and by incipient wetness impregnation, and used in the oxidation of ethanol and toluene. It was observed that the preparation method can have a significant effect on the dispersion of the metallic phase and consequently on the catalytic performance.

Platinum was found to be the most active metal, independently of the preparation method. Furthermore, it was established that the oxidation reactions of ethanol and toluene in the presence of Pt or Pd catalysts are structure sensitive, the intrinsic activity increasing with the metal particle size.

The effect of several parameters on the oxidation of ethyl acetate was investigated, such as the crystalline phase of the support, the nature and amount of noble metal (platinum or palladium), the metal dispersion, and the activation conditions. Platinum was also found to be more active and selective to CO_2 than palladium, and the presence of pre-reduced platinum was also found to improve catalyst performance. Relatively to the effect of the metal disperson, it was observed that the oxidation of ethyl acetate is also structure sensitive.

The catalytic oxidation of ethanol /toluene mixtures was also studied over platinum supported catalysts. Mutual inhibitory phenomena were observed, being much more evident in the case of ethanol. It was proposed that the inhibition effect results from the competition for the oxygen atoms chemisorbed on the Pt particles.

10.3 Comparison between supported noble metals catalysts and manganese oxides

The efficiency of the catalytic oxidation largely depends on the physical and chemical properties of the catalyst and the nature of the compound to be degraded. Cryptomelane doped with small amounts of Mn_3O_4 and platinum supported on titania were the most active systems. The choice between using the metal oxide or the noble metal to catalyse VOC oxidation depends on several factors, namely the nature of the stream to be treated and the presence of contaminants. It can be concluded from the present work that it is preferable to use supported noble metals for the oxidation of the aromatic hydrocarbons (toluene), while cryptomelane is by far the most attractive system for oxygenated compounds. Moreover, in this case, cryptomelane is also less sensitive to the presence of water vapour in the gas stream than noble metals, due its hydrophobic nature.

10.4 Suggestions for forthcoming work

There is still much work to be done regarding the catalytic oxidation of VOC. The work presented in this thesis was mainly focused on the study of cryptomelane – type manganese oxides in the oxidation of VOC. The good results obtained with the cesium modified cryptomelane catalyst opened up some new frontiers for further research. Other cations such as Na^+, Li^+ or H^+ could be introduced in the tunnel structure of cryptomelane in order to further improve its catalytic properties. Moreover, other elements like cerium, copper and zirconium can also be incorporated into the framework of cryptomelane.

An additional effort should be invested in the catalytic oxidation of mixtures, since real effluents contain several different compounds. Binary and ternary mixtures with different compositions should be tested.

The application of this technology in industry requires the use of structured catalysts. In this context, the preparation, characterization and utilization of monoliths would be of great interest.

Appendices

Appendix A- Schematic representation of the experimental set-up

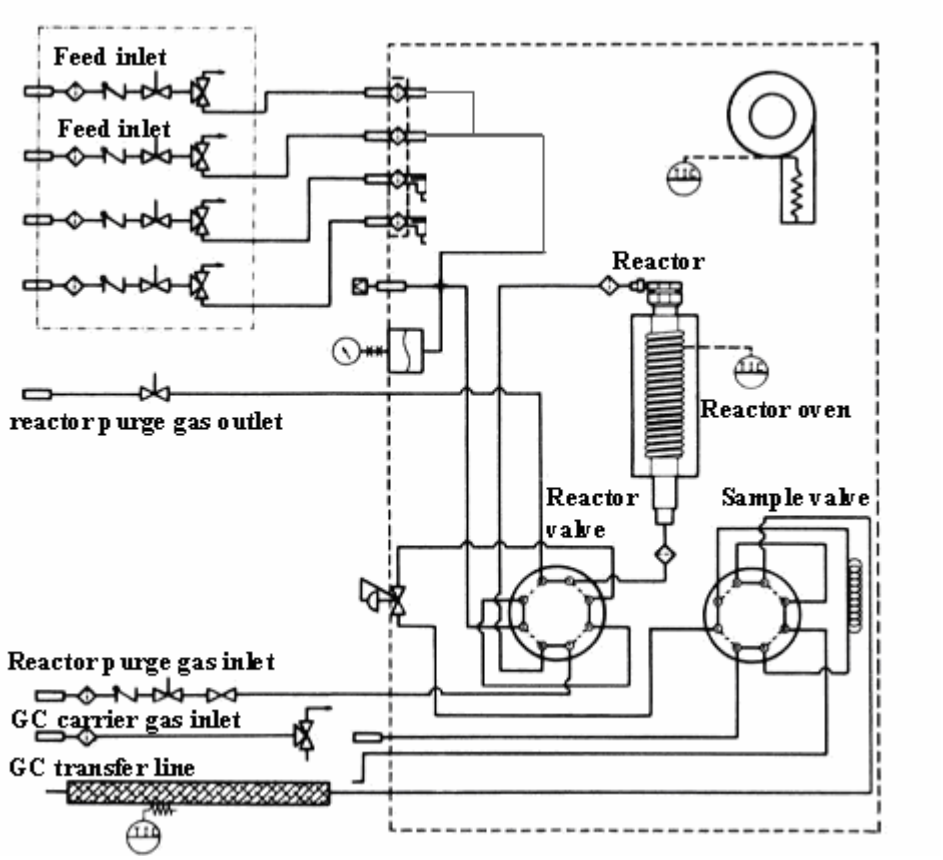

Figure A- Reactor scheme.